GAW Report No. 275

IG^{3}IS Urban Greenhouse Gas Emission Observation and Monitoring Good Research Practice Guidelines

WEATHER CLIMATE WATER

WORLD METEOROLOGICAL ORGANIZATION

GLOBAL ATMOSPHERE WATCH

IG3IS Integrated Global Greenhouse Gas Information System

GAW Report No. 275

IG³IS Urban Greenhouse Gas Emission Observation and Monitoring Good Research Practice Guidelines

WEATHER CLIMATE WATER

WORLD
METEOROLOGICAL
ORGANIZATION

GLOBAL
ATMOSPHERE
WATCH

IG3IS
Integrated
Global Greenhouse Gas
Information System

Chair, Publications Board
World Meteorological Organization (WMO)
7 bis, avenue de la Paix
P.O. Box 2300
CH-1211 Geneva 2, Switzerland

Tel.: +41 (0) 22 730 84 03
Fax: +41 (0) 22 730 81 17
Email: Publications@wmo.int

IG^{3}IS Urban Greenhouse Gas Emission Observation and Monitoring Good Research Practice Guidelines

Lead Authors:

Jocelyn C. Turnbull[1,2,3], Phil DeCola[3,4], Kim Mueller[5], Felix Vogel[6]

Authors:

Anna Agusti-Panareda[7], Doyeon Ahn[8], Sunil Baidar[2,9], Heinrich Bovensmann[10], Alan Brewer[9], Dominik Brunner[11], Huilin Chen[12], Jia Chen[13], Frédéric Chevallier[14], David Crisp[15], Andreas Christen[16], Ron Cohen[17], Kenneth J Davis[18], Florian Dietrich[13], Richard Engelen[7], Christian Feigenwinter[19], Andreas Fix[20], Beniamino Gioli[21], Kevin Gurney[22], Kristian Hajny[23], Janne Hakkarainen[24], Samuel Hammer[25,26], Frank Hase[27], Timothy W. Hilton[1], Lucy Hutyra[28], Leena Järvi[29], Sujong Jeong[30], Anna Karion[5], Jooil Kim[31], Thomas Lauvaux[14], John Lin[32], Zoë Loh[33], Israel Lopez-Coto[5], Bradley Matthews[34], Natasha Miles[18], Logan Mitchell[32], Lee Murray[35], Thomas Nehrkorn[36], Nasrin Mostafavi Pak[6], Dario Papale[37], Hayoung Park[30], Ignacio Pisso[38], Joseph Pitt[22], Michel Ramonet[14], Peter Rayner[39], Thomas Röckman[40], Anke Roiger[20], Paul Shepson[22], Peter Sperlich[41], Erik Velasco[42], Alex Vermuelen[43], Isaac Vimont[44], Roland Vogt[19], James R. Whetstone[5], Joy Winbourne[45], Irene Xueref-Remy[46]

Author affiliations

1. GNS Science, Te Pū Ao, Lower Hutt, New Zealand
2. CIRES, University of Colorado at Boulder, CO, USA
3. Integrated Greenhouse Gas Information System (IG^{3}IS) Scientific Steering Committee Co-Chair, World Meteorological Organization
4. University of Maryland, Department of Atmospheric and Oceanic Sciences, USA
5. National Institute of Standards and Technology (NIST), Gaithersburg, Maryland, USA
6. Environment and Climate Change Canada, Canada
7. European Centre for Medium-Range Weather Forecasts, Reading, United Kingdom
8. The George Washington University, Washington, D.C., USA
9. NOAA Chemical Sciences Laboratory, Boulder, CO, USA
10. University of Bremen, Institute for Environmental Physics, Germany
11. Empa, Dübendorf, Switzerland
12. University of Groningen, The Netherlands
13. Technical University of Munich, München, Germany
14. Laboratoire des Sciences du Climat et de l'Environnement, Gif sur Yvette, France
15. Jet Propulsion Laboratory/California Institute of Technology, CA, USA
16. Albert-Ludwigs-Universität Freiburg, Freiburg, Germany
17. University of California, Berkeley, California, USA
18. Pennsylvania State University, University Park, Pennsylvania, USA
19. University of Basel, Department of Environmental Sciences, Basel, Switzerland
20. German Aerospace Centre, Institute of Atmospheric Physics, Germany
21. Italian National Research Council, Institute of BioEconomy, Firenze, Italy
22. Northern Arizona University, Flagstaff, Arizona, USA
23. Stony Brook University, School of Marine and Atmospheric Sciences, NY, USA
24. Finnish Meteorological Institute, Helsinki, Finland
25. Institute of Environmental Physics, Heidelberg University, Germany
26. ICOS Central Radiocarbon Laboratory, Heidelberg University, Germany
27. Karlsruhe Institute of Technology, Karlsruhe, Germany
28. Boston University, Department of Earth & Environment, Boston, MA, USA

29. University of Helsinki, Institute for Atmospheric and Earth System Research, Finland

30. Seoul National University, Seoul, Korea

31. Scripps Institution of Oceanography, University of California San Diego, La Jolla, CA, USA

32. The University of Utah, Department of Atmospheric Sciences, Salt Lake City, UT, USA

33. Commonwealth Scientific and Industrial Research Organization (CSIRO), Melbourne, Victoria, Australia

34. University of Natural Resources and Life Sciences, Vienna, Austria

35. Earth and Environmental Sciences, University of Rochester, NY, USA

36. Atmospheric and Environmental Research, Lexington, MA, USA

37. Università degli Studi della Tuscia, Viterbo, Lazio, Italy

38. Norwegian Institute for Air Research (NILU), Atmosphere and climate department, Kjeller, Norway

39. University of Melbourne, School of Earth Sciences, Climate and Energy College, Victoria, Australia

40. University of Utrecht, The Netherlands

41. NIWA, Wellington, New Zealand

42. Molina Centre for Energy and the Environment, USA

43. Integrated Carbon Observation System (ICOS), Helsinki, Finland

44. NOAA Global Monitoring Laboratory, Boulder CO, USA

45. University of Massachusetts, Department of Earth, Environmental, and Atmospheric Sciences, Lowell, MA, USA.

46. Institut Méditerranéen de Biodiversité et d'Ecologie Marine et Continentale, Universitaires d'Aix-Marseille, France

Table of Contents

1. Summary of Purpose 6
2. Introduction 7
3. Urban Inventory and Flux Models 9
4. Atmospheric Observational Methods 13
5. Data Assimilation Systems 29
6. Data management, archiving and distribution 35
7. References 36

Annex A. Inventory or emission flux models 38
- A.a. Fossil fuel CO_2 emission data products 38
- A.b. Biogenic CO_2 flux models/products 47
- A.c. Methane flux models/products 60

Annex B. Atmospheric Observational Methods 66
- B.a. Tower and other elevated point observations 67
- B.b. Tower and elevated point measurement data analysis 72
- B.c. Greenhouse gas and other trace gas vertical profile measurements 76
- B.d. Mobile (ground-based) surveys 83
- B.e. In situ airborne GHG mole fraction observations 87
- B.f. Mass balance 90
- B.g. Discrete flask sampling 102
- B.h. Isotope, Correlate Tracer and Tracer Ratio Methods 106
- B.i. Eddy covariance flux observations 114
- B.j. Ground-based Remote Sensing for Urban Monitoring 124
- B.k. Dense networks 130
- B.l. Choice of background 132
- B.m. Meteorological Observations for Urban Greenhouse Gas Analysis 138
- B.n. Satellite Remote Sensing of XCO_2 145

Annex C. Data Assimilation Systems 154

C.a. Meteorological Inputs Needed for Urban Monitoring Systems 154

C.b. Forward modelling 163

C.c. Calculation of atmospheric footprints needed for urban monitoring 166

C.d. Use of inverse modelling methods for urban monitoring 172

Annex D. Recommendations for Data Management, Archiving and Distribution 175

D.a. FAIR data principles 175

1. Summary of Purpose

The Integrated Global Greenhouse Gas Information System (IG³IS) aims to coordinate an Integrated Global Greenhouse Gas Information System, linking inventory and process model-based information with atmospheric observations and atmospheric modelling, to provide the best possible estimates of greenhouse gas emissions at the national and urban scales. Linkages to stakeholders and policy outcomes are a critical goal of IG³IS. The IG³IS Implementation Plan outlines the IG³IS ambition at a broad scale (DeCola et al., 2018).

These Good Research Practice Guidelines are intended to provide technical guidance on current state of the art technologies in urban greenhouse gas information systems. They lay out the available methodologies and how they can best be implemented, as well as guidance on the end user outputs that might be obtained from each methodology. There are many unresolved challenges in this evolving field of research, and we include discussion of ongoing research and considerations.

A note on the relationship between these Good Research Practice Guidelines and “Standards”. The metrology community is working in parallel to develop standards for urban greenhouse gas measurements. These Good Research Practice Guidelines are aimed at the research community developing emerging methods. Documentary standards will be the logical follow-on as best practices coalesce into widely accepted methodologies that can be implemented in operational situations. IG³IS, the International Bureau of Weights and Measures (BIPM), US National Institute of Standards and Technology (NIST) and other metrology organizations will work together to ensure alignment between best practices and standards.

The process of creating these Good Research Practice Guidelines began with the IG³IS Steering Committee identifying experts for each sub-topic. At a workshop convened in June 2020, each section was written by the identified lead author and others from the research community, reviewing the state of the art for each topic. Following the workshop, the authors consulted with other experts to provide a draft document. The draft was available for public comment from November 2021 to January 2022, following which public comments were incorporated into the final document. Additional expert contributors were identified during this review process. This is an evolving field of research, and we anticipate that the best practices will require regular updating as knowledge develops. We recommend updates to this document every two years, through the biannual IG³IS Science meetings as well as dedicated workshops. Researchers, experts and stakeholders are invited to participate in these future revisions.

2. Introduction

There is a growing ambition across many cities to mitigate their greenhouse gas emissions, due to carbon dioxide (CO_2), methane (CH_4), nitrous oxide (N_2O) and fluorinated gases. Since the majority of anthropogenic emissions originate in urban areas, this is a key component of national and international mitigation efforts. Currently, cities rely on inventory-based methods to evaluate their emissions, typically estimating total city-wide CO_2 emissions for each source sector on an annual basis. While there is no compulsion to use specific methodologies, most cities follow a general set of guidelines to create city-wide inventories (Fong et al. 2014). However, as efforts to mitigate emissions expand, the need for more detailed, timely emissions information at sub-national scales is growing.

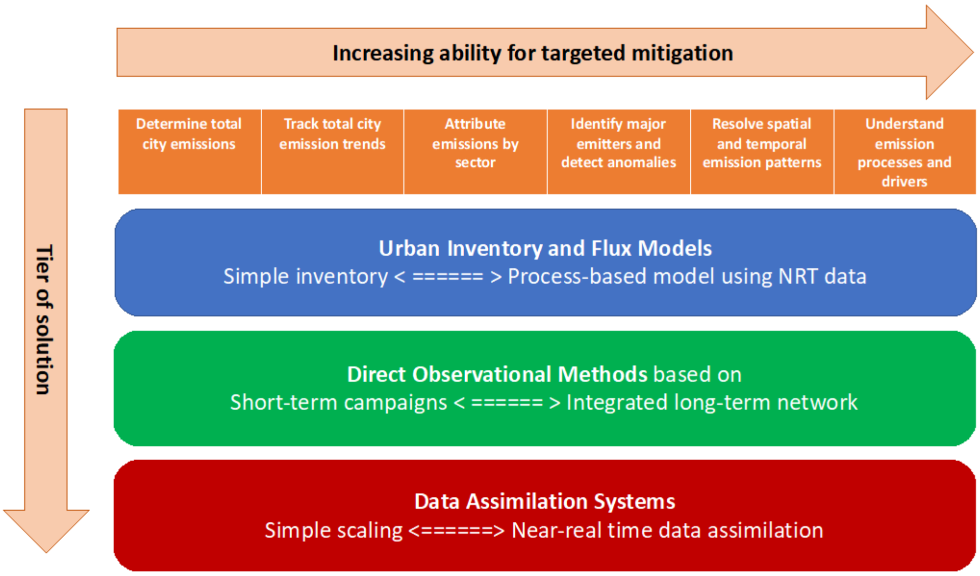

Figure 1: Solutions for Targeted Mitigation.

This document considers information needs for targeted mitigation efforts and available solutions. The level of emissions information required can range from a one-time determination of total city emissions, to spatially, temporally and source sector resolved emissions information. As the complexity of the emissions information grows, so too does the ability to use the information for targeted mitigation (Figure 1). Research on urban greenhouse gas emissions continues to evolve, and there is no single emission estimation method that can be applied to every situation. Instead, there are a variety of available methods which can be applied depending on the particular urban environment and desired outcomes. In this document, we detail the solutions available, categorizing them by three tiers of increasing sophistication: urban inventory and flux models, direct observational methods, and data assimilation systems. Within each of these categories, multiple methodologies may be applied. If the goal is to identify major emitters and detect anomalous (undocumented) emission sources, short-term campaigns using mobile surveys and inventory validation may be sufficient. When the goal is detailed quantification of changes in emissions, separated by source sector, long-term observations and near-real-time data assimilation may be needed to complement inventory methods.

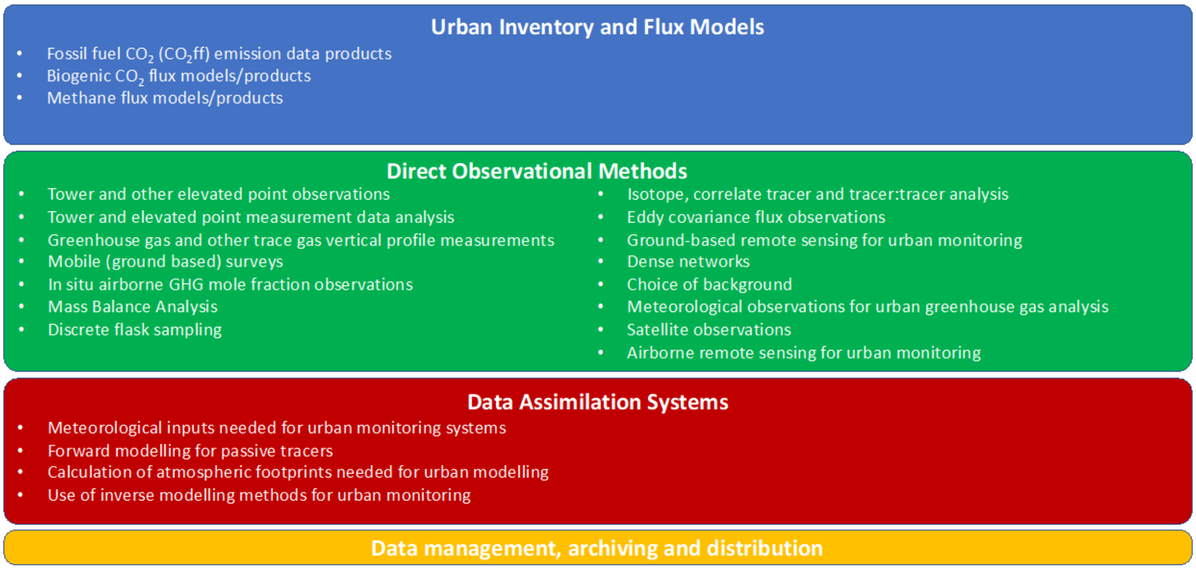

Figure 2: Emission information methodologies presented in this document

Within the three tiers of solution (Figure 1), multiple methodologies exist (Figure 2), and here we describe each of those methodologies and techniques. First, in Section 3, high-resolution urban inventory-based methods are discussed, including those for fossil fuel CO_2 emissions, biogenic CO_2 fluxes, and methane emissions and fluxes. We follow this in Section 4 with Direct Observational Methods. A number of different techniques can be used to make atmospheric observations of greenhouse gases (GHGs) in urban areas, and these lead to a variety of different methods to directly evaluate emissions depending on the type of observation and outcome required. In Section 5, we lay out the data assimilation systems and components thereof that can be used to relate atmospheric observations to inventory-based data products and produce refined and validated “posterior” detailed emission maps at high spatial and temporal resolution. Section 6 provides recommendations for Data Management. Finally, the Annexes provide expanded detail on individual methods, appropriate for practitioners looking for detailed guidance to implement these methods.

3. Urban Inventory and Flux Models

In this chapter, we summarize the state-of-the-art approaches used to create urban-scale emission data products from flux observations, and statistical or proxy information. These data products are the first tier of solutions that respond to the information needs of stakeholders planning mitigation efforts (see Figure 1). City-wide emission inventories have been developed by different groups and actors for very different purposes, including self-reporting or carbon disclosure activities to support policymaking as well as fundamental research. While other types of inventories such as those developed following the Global Protocol for Community-Scale Greenhouse Gas Emission Inventories (Fong et al., 2014) are mentioned here, the core focus is on spatially and temporally explicit data products which are commonly required when comparing to emission estimates derived from atmospheric observations.

The level of detail required and achievable may differ significantly depending on factors such as data availability, complexity of terrain, mix of sources and sinks, etc. In general, emission products for CO_2 from combustion of fossil fuels are most mature and building/street-level resolution and sector-specific information has been achieved in some cases. Combustion, which is the core process here, is well understood and fuel use data or proxies for fuel use can be found in many regions.

In contrast, our understanding of the spatial and temporal variability of biogenic CO_2 fluxes in urban areas is still developing. Even in cities where inventories of urban vegetation are available (e.g. from remote sensing) it is still a matter of cutting-edge research to translate this proxy data into photosynthesis and respiration as well as carbon loss and storage terms, which respond to external drivers, such as water availability, weather, urban heat islands, fertilization, etc.

In contrast to CO_2, emission data products for methane are often even more challenging as the spatial distribution of infrastructure and consumption proxies are often only a limited predictor of emissions. Methane emissions are usually driven by unintended leaks and/or faulty equipment. Many studies have also found that a small share of sources disproportionately contribute to overall emissions. Nevertheless, spatially and temporally explicit CH_4 emission products have been created for a few cities.

Creating either a CO_2 or CH_4 inventory is often time and labour intensive, which requires collections and quality control of large amounts of consumption information, emission factors, and proxy data. While a more detailed description of the process is given in the annexes, we focus on the core elements here.

3.1 Fossil fuel CO_2 emission data products

Often referred to as “bottom-up” approaches or “emissions models” these include a wide variety of approaches that attempt to estimate fossil fuel CO_2 (CO_2ff) fluxes independently of the use of atmospheric mixing ratios. They generally include approaches such as: activity data multiplied with associated emission factors; emissions based on fuel consumption statistics; emission ratios to emission estimates for other gases (e.g. air quality species); direct stack flux monitoring; or more complex emissions models. They also include use of remote sensing attributes other than a column trace gas measurement.

There are two general aims in producing CO_2ff emission data products. The first is usable/useful to policy stakeholders (citizens, government, practitioners, businesses). The second broad aim is to incorporate these data products into “information systems” such as data assimilation (Section 5), which often requires spatially and temporally resolved emissions information rather than annually aggregated data. Emissions can be divided into three scopes. Scope 1 is emissions that physically occur within the region of interest. Scope 2 accounts for emissions that are generated elsewhere but consumed in the region of interest (e.g. electricity generation in one place but used in another), and Scope 3 is embedded emissions from the manufacturing of goods.

Considerations

- Fluxes should be gridded at resolutions below that of atmospheric transport models.
- High temporal resolution is needed – hourly temporal resolution is preferred.
- Fluxes should reflect a continuous time series as opposed to “snapshots” in time.
- Data products should be provided as close to real time as possible.
- Scope 1 emissions are needed for comparison with atmospheric observations– this is what the atmosphere “sees”. Though Scope 2 and Scope 3 are useful for context, they must remain discrete from Scope 1.
- Emissions should be separated by sector/fuel in anticipation of the growing multi-tracer work which is fuel/sector-specific.
- Include uncertainty estimation. This is important for use as “prior” flux where the prior uncertainty can leverage considerable control over the outcomes of inversion/data assimilation modelling.
- Estimates should be documented, peer-reviewed with transparent traceable methods and available in a downloadable/usable form.
- Human respiration and biofuel combustion emissions may be included.

Ongoing Research

- Currently, multiple self-reporting standards for urban GHG inventories co-exist with different emission models developed within the scientific community. Therefore, an in-depth analysis of the self-reporting approaches and scientific products is crucial to ensure comparability of results and to assess if all approaches can achieve the required completeness and precision to be relevant for stakeholders.
- Beyond the classical approach, systems have been developed that construct gridded emissions relying on explicit models constrained by proxy data, often using Bayesian techniques to achieve quantitative uncertainty estimates as well as prognostic and diagnostic capabilities.

See also Annex A.a.

3.2 Biogenic CO_2 flux models/products

The impact of biological fluxes on urban CO_2 mixing ratios is poorly constrained but has been suggested to offset between 0% and 100% of local fossil fuel emissions depending on the locale, season, and hours of the day considered although in general the offset capacity at daily to annual scale is rather small. The mixing ratio of CO_2 and other greenhouse gases in cities is the result of the composition of inflowing air, local emissions source, local atmospheric chemistry, and biological uptake/loss processes. The biological influence on CO_2 varies across multiple temporal and spatial scales. For example, fluxes vary geographically with urban form; fluxes vary seasonally with climate and vegetation composition; fluxes vary diurnally with weather and physiology; and fluxes vary across all timescales and geographies with landscaping management choices. Urbanization alters photosynthetic and respiration processes of plants and soils through a mix of increased resource availability as well as constraints on net ecosystem productivity. Net productivity per unit plant may be stimulated by modified climate through heat and irrigation islands; extended growing season duration; increasing local mole fractions of CO_2; increased availability of limiting nutrients through direct and indirect fertilization; and by the relatively high light environments experience by urban plants. Net productivity can also be decreased through increased pollutant loads, management choices (e.g. road salting, extensive pruning, and removal of hazard trees), poor quality soils, and the amplified effects of heat waves. Existing urban biosphere models are at a nascent point in development, largely relying on modified light-use efficiency photosynthetic models developed in rural ecosystems and temperature-derived respiration models.

Considerations

- The influence of biogenic CO_2 fluxes in urban areas can range from negligible to dominant depending on timescale, geography, and detail of analysis.
- Management decisions, urban form, and the extent of the urban greenspace are fundamental controls on biogenic CO_2 fluxes. Decisions such as how to manage plant organic waste (leaf litter) or implement ‘nature-based’ climate solutions to expand urban canopy can radically alter biogenic fluxes across a range of scales. All these factors are under affected by policy.
- The functional traits of urban vegetation strongly influence biological CO_2 fluxes and the ecosystem resilience to climate change.

Ongoing Research

- Models with varying process-based and management details are under development including those operating at the individual tree scale, remote sensing driven models, and generalized first order models. All these classes of models can be useful in the IG^{3}IS context depending on the city and specific application.
- Field studies are being conducted to better understand the biogeochemical and biophysical cycles in urban ecosystems.
- Development of allometric and prediction growth models for urban vegetation vis needed along with research into the of urban land management practices.

See also Annex A.b.

3.3 Methane flux models/products

The general principles of creating an anthropogenic methane emission product are similar to studies for CO_2: using activity or consumption data in concert with related emission factors to calculate total (most often annual) emissions for each sector. Alternatively, reported regional methane emissions can be downscaled to city scale based on proxy data. However, methane emission products often have much higher relative uncertainties than CO_2 emission products, as methane is most commonly released as a non-intentional by-product of human activities. Therefore, consumption-based approaches are less reliable and can cause discrepancies. This also means relative uncertainties are similar for large and small emitters. Emission factors within an economic sub-sector or activity often do not follow a normal distribution but are heavy-tailed (‘super-emitter problem’).

Considerations

- Collect site specific data where possible and otherwise use IPCC recommended approaches
- Provide sector-specific information (possibly include isotope and co-emitted species in the inventory)
- If possible, use different approaches to create an ensemble of emission products to capture systematic uncertainties
- Use atmospheric information to validate emission factors (and their distributions) for local infrastructure and facilities
- It is important to provide information in clear and well-defined categories
- For the waste sector, include landfills (open and closed), wastewater treatment plants, sewage collection networks
- For the natural gas sector, include storage facilities, compressor and feeder stations, distribution pipelines, consumer appliance emissions
- For the industrial sector, include power plants, solvent and chemical industries
- Agricultural sources may be included within cities, including ruminants, and crops
- Other biogenic sources may include wetlands, waterways, lakes, and coastal ecosystems
- Incomplete combustion of transportation fuels should be included.

Ongoing Research

- Complete urban methane inventories have only been created for a limited number of cities in high-income countries, so more research into factors influencing urban CH_4 emissions in all global regions is critical.
- To date urban methane inventories have been focussed on Scope 1 emissions and have been predominantly used to compare to atmospheric observations and mobile survey data. For policymakers Scope 2 and Scope 3 could be highly relevant as well.

See also Annex A.c.

4. Atmospheric Observational Methods

Atmospheric observations greenhouse gases, related tracers and meteorological factors are used to infer GHG emissions. In this section, we discuss a variety of measurement methods along with techniques and conceptual models to infer GHG emissions from these observations. Each method has advantages and disadvantages that are more suited to particular applications and targeted mitigation outcomes. These observational methods form the second tier of information for targeted mitigation outcomes (see Figure 1), adding a layer of emission information that may not be obtainable from inventory-based methods, as well as providing an independent constraint on emissions. Currently, the most widely used methods utilize high precision GHG instrumentation placed on towers or other elevated points, in aircraft or ground-based vehicles, and we describe the observational methods and analysis techniques in sections 4.1. to 4.6. Flask measurements of additional trace gases and isotopes are often made in tandem with the in situ equipment, and these are discussed in sections 4.7 and 4.8. Other techniques involve ground or satellite-based remote sensing (section 4.10 and 4.14), dense networks, typically using lower cost sensors (section 4.11) and the eddy covariance technique (section 4.9). All observational methods require consideration of background or incoming air composition as well as meteorological information, discussed in sections 4.12 and 4.13. While the different methods are described in the following sections (and annexes) individually, there is of course considerable scope for, and advantages of, applying different observational methods together within a city.

Practitioners making GHG observations should also refer to the WMO/GAW Greenhouse Gas Measurement Techniques Recommendations (Crotwell et al., 2020). These recommendations, updated every two years, provide detailed explanations of how greenhouse gas measurements should be performed, including international consensus on calibration and standardization, data quality and other factors.

4.1 Tower and other elevated point observations

Monitoring atmospheric mole fractions of greenhouse gases from elevated points in and around cities aims to measure the local enhancements in these mole fractions due to urban emissions. Measuring at elevated points such as roof tops or higher (tall towers, mountains) and sites downwind of the city, compared to surface measurements performed at the street-level, makes it possible to extend the footprint of the observations and to reduce as much as possible the surface layer vertical gradients.

Considerations

- Long-term multi-year measurements are essential to monitor the trends associated with, for example, the emission reduction strategies set up by the city.
- Continuous measurements are needed due to the high signal variability.
- At a minimum, CO_2 should be measured. CH_4 and CO are also recommended, with additional species where possible.
- Near-real-time data products are important for a rapid detection of technical problems and to analyse the observed variability (Section 4.2).
- A minimum of two sites, one upwind and one downwind of the city are needed. Depending on the wind patterns, several pairs of upwind-downwind sites might be required to cover the airmass paths from upwind to downwind of the city under various wind conditions.
- Generally the choice of sites results from a compromise between a conceptually optimal network and existing, accessible structures, since infrastructure is rarely built for atmospheric measurements.
- In all cases, it is essential to assess the risk of local contamination, which is particularly important on the roofs of buildings due to venting of emissions from inside the building.
- More complex in-depth network design studies are highly recommended.
- Co-located flask sampling for additional species is advantageous.

Ongoing Research

- It is recommended to link the urban networks to WMO reference scale (see GGMT recommendations) but access to reference gases can be an issue, and new instruments (e.g. open path) may be difficult to calibrate. More important for urban networks may be the internal compatibility of the stations.

See also Section 4.2. and Annex B.a.

4.2 Tower and elevated point measurement data analysis

The interpretation of tower-based greenhouse gas (GHG) observations is strongly dependent on sound practices in general observational techniques (Section 4.1) and data quality control (Section 6), and dependent on background mole fractions defined for the network (Section 5.6). Here, we outline strategies that may be useful in analysing the data, once the prerequisite data needs have been fulfilled. Generally, analysis can be done on mole fractions directly, or on "enhancements" (mole fractions after removal of a baseline). Calculation of enhancements isolates the signal from the region of interest, removing larger scale contributions. When determination of the background also takes into consideration the biogenic signal, the enhancements more directly represent the signals from anthropogenic emissions but defining a clear background can be challenging (Section 5.6). Of interest is identifying significant patterns in the variability observed, and in the complex urban environment, one should expect a mix of factors to drive this variability.

Considerations

- Variability at various temporal scales: Annual trends in the variability of mole fractions and their enhancements. Analysis should consider whether significant patterns exist in the variability over annual timescales. Consider composite plots of mole fractions at hour-of-day, day-of-week, day-of-year, month-of-year, seasonal, multi-annual, etc. Caution is necessary in interpreting patterns, as changes can be driven by meteorology as well as a change in emissions. In general, higher standard deviation within an hour indicates larger local sources.
- Site-to-site variability of mole fractions and mole fraction enhancements: Comparing sites may help understand the factors that dominate variability across the network.
- Tower observations can be used in combination with air mass back trajectory footprints, which become an integral part of forward modelling and inversions (Section 5).
- Wind roses and polar plots: Mole fraction enhancements can be plotted against wind speeds/directions to analyse correlations between wind and pollution patterns.
- Significant filtering of the data (e.g. In terms of wind speed, wind direction, time of day, day-of-year) may be necessary to derive coherent plots, and the recommendation is to use flexible software plotting tools that allow for experimentation in sensitivity studies.

Ongoing Research

- Analysis of GHG emission reductions during the COVID-19 shutdown; note that larger signals are captured using from lower elevations (e.g. 10 m).
- Development of common data formats to allow coherent analysis of observations across different networks (e.g. CO2-USA, ICOS-cities).
- Analysis of the cumulative summing of the enhancement mole fractions over a period of time to identify the timing of significant change in emission patterns (caution is necessary of gap filling if missing data is required).
- Analysis of tracer-tracer ratio between co-measured compounds to effectively factor out meteorology and help identify a direct source emission signature (Section 4.8).
- Analysis of vertical gradients measured at multiple inlet heights to better understand the surface fluxes nearby the measurement site (Section 4.3).
- Analysis of GHG variability as a function of atmospheric boundary layer height.

See also Annex B.b.

4.3 Greenhouse gas and other trace gas vertical profile measurements

Measurements of greenhouse gases (GHGs) and other trace gases are often collected at discrete altitudes with in situ sensors. The altitude of the measurement has important implications for data interpretation. Measurements at multiple altitudes makes the measurement system more robust and opens new data analysis options.

Considerations

- Measure vertical GHG profiles at sites representative of the urban area. Urban enhancements are the primary observation used at present for urban emission estimates (Section 4.1 and 4.2). These enhancements effectively capture emissions from an entire urban area. Ideally the measured enhancements are close approximations to the atmospheric boundary layer (ABL). It is generally advantageous, therefore, to collect GHG measurements high enough to avoid strong vertical differences driven by local fluxes that will mix with and complicate interpretation of the urban enhancement. The sensitivity of a measurement network to local fluxes and vertical gradients can be assessed with profile measurements at sites representative of your urban area.
- Measure at common altitudes, if practical. Measurements collected at common altitudes across a network make comparison across profile measurements easier, since the vertical gradients in the lower ABL are strong functions of altitude above ground.
- Measure GHG profiles at upwind sites to improve background characterization. Vertical profile measurements, particularly on tall communications towers, can provide valuable upwind constraints particularly in meteorological conditions when the atmosphere is vertically stratified.
- Measure GHG profiles at urban or downwind sites to explore experimental night-time enhancement measurements. It is likely that night-time measurements can be used to constrain urban emissions as our understanding of the nocturnal, urban boundary layer improves. Vertical profile measurements are likely to contribute to that improved understanding and improve the accuracy of night-time emissions estimates.
- Measure GHG profiles for local flux inference. GHG profiles can be used to infer local fluxes. While absolute quantification with flux-gradient relationships is challenging, relative changes over time can be tracked. Low altitude sampling points are beneficial to this objective.
- Consider coupling vertical GHG profile measurements with eddy covariance flux measurements (Section 4.9). Micrometeorological measurements of atmospheric turbulence, energy fluxes, and GHG fluxes are complementary to profile measurements, and enable additional quantification of flux-gradient relationships and local fluxes. Atmospheric profiling using lidar, rawinsondes, sodar or radar are similarly complementary to GHG profile measurements.

Ongoing Research

- To date, urban networks with inlet heights determined mostly by practical considerations. Using sites with multiple inlet heights might help to develop recommendations on what inlet heights are most suitable for certain applications/cover a certain footprint of a city.

See also Annex B.c.

4.4 Mobile (ground-based) surveys

Over recent years mobile ground-based surveys have been used in many studies to detect and quantify greenhouse gas sources and to identify unknown/untapped mitigation potentials. Especially the work on methane sources from facilities and infrastructure has progressed significantly.

Many studies have used mobile surveys in combination with tracer release experiments or modelling to infer CH_4 emissions from facilities (landfills, wastewater treatment plants, etc.). Typically, emission rates can be estimated with an individual uncertainty of 50–70%.

Larger scale studies in urban areas have often focussed on mapping enhancements of atmospheric methane resulting from natural gas infrastructure emissions. These studies were initiated in US cities and used empirical calibrations to translate CH_4 enhancement maps to emission rate estimates. Beyond these short-term studies targeting specific events of facilities, the use of third-party platforms has emerged as a viable option for city scale monitoring (e.g. public transit vehicles). Campaigns as well as more routine surveys follow similar principles and the core issues to address in our recommendation are survey planning, technical requirements and auxiliary observations.

Considerations

- For facility monitoring it is critical to ensure that the observed GHG variability is caused by the target facility, and that the observed enhancements are representative to allow upscaling of results.
- For urban surveys it is important that the measurement plan should aim to reflect the whole domain. If not all roads or areas in a city can be accessed this is even more important as a sampling bias can limit the ability to upscale the results from the survey.
- Ensure that the measurements are not contaminated by the vehicle.
- As many instruments provide continuous observations a precise determination of the residence time of the gas in the inlet and the response time of the instrument is critical.
- For urban GHG surveys the most relevant quantity is the local GHG enhancement. To properly determine this quantity frequent measurements are required (multiple times per minute) as well as the use of stable instruments. Ideally, the short-term and long-term repeatability of the instrument used should allow a signal to noise ratio of better than about 20.
- Geolocation information is vital and should be recorded on the exact same time stamp as the GHG data.

Ongoing Research

- IG^{3}IS should consult with other groups conducting urban methane surveys to continuously improve these recommendations.
- Further investigation of the (empirical) relationship proposed between emission rate of a GHG source and the observed GHG enhancements in different conditions is needed.
- The usefulness of mobile weather stations in urban survey studies should be further investigated.

See also Annex B.d.

4.5 In situ airborne GHG mole fraction observations

For urban monitoring of GHGs, airborne platforms provide a unique way of making in situ vertical profile measurements and surveying the entire urban area for quantification of surface fluxes, e.g. using a mass balance approach (Section 4.6) or inversion technique (Section 5). The mobile platform includes aircraft, unmanned aerial vehicles (UAVs), helicopters, zeppelins, balloons, etc. Besides GHGs, airborne platforms also provide collocated meteorological measurements, other trace gases, and aerosols.

Considerations

- Make continuous measurements of CO_2, CH_4, N_2O and other useful tracers such as CO, C_2H_6, NO_2, H_2O (or RH, T, P), wind speed and wind direction.
- Flask sampling for offline analysis can provide complementary data, e.g. $^{14}CO_2$, ^{13}C and ^{2}H in CH_4.
- Background observations shall be carefully measured (see details in Section 4.12 Choice of background).
- Make use of the synergy with commercial airliner greenhouse gas measurement programs.
- The stability or accuracy of GHGs mole fraction measurements is more important than the short-term precision, and measurements should be compatible or traceable to the WMO scales.
- Besides the accuracy of GHGs mole fractions, attention should also be paid to the accuracy of altitude measurements, especially for small UAVs.

Ongoing Research

- We encourage the development and validation of simultaneous wind speed and direction measurements.
- We encourage the development of quantification techniques using UAVs, e.g. by performing tracer release experiments or comparisons with other methods such as the tracer ratio method, the mobile van method, the integrated open path method.

See also Section 4.6. and Annex B.e.

4.6 Mass Balance Analysis

The mass balance method is a conceptually simple approach that does not rely on numerical transport modelling or sophisticated statistical methods. Greenhouse gas emission estimates have been made for many cities across the world using an aircraft mass balance approach based on the principle of conservation of mass.

Considerations

- Measurements of mole fraction, temperature, pressure and wind covering the spatial extent of the urban emission plume (in both the horizontal and vertical dimensions) are required.
- Ideally both vertical and horizontal structure of the plume are resolved by multiple horizontal transects. In some cases it can be assumed that the convective boundary layer is well mixed in the vertical, simplifying the calculation.
- Convective boundary layer height must be determined.
- Background mole fraction estimates are typically from downwind of the city either side of the plume (see also Section 4.5). Upwind transects can also be used as background.
- Suitable flight days will have steady-state winds with minimal vertical shear.
- These measurements represent a snapshot in time, and the source region may be difficult to identify.

Ongoing Research

- To calculate the urban emission rate, it is necessary to measure a background mole fraction, representing what would have been measured downwind of the city in the absence of urban emissions. This quantity is often hard to measure, as emissions from outside the urban area can have different impacts on the background measurements and the in-plume measurements.
- The best way to attribute the calculated emission rate from the mass balance approach to a specific surface area has not yet been resolved.
- The mass conservation equation is usually simplified by assuming steady-state winds. At the spatial and temporal scales typical of advection across urban areas, this assumption is often violated. Numerical weather prediction model data or ancillary meteorological measurements can be used to assess the validity of this assumption, and in some cases to correct for temporal and spatial variability in the wind field.
- Like other methods based on aircraft sampling, emission rates calculated using the mass balance method represent snapshots in time. Multiple flights across different months and days of the week will be necessary to estimate annual emissions. The meteorological conditions required to calculate emission rates using this method typically occur during afternoon hours, making it difficult to capture diurnal patterns in emission rates.

See also Annex B.f.

4.7 Discrete flask sampling

Flasks are widely used for discrete greenhouse gas and associated tracer measurements. The first objective is to obtain higher precision than might be possible from current in situ sampling systems and provide a way to routinely intercompare multiple in situ sampling systems. Flask samples provide the ability to measure numerous species from the same discrete atmospheric sample, and to use a single instrument to measure a species at multiple sites. Finally, flasks give capability to measure species that are currently impossible using any other method, namely radiocarbon in CO_2 ($^{14}CO_2$). Careful consideration of several factors must be done to ensure the flask sampling method or the materials of the flasks themselves do not corrupt the sample during collection, transport, storage, and analysis.

Considerations

- Inlets co-located with in situ systems are recommended to allow direct comparison.
- Use of an integrating volume to collect ~hourly samples is recommended for urban flask samples to obtain more representative samples with less influence from short-term local sources.
- Species that may be measured include CO_2, CO, CH_4 (for comparison with in situ measurements), CO, COS, N_2O, hydrocarbons, and halocarbons, radiocarbon (^{14}C) in CO_2 and/or CH_4, stable isotopes in CO_2, CH_4, and many other species.
- Reactive species are often not readily measured from this type of system.
- Sampling systems must consider possible contaminants for each species being measured, along with leakage and alteration during storage. It may be possible to remove such contaminants prior to flask filling.
- Glass flasks are most commonly used for GHG measurements, but stainless steel canisters and bags can be appropriate for some species. Some species can be contaminated, or mole fractions altered by the storage medium.
- Some species are vulnerable to contamination from components of the filling system (inlet lines, valves, o-rings, vacuum grease, etc.).
- Water is the most common contaminant, with varying effects dependent on species, the flask type and the pressure. Drying prior to flask filling is recommended in most instances.
- Conditional sampling based on wind direction or other factors can be useful to ensure that every collected flask is worthwhile. However, any biases induced by conditional sampling must be considered.
- The amount of air collected should factor in the air volume and pressure requirements of each analysis.
- Replicate samples are recommended for QA/QC where practical.

Ongoing Research

- There is ongoing development of air collection systems, particularly associated with airborne sampling where weight and space for flasks is challenging, and for species which require larger volumes of air for analysis.
- Additional species are continually being added to the analysis list, so careful characterization of the measurement method and its uncertainty, and any biases or contamination introduced by the sampling and measurement method are being routinely developed.

See also Annex B.g.

4.8 Isotope, correlate tracer and tracer ratio analysis

Isotopes have long been used to partition trace gas sources and sinks, taking advantage of the different isotopic signatures of the various sources and the fractionation factors of the sinks. Correlate tracers are tracers that are co-emitted with the greenhouse gas of interest, or whose emissions are co-located, thus allowing these gases to be used as proxies for the greenhouse gas source type of interest. Quantitative estimates of GHG source and sink contributions can be drawn from observed changes in atmospheric isotopic composition or the surplus of the correlate tracers using appropriate modelling approaches.

Considerations

- $^{14}CO_2$ measurements can be used to determine recently added fossil fuel CO_2 (CO_2ff). Requires both background and urban $\Delta^{14}CO_2$ measurements, and either background or urban CO_2 mole fraction. Other CO_2 contributions (typically net biogenic) can also be obtained by comparing CO_2ff with the CO_2 enhancement.
- Similarly, the contributions of fossil and biogenic CH_4 sources can be separated using $^{14}CH_4$. Background and urban $^{14}CH_4$ content and CH_4 mole fraction observations are required.
- $\delta^{13}C$ can be used in some cases to further partition CO_2ff into petroleum, coal and natural gas sources. Requires that biogenic CO_2 $\delta^{13}C$ is well constrained.
- CH_4 fluxes can be partitioned using $\delta^{13}C$ and $\delta^{2}H$ or correlate species (e.g. ethane).
- CO is used as a correlate tracer for CO_2ff. The CO:CO_2ff emission ratio is typically determined empirically from $^{14}CO_2$ and CO observations and applied to high temporal resolution CO measurements. Non-fossil CO sources must be considered.
- When emissions of one species are well known, emissions of a second species can be estimated from the observed mole fraction ratio, assuming that the emission ratio is conserved in the atmosphere. This method avoids explicit transport modelling, but implicitly assumes that the spatial and temporal source distributions of both tracers are comparable, e.g. with regard to point and area sources.

Ongoing Research

- Carbonyl sulfide (COS) may be used to diagnose photosynthetic uptake, but the methodology for urban areas is not yet well developed.
- CO is the most widely used correlate tracer, but many questions remain regarding the best uses of CO and the potential for biases from non-fossil sources and sinks as well as the spatial and temporal variability of the CO:CO_2ff emission ratio.
- Other correlate tracers (NOx, volatile organic compounds (VOC), halocarbons) are the subject of current research but not yet well developed. Some tracers may relate to a specific CO_2ff emission sector or sectors, allowing further partitioning of emissions. Chemically reactive correlate tracers face the fundamental challenge that the shorter their atmospheric lifetime, the better the relevant air chemical processes must be described in order to draw quantitative conclusions.
- The use of APO (atmospheric potential oxygen) as a direct tracer for CO_2ff contributions is currently under active development. The detection principle is based on the different carbon to oxygen stoichiometry of fossil fuels compared to biological processes or fuels.
- Other methods for diagnosing the CO_2ff fraction of CO_2 are being developed, including atmospheric oxygen and clumped isotope techniques.

See also Annex B.h.

4.9 Eddy covariance flux observations

The Eddy Covariance (EC) technique measures the exchange of any scalar entity, including greenhouse gases (GHG) between the urban surface and the atmosphere at high temporal resolution (e.g. half-hourly). It is the only method by which local net fluxes are inferred directly from measurements at single locations. The footprint (monitored source area) of the measurements is variable and depends on the measurement height, atmospheric conditions and wind direction. It typically extends hundreds of meters around the measurement site. Eddy Covariance can be used to measure GHG fluxes to be analysed in relation to emission control strategies (e.g. vehicular traffic limitations, house heating strategies, etc.), to infer integral emission factors and integral emission signatures for an entire urban area, or to assess the role of urban vegetation in the carbon balance of cities. The method provides unique information in terms of temporal resolution and integration of emission sources (e.g. traffic, building emissions, human metabolism, etc.) and sinks (e.g. vegetation uptake). The flux measurements are in situ, non-intrusive, quasi-instantaneous and with proper selection of the footprint can represent a large upwind extent similar to the size of a complete urban neighbourhood (i.e. a few square kilometres). However, its application is challenging, but not impossible due to the heterogeneity of the urban surface in terms of land use, roughness elements (buildings and trees) and mix of emission sources and sinks in comparison to more uniform natural ecosystems.

Considerations

- The measurement system requires an ultrasonic 3D anemometer and a fast gas analyser that must be synchronized. Data are in general collected at high frequency (10–20 Hz) to capture the smaller eddies that contribute to the turbulent mixing of the GHG.
- The EC system should ideally be placed high enough to avoid influence of local emission sources and flow interference from nearby buildings. The optimal height is above the roughness sublayer which is typically 2–5 times the mean surrounding.
- An urban EC system must be placed in an area with roughly uniform landscape with buildings of similar height, and emission sources and sinks in all directions.
- Measurement site will depend on research objectives.
- The method is based on turbulence. In case of low turbulence (e.g. calm periods at night), the fluxes at the surface can be decoupled from the overlying atmosphere.

Ongoing Research

- Partitioning fluxes into source emission sectors is not straight forward and no standard method exists.
- Urban storage and advection fluxes are not usually estimated. Further work is required to develop methods to estimate these terms.
- It is required to assess the applicability of current data quality control procedures and flux footprint models for urban environments and harmonize their application.
- EC flux observations in cities may not always satisfy all the underlying assumptions for their application. There is a need to investigate the impact on uncertainties and biases in derived flux estimates.

See also Annex B.i.

4.10 Ground-based remote sensing for urban monitoring

In order to quantify the GHG emissions of large area sources such as cities, ground-based remote sensing approaches that determine column average dry air mole fractions are of growing interest. In comparison to the state of the art in situ measurements, they are less influenced by the variation of the planetary boundary layer height and nearby point sources. Furthermore, they are more compatible with the scale of atmospheric models and remote sensing data collected by space missions.

Considerations

- The current recommended instrument choice is a low-resolution (in the range of ~ 0.2 to 1 cm^{-1}) compact robust FTIR spectrometer performing solar absorption measurements in the near infrared spectral region (the same spectral region used by Total Carbon Column Observing Network (TCCON)).
- The FTIR spectrometer should record DC-coupled interferograms for allowing the compensation of variable atmospheric transmission during recording.
- Recording of double-sided interferograms should be regarded as a requirement. The photometric accuracy of the resulting spectra then is significantly higher.
- For the purpose of source attribution, it is desirable that the device also records XCO.
- The spectrometer needs to be equipped with an actively controlled solar tracker for ensuring proper line-of-sight control.
- The spectrometer requires a shelter and additional software solutions achieving autonomous and permanent operation.
- It is preferable to set up these instruments on rooftops or open areas to minimize shading by obstacles throughout the day and seasons.
- For the network configuration, at least a pair of spectrometers is required with a focus on mole fraction enhancements (upwind to downwind difference). An array (e.g. five units) emphasizing the peripheral line of the region of interest is the preferred configuration as it results in a better sampling. For hilly and coastal cities, specific configurations might result.
- Retrieval algorithms can be used to translate observations to mole fraction values that are intercomparable within different groups and study regions.
- The derivation of mole fraction values from spectral observations requires knowledge of the ground pressure, so at least one accurate ground pressure record in the centre of the region of interest needs to be available (accuracy < 0.1 hPa) and the altitude of all spectrometers must be known (knowledge better than 1 m).
- A centralized facility is desirable: it tests new units before deployment, develops procedures for and supports performance checks on-site, and covers the calibration between different city observatories and with respect to TCCON.

Ongoing Research

- Modelling framework has been currently developed to use the column measurements for assessing city emissions. The city column measurements have been used to not only validate the absolute mole fractions measured by the satellites but also the urban-rural gradients.

See also Annex B.j.

4.11 Dense networks

Dense networks are an approach to urban GHG emissions assessment that relies on large numbers of sensors, each with a small, locally dominated, footprint of two-five kilometres diameter that overlaps with the footprint of adjacent observing stations. In principle, such networks could use any instruments, however, in practice low-cost sensors make the idea attractive. The conceptual advantages of the approach include 1) much lower capital investments than some of the alternatives, 2) the small footprint of each sensor allows for more direct attribution to individual source types, 3) addition of low-cost air quality observations can enhance attribution to sectors for an incremental additional cost that is a small percentage of overall capital cost and 4) there is a square root N advantage in signal to noise of some analyses. Within the mix of approaches described in this document, dense networks are a newer idea, one that is not as extensively vetted as the others.

There is also growing interest in mapping experiments that rely on instrumented vehicles including cars and trucks whose path can be user defined or public transit that repeatedly samples the same route through a city (See Section 4.4). These have some parallel benefits to dense networks in that they can map the city emissions with many small footprints at an affordable price point.

Considerations

- Locations should generally follow the guidelines for tower and elevated site measurements, but the denser network means more variety of sites is possible.
- Sensors may be placed close to particular sources, with care taken to interpret the results accordingly.
- Accuracy, precision, calibration and intercomparibility can be challenging with lower cost sensors but remain critical.

Ongoing Research

- Calibration and intercomparibility remain challenging.
- Dense networks for GHG measurement are still under development and consensus on the types and quality required has not yet been reached.
- Dense networks with sensors close to individual sources require different interpretation than tower and elevated site networks.
- The optimal spatial density of instruments has not yet been established, and in any case will be dependent on the desired outcomes, data analysis and modelling methods to be employed, and the particular city geography and meteorology.
- Examples show that emissions can be retrieved to 10% accuracy with a few months of data. Ongoing research to show that dense networks can measure annual trends of 3%–5% per year will be needed to fully assess the promise of this approach.

See also Annex B.k.

4.12 Choice of background

Analysis of urban area greenhouse gas (GHG) concentration (or mole fraction) data for the purpose of estimating emissions requires isolating the portion of the observed mole fraction that is attributed to emissions from the domain of interest. Here we refer to the portion not attributable to emissions within the domain as "background". For urban analyses, the domain of interest is often small compared with the domains of regional or continental analyses, complicating the choice of background. Air masses entering an urban area are influenced by emissions (and depletions) upwind that occurred in the recent past, and upwind terrestrial and anthropogenic fluxes of both carbon dioxide (CO_2) and methane (CH_4) can be quite large and heterogeneous. Thus, unlike background conditions for global or continental analyses, the incoming air mole fraction can have significant variability both in space and time. Each urban research project must determine the level of variability to be expected, and if a background analysis method is chosen should take steps to evaluate that background as much as possible. Evaluation of background mole fraction and variability not only aids in the selection of the best possible background for the application at hand, but it also helps quantify uncertainties that should be propagated to the analysis.

The choice of background can be the largest contributor to uncertainty in urban studies, especially in metropolitan areas with smaller enhancements.

Considerations

- Towers and other elevated sites typically use a similar site upwind of the city as background. Data may be sampled at the same time as the observations inside the urban area or may use a more sophisticated backward trajectory method to determine the upwind sampling time.
- "Clean air" stations may be used as background. These may be filtered or smoothed to achieve background conditions and remove synoptic pollution events.
- Lowest percentile data for a given day or days can be used, but this method can yield incorrect values depending on the goal of the study, so care should be taken to validate them.
- Background stations should be located so that they are well exposed to regional atmospheric flow, and not contaminated by local anthropogenic emissions, as much as possible.
- Alternatives to using upwind measurements for in situ enhancement analyses include solving for the boundary condition within an inversion or nesting the urban domain inside a large global model in order to propagate the background into the domain.

Ongoing Research

- Caution must be exercised when using upwind or rural stations to define a background, no matter which of the above methods are employed. For CO_2 in the summer, for example, strong local biospheric fluxes near the rural station may bias the background time series. Thus, additional understanding of the biosphere in the rural area surrounding the upwind or background measurement sites may be required.
- It may be necessary to select or filter data according to wind speed and wind direction relative to the upwind site in analysis.
- Complex meteorology (e.g. recirculation, land-sea breeze) also complicates the choice of background, so additional considerations for data filtering and upwind station choice are required.

See also Annex B.I.

4.13 Meteorological observations for urban greenhouse gas analysis

Meteorological measurements are essential for improving the accuracy and precision of GHG emissions inferred from atmospheric GHG observations. Meteorological parameters like wind speed and direction are often concurrently measured with greenhouse gases for the purpose of filtering and interpreting GHG data for different atmospheric conditions. Regional backgrounds needed to quantify local excess GHG mole fractions may strongly depend on the meteorological conditions (wind speed, direction, mixing height). Methods such as mass balance used to estimate GHG fluxes from source regions also require knowledge of wind speed, direction and mixing height. Atmospheric models used for inverse modelling of GHG emissions either assimilate meteorological observations to improve model performance or use the meteorological observations to independently evaluate model performance.

The WMO Guide to Meteorological Instruments and Methods of Observations provide information about different instruments for measuring various meteorological parameters and should be followed.

Considerations

- Urban ABL wind speed and direction, and mixing height are the main measurements that can constraint atmospheric transport errors in inverse modelling of GHG fluxes.
- We recommend urban ABL measurements both inside and downwind of the city, since ABL height can vary, as well as capturing the full diurnal cycle.
- Measurements of the ABL depth, wind speed and wind direction in the upwind environment, paired with the same urban measurements, enable this to be examined as a source of bias in the urban meteorological simulation.

Ongoing Research

- More exchange with the WMO/GAW Urban Research Meteorology and Environment (GURME) initiative on urban meteorological information and air quality
- Incorporation of information on urban heat island and surface roughness in urban GHG analysis.

See also Annex B.m.

4.14 Satellite Remote Sensing of XCO_2

Space-based estimates of the column-averaged dry air mole fraction of CO_2 (XCO_2) complement ground-based and aircraft measurements with much greater spatial resolution and coverage. XCO_2 estimates can be analysed with mass balance or plume models or with more sophisticated Lagrangian particle dispersion models (LPDMs) to estimate urban CO_2 fluxes. It is challenging to detect urban emission plumes in the atmospheric signal of CO_2 given the fundamental linkage of atmospheric CO_2 with biospheric sources, the large background CO_2 mole fraction, and influences from other processes such as atmospheric transport.

Considerations

- A number of ongoing satellite missions that observe greenhouse gases may be useful, each with its own suite of specific species measured, varying instantaneous fields of view, and revisit times.
- Satellite retrievals are prone to cloud and aerosol contamination, which results in limited data availability, and the swath width may also limit detection of specific sources.
- To isolate the local effect of anthropogenic emissions at the urban scale, it is necessary to remove the biospheric and background portion of the atmospheric signal, which are large relative to the anthropogenic signal. To date this has been done by comparing with nearby “clean” observations, or daily median values from the selected study region.
- Using a synergy of multiple satellites and including correlate tracers (like NO2 and CO) can help to disentangle anthropogenic and natural sources.

Ongoing Research

- Better quantification of greenhouse gas and pollutant co-emission patterns and characteristics would help disentangle CO_2 sources.
- Future missions are being designed to allow for better coverage and more sampling over urban areas.
- Models using space-based measurements can be used to estimate CO_2 fluxes, but further development of models and satellite constellations are needed for precise observations to reduce errors and uncertainties.

See also Annex B.n

4.15 Airborne atmospheric remote sensing of GHGs

For urban monitoring of GHGs, the quickly evolving technique of airborne atmospheric remote sensing – either passive using spectrometers, or active using LIDAR technologies – provides a unique way of making measurements of the spatial distribution of atmospheric column average dry air mole fraction below the aircraft during single overflights. These methods allow surveying of an entire urban area to quantify surface fluxes, e.g. using a mass balance approach (Section 4.6) or inverse studies (Section 5). In addition, using imaging sensors to localize strong emitting sources in urban areas is feasible. In comparison to the state of the art in situ measurements, airborne remote sensors are less influenced by the variation of the planetary boundary layer height and allow imaging of point sources. Furthermore, they are more compatible with remote sensing data collected by space missions and ground-based remote sensing (see Section 4.10). Lidars are intrinsically independent from sunlight and thus can measure at night and below clouds. They are considered less prone to aerosol interference, not to be neglected in urban environments.

Considerations

- Make measurements of CO_2 and CH_4 in combination with useful tracers such as CO, NO_2, H_2O, wind speed and wind direction.
- When combined with in situ sampled (airborne and ground) mole fraction observations, total area fluxes and emissions from strong individual sources within that area can be derived.
- Background mole fractions must be carefully measured (Section 4.12).
- When evaluating point sources, the relative error of GHG column measurements with respect to the background mole fraction (gradients) is more important than absolute accuracy of the column measurement.
- For larger scale applications (urban agglomerations and beyond) the accuracy of the GHG column measurement also becomes important. Measurements should be compatible or traceable to the WMO scales.

Ongoing Research

- We encourage the validation of flux estimates using airborne remote sensed column mole fractions by in situ mole fraction and simultaneous wind speed and direction measurements.
- We encourage the development of quantification techniques using various airborne platforms, by performing tracer release experiments or comparisons with other methods.
- We encourage the combined use of active and passive remote sensing techniques onboard aircraft.
- We encourage attempts to provide profile data using differential absorption lidar (see also Section 4.3).

5. Data Assimilation Systems

Data assimilation systems (DAS) are a broad class of methods that are used to combine multiple streams of data/observations to estimate possible states of a system as it evolves over time. At the very general view, data assimilation can provide a range of possible states and the probabilities they represent. A state could represent any type of variable, temperature, pressure, GHG emissions, etc. Data assimilation systems are applied in a vast number of fields. For example, meteorological numerical models have been successfully assimilating large amounts of data for decades to predict weather and climate.

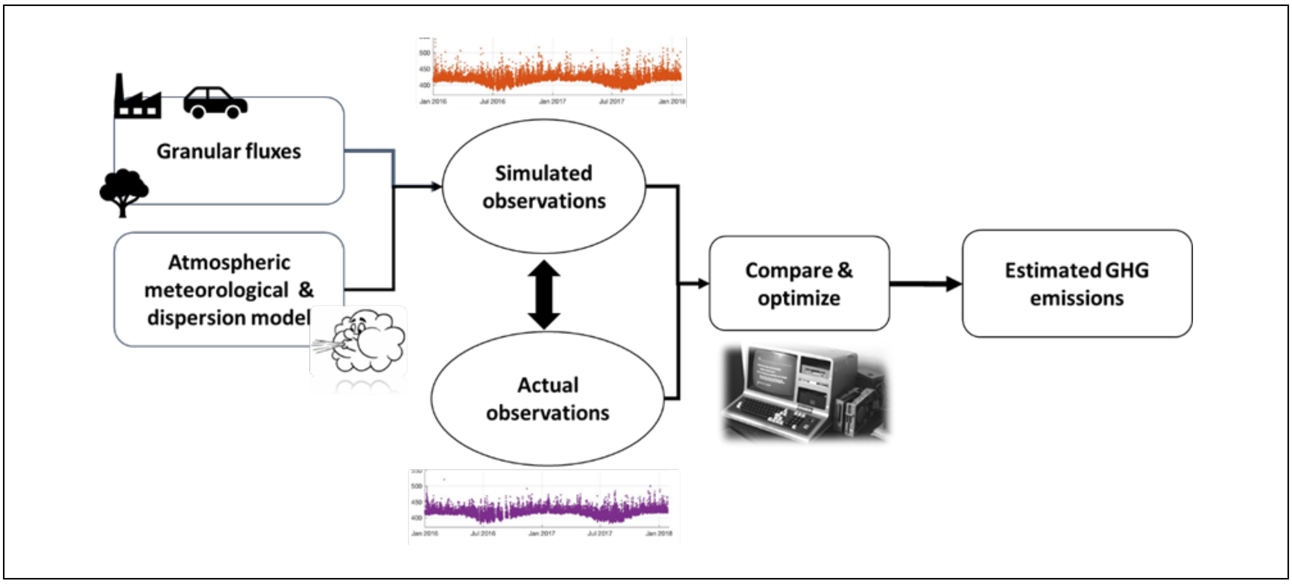

Figure 3: DAS/AIM: Conceptual diagram of a combined data assimilation and atmospheric inversion modelling framework.

Data assimilation can have many names, depending on the field of application, and take different forms. Atmospheric inverse models (AIM) are a type of data assimilation system. AIMs are applied to extract the maximum information from observations, meteorological/dispersion models, and prior information, e.g. to estimate greenhouse gas (GHG) emissions. The combination of data and models is needed for a variety of reasons. Atmospheric GHG observations are usually sparse, not made on a grid, and measured at different times. They measure abundance and therefore, are an indirect measurement of emission rates. Meteorological models, which account for atmospheric transport and dispersion, mathematically transform observations of GHG abundance to upwind mole fractions and/or emissions at a location in time and space. Additional prior information, such as granular emission information is assimilated to help constrain estimates of emissions at fine temporal and spatial resolutions. In the literature, AIMs can take many forms from simple scaling methods to full variational systems akin to weather prediction models. The development and application of AIM depends on the types of questions that need to be answered (e.g. ascertaining trends versus specifying emissions at a particular location, etc.) along with the sensitivity of the method/emission estimates to assumptions that could lead to bias. These methods form the third tier of action for targeted mitigation (see Figure 1), requiring a suite of data streams that makes them more complex to implement, but with the potential to provide the best possible detailed emission information.

In this section, we describe various aspects of data assimilation for the goal of estimating greenhouse gas emissions and their associated uncertainties. Note that full descriptions of specific inputs, models including AIMs (which span from simple scaling approaches to full variational methods, etc.) are not provided in the text which requires practitioners to further review literature cited within the Annexes. A general concept is shown in Figure 3. The section is organized as follows:

1. **Meteorological inputs needed for urban monitoring systems**: Describes the concepts and considerations when modelling meteorology.

2. **Forward modelling**: Explains how emission information is transported (using a meteorological model) to create 4-D atmospheric GHG concentration (x, y, z, t) fields that can be sampled to create simulated observations.

3. **Calculation of atmospheric footprints needed for urban modelling**: Describes method for using an atmospheric meteorological model coupled to a particle transport model (simulating dispersion within the atmosphere) to simulate the transport of particles released at an atmospheric observation location backward in time. The resulting output provides a linear operator (link) that translates an observed abundance of GHG to an emission location. This link can be used with granular emission information to create simulated observations. Some simple AIMs simply scale simulated observations to observed mole fractions.

   Use of inverse modelling methods for urban monitoring: Outlines AIMs that use meteorology and dispersion, atmospheric observations, granular emission information in an optimization method to estimate emission and associated uncertainties. AIMs cover many types of optimization methods. This section is a broadly describes AIMs in general. The AIMs that fall under this section include traditional Bayesian, geostatistical Bayesian, and 4-D Var approaches.

5.1. Meteorological inputs needed for urban monitoring systems

All urban greenhouse gas (GHG) monitoring systems rely on meteorological inputs. In general, advection (by wind fields resolved by the model) drives the transport while the turbulence (by generally unresolved/parameterized turbulent velocities, represented as needed for each model type) drives the mixing. Thus, an effort must be made to ensure that winds, mixing depth, and velocity variances are as accurately reproduced throughout the boundary layer as possible.

This is important for both the urban environment and rural areas surrounding it. The residence time of air over any urban environment is limited, and biases in the air inflow to the urban area may persist throughout the entire urban domain. The accuracy and uncertainty of the meteorological fields are assessed using a variety of techniques. Any model performance assessment should be in line with the specific application to quantify urban emissions.

Considerations

- Define a horizontal resolution relevant to the target problem size and terrain complexity. Depending on the application and feasibility, finer resolution models are preferred up to the limit that the physics approximations intrinsic to the parameterizations adopted in the model hold. Nested domains or adaptive grid solutions may be considered.
- The vertical resolution should be fine enough to resolve the vertical development of the Planetary Boundary Layer (PBL) over time and to resolve vertical gradients in GHGs corresponding with the atmospheric GHG measurements used within the AIM.
- The size of the domain should also be in accordance with the target problem domain. In general, the area for which emissions are to be estimated should be far enough from the domain's edges to avoid boundary effects and allow for some spatial spin up of the simulation so that numerical anomalies are minimized.
- If "off-the-shelf" meteorological products are used, preference should be given to well known products generated by national or international agencies or other certifiable sources, like the NOAA-NWS, ECMWF, or similar.
- Reanalysis, analysis and forecast products should be considered in that order.
- For city scale modelling, finer horizontal, vertical and temporal resolutions might be needed. Specifically, if GHG measurements are within urban canyons and/or within building wakes, much higher fidelity modelling including large eddy simulations may be needed.
- Mesoscale models should not be used on grid spacings less than ~1 km without careful consideration of "grey zone" issues.
- In all cases, evaluation against independent observations of the most important variables affecting tracer transport (e.g. wind direction, wind speed, mixing depth and turbulence) should be used – if available.
- It is desirable to use at least two meteorological models to evaluate the impact of the choice of atmospheric transport on inferred emissions. If possible given resources, an ensemble of transport models should be used to help quantify transport model uncertainties.

Ongoing Research

- Evaluation and resolution of biases in meteorological models that are pertinent to atmospheric composition studies.

See also Annex C.a.

5.2. Forward modelling

Atmospheric modelling of GHGs in forward mode remains common practice at global scale. At regional and urban scales, backward in time simulations (e.g. using Lagrangian particle dispersion modelling) become more computationally efficient. Despite the computational disadvantage, forward models remain a valuable tool when interpreting complex observations at regional scale. For point sources or whole-city emissions, forward simulations produce the link between mole fractions and sources, and they are also a means to evaluate transport model errors. Forward modelling provides information for unobserved areas and offers more flexibility in observing systems by simulating the whole spatio-temporal dimensions of the concentration space. However, accurately representing the atmospheric transport of passive tracers requires careful consideration of the model configuration and its numerical schemes.

Considerations

- Conservation of mass remains the foremost challenge in modelling systems. Relatively small imbalanced terms can generate large losses/gains in mass.
- All Eulerian models are subject to numerical diffusion. It is impossible for a model to resolve concentrated plumes that exist at finer horizontal and vertical resolutions than those of the model unless one transports higher-order moments of the sub-grid tracer distribution. In practice, this is rarely done due to computational cost.
- Continuous injection of mass fluxes into the atmosphere guarantees the fair representation of plume structures. The injection height for point sources should also be considered.
- Conservation of GHG mass/concentration at the boundaries (e.g. global to regional scale) of any bounded simulation domain involves different horizontal resolutions, hence different surface pressures that makes it nearly impossible to reconcile mass and mole fraction over the column. Depending on the observing systems either: conserve the total mass coming from outside the domain (path-integrated), or modify the mass but conserve the mole fraction (in situ).
- Spin up time ensures that the modelling system is theoretically at equilibrium.
- Convection schemes, which involve multiple phases being constantly adjusted within clouds, can pose major challenges to accurately dry air masses when calculating mixing ratios.
- For online forward models, regional models tend to deviate from the meteorological analysis. It is highly recommended to re-start simulations on a regular basis (i.e. every week at most).
- Beware of inconsistencies between meteorological parameters and regional transport models.

Ongoing Research

- Global simulations with adaptive mesh models to simulate parts of the globe at higher resolution.
- Online adjoint modelling at regional scales able to invert for surface and boundary fluxes.
- Convection and advection schemes including accurate representation of vertical transport, aerosol interactions, and mass balance conservation.
- Near-surface mole fractions remain challenging as the surface is often poorly represented and the vertical resolution is too coarse compared to existing structures on the ground.

See also Annex C.b.

5.3. Calculation of atmospheric footprints needed for urban modelling

The use of GHG measurements to provide quantitative information about GHG emissions requires knowledge about the sensitivity of the receptor observation to a particular source area. The “footprint” or the “source-receptor relation” is the amount of change in GHG mole fraction at the receptor, given a unit emission at a source area. The transported quantity in the models is often a conserved one, such as mixing ratio (sinks and sources are explicitly represented). The footprint is the quantitative information used to construct the Jacobian matrix in inverse analysis (Section 5.4). Atmospheric transport within the PBL is strongly dominated by turbulence and turbulent dispersion. The stochastic nature of turbulence means that the path between the source and the receptor can never be defined by a single air parcel trajectory. Instead, the transport is more closely approximated by an ensemble of air parcels, each of which traces a stochastic trajectory incorporating the random nature of turbulent eddies. Models which adopt the stochastic, ensemble trajectory approach are referred to as LPDM.

Considerations

- Footprints can be constructed forward or backward in time depending on the number of sources vs receptors. Urban applications typically use backward footprints.
- Footprints are often the input into inverse analysis systems but can also be used in a simple scaling method to evaluate emissions from observations and are useful as a stand-alone product for tracer ratio evaluations (Section 4.8).
- Discrepancies between time-forward versus time-backward simulations have been used to reveal internal inconsistencies and violations of physical principles within the model. LPDMs should also be evaluated against real-world atmospheric dispersion.
- Tiers of footprint information:
  - No footprint generation, per se. Atmospheric transport information is instead gleaned from simple wind rose analyses or single backward trajectories originating from the receptor that only accounts for mean winds (no turbulence).
  - Footprint generated using LPDMs.
  - Footprint generated using LPDMs, as well as an assessment of transport errors in both the meteorological fields using meteorological observations and the atmospheric dispersion using tracer release data.
  - Footprint generated using LPDMs, combined with an assessment of transport errors within an inverse analysis system.

See also Annex C.c.

5.4. Inverse modelling methods for urban monitoring

The use of inverse modelling methods as a tool for estimating surface fluxes of atmospheric trace gases has become increasingly common to quantify urban, metropolitan, and regional emissions. Inverse methods attempt to deconvolute the effects of atmospheric transport and recover source emissions based on atmospheric measurements (e.g. GHG mole fractions from an in situ site or satellite retrievals). Since inverse models are ill-posed (many possible solutions) and under-determined (observations are limited in spatial coverage/quality compared to the number of emission estimates), additional/prior information is generally needed to guide the inversion to a set of plausible emissions. Prior knowledge refers to something that is reasonably well known about emissions (e.g. available emission information derived from statistical information, emission uncertainties, or even the sign of the emissions). An inversion model aims to achieve the best statistical (optimal) compromise between the various information pieces, such as observations, priors, and meteorological inputs.

Considerations

- Determine which target variables are required, e.g. total, sectoral emissions, etc.
- Determine the atmospheric model appropriate for the inverse model application including resolution in space and time, other input variables.
- Data selection must be considered, and choices should be made as appropriate for the application (e.g. wind direction, local time daily periods, outlier detection).
- Ensure that the inversion model is appropriately linear.
- Consider the errors associated with atmospheric GHG observations, atmospheric transport, and any prior emission information especially if it is likely that the errors for any of these components are correlated (highly plausible at finer resolutions.). All errors must be appropriately accounted for in the inversion model.
- Consider any suspected biases in the inversion system. Biases in the prior may not be a problem but will still distort the emission estimates. “Large” model or observational biases may dominate the inversions if not corrected.
- Consider how the inversion is solved and if additional statistical assumptions are needed.
- Attempt to use any independent data for evaluation.
- All elements of an inverse model should be made explicit within the appropriate mathematical framework. For this reason, a Bayesian framework should be favoured over other methods such as artificial intelligence.
- The inversion data provider should also communicate about the following diagnostics: (1) the underlying cost function, (2) the gradient of the cost function, (3) realism of ALL optimized variables, (4) uncertainty estimates for all optimized variables, (5) statistical consistency between the various internal elements (e.g. chi-squares), (6) statistical consistency when comparing with external information.

Ongoing Research

- Transparency, such as availability of the full model, the inversion system and the observations are desired but is more likely a long-term goal.

See also Annex C.d.

6. Data Management, Archiving and Distribution

Urban greenhouse gas and ancillary data should follow 'FAIR' data principles, meaning they should be Findable, Accessible, Interoperable, and Reusable/Reproducible. A key component of creating data sets that follow FAIR principles is utilizing the Climate and Forecast (CF) conventions for data and metadata (http://cfconventions.org/).

Considerations

- Findable data sets. A globally unique and persistent identifier such as a Handle PID or Digital Object Identifier (https://www.doi.org/).
- Accessible data. Data and metadata should be accessible in open data formats such as NetCDF (https://www.unidata.ucar.edu/software/netcdf/), HDF5 (https://www.hdfgroup.org/) or plain text.
- Interoperable data. Data and metadata should follow CF naming conventions for the description of the measured variables.
- Reusable/reproducible data. Methods to produce data should be well documented so that results or products can be reproduced by others.

Ongoing Research

- Expanding new and existing urban data set repositories to include additional cities and data streams (e.g. flask data).

See also Annex D.

7. References

Crotwell A.M., Lee H., Steinbacher M. (2020) *20th WMO/IAEA Meeting on Carbon Dioxide, Other Greenhouse Gases and Related Measurement Techniques (GGMT-2019)*, (WMO-GAW Report No. 255).

DeCola P.L., Tarasova O., Brunner D. et al. (2018) An Integrated Global Greenhouse Gas Information System (IG^3IS) Science Implementation Plan.

Fong W.K., Sotos M., Doust M. et al. (2014) Global Protocol for Community-Scale Greenhouse Gas Emission Inventories: An Accounting and Reporting Standard for Cities, World Resources Institute, C40 Cities, ICLEI.

Annexes to the IG^{3}IS Urban Greenhouse Gas Emission Observation and Monitoring Guidelines for Good Research Practices

These Annexes provide expanded information on methodologies and techniques that will be useful to practitioners applying these methods. Readers should refer to the main document for summary information and to these Annexes for more detailed information. These Annexes are divided into four groups. Annex A provides detailed information on the construction of urban inventory and flux models. Annex B describes atmospheric observational techniques and the direct methods for interpretation of these observations. More elaborate data assimilation systems for evaluating emissions from bottom-up and observational information are detailed in Annex C. Finally, Annex D addresses data management and distribution.

Annex A. Urban Inventory and Flux Models

A.a. Fossil fuel CO_2 emission data products

Kevin R Gurney[1]

[1]Northern Arizona University, Flagstaff, Arizona, USA

A.a.1. Introduction

Often referred to as "bottom-up" approaches or "emission models" they increasingly include a wide variety of techniques that attempt to estimate fossil fuel CO_2 (CO_2ff) fluxes in ways independent of the use of atmospheric mixing ratios. They generally include approaches such as, activity x emission factor, fuel consumption statistics, ratio to monitored air quality (AQ) species, criteria pollutant species, direct stack flux monitoring, emission models, etc. They also include use of remote sensing attributes other than a column trace gas measurement (often referred to as "top-down" approaches in some circles) - examples include use of nightlights.

There are two general aims in producing CO_2ff emission data products. The first is usable/useful to policy stakeholders (citizens, government, practitioners, businesses). We are fairly confident that policy stakeholders are interested in quantified fluxes with categorization by sector (onroad transport, residential, commercial, industrial, electricity generation, airports and air traffic, ports and shipping, rail, offroad transport) and fuel (natural gas, petroleum, coal). Emissions can be divided into three scopes. Scope 1 is emissions that physically occur within the region of interest. Scope 2 accounts for emissions that are generated elsewhere but consumed in the region of interest (e.g. electricity generation in one place but used in another), and Scope 3 is embedded emissions from the manufacturing of goods. Users are generally interested in all scopes, but the interest varies and often what is used is a mixture of scopes. Evidence for that is seen in the self-reported inventories (SRI) that many cities have made where scope 2 is typically how electricity generation is characterized and some scope 3 is included. Furthermore, existing SRIs will have gaps in scope 1 depending upon data availability and notions of responsibility because different jurisdictional levels having varying types of policy/mitigation levers. For example, airport emissions may be reduced to attempt to account for only the local population use of airport (as opposed to a larger population and/or transit passengers). Also desirable are estimates that have a clear geographic boundary – they currently build SRIs according to governance city boundaries due to political purview but "metro" or aggregate settled areas are also useful. Self-reported inventories are generally constructed at an annual resolution of interest with both a base year and a target year (assuming a target year has passed) although there is no formal standard on what constitutes a base year and whether the base year remains constant There appears to be little interest in sub-annual temporal resolution.

Recently, a few cities have started to release documentation accompanying SRIs. Our aim here is to provide clarity on methods, boundaries, and scopes. Information used currently by cities is in tabular form, normally an Excel spreadsheet that has compiled emission factors (based on national or international numbers).

Though not fully established, cities may be interested in some of the more advanced products being developed in the scientific community. Examples are more spatial granular estimates, sub-annual temporal resolution, time series of emissions that are regular or complete (as opposed to a single base year and target year), uncertainty estimations, and process/technology resolution. There may be interest in emissions information placed into formats that would integrate with city planning "toolchains". Typically, that means shapefiles (GIS) with multiple attributes relevant to planning. Shapefiles would help geolocate places that have higher emissions that could be mapped to a database with hourly emission information. Early versions of such products have revealed their usefulness as outreach tools to reach civil society as well as government entities. Finally, and perhaps most importantly, users they may be interested in knowing that estimates are consistent with atmospheric measurements. The scientific community has placed emphasis on this and with real policy and/or financial exchange, this will become critical even if the interest is limited as of now.

The second broad aim in producing CO_2ff emission data products is to incorporate them into “information systems” such as the data assimilation/inversion work, bottom-up/top-down comparisons within ongoing scientific research. This places specific demands on the way the information is produced and how the results are fashioned. The attributes can be listed as follows:

- Gridded at resolutions below atmospheric transport model resolution (so regridding does not alter spatial structure dramatically).
- Continuing sub-annual temporal resolution – hourly is preferred.
- Reflect a continuous time series as opposed to “snapshots” in time.
- Generate estimates as close to real time as possible – traditionally challenging but new work using anonymized mobility data (e.g. Google Community Mobily Reports and Apple Mobility Trends Reports) stimulated by the COVID-19 pandemic shows promise.
- Estimates can isolate scope 1 – this is what the atmosphere “sees”. Though Scope 2 and Scope 3 are useful for context, they must remain discrete from Scope 1.
- Estimates containing sector/fuel resolution in anticipation of the growing multi-tracer work which is fuel/sector-specific.
- Include uncertainty estimation. This is important for use as “prior” flux where the prior uncertainty can leverage considerable control over the outcomes of inversion/data assimilation modelling.
- Estimates are documented, peer-reviewed with transparent traceable methods. Data online in downloadable/usable form.

A.a.2. Hierarchy of products

There is a fairly rich array of inventory/data products out there that span spatial scale, domain, and methodology. Here is a breakdown of the spectrum.

A.a.2.1 Global/granular

In this category are ODIAC, FFDAS, EDGAR, CDIAC, PKU-FUEL. These are primarily starting with national accounts and performing a downscaling to the sub-country spatial scale and regularize the results into grids. In this sense they are often referred to as “top-down” – a term that, in this case, comes from econometric research. This term can be confusing because the atmospheric inverse/assimilation approaches also use the term “top-down”. As such, these types of emission products might be better referred to as global “downscaling” efforts. The proxies used to downscale vary and some are incorporating portions of bottom-up (as described in the following section) with in the estimation so are emerging as “hybrid downscaling” efforts. However, their accuracy and precision are largely dependent on the quality of the proxy data used in the downscale process. Because national “bottom-up” efforts (see next bullet) can vary widely in terms of data sources, quality and methods, these global downscaling data products are important for their consistency in space. They remain important efforts in characterizing emissions globally.

A.a.2.2 National/granular

These data products are almost entirely limited to industrial/high-income countries at this stage. Examples include Vulcan (Gurney et al., 2009), ACES (Gately and Hutyra, 2017), Poland (Bun et al., 2019), work by Ivanova et al. (2020) and a few efforts within China. These are “bottom-up” efforts primarily (though elements of downscaling occur in these methods as well) and hence, constructed from multiple datasets related to the classic “activity x emission factor” (AFxEF). However, it is important to note that the IPCC AFxEF approach is a much simplified representation of what many of these data products are doing. They will often include direct flux monitoring (e.g. CEMS at powerplants), fuel statistics, and co-pollution monitoring. These approaches are deterministically tied to emissions and hence, are not well-described by the notion of activity data. These national bottom-up efforts continue to evolve with new efforts at intercomparison (Gurney et al., 2021).

A.a.2.3 Urban/whole-city

There are many papers and project on determining whole-city emissions though they are predominantly from high-income countries. The vast majority of these are either single-city estimates or city collections (e.g. Ramaswami et al. 2008; Kennedy et al., 2009). Some extend to very large data sets such as that found in Moran et al. (2022). In addition to what can be found in the peer-reviewed literature, there are many projects with cities generating self-reported inventories. These are mostly reported in the grey literature and are difficult to trace in terms of methods, data, and uncertainty. The SRI efforts follow one of a few protocols that are out in the public domain via effort by a few NGOs. One of the challenges with using this work – either the peer-reviewed literature or the SRIS – is that they reflect an array of scope and scope mixtures in the results. Methods vary as well, although there has been some effort to harmonize methods across cities (Fong et al., 2014; Nangini et al., 2019). There is a growing literature on full scope 3 accounting but that is mostly in the peer-reviewed literature, cities generating SRIs have faced challenges in performing full scope 3 analysis due to difficulties in determining global supply chains. The scope 3 results are difficult to incorporate into atmospheric-based methods but remain important to policymakers and hence, should be considered part of a structured construction of information for cities on urban emissions. Each method uses various definition of the “city” domain as well as different definitions of sectors which can make comparisons difficult. For the works in the published literature – this is especially true which renders much of the value of these estimates for city stakeholder of little use.

A.a.2.4 Urban/granular

Sub-city granularity is less common in the literature (both peer-reviewed and grey). There are a growing number of cities for which these types of data products have been produced. Hestia is an example with results for Salt Lake City, Indianapolis, Los Angeles Megacity, Baltimore and work underway in the USA Northeast corridor which will include both Baltimore and Washington D.C. However, there are a number of additional notable efforts in Toronto, Paris, Melbourne, Tokyo, Auckland, Beijing, and Mexico City, among other cities. There are probably other cities where work is underway, but it is not reported as of yet such as Sao Paulo and Recife, Brazil.

A.a.3. Input data

The input data needed to build the granular urban data products varies widely in the practical examples available in the literature. A few common needs are clear. The following is an attempt at a fairly comprehensive list of data divided into four categories: emissions magnitude, spatial distribution, temporal distribution, and uncertainty.

A.a.3.1 Emissions magnitude

Emissions magnitude can come as a sector-specific multi-sector input data. National accounts of emissions remain important in urban assessments. They will continue to be used in urban data products in places where local data are scarce. Direct fuel consumption data are also important though rarely provided at the local scale. Hence, this information may require downscaling but remains an important check at the aggregate scale. However, local utility data may be available and is valuable. Clearly the geographic definitions, the comprehensiveness of the data, and what scope are critical to know in order to rationally use such data. Utility data in particular is generally defined in a service area which may not map to city boundaries.

- For onroad sources, traffic data are crucial and may consist of vehicle distance travelled type of data, vehicle counts at individual stations, statistics on vehicle fleet in a given geography, mobility data (such as derived from smartphone or GPS data), and congestion indices.
- For buildings and related sources, information on building infrastructure including information on the footprint or use floor area, the type of fuel used on-site, the age of the built structure. Building energy models can also provide important information assuming building envelope information is available. If building energy modelling has been performed these can be a rich source of both estimates on energy consumption and/or helpful information on key building attributes.
- Air quality data has been used in the Vulcan/Hestia system and can be useful insofar as the species considered is co-emitted with CO_2ff emissions. Carbon monoxide (CO) is the best example of this. It can be traced back to fuel with emission factors.
- The smaller transportation source sectors (airport, rail, commercial motor vehicles, non-road) often have relevant data though rarely at the local scale. Airport, commercial marine vessel, and rail activity (volume, frequency, fleet characteristics) are typically archived nationally with the air/land/sea traffic or general transportation national agency.
- Non-road is typically the most difficult sector regarding data acquisition. For this reason, it is often missing in many urban inventories. However, it can account for a non-negligible amount of emissions and should be included if possible. Often a scale factor applied to population statistics is used, but there are other indirect means to estimate non-road emissions.
- Point sources, which typically include electricity production facilities and industrial facilities have varying degrees of data availability. Typically, power production is well-tracked given the magnitude and relatively small number of sources. Many countries have example of databases with attributes that allow for characterization of emission. This is often a result of these facilities being in the public domain. Industrial facilities, by contrast, are more difficult to quantify given the paucity of data which, in turn, is often a reflection of private ownership and concerns over competition. Local air pollution, water pollution, or toxic emission databases are a potentially useful place to look for information about industrial facilities. Point sources have various degrees of errors that should be assessed, e.g. powerplants can be in the wrong location, which could impact total emissions.
- In some cases, direct stack monitoring is available (e.g. CEMS units) and this is an extremely useful source of information for emissions. Uncertainty characteristics such as bias in monitoring flow or concentration are worth examining if that data is available.
- Finally, census data offers useful proxy information that can be used to generate emissions estimates based on attributes of population and housing characteristics.

A.a.3.2 Spatial distribution of emissions

One of the advantages of the new bottom-up urban estimation methods, is the ability to place emissions in space at resolutions high enough to resolve individual buildings and street segments. Though resolution at these scales (buildings, street segments) is, thus far, not required by atmospheric inverse/assimilation systems (Section 6), space-resolved priors are a critical ingredient. Furthermore, there is often a dearth of information between the scales of province/county and building/street and hence, quantification at the finer scales is often a logical step after which aggregation can be used to best match the high-resolution inverse/assimilation modelling typical for urban domains.

Essential for all sources is correct geolocation. Often this is correcting or originating the location of emitting elements within the resolved geography considered (e.g. grid cells, points, lines, polygons).

- For point sources, there is a large amount of information within applications such as Google Earth Engine, Google mapping, ESRI database mapping and related efforts. Oftentimes, simple manual visual identification of notable facilities can correct geolocation. For example, electricity production facilities, refineries, airports, railyards, and commercial motor vehicle terminals can all be readily identified with the very high-resolution imagery found in the above applications. Though ambiguity can sometimes be present (when there are multiple facilities of the same type all proximal to the mis-located facility), even these instances can be resolved with additional information available through online address searching or ground-truthing.
- Cities often have civil bureaucracies with GIS-based information on buildings, roads and other important urban infrastructure. Planning departments and transportation authorities often archive GIS-based datasets on such infrastructure information, and these can be critical in distributing or allocating emissions at larger scales. Some of these data can come from crowd-sourced efforts such as OpenStreetMaps which is a rich archive of roads and buildings and is freely available.
- Finally, there are new sources of information being created from “big” data sources such as GPS and smartphone locations. There are numerous examples of information relevant to traffic, movement of people in relation to businesses, and crowd densities derived from these data that offer additional spatial proxy information. Comprehensiveness i.e. biased samples) and availability vary, however as well as data access.

In summary, information available to distribute emissions in space to spatial scales at the sub-city scale are primarily acting as spatial proxies when either direct information (e.g. stack flux monitoring) or deterministic spatial identification (e.g. building utility data) is lacking. As such these approaches have to be considered approximate and where possible included with uncertainty information (see below).

A.a.3.3 Temporal distribution of emissions

Temporal data is usually the most difficult to find. There are very limited sub-annual data in general. However, in order to capture important cyclic behaviour, a sample of time may be adequate (e.g. one day, one week) for understanding repeating cycles of emissions behaviour. Aside from the datasets described thus far on emissions magnitude and spatial content, which may contain sub-annual information, there are a number of proxies that can provide additional information.

- Onroad emissions are the most straightforward and traffic monitoring at sub-annual timescales is common. For onroad, it is crucial to attempt to retrieve hourly-resolved data given that morning and evening rush hours (associated with the daily commercial/business commute cycles) are often the largest temporal variation in onroad emissions. The next important cycle is weekdays, followed by months.

- For buildings, energy modelling is often helpful (e.g. eQUEST).
- Airport emissions can often be characterized in time by gathering flight times/volumes.
- Similarly with rail and shipping, commercial vehicle schedules can often be gathered.
- Industrial sources as always pose some of the biggest challenges due to privacy and proprietary concerns. Manufacturing sub-sector output data can provide some insight into temporal variations.
- In all sectors, it is important to have information on the local calendar – for example what constitutes the work week and holidays.

A.a.3.4 Uncertainty

Three forms of uncertainty have been used in bottom-up granular studies thus far. The first, expert judgement, is best avoided but is oftentimes required given the paucity of uncertainty in incoming data. Without true characterization of probability densities of incoming data, sensitivity studies such as those that characterize a “high/low” or upper bound/lower bound to the variable/parameter space, can be useful. By propagating these boundaries across a number of variables/parameters in a calculation, the final boundaries can be explored and used as confidence intervals. Finally, if probability density is available on incoming data, a Monte Carlo approach can be used in which ensemble runs propagating uncertainties through the calculation process can be used.

A.a.4. Considerations when integrating with atmospheric data approaches

Integration of granular bottom-up estimation with atmospheric inverse/assimilation approaches requires a number of considerations. This can dictate elements of the estimation process.

It is worth asking a few questions to the atmospheric inverse/assimilation modellers in order to target the bottom-up effort correctly (Section 5 and Annex C). These include: what does the atmospheric data support? What is the model resolution? What is the observing density? What are the expected spatial gradients like?

A.a.4.1 Gridding

Since most bottom-up efforts will not naturally be quantified onto a grid, given the typical types of data used to construct the bottom-up estimates, gridding to the atmospheric inverse/assimilation process is necessary. This is best done using the underlying “native” resolution (points, lines, polygons) directly to the required grid as opposed to regridding directly from one grid resolution to another. This is due to the fact that pointwise sources can be misallocated in the regridding process leading to errors. It is important to establish whether or not the grid can be represented as a cartesian or spherical grid. Much bottom-up input data are cartesian. Reprojection can cause distortion. Since most atmospheric inverse/assimilation systems will run an urban experiment using some form of nested grid, it is best to consider how the bottom-up might simply characterize an outer domain or a larger regional estimate within which the detailed urban estimate resides. This can be done at lower resolution than done for the urban estimate but creating this alongside the detailed urban estimate is important as it can avoid “cliffs” or other forms of misspecification if done independently.

A.a.4.2 Uncertainty

Because atmospheric inverse/assimilation systems are dependent upon prior uncertainties, they remain important to quantify. As with uncertainty in general this is often challenging. In the instance where a complete error analysis can be performed, spatial and temporal error covariances should be attempted. This can have a significant impact on outcomes.

A.a.4.3 Scope

Though perhaps obvious it is worth repeating that for integration with atmospheric inverse/assimilation efforts, the bottom-up estimation must be a scope 1 accounting only. While other scopes are useful and encouraged as being helpful for stakeholders, the atmosphere only “sees” a scope 1 estimate and hence, it is critical that this be the basis for prior fluxes used.

A.a.5. Recommendations

The aim of bottom-up guidelines is to encourage the best practices under all conditions recognizing that conditions vary widely across the global geography. Hence, a tiered set of guidelines are likely needed. First, a few other key attributes of a guideline document must reflect.

- Transparency. Data transparency is necessary to collect the type of data needed for granular bottom-up estimation. Transparency varies by country and province. Often data is collected but not publicly available. There are techniques by which privacy information and other identifying factors can be removed from data records such that privacy barriers can be overcome.
- Social norms. In some cases, the social norms will dictate the availability and transparency of data in country/province. Understanding what those are and proposing solutions can be a strategic choice in these conditions.
- Governance (ratios of public to private) and proprietary barriers. Even with high official and unofficial transparency, data may be difficult to acquire due to proprietary barriers among specific private interests. For example, this may be due to a small number of private businesses within a sector within the domain of interest. Again, finding techniques to overcome the data concern through processing or removal of important identifying information can improve the data availability.
- Capacity – the human and technical capacity available in a given location to perform the work associated with generating bottom-up estimation. The demands can be considerable, and this may be more readily available in some places and not others. A useful partnership can be established with a local academic institution, and this can lower the barrier on human labour and expertise.

Given the variation in availability, transparency, and capacity, a tiered system, as described by the IPCC, is a sensible way to guide potential projects aimed at developing granular bottom-up GHG estimates.

- **Tier 1.** This would represent the simplest guidance and used where local or granular data are difficult to acquire or non-existent. Recommended techniques would include downscaling using proxy measures from national estimates or from existing gridded global data products such as ODIAC, FFDAS, or EDGAR. These may stop at the whole-city without further granularity. This understand that where there is limited data and limited capacity, any estimate may be better than nothing. Assumed uncertainties must be large so as to allow atmospheric monitoring more leverage in the inverse/assimilation work. May only be possible for a single year.
- **Tier 2.** Like tier 1 with the exception that an existing SRI estimate has been made and can act as a starting point for further improvement or downscaling. Work on this tier can investigate the scoping used and adjust to conform to a scope 1 only result. Any independent data can be used to evaluate the SRI results and downscaling using available proxies employed. May only be possible for a baseline and recent year.
- **Tier 3.** This would represent a complete space/time-explicit bottom-up effort like what might be found in the Hestia Project. Should be multiyear with potential latencies.

- **Tier 4.** This uses the results from tier 3 in a complete inverse/assimilation system with optimization of the bottom-up to best match the atmospheric monitoring. This will include a multiyear effort and building out results into near-real-time. Used in a trend detection mode.

All tiers share a few common features that are strongly encouraged.

- The first is the need for and importance of documentation on the procedures used and scoping represented by the emissions output. This may include a standardized form and must identify sectors included/not included, scoping definitions, boundaries, and numerical methods, input data, and output formats. The goal is to achieve standardized consistency across city projects.
- Internal consistency can be checked via the use of normalization such as to population (per capita) or per unit area (i.e. in buildings) as ways to performed order-of-magnitude checking of results. These can be compared to national assessments as well.
- Clarity on scoping definitions. This is critical to achieving linkage to atmospheric inverse/assimilation approaches.
- The consideration of biotics must be clearly described. The inclusion of informal economies, relevant in many global cities, must be clearly described and methods presented.
- Quantification of uncertainty. Even if using expert judgement, quantification of uncertainty is critical to the application of the bottom-up estimate to use in, and comparison to, other approaches including atmospheric inverse/assimilation studies.
- There should be emphasis on what inputs or portions of the emissions drive the majority of variability in the urban landscape.
- Explicit linkage to the IPCC tiers may be helpful and will be recognizable to the larger community.
- We have new opportunities due to the emergence of a number of new or “big” data type of data products. Among these are GPS and smartphone data, new very high-resolution optical imagery, and other forms of social media tracking. At the least, these are dense enough to offer information on space/time proxies. It is sensible to embrace these datasets as much as possible and provide further guidance on use and practices.
- Encourage the quality control (QC) of the large amount of data being ingested into these estimates. We may want to provide guidelines on QC procedures or best practices.
- Intercomparisons are strongly encouraged – these can further enumerate best practices and propagate knowledge. Assuming enough projects, a formal intercomparison is possible.

A.a.6. References

Bun R., Nahorski Z., Horabik-Pyzel J. et al. (2018) Development of a high-resolution spatial inventory of greenhouse gas emissions for Poland from stationary and mobile sources, *Mitigation and Adaptation Strategies for Global Change*, 24, 853–880, DOI:10.1007/s11027–018–9791–2.

Fong W.K., Sotos M., Doust M. et al. (2014) Global Protocol for Community-Scale Greenhouse Gas Emission Inventories: *An Accounting and Reporting Standard for Cities, World Resources Institute*, C40 Cities, ICLEI.

Gately C.K. and Hutyra L.R. (2017) Large Uncertainties in Urban-Scale Carbon Emissions, *Journal of Geophysical Research Atmospheres*, 122, 11242–11260, 10.1002.

Gurney K.R., Mendoza D.L., Zhou Y. et al. (2009) High resolution fossil fuel combustion CO_2 emission fluxes for the United States, *Environmental Science and Technology*, 43, 5535–5541.

Gurney K.R., Liang J., Roest G. et al. (2021) Under-reporting of greenhouse gas emissions in US cities, *Nature Communications*, 12, 10.1038/s41467–020–20871–0.

Ivanova D., Barrett J., Wiedenhofer D. et al. (2020) Quantifying the potential for climate change mitigation of consumption options, *Environmental Research Letters*, 15, 10.1088/1748–9326/ab8589.

Kennedy C., and Steinberger J. (2009) Greenhouse gas emissions from global cities, *Environmental Science & Technology*, 43, 7297–7302.

Moran D., Pichler P.-P., Zheng H. et al. (2022) Estimating CO_2 emissions for 108,000 European cities, *Earth System Science Data*, 14, 845–864, https://doi.org/10.5194/essd-14–845–2022.

Nangini C., Peregon A., Ciais P. et al. (2019) A global data set of CO_2 emissions and ancillary data related to emissions for 343 cities, *Scientific Data*, 6, 180280,.

Ramaswami A., Hillman T., Janson B. et al. (2008) A Demand-Centred, Hybrid Life Cycle Methodology for City Scale Greenhouse Gas Inventories, *Environmental Science & Technology*, 42, 6455–6461.

A.b. Biogenic CO_2 flux models/products

Lucy R. Hutyra[1] and Joy B. Winbourne[2]

[1]Boston University, Department of Earth & Environment, Boston, MA USA

[2]University of Massachusetts, Department of Earth, Environmental, and Atmospheric Sciences, Lowell, MA, USA.

Biological carbon sources and sinks, primarily from plants and soils, strongly influence atmospheric composition globally and locally within cities (Sargent et al. 2018). The spatial and temporal influence of biogenic CO_2 fluxes in cities introduces biases of unknown magnitude into measurement and modelling of anthropogenic emissions when treated as known, neutral or negligible (Gurney et al., 2005; Kennedy et al., 2012) as has historically been the case. Correcting for temporal aliasing of biogenic and anthropogenic fluxes will require careful partitioning of each to attribute sources when generating an accurate atmospheric CO_2 monitoring system (Briber et al., 2013; Gurney et al., 2005; Hutyra et al., 2014; Myeong et al., 2006).

Broadly, the urban mixing ratio of CO_2, and other greenhouse gases, is the result of the composition of the inflowing air, local emission sources, local atmospheric chemistry, and biological uptake/loss processes. The biological influence on CO_2 mixing ratios vary geographically with the urban form, seasonally with the climate and functional traits of vegetation, diurnally with weather and physiology, and across all timescales and geographies with the landscaping management choices (Bergeron and Strachan, 2011; Crawford et al., 2011; Järvi et al., 2012; Sargent et al. 2018; Velasco et al. 2021; Hill et al. 2021). Both bottom-up (Winbourne et al. 2021; Briber et al., 2015; Gough and Elliott, 2012) and top-down (Pataki et al., 2006; Turnbull et al., 2015; Sargent et al. 2018; Lauvaux et al. 2020) have demonstrated the enhanced productivity of urban vegetation in some urban areas. Across many biomes, inventory studies show the potential for large C sequestration rates in cities by individual trees (Churkina et al., 2010; Jo, 2002; Nowak and Crane, 2002; Zhao et al., 2012; Lal and Augustin 2012). Indeed, growth rates of urban vegetation have been observed to be upwards of four times those observed in nearby rural forests (Smith et al. 2019). Biological uptake by plants and soils has been estimated to offset between 0–100% of local fossil fuel emissions depending on the locale, season, and hours of the day considered (McPherson and Simpson, Zhao et al., 2010; Sargent et al. 2018; Lauvaux et al. 2020). The carbon sequestration potential of urban vegetation, however, can be dampened by corresponding contributions from land management choices that alter soil respiration rates (Hundertmark et al. 2021; Reinmann et al. 2020; Garvey et al. 2022; Hill et al. 2021).

This overview describes the current understanding of net ecosystem biogenic CO_2 flux and the components of gross primary productivity (GPP) and respiration across a range of urban ecosystem types. A discussion of current measurement and modelling approaches, data requirements, and limitations is provided in the content of urban CO_2 observing systems.

A.b.1. Net Ecosystem Exchange

The net ecosystem exchange of CO_2 is the residual difference of the carbon released through respiration and taken up through photosynthesis. Photosynthesis is an important CO_2 flux component in highly vegetated urban areas. This process requires light reactions and occurs at higher rates with warm and sunny conditions (maximized during midday) during the growing season. However, under severe environmental conditions (i.e. high radiation, temperature, and vapour pressure deficit) photosynthesis can be reduced (Velasco et al. 2021, 2013). In contrast, respiration occurs during day and night hours. Ecosystem respiration is comprised of both autotrophic sources (leaf, stem and root associated) and heterotrophic sources (decomposition of coarse woody debris pools and C substrates in the soils). Autotrophic respiration is strongly coupled to variables that drive patterns in photosynthesis. Heterotrophic respiration has an approximately exponential relationship with soil temperature, increasing until ~25ºC (Carey et al. 2016) and is strongly influenced by soil moisture content and regimes

(Davidson et al. 1998; Velasco et al. 2021). During growing season midday hours the net biological CO_2 flux will be small or negative (potentially offsetting a fraction of FF-CO_2 through net ecosystem uptake); during night-time growing season hours the net biological flux will be maximized with respiration processes releasing CO_2. Ecosystem respiration and photosynthesis both have other tracers that can be very powerful validation of carbon source/sink dynamics (link to tracer chapter). Sargent et al. (2018) found that during the afternoons in the growing season, net biogenic uptake of CO_2 almost completely balanced anthropogenic CO_2 emissions in mesic city of Boston, MA. Conversely, in the cold winter (non-growing season), ecosystem respiration produced 17 to 20% of the total CO_2 flux in the urban study domain. Similarly, Velasco et al. (2013) found in Telok Kurau, Singapore that daytime net biogenic uptake of CO_2 accounted for 8% of the observed anthropogenic CO_2 flux in the study area. Omission of biological fluxes from atmospheric inversion can result in substantial biases (Hutyra et al. 2014).

A.b.2 Gross Primary Productivity (GPP) – Biological Carbon Uptake

Vegetation sequesters atmospheric CO_2 through the process of photosynthesis and a fraction of that photosynthate is stored in plant tissues (e.g. wood, leaves, roots) and soils. In urban areas, land management decisions often result in some of that plant biomass being removed and either composted or incinerated (Velasco et al. 2021; Templer et al. 2015). Researchers have employed various techniques that estimate CO_2 fluxes. Several urban studies of biogenic carbon sequestration have focus on aboveground plant productivity and neglected the contributions of carbon losses from soil respiration and leaching of dissolved carbon in soil (Kindler et al. 2011; Lal and Augustin 2012). Studies that include carbon losses have used approaches such as scaling CO_2 fluxes of leaves through chamber measurements (e.g. Winbourne et al. 2021) to whole ecosystems through partitioning of eddy flux data (Section 4.9, Annex B.i). The key determinant of biogenic fluxes among urban cities is variation in vegetation (species, size, density), canopy extent, and properties and history of soils across cities (Winbourne et al. (in prep); Havu et al. 2021; Pouyat et al. 2006). While historically considered negligible in urban areas, urban vegetation can constitute a significant portion of land cover within the urban mosaic. Greenspace in urban areas range from 10% to 30% of urban land area in US cities (Nowak et al. 2001) and 4 to 53% in Europe (Lavalle et al. 2002). It is important to note, that "urban" is often an inconsistent land cover definition with vegetation carbon stock density varying based on the urban definition used. For example, in the Boston metropolitan area estimates in vegetation carbon stock density varied from 37 ± 7 to 66 ± 8 Mg C ha^{-1} among three commonly used urban definitions (Raciti et al. 2014).

The biophysical factors that affect rates of photosynthesis vary between rural and urban environments, as well as across the urban landscape. The net productivity per unit plant in cities is stimulated by conditions that release plant growth from temperature, water, light, CO_2, and nutrient constraints (Zhao et al., 2016). For example, urban areas experience elevated ambient air temperatures (the urban heat island effect; Kim 1992; Oke 1982) that cause seasonally dependent changes in C fluxes from urban vegetation (Pataki et al., 2006; Zhang et al., 2004; Zhao et al., 2012) and an extension of the urban growing season (Melaas et al., 2016a, 2016b; Zhang et al., 2004). Net productivity can be stimulated by elevated ambient CO_2 mole fractions (Ainsworth et al. 2005), higher nutrient availability from direct fertilization or indirectly from deposition (Rao et al. 2014; Decina et al. 2016), high light environments (Trlica et al. 2020; Reinmann et al. 2020), and potential for higher water availability from irrigation and leaking infrastructure (Stål 1998). Conversely, net productivity of vegetation can be decreased through increased pollutant loads (e.g. ozone, heavy metals; Ainsworth et al. 2012; Krupa and Manning, 1988; Ollinger et al., 2002), poor soil conditions (Rahman et al. 2011; Roman and Scatena 2011; Pickett and Cadenasso 2009), management choices (e.g. road salting, extensive pruning, and removal of hazard trees; Roman and Scatena 2011), and the amplified impacts of heat waves, droughts, and other weather extremes that are becoming more frequent with climate change (Teskey et al. 2014; Li and Bou-Zeid 2013).

The combination of biophysical factors influencing vegetation vary among urban areas. In resource limited regions increases in nutrient availability through nitrogen deposition (Decina et al. 2020) and through increased water availability in arid areas (Buyantuyev and Wu 2009; Zhang et al. 2013). However, elevated mole fractions of NOx and tropospheric O_3 can potentially offset stimulated rates of primary productivity (Reich 1987). Ozone exposure can negatively affect photosynthesis rates (Krupa and Manning 1988; Ollinger et al. 2002). Extensive national-scale nitrogen deposition monitoring networks exist in the US and Europe, but similar to the global CO_2 monitoring networks, sites are intentionally located away from urban areas and point sources of pollution in order to capture background regional trends. The elevated levels of ozone coupled with high temperatures resulted in reductions of 50–75% in photosynthesis by urban oak (*Quercus*) in Houston, TX relative to rural woodlands (Lahr et al. 2015). In contrast, in mesic Boston, MA urban tree growth rates were four times greater relative to rural forests when accounting for species and size but also die much younger (Smith et al. 2019). Similarly, urban conditions in Raleigh, North Carolina was shown to elevate photosynthetic rates in Red Maple (*Acer rubrum*) in urban areas relative to suburban/rural settings (Lahr et al. 2018). The net urban impacts on GPP are variable depending on the context and management.

A.b.3 Ecosystem Respiration – Biological Carbon release

Ecosystem respiration, or the release of CO_2 from the oxidation of organic carbon for energy, is composed of autotrophic (leaves, stems, roots) and heterotrophic sources (decomposition of soil and woody debris such as mulch). The major driver of ecosystem respiration is the efflux of CO_2 from soils (Luyssaert et al. 2007) accounting for 60–90% of total ecosystem respiration in temperate forests (Davidson et al., 2002). Soil respiration is due to the heterotrophic decomposition of organic material and autotrophic root respiration (Trumbore, 2006). Respiration rates are a function of carbon substrate characteristics and content, microbial community composition and diversity, moisture, temperature, soil texture, pH, and nutrient content (Crum et al., 2016; Davidson et al., 1998). Many of these parameters can be considerably altered in urban ecosystems. For example, in urban areas soil respiration patterns (spatial and temporal) may differ due to elevated ambient air temperatures, nutrient loading, impervious surface areas (ISA, i.e. pavement and buildings) that restrict diffusion of CO_2 from soils, compaction by pedestrians, and human addition of labile C sources (George et al., 2007; Ziska et al., 2004, Hundertmark et al. 2021).

Variation in urban form and management decisions result in urban soil respiration fluxes that can span orders of magnitude. Studies have reported temperate soil respiration rates in urban areas that range from <1 μmol CO_2 m^{-2} s^{-1} to >10 μmol CO_2 m^{-2} s^{-1} depending on climate, management, and soil water content. For example, in the mesic city of Boston, MA Decina et al. (2016) found soil respiration rates in residential landscaped areas were 6.73 $\pm$ 0.16 μmol CO_2 m^{-2} s^{-1}, while urban forests respired significantly less (2.62 $\pm$ 0.15 μmol CO_2 m^{-2} s^{-1}). Hill et al. (2021) found rates of soil CO_2 efflux in residential lawns of Baltimore, MD to be twice as high as those in adjacent forest edge soils. Similarly, in Beijing, China respiration rates in an unmanaged urban forest were lower (ranging seasonally from 0.28 μmol CO_2 m^{-2} s^{-1} to 3.62 μmol CO_2 m^{-2} s^{-1}; Chen et al. 2013) than those in a suburban park outside of Beijing (10.09 μmol CO_2 m^{-2} s^{-1}; Wu et al., 2015). In contrast, urban grass dominated parkland soils in Auckland, New Zealand had lower rates of soil CO_2 efflux when compared to urban forest soils (Weissert et al. 2016). In Seoul, South Korea, a threefold difference was observed in soil CO_2 efflux between different forest types, lawn, wetland, and bare soil (Bae and Ryu 2017). In the arid climate of Phoenix, Arizona, soils associated with golf courses, agricultural systems, hotels, and other tourism centeres respired CO_2 at the highest rates (~5 μmol CO_2 m^{-2} s^{-1}) compared to native desert soil respiration of 0.47 μmol CO_2 m^2 s^{-1} (Koerner & Klopatek, 2002). In Southern California lawns exhibited the highest observed respiration rates, which was up to 14.26 mol CO_2 m^{-2} s^{-1} or 53 times higher than that of wildlands in summer (Crum et al., 2016). High rates of soil CO_2 efflux were observed during the early stages of turf development in study conducted in Moscow, Russia (Shchepeleva et al. 2017). Urban landfills also exhibit high respiration rates of 13.6 μmol CO_2 m^{-2} s^{-1}, that do not vary with either soil moisture content or temperature (Koerner & Klopatek, 2002). The elevated rates of respiration in managed land use corresponded to increased nutrient additions, irrigation, and mulching.

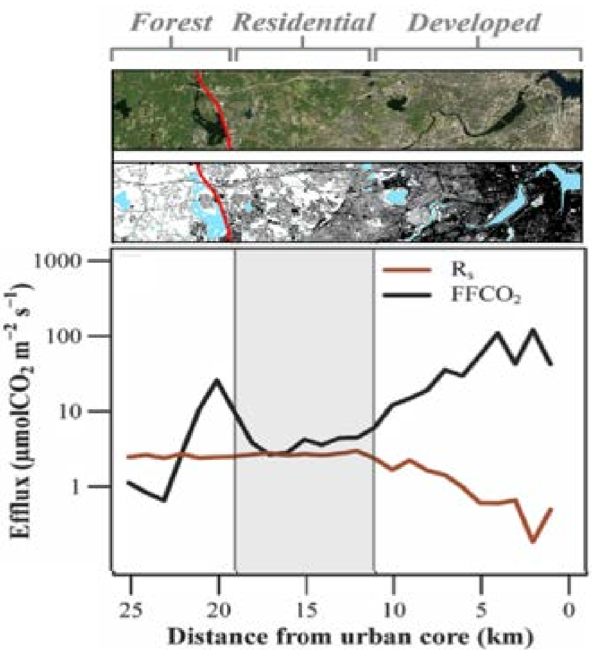

Figure 4: Top: Aerial image of land cover along a 25 km urban to rural transect in Boston, MA. Middle: Impervious (black) and pervious (white) areas. Bottom: Growing season modelled soil CO_2 efflux (R_s) and CO_2ff emissions; CO_2ff enhancement at 20 km due to I-95 (red line in panels denotes I-95). Grey band (11–18 km) denotes a shift from predominately developed to highly pervious residential land covers. [After Decina et al. 2016]

The high levels of impervious surfaces in urban cores leads to lower respiration contributions as there is less soil connected to the atmosphere and accounts for a smaller fraction of the fossil fuel emissions than in greener residental suburbs. For example, Decina et al. (2016) found soil respiration was equivilent to ~1% of CO_2ff in urban centres, while in residental areas soil respiraiton constitutes ~72% of CO_2ff (Figure 4). Collectively, these studies consistently show that even in developed areas with expansive impervious surface coverage, biological respiration fluxes can represent a significant source of CO_2 efflux.

Management practices disturb the C cycle by catalysing C decomposition through mulching fertilizer application (Townsend-Small & Czimczik, 2010; Livesley et al. 2010; Stefaner et al. 2021) or removing individual components that contribute to carbon cycling (Templer et al. 2015; Velasco et al. 2021). There are additional contributions of CO_2 to the atmosphere from maintenance activities that are typically generated from fossil fuel sources (e.g. mowing, leaf blowers) (Velasco et al. 2021). Templer et al. (2015) found that up to 52% leaf litter and grass clippings are removed from the local ecosystem in Boston and composted elsewhere. While a portion of this C may be reintroduced into the ecosystem through application of compost in urban gardens, it is evident that the C cycle is disrupted twice; first through removal of nutrients and later through the addition of compost, thereby creating hotspots of nutrient addition (Templer et al., 2015). Similarly, fallen branches and other woody debris is removed and chipped or sold as firewood. Similarly, Velasco et al. (2021) found impacts to the C cycle from land management decisions with organic waste. In residential lawns of Singapore, Velasco et al. (2012) found lawns as a net carbon source when organic waste was removed and incinerated rather than composted. Stefaner et al. found a reduction in need for fertilizers and in CO_2 fluxes when planting herbaceous legumes rather than turf grass in Singapore. Shifts in urban landscape design and management can alter C cycling by helping to promote carbon storage and reduce the impact of GHG produced from maintenance activities (Velasco et al. 2021).

A.b.4 Urban Biogenic Flux Models

The current generation of ecosystem and climate models used by the scientific community were not developed or parameterized to effectively capture urban biogenic CO_2 fluxes. This is a consequence of urban areas historically being omitted from modelled or remote sensing-based estimates of landscape level biogenic C fluxes (Churkina 2008). Several processed based models developed and parameterized for natural ecosystems have been applied to urban areas (Milesi et al. 2005; Imhoff et al. 2004; Bandaranayake et al. 2003). The current models are under development having varying process-based and management details relevant to urban areas, including those operating at the individual tree scale such as Ufore (Nowak and Crane 2000), remote sensing driven models like Urban Vegetation Photosynthesis and Respiration Model (VPRM) (Hardiman et al. 2017; Winbourne et al., 2021), and first order models such as ICLEI – Land Emissions And Removals Navigator (LEARN) tool (https://icleiusa.org/learn/). All these classes of models can be useful in the IG³IS context depending on the city and specific application.

Most models of urban biogenic C flows are not spatially explicit and those that are have relied on coarse-scale remote sensing imagery, and/or use relatively simple light-use efficiency models (e.g. Zhang et al., 2008; Zhao et al., 2012). Some flux studies have related seasonal patterns to land cover variability (e.g. urban vegetation) only in broad, qualitative terms or to spatially limited areas (i.e. immediately surrounding a flux tower), which limits city scale understanding of the urban C cycle (Bergeron and Strachan, 2011; Crawford et al., 2011; Helfter et al., 2011; Järvi et al., 2012; Kordowski and Kuttler, 2010). At the global scale, Churkina (2016) estimated C fluxes of urban areas based on calculating uptake and respiration rates for vegetation and other contributors of the urban carbon cycle by multiplying the urban extent with the fraction of greenspace in urban areas globally and the gross CO_2 uptake rates of urban vegetation, but assuming uptake rates of a temperate humid forest (Churkina, 2016; LUYSSAERT et al., 2007). Similarly, most existing ecosystem C exchange models have been developed and parameterized for grassland, agricultural, and forest ecosystems and then modified for application to urban systems assuming urban vegetation response to environmental conditions in a similar manner as vegetation in rural settings. This assumption has proven incorrect on many occasions (Kaye et al. 2006; Hutyra et al. 2014; Hardiman et al. 2017; Smith et al. 2019).

Several of the most detailed urban ecological modelling approaches were created for purposes that do not easily align with IG³IS. For example, urban biological life cycle (Strohbach and Hasse 2012) and individual tree models (Ufore; Norwak and Crane 2000) developed in recent years require detailed tree-level and spatially explicit inventories, and/or yield data at only annual temporal resolution. To capture the management impacts requires even further detail (Hundertmark et al. 2021). A new ICLEI – LEARN model (https://icleiusa.org/learn/) was created for urban greenhouse gas budgeting purposes and following an approach analogous to Churkina (2016), but focusing on urban tree sequestration for city climate action plans and it does not currently include processes or the temporal/spatial resolution needed to be useful for IG³IS atmospheric observing systems.

A model approach that shows promise to align with the goals of IG³IS is the VVPRM; Mahadevan et al., 2008) modified by Hardiman et al. (2017) to include factors unique to urban C cycling (in particular fraction of impervious surface area and impacts of urban heat island on air temperatures). The Urban-VPRM provides high temporal (hourly) and spatial resolution either at 500 m using Moderate Resolution Imaging Spectroradiometer (MODIS) or recently with 30 m using Landsat (Winbourne et al. 2021). The VPRM has been parameterized for a range of forest types, agricultural, and grassland ecosystems and has been extended to deciduous forests (Hardiman et al. 2017; Sargent et al. 2018), agricultural-urban systems (Lauvaux et al. 2020), and arid urban systems (Feng et al. 2016). The model generates estimates of GPP based on light-use efficiency and ecosystem respiration based on phenology and air temperature (or soil temperature in some cases; Luus and Lin 2015). Specifically, the VPRM is driven by remote sensing products such as enhanced vegetation index (EVI) or normalized difference vegetation index (NDVI) and meteorological data on temperatures and photosynthetically active radiation. Solar Induced fluorescence (SIF) has also started to be integrated into VPRM models (Luus et al. 2017), but the current SIF resolution and repeat times creates challenges for widespread application.

Advances in data products in urban areas will facilitate improved modelling of urban productivity and net C fluxes across different urban contents. For example, recent maps of urban biomass at very high resolution with remote sensing approaches such as LIDAR are improving the understanding of forest structure and extent (Davies et al., 2011; Raciti et al., 2014; Hardiman et al 2017). Harmonized Landsat-Sentinel products are offering rapid improvements in both data resolution and frequency, with resolutions down to 10m and repeat times of less than four days (Claverie et al. 2018). Widespread improvements in SIF data availability are rapidly emerging OCO-3 target mode capabilities and upcoming satellite missions like GeoCarb that will offer wall-to-wall across the Americas.

A.b.5 Model Limitations

The key limitations to modelling biogenic carbon fluxes including the lack of validation data, limited availability of data inputs required by existing modelling approaches, and the omission of urban management features and data.

Studies validating biogenic carbon flux models are rare. Rather urban ecosystems are frequently assumed to function as their rural counterparts with models being parameterized as more well-studied rural systems. While existing models of biogenic carbon fluxes provide some insights on the different CO_2 flux sources and magnitudes, the lack of model validation continues to limit policy application. Studies that have assessed urban biogenic C fluxes using models have raised concerns in relying on literature values from rural or forested systems to parameterize algorithms as these do not apply in urban settings (e.g. Pataki et al., 2003). A recent validation of the Urban-VPRM with a bottom-up inventory of biogenic carbon fluxes showed that the Urban-VPRM shows promise for providing accurate estimates of gross ecosystem exchange, however the model severely overestimated respiration in the winter (Winbourne et al. 2021). Improved estimates of ecosystem respiration could be achieved with either a seasonally dynamic parameterization of ecosystem respiration (versus annual parameterization) or the use of soil rather than air temperature.

Sufficient input data can limit where and when biogenic C flux models can be applied. Models such as Urban-VPRM require detailed land cover classification, climatological, and impervious surface area metrics that are not consistent in resolution, quality, or characteristic across different regions of the globe. Many standard remote sensing products, like leaf area index and MODIS NPP, are unavailable for urban areas due to retrieval challenges (Hardiman et al. 2017). Impervious surface can also be overlaid by green canopy which can introduce systematic biases in respiration estimates. The parameterization of the VPRM model has largely been done using North American flux tower measurements (Mahadevan et al. 2008, Hilton et al. 2013), and these parameters may not apply in other regions or biomes. Further, the VPRM relies on greenness metrics which conflate green grass with green trees. Irrigation and fertilizer applications in urban areas can lead to urban grass being bright green and these two functional groups cycle C differently.

Lastly, current modelling approaches do not capture the management processes that fundamentally impact biogenic C fluxes. Urban vegetation is exposed to suite of management choices that have significant impacts on biogenic C fluxes. GPP is impacted by decisions on when, where, and whether to irrigate, fertilize, mow, or prune vegetation (Pataki et al. 2011). Ecosystem respiration rates are influenced by management decision on the size of soil surface area around street trees, and choices around use of mulch which has significantly higher rates of C loss from soil respiration than lawns (Hundertmark et al. 2021).

A.b.6 Conclusions

The impact of biological fluxes on urban CO_2 mixing ratios is poorly constrained but has been clearly demonstrated to significantly influence CO_2 mixing ratios and alias daytime fossil fuel emissions. Models such as the Urban-VPRM offer hourly estimates of fluxes at high spatial resolutions, but there are few validation studies, parameterizations largely rely on rural vegetation, driver data is variable in quality and resolution across the globe, and the model does not capture urban management effects. As cities adopt 'nature-based solutions' and efforts to expand urban canopy cover, the biological impacts on biogenic CO_2 fluxes can be expected to increase in both magnitude and complexity.

A.b.7 References

Ainsworth E.A., Yendrek C.R., Sitch S. et al. (2012) The effects of tropospheric ozone on net primary productivity and implications for climate change. *Annual Reviews of Plant Biology* 63, 637–661.

Bae J. and Ryu Y. (2017) Spatial and temporal variations in soil respiration among different land cover types under wet and dry years in an urban park. *Landsc. Urban Plann*., 167, 378–385, doi.org/10.1016/j.landurbplan.2017.07.020.

Bandaranayake W., Qian Y.L., Parton W.J. et al. (2003). Estimation of Soil Organic Carbon Changes in Turfgrass Systems Using the CENTURY Model. *Agronomy Journal*, *95*(3), 558.

Bergeron O. and Strachan I.B. (2011) CO_2 sources and sinks in urban and suburban areas of a northern midlatitude city. *Atmospheric Environment* 45(8): 1564–1573.

Briber B., Hutyra L., Dunn A. et al. (2013) Variations in atmospheric CO_2 mixing ratios across a Boston, MA urban to rural gradient. *Land* 2 (3), 304–327.

Briber B., Hutyra L., Reinmann A.B. et al. (2015) Tree productivity enhanced with conversion from forest to urban land covers. *PLoS ONE* 10(8): e0136237.

Buyantuyev A. and Wu J. (2009) Urbanization alters spatio-temporal patterns of ecosystem primary production: A case study of the Phoenix metropolitan region, USA, *Journal of Arid Environments*, *71*(4–5), 512–520.

Carey J.C., Tang J., Templer P. H. et al. (2016). Temperature response of soil respiration largely unaltered with experimental warming. *Proceedings of the National Academy of Sciences*, *113*(48), 13797–13802.

Chen W., Jia X., Zha T. et al. (2013). Soil respiration in a mixed urban forest in China in relation to soil temperature and water content. *European Journal of Soil Biology*, *54*, 63–68.

Chen Y., Day S.D., Shrestha R.K. et al. (2014) Influence of urban land development and soil rehabilitation on soil atmosphere greenhouse gas fluxes. *Geoderma* 226e227, 348–353.

Claverie M., Ju J., Masek J.G. et al. (2018). The Harmonized Landsat and Sentinel-2 surface reflectance data set. *Remote Sensing of Environment*, *219*, 145–161.

Churkina G. (2008) Modelling the carbon cycle of urban systems. *Ecological Modelling* 216: 107–113.

Churkina G., Brown D.G. and Keoleian G. (2010), Carbon stored in human settlements: The conterminous United States, *Global Change Biology*, *16*, 135–143.

Crawford B., Grimmond C.S.B., Christen A. (2011). Five years of carbon dioxide fluxes measurements in a highly vegetated suburban area. *Atmospheric Environment* 45:896–905.

Crum S.M., Liang L.L. and Jenerette G.D. (2016). Landscape position influences soil respiration variability and sensitivity to physiological drivers in mixed-use lands of Southern California, USA: variability of soil respiration. *Journal of Geophysical Research: Biogeosciences*, *121*(10), 2530–2543.

Davies Z.G., Edmondson J.L., Heinemeyer A. et al. (2011) Mapping an urban ecosystem service: Quantifying above ground carbon storage at a city-wide scale, *Journal of Applied Ecology*, *48*, 1125–1134.

Davidson E.A., Belk E., Boone R.D. (1998) Soil water content and temperature as independent or confounded factors controlling soil respiration in a temperate mixed hardwood forest. *Global Change Biology.* 4, 217–227.

Davidson E.A. et al. (2002) Belowground carbon allocation in forests estimated from litterfall and IRGA-based soil respiration measurements, *Agric. For. Meteorol*., 113, 39–51.

Decina S.M., Hutyra L.R., Gately C.K. et al. (2016) Soil respiration contributes substantially to urban carbon fluxes in the greater Boston area. *Environmental Pollution* 212:433–439.

Decina S.M., Hutyra L.R. and Templer P.H. (2020) Hotspots of nitrogen deposition in the world's urban areas: a global data synthesis. *Frontiers in Ecology and the Environment* 18(2):92–100.

Feng S., Lauvaux T., Newman S. et al. (2016). Los Angeles megacity: a high resolution land–atmosphere modelling system for urban CO_2 emissions. *Atmospheric Chemistry and Physics*, *16*(14), 9019–9045.

George K., Ziska L.H., Bunce J.A. et al. (2007). Elevated atmospheric CO_2 con- centration and temperature across an urban-rural transect. *Atmospheric Environment* 41: 7654–7665.

Gough C.M. and Elliott H.L. (2012) Lawn soil carbon storage in abandoned residential properties: an examination of ecosystem structure and function following partial human-natural decoupling. *Journal of Environmental Management* 98:155–162.

Gurney K.R., Chen Y.H., Maki T. et al. (2005), Sensitivity of atmospheric CO_2 inversion to seasonal and interannual variations in fossil fuel emissions, *Journal of Geophysical Research*, *110*(D10), 10308–10321.

Hardiman B.S., Wang J.A., Hutyra L.R. et al. (2017) Accounting for urban biogenic fluxes in regional carbon budgets *Science of the Total Environment* 592: 366–372.

Havu M., Kulmala L., Kolari P. et al. (2021) Carbon sequestration potential of street tree plantings in Helsinki. *Biogeosciences Discussions*. doi.org/10.5194/bg-2021–242.

Helfter C., Famulari D., Phillips G.J. et al. (2011). Controls of carbon dioxide concentrations and fluxes above central London. *Atmospheric Chemistry and Physics* 11:1913–1928.

Hilton T.W., Davis K.J., Keller K. et al. (2013) Improving North American terrestrial CO_2 flux diagnosis using spatial structure in land surface model residuals. *Biogeosciences* 10: 4607–4625.

Hill A.C., Barba J., Hom J. et al. (2021) Patterns and drivers of multi-annual CO_2 emissions within a temperate suburban neighbourhood. *Biogeochemistry*, 152(1): 35–50.

Hundertmark W.J., Lee M., Smith I.A. et al. (2021) Influence of landscape management practices on urban greenhouse gas budgets *Carbon Balance Management* 16: 1–12.

Hutyra L.R., Duren R., Gurney K. et al. (2014) Urbanization and the carbon cycle: current capabilities and research outlook from the natural sciences perspective. *Earth Future 2* (10), 473e495.

Imhoff M.A., Bounoua L., DeFries R. et al. (2004) The consequences of urban land transformation on net primary productivity in the United States, *Remote Sensing of the Environment*, *89*, 434–443.

Järvi L., Nordbo A., Junninen H. et al. (2012) Seasonal and annual variation of carbon dioxide surface fluxes in Helsinki, Finland, in 2006–2010. *Atmospheric Chemistry and Physics* 12:8475–8489.

Jo H.-K. (2002). Impacts of urban greenspace on offsetting carbon emissions for middle Korea. *Journal of Environmental Management.* 64:115–126.

Kaye J.P., McCulley R.L., Burke I.C. (2005). Carbon fluxes, nitrogen cycling, and soil microbial communities in adjacent urban, native and agricultural ecosystems. *Global Change Biology* 11 (4), 575e587.

Kennedy C., Baker L., Dhakal S. et al. (2012) Sustainable Urban Systems. *Journal of Industrial Ecology*. 16(6):775–779.

Kim H.H. (1992) Urban heat island*. International Journal of Remote Sensing* 13, 2319–2336.

Kindler R., Siemens J.A.N., Kaiser K. et al. (2011) Dissolved carbon leaching from soil is a crucial component of the net ecosystem carbon balance. *Global Change Biology*, 17, 1167–1185, doi.org/10.1111/j.1365–2486.2010.02282.x.

Krupa S.V. and Manning W.J. (1988) Atmospheric ozone: formation and effects on vegetation. *Environmental Pollution* 50, 101–137.

Koerner B. and Klopatek J. (2002) Anthropogenic and natural CO_2 emission sources in an arid urban environment. *Environmental Pollution*, *116*, S45–S51.

Kordowski K. and Kuttler, W. (2010) Carbon dioxide fluxes over an urban park area. *Atmospheric Environment* 44 (23), 2722–2730.

Lahr E.C., Dunn R.R., Frank S.D. (2018) Variation in photosynthesis and stomatal conductance among Red Maple (*Acer rubrum*) urban planted cultivars and wildtype trees in the southeastern United States. *PLOS ONE* 13, e0197866–19.

Lal R. and Augustin B. (editors), (2012) Carbon sequestration in urban ecosystems *Springer: New York*.

Lauvaux T., Gurney, K.R., Miles, N.L. et al. (2020) Policy-relevant assessment of urban CO_2 emissions. *Environmental Science and Technology*, 54: 10237–10245, 2020.

Lavalle C., Demicheli L., Kasanko M. et al. (2002) Towards an urban atlas. Assessment of spatial data on 25 European cities and urban areas. *Environmental issue report No 30. European Environment Agency*, Copenhagen, Denmark.

LEARN https://icleiusa.org/learn/

Li D and Bou-Zeid E. (2013) Synergistic interactions between urban heat islands and heat waves: The impact in cities is larger than the sum of its parts. *Journal of Applied Meteorology and Climatology* 52: 2051–2064.

Livesley S.J., Dougherty B.J., Smith A.J. et al. (2010) Soil atmosphere exchange of carbon dioxide, methane and nitrous oxide in urban garden systems: impact of irrigation, fertilizer and mulch. *Urban Ecosystems*, *13*(3), 273–293, doi.org/10.1007/s11252–009–0119–6.

Luus K.A., Commane R., Parazoo N.C. et al. (2017) Tundra photosynthesis captured by satellite-observed solar induced chlorophyll fluorescence *Geophysical Research Letters* 44(3): 1564–1573.

Luus K.A. and Lin J.C. (2015) The Polar Vegetation Photosynthesis and Respiration Model: a parsimonious, satellite-data-driven model of high-latitude CO_2 exchange, *Geoscience Model Development*, 8, 2655–2674.

Luyssaert S., Inglima I., Jung M. et al. (2007) CO_2 balance of boreal, temperate, and tropical forests derived from a global database. *Global Change Biology* 13, 2509–2537.

McPherson E.G., and Simpson J.R. (1999) Carbon dioxide reduction through urban forestry. *Gen. Tech. Rep. PSW-171,* USDA For. Serv. Pacific Southwest Res. Station, Albany, CA.

Mahaedevan P., Wofsy S.C., Matross D.M. et al. (2008) A satellite-based biosphere parameterization for net ecosystem CO_2 exchange: Vegetation Photosynthesis and Respiration Model (VPRM) *Global Biogeochemical Cycles* 22: 1–17.

Melaas E.K., Friedl M.A. and Richardson A.D. (2016a) Multi-scale modelling of spring phenology across deciduous forests in the eastern United States. *Global Change Biology* 22: 792–805.

Melaas E.K., Wang J.A., Miller D.L. et al. (2016b) Interactions between urban vegetation and surface urban heat islands: a case study in the Boston metropolitan region. *Environmental Research Lett*ers 11:54020.

Milesi C., Elvidge C., Nemani R.R. et al. (2003) Assessing the impact of urban land development on net primary productivity in the southeastern United States. *Remote Sensing of the Environment* 86: 401–410.

Myeong S., Nowak D., Duggin M. (2006) A temporal analysis of urban forest carbon storage using remote sensing. *Remote Sensing of the Environment* 101:277–282.

Nowak D.J., Noble M.H., Sisinni S.M. et al. (2001) Assessing the US urban forest resource, *J. For.*, *99*, 37–42.

Norwak D.J. and Crane D.E. (2000) The Urban Forest Effects (Ufore) model: quantifying urban forest structure and functions. In: Hansen, M. Burk, T. eds integrated tools for natural resources inventories in the 21st century. *Gen. Tech. Rep. NC-212.* St. Paul, MN: US. Dept. of Agriculture, Forest Service, North Central Forest Experiment Station, 714–720.

Nowak D.J. and D. E. Crane (2002) Carbon storage and sequestration by urban trees in the USA, *Environmental Pollution*, *116*, 381–389.

Oke T.R. (1982) The energetic basis of the urban heat island, *Q. J. R. Meteorol. Soc.*, *108*, 1–24.

Ollinger S.V., Aber J., Reich P.B. (2002) Interactive effects of nitrogen deposition, tropospheric ozone, elevated CO_2 and land use history on the carbon dynamics of northern hardwood forests. *Global Change Biology* 8:545–562.

Pataki D.E., Bowling D.R., Ehleringer J.R. (2003) Seasonal cycle of carbon dioxide and its isotopic composition in an urban atmosphere: anthropogenic and biogenic effects. *Journal of Geophysical Res*earch 108 (D23)

Pataki D.E., Alig R.J., Fung A.S. et al. (2006), Urban ecosystems and the North American carbon cycle, *Global Change Biology 12*, 2092–2102, 12: 1–11

Pataki D.E., Carreiro M.M., Cherrier J. et al. (2011) Coupling biogeochemical cycles in urban environments: Ecosystem services, green solutions, and misconceptions, *Front. Ecol. Environ.*, *9*, 27–36.

Pickett S.T.A. and Cadenasso M.L. (2009) Altered resources, disturbance, and heterogeneity: A framework for comparing urban and non-urban soils. *Urban Ecosystem* 12: 23–44.

Pouyat R.V., Yesilonis I.D., Szlavecz K. et al. (2008) Response of forest soil properties to urbanization gradients in three metropolitan areas. *Landscape Ecology* 23, 1187–1203

Raciti S.M., Hutyra L.R., Newell J.D. (2014) Mapping carbon storage in urban trees with multi-source remote sensing data: relationships between biomass, land use, and demographics in Boston neighbourhoods. *Sci. Total Environ*. 500e501C, 72e83.

Rahman M.A, Smith J.G., Stringer P. et al. (2011) Effect of rooting conditions on the growth and cooling ability of *Pyrus calleryana*. *Urban Forestry and Urban Greening* 10: 185–192.

Rao P., Hutyra L.R., Raciti S.M. et al. (2014) Atmospheric nitrogen inputs and losses along an urbanization gradient from Boston to Harvard Forest, MA. *Biogeochemistry* 121:229–245.

Reinmann A., Smith I.A., Thompson J.R. et al. (2020) Urbanization and fragmentation mediate temperate forest carbon cycle response to climate. *Environmental Research Letters* 15:114036.

Reich P.B. (1987). Quantifying plant response to ozone: a unifying theory. *Tree Physiology*, *3*(1), 63–91.

Roman L.A. and Scatena F.N. (2011) Street tree survival rates: Meta-analysis of previous studies and application to a field survey in Philadelphia, PA, USA. *Urban Forestry and Urban Greening* 10: 269–274.

Sargent M., Barrera Y., Nehrkorn T. et al. (2018) Anthropogenic and biogenic CO_2 fluxes in the Boston urban region. *Proceedings of the National Academy of Sciences of the United States of America*, doi:10.1073/pnas.1803715115.

Shchepeleva A.S., Vasenev V.I., Mazirov I.M. et al. (2017) Changes of soil organic carbon stocks and CO_2 emissions at the early stages of urban turf grasses' development. *Urban Ecosyst.,* 20 (2), 309–321 doi.org/10.1007/s11252–016–0594–5.

Smith I.A, Dearborn V.K., Hutyra L.R. (2019) Live fast, die young: Accelerated growth, mortality, and turnover in street trees. *PLOS ONE* 14.

Stål Ö. (1998) The interaction of tree roots and sewers: The Swedish experience. *Arboricultural Journal* 22: 359–367.

Stefaner K., Ghosh S., Yusof M.L.M. et al. (2021) Soil greenhouse gas fluxes from a humid tropical forest and differently managed urban parkland in Singapore. *Science of the Total Environment*, *786*,147305, doi.org/10.1016/j.scitotenv.2021.147305.

Strohbach M.W., Arnold E. and Haase D. (2012). The carbon footprint of urban green space—A life cycle approach. *Landscape and Urban Planning*, *104*(2), 220–229.

Teskey R., Wertin T., Bauweraerts I. et al. (2014) Responses of tree species to heat waves and extreme heat events. *Plant, Cell and Environment* 38: 1699–1712.

Templer P.H., Toll J.W., Hutyra L.R. et al. (2015) Nitrogen and carbon export from urban areas through removal and export of litterfall. *Environmental Pollut*ion 197, 256–261

Trlica A., Hutyra L.R., Morreale L.L. et al. (2020) Current and future biomass carbon uptake in Boston's urban forest. *Science of the Total Environ*ment 709:136–96.

Townsend-Small A. and Czimczik C.I. (2010) Carbon sequestration and greenhouse gas emissions in urban turf: Global Warming Potential of Lawns. *Geophysical Research Letters*, *37*(2), L02707.

Turnbull J.C., Sweeney C., Karion A. et al. (2015) Toward quantification and source sector identification of fossil fuel CO_2 emissions from an urban area: results from the INFLUX experiment. *Journal of Geophysical Research Atmos*pheres 292–312.

Velasco E., Segovia E., Choong A.M.F. et al. (2021) Carbon dioxide dynamics in a residential lawn of a tropical city. *Journal of Environmental Management* 280:11752

Weissert L.F., Salmond J.A., Schwendenmann L. (2016) Variability of soil organic carbon stocks and soil CO_2 efflux across urban land use and soil cover types. *Geoderma* 271, 80–90. (https://doi.org/10.1016/j.geoderma.2016.02.014).

Winbourne J.B., Smith I., Stoynova, H. et al. (2021) Quantification of urban forest and grassland carbon fluxes using field measurements and a satellite-based model in Washington D.C./Baltimore Area. *JGR Biogeosciences*: 10.1029/2021JG006568.

Winbourne J.B., Schifman L., Palzozzo I. et al. Spatial and seasonal trends in biogenic and fossil fuel carbon dioxide fluxes among three metropolitan regions. In prep.

Wu X., Yuan J., Ma S. et al. (2015) Seasonal spatial pattern of soil respiration in a temperate urban forest in Beijing. *Urban Forestry & Urban Greening*, *14*(4), 1122–1130.

Ziska L.H., Bunce J.A. and Goins E.W. (2004) Characterization of an urban-rural CO_2/temperature gradient and associated changes in initial plant productivity during secondary succession. *Oecologia* 139, 454–458. doi:10.1007/s00442–004–1526–2.

Zhang X., Friedl M.A., Schaaf C.B. et al. (2004) The footprint of urban climates on vegetation phenology. *Geophysical Research Lett*ers 31:10–13.

Zhang C., Tian H., Pan S. et al. (2008) Effects of Forest Regrowth and Urbanization on Ecosystem Carbon Storage in a Rural–Urban Gradient in the southeastern United States. *Ecosystems*, *11*(8), 1211–1222.

Zhang C., Tian H., Pan S. et al. (2014) Multi-factor controls on terrestrial carbon dynamics in urbanized areas. *Biogeosciences* 11:7107–7124.

Zhao M., Kong Z.H., Escobedo F. et al. (2010) Impacts of urban forests on offsetting car- bon emissions from industrial energy use in Hangzhou, China. *Journal of Environmental Management* 91: 807–813.

Zhao S., Liu S., Zhou D. (2016) Prevalent vegetation growth enhancement in urban environment. *Proceedings of the National Academy of Sciences of the United States of America* 201602312.

Zhao T.T., Brown D.G., Fang H.L. et al. (2012) Vegetation productivity consequences of human settlement growth in the eastern United States, *Landscape Ecology*, *27*, 1149–1165.

A.c. Methane flux models/products

Felix Vogel[1], Nasrin Mostafavi Pak[1]

[1]Environment and Climate Change Canada, Canada

A.c.1. Introduction

Methane is a short-lived climate pollutant with a large global warming potential of 34 on a 100-year time horizon (Gasser et al., 2017), which makes it low-hanging fruit for mitigation policies. As an ozone precursor methane is also relevant for air quality studies. Compared to carbon dioxide it is important to note that methane does not have strongly localized sinks but is decomposed through chemical processes in the atmosphere or by microbial activity in soils. Furthermore, many anthropogenic methane sources are not related to fossil fuels but bacterial processes in landfills, wastewater or ruminants (Saunois et al., 2019), which can complicate a proper determination of emission rates.

To include emission models (process-oriented), emission inventories (statistics-based or reported) as well as other 'bottom-up' techniques we will refer all of them as *emission data products* here.

Emission data products, which are typically based on socio-economic information, play a crucial role in understanding atmospheric methane levels in urban areas as they allow to infer which (known) sources contribute to local enhancements. Furthermore, when combined with atmospheric transport models they help to interpret atmospheric observations, while atmospheric data in return can help provide independent constraints on local and regional methane emission rates and fluxes. To date atmospheric-based techniques often lack the ability to provide spatially explicit and sector-specific emission information to the same degree as high-resolution city-specific emission data products can. Compared to urban carbon dioxide emission products, which have been developed for multiple cities, there is only a very limited number of spatially explicit city-specific emission data products available at this point (e.g. Hopkins et al., 2016; McKain et al., 2015).

The general principles of creating an anthropogenic methane emission product are similar to studies for carbon dioxide, i.e. using activity or consumption data in concert with related emission factors to calculate total (most often annual) emissions for each sector. Alternatively, reported regional methane emissions can be downscaled to a city based on proxy data. However, methane emission products often have much higher relative uncertainties than carbon dioxide emission products (Ganesan et al., 2019) as methane is most commonly released as a non-intentional by-product of human activity. Therefore, consumption-based approaches are less reliable and can cause discrepancy. This also means relative uncertainties for large emitters are often not better compared to smaller sources. Emission factors are also not always normally distributed for the economic sub-sector or activity but heavy-tailed ('supper-emitter problem') (Weller et al.,2020; von Fischer et al., 2010).

A.c.2 Recommendations

- Collect site specific data where possible and otherwise use IPCC recommended approach (see methods in Section 4.1. and Annex A.a.)
- Provide sector-specific information (possibly add isotope and co-emitted species in inventory).
- If possible, use different approaches to create an ensemble of emission products to capture systematic uncertainties.
- Use atmospheric information to validate emission factors (and their distribution) for local infrastructure and facilities.
- Emission products from atmospheric observations only (e.g. mobile NG infrastructure surveys, detection of hotspots using satellites).

- To date urban methane inventories have been focussed on Scope 1 emissions and have been predominantly used to compare to atmospheric observations and mobile survey data. For policymakers Scope 2 and Scope 3 could be highly relevant as well. Especially, Scope 2 plays a crucial role as many cities export waste to landfills outside their city limits.
- It is important to provide information in clear and well-defined categories. SNAP or CFR definitions could be used, or explicit definitions can be made. The most important sectors are given below and a table with important activity data and proxies is given in Table A.c.1.
  - Waste management: landfills, wastewater treatment plants, sewage collection network
  - Natural gas infrastructure: storage facilities, compressor and feeder stations, distribution pipelines, consumer appliance emissions
  - Industrial sources: power plants, solvent and chemical industry
  - Agricultural sources: ruminants, crops
  - Natural: wetlands, waterways, lakes, mangroves
  - Transportation (-> incomplete combustion): onroad traffic, shipping
- Role of atmospheric observations:
  - Can provide information on emissions from important facilities
  - Help to understand range of emission factors. e.g. natural gas distribution infrastructure and identify super-emitters
  - Provide a benchmark to assess spatial and temporal disaggregation of emissions
  - Combined with inverse modelling can provide a constraint on total urban emissions
  - Including carbon isotopes and co-emitted species can constrain sector-specific emissions.

Table A.c.1. Methane emission sectors and emission estimation methods.

Sector / Subsector	Total Emissions	Temporal Disaggregation	Spatial Disaggregation	Uncertainty Considerations
Waste management				Waste sector activity is often the most important source sector and correctly estimating emissions is critical.
Solid waste management (landfills)	* history of amount and type of waste deposited * type of operations and technologies used * installation and efficient of landfill gas collection system	* process models can provide information based on atmospheric and soil parameters such as temperature, pressure, moisture, etc.	* site specific information	The uncertainty of this sector can strongly depend on the efficiency of landfill gas recovery systems.
Wastewater treatment	* total amount of water treated (population equivalent) * type of treatment and stages used (e.g. aerobic, anaerobic)	* amount of water treated	* site specific information	On-site operations can change throughout the season or in response to water levels or treatment demand, this contributed to emission uncertainties.
Wastewater collection	* total amount of wastewater produced (population equivalent) * type of sewage system (e.g. gravity-drained, pumped, mixed water)	* climatic and weather parameters are likely influences	* information on sewage network * road network data can act as a proxy	To date emissions from sewage collection systems are not well understood and should be considered as highly uncertain. As default temporally constant emissions could be used.
Natural gas infrastructure				Estimating emissions from natural gas infrastructure has proven difficult in some regions as overall emissions are often dominated by 'super-emitters', i.e. a small portion of the network contributes to the majority of emissions.
Compressor and feeder stations	* natural gas transmitted	* natural gas quantities transmitted * on-site operations	* site specific information	Studies have shown that emissions change strongly over time due to on-site operations.

Sector / Subsector	Total Emissions	Temporal Disaggregation	Spatial Disaggregation	Uncertainty Considerations
Storage facilities	* type and count of storage systems * amount of gas/oil stored and system pressure * amount of gas/oil loaded and unloaded	* natural gas quantities transmitted * site operations	* site specific information	Besides the super-emitter problem, storage facility emissions can also be intermittent, e.g. due to unclosed hatches.
Distribution pipelines	* amount of gas distributed per year * age of infrastructure * length of pipeline system * type of pipeline by pressure (low, mid, high) * type of pipeline by material (cast-iron, polymer, etc.)	* natural gas distributed	* natural gas network maps * road network as proxy	Spatial disaggregation is very challenging as a small portion of the network can contribute the majority of emissions.
Consumer / household emissions	* natural gas used * amount of energy used	* natural gas consumption	* census data on households * population density as proxy	Emission factors for household emissions (water boilers, stoves, etc.) are still highly uncertain.
Industrial emissions				Industrial emissions vary considerably across urban areas. Where chemical industry is important this can be a major source.
Fossil fuel power plants	* annual natural gas consumption * annual energy production	* natural consumption * energy production	* site specific information	Temporal disaggregation is challenging and uncertain as emissions might not be correlated with production.
Solvent, chemical industries and other	* annual production * annual sales (e.g. gas stations)	* production * sales data	* site specific information	Temporal disaggregation is challenging and uncertain as emissions might not be correlated with production or sales.
Agricultural sources				At national and regional scale agriculture is often an important source, but are typically a minor contribution in dense urban areas.

Sector / Subsector	Total Emissions	Temporal Disaggregation	Spatial Disaggregation	Uncertainty Considerations
Ruminants	* head count and dry weight of ruminants * type of ruminants (cattle, heifers, goats, sheep, etc.) * type of feed	* daily emissions related to feeding times * information on head count and dry weight changes (seasonal)	* county-specific head count and dry weight * Information of farm locations	Typically, information about livestock counts are found to be reliable, but uncertainty on emissions factors exist.
Crops and other	* amount of farmed area (e.g. rice) * amount of crop produced	* track seasonally changing managing practices	* information on farm locations	Annual crop information is often available, but emission factors are often highly uncertain.
Natural emissions				Natural emission models have a large uncertainties but are typically a minor contribution in dense urban areas.
Wetlands	* wetland process models (e.g. WetCharts)	* changes in soil moisture, wetland extent, temperature	* wetland databases * remote sensing information	Wetland extent can change significantly interannually and seasonally, which contributes significantly to the uncertainty in this sector.
Fresh water (rivers, lakes, canals)	* upscaling from known water surface area * dissolved organic matter content of water	* changes in water temperature	* regional maps * remote sensing information	Emissions from freshwater are still an active area of research and emission predictions very difficult.
Transport				Methane emissions from combustion in mobile sources are typically a minor contribution to urban emissions.
Road traffic	* vehicle kilometres travelled * methane emission factors for vehicle fleet	* traffic counts * congestion index	* road network data	Emissions might differ by vehicle type.
Shipping and other	* shipping volume from ports	* shipping volume information	* shipping lanes	Emissions from this sector are typically minor, but a likely source of uncertainty is related to different type of cargo vessels being used.

A.c.3. References

Ganesan A.L., Schwietzke S., Poulter B. et al. (2019) Advancing Scientific Understanding of the Global Methane Budget in Support of the Paris Agreement, *Global Biogeochemical Cycles*, 33, 1475–1512, doi:10.1029/2018gb006065.

Gasser T., Peters G.P., Fuglestvedt J.S. et al. (2017), Accounting for the climate–carbon feedback in emission metrics, *Earth System Dynamics*, 8(2), 235–253, doi:10.5194/esd-8–235–2017.

Hopkins F.M., Kort E.A., Bush S.E. et al. (2016), Spatial patterns and source attribution of urban methane in the Los Angeles Basin, *Journal of Geophysical Research: Atmospheres*, 121(5), 2490–2507, doi:10.1002/2015jd024429.

McKain K., Down A., Raciti S.M. et al. (2015), Methane emissions from natural gas infrastructure and use in the urban region of Boston, Massachusetts, *Proceedings of the National Academy of Sciences*, 112(7), 1941–1946, doi:10.1073/pnas.1416261112.

Saunois M. et al. (2020), The Global Methane Budget 2000–2017, *Earth System Science Data*, 12(3), 1561–1623, doi:10.5194/essd-12–1561–2020.

Von Fischer J.C., Rhew R.C., Ames G.M. et al. (2010), Vegetation height and other controls of spatial variability in methane emissions from the Arctic coastal tundra at Barrow, Alaska, *Journal of Geophysical Research*, 115, doi:10.1029/2009jg001283.

Weller Z.D., Hamburg S.P. and von Fischer J.C. (2020), A National Estimate of Methane Leakage from Pipeline Mains in Natural Gas Local Distribution Systems, *Environmental Science & Technology*, 54(14), 8958–8967, doi:10.1021/acs.est.0c004

Annex B. Atmospheric Observational Methods

This Annex B details the atmospheric observation techniques, as well as methods for direct analysis of these observations. Readers should also refer to the main document for shorter summaries of each method.

The WMO/GAW Greenhouse Gas Measurement Techniques recommendations (Crotwell et al., 2020) provide detailed explanations of how greenhouse gas measurements should be performed. The precision requirements outlined in that document can be relaxed for many urban measurements where the signals of interest are large, but the general principles of calibration and standardization, data quality and measurement methodologies hold for urban areas.

B.a. Tower and other elevated point observations

Michel Ramonet[1]

[1]Laboratoire des Sciences du Climat et de l'Environnement, Gif sur Yvette, France

B.a.1 Introduction

Monitoring atmospheric mole fractions of greenhouse gases from elevated points in and around cities aims to measure the enhancements of these mole fractions due to urban emissions. The use of elevated points, compared to surface measurements, makes it possible to extend the footprint of the observations and avoid surface layer vertical gradients (Section B.c). Telecommunication towers, higher than 100 m, have been integrated for many decades in continental and global networks [Andrews et al., 2014; Stanley et al. 2018, Ramonet et al. 2020], with in general only weather sensors installed on the structure of the tower, while GHG analysers are installed in a building at the foot of the tower, connected to the air intakes by tubes and pumps allowing fairly rapid response times. This configuration allows the use of sophisticated analysers for high precision measurements, with minimal installation and maintenance on the tower infrastructure itself. This type of installation on tall towers is now deployed in and around several cities such as Indianapolis, Toronto, Paris, Washington D.C. and Baltimore. However, the development of dense measurement networks (Section 4.11. and Annex B.k.) based on the use of low-cost instruments may be based on the installation of sensors on other kinds of infrastructures, and in many case the roofs of buildings may be more accessible than tall towers.

B.a.2 Data quality considerations

The WMO/GAW GGMT recommendations specify the following with regards to the compatibility of urban greenhouse gas measurements: "The required uncertainty of measurements and tolerable maximum bias within the network in high-density emissions areas is a function of the magnitude of the enhancement, with stricter requirements where the local GHG excess is small. Requirements for measurements in areas with small GHG excess values should be comparable to the WMO requirements for measurement of background air. For elevated measurements, we recommend network compatibility of 5% (or better) of the excess dry mole fraction over the appropriate regional background. At this level, measurement uncertainties and biases will be small relative to other sources of uncertainty in calculated fluxes based on imperfect knowledge of atmospheric transport. However, we recommend that high-density emissions area measurements still adhere to WMO guidelines for near background level observations including traceability to WMO scales, but we recognize that compatibility requirements for elevated measurements are far less stringent." (Crotwell et al., 2020).

Recommendations:

- Long-term measurements are essential to monitoring trends in emissions associated with reduction strategies implemented by cities.
- Continuous measurements are needed due to the high signal variability.
- It is recommended to link the urban networks to WMO reference scale (see GGMT, Crotwell et al., 2020). but access to reference gases can be an issue, and new instruments (e.g. open path) may be difficult to calibrate. More important for urban networks maybe the internal compatibility of the stations.
- Near-real-time data products are important for a rapid detection of technical problems and to analyse the observed trends and variability.

B.a.3 Sampling strategy – locations, frequency, number of sites

The selection of measurement sites for a new monitoring network is one of the most critical steps, which will greatly affect the ability to provide relevant information on the city emissions. An essential first step is to consider the dominant wind directions in order to determine areas most often upwind and downwind of the city. More complex network design studies (Turner et al., 2016; Wu et al., 2016; Lopez-Coto et al., 2017) are highly recommended, if possible. Depending on wind patterns, several pairs of upwind-downwind sites might be required to cover the city (e.g. Turnbull et al, 2015; Xueref-Remy et al, 2018). Generally the choice of sites results from a compromise between the a priori optimal network, and the existing infrastructures available insofar as it is generally cost prohibitive to build towers specifically for atmospheric measurements. A logical strategy is to first define favoured areas in view of predominant wind directions and possibly mole fraction gradients simulated by a high-resolution atmospheric transport model. The second step is to identify existing elevated structures within those areas and check the environment of those elevated structures for local anthropogenic contamination and biospheric influence (Section 4.12 and Annex B.l. on background selection). For cities with notable orography, measurement locations on hilltops or mountaintops are an option, but such sites do make the representation of observations by atmospheric transport models more complex. For coastal cities, it is important to set an upwind site at the seashore or in the bay of the city (e.g. Verhulst et al, 2017).

B.a.3.1 Determination of ideal measurement locations

The minimum configuration of an urban network is usually to have two towers upwind and downwind of the city in the direction of the prevailing winds in order to have as many mole fraction gradients as possible with a background site (the upwind site; see also Section 4.12 and Annex B.l. on background selection). To increase the number of situations where the upwind to downwind gradient of the city is measured, a network of towers on the outskirts of the city seems to be the preferred option. In addition to one or more upwind-downwind pairs, dedicated site(s) downwind of specific hotspots may be desirable. Depending on the signal and the distance from the hotspot low-cost sensors may be appropriate for such purpose. Furthermore, in regions where low windspeed situations often occur and the urban emissions accumulate, it may be useful to install a measurement site within the city itself to quantify the local urban CO_2 dome by calculating the excess of mole fraction measured at that site relative to background mole fraction level (as defined in Section 4.12) (e.g. Xueref-Remy et al, 2018; Mitchell et al., 2018; Karion et al., 2021).

B.a.3.2 What types of elevated points should be used?

Telecommunication towers (100m high or more) seem optimal because they generate little perturbation of the atmospheric circulation (important for consistency with the simulations) and no risk of very local influences at the top. But this option can be expensive when tower operators require annual usage fees, and such towers are more common in some cities than others. Other options are for example water towers (e.g. Lian et al, 2019), churches, monuments such as the Eiffel tower in Paris (Xueref-Remy et al, 2018) and the roofs of residential and office buildings (e.g. Sargent et al, 2018). In the latter case, the risk of local contamination is higher due to the potential for building air exhaust onto the roof. For this type of site, it is recommended, if possible, to perform a measurement campaign of at least one week in order to determine the CO_2 variability, and the possible presence and location of spikes indicating local contamination associated with the 'breathing' of the building. One option is also to install several sampling lines on the corners of the roof, sampled one after the other to detect possible local contamination sources, and using post-hoc selection of the optimal data based on wind direction and/or other contamination parameters (Sargent et al., 2018).

Administrative authorizations to access elevated structures can be very slow to obtain. Beyond the possible discussions on rental prices, safety conditions must be discussed, in particular for installation of inlet lines and the use of compressed air tanks for the calibration of analysers.

B.a.3.3 What types of essential and useful collocated measurements?

The variations of GHG mole fractions are very strongly linked to meteorological conditions, and therefore weather sensors for measuring temperature and wind speed/direction are essential for the interpretation of the data, and for the validation of atmospheric transport models. Furthermore, co-location with measurements of gases and / or particles characteristic of a given sector of activity is very useful in making it possible to attribute variations in GHG to these sectors (Nathan et al., 2018). The most frequently considered components are CO as a tracer for combustion and NOx as a tracer for automobile traffic. These two gases are generally measured in air quality networks, and it is therefore possible to benefit from these existing measurements. However, the co-location of the GHG and air quality measurement sites is not always optimal because the latter generally seek to be close to the sources, while a larger footprint is sought for the GHG measurements. Many other compounds can be considered for collocated measurements but the link with a specific process remains generally difficult to establish. Pilot measurement programs are being deployed in different cities to quantify the added values of possible tracers. The radiocarbon measurement represents the most direct information to discriminate between fossil and biogenic CO_2 emissions (Miller et al. 2020; Niu et al., 2018; Wang et al., 2018). Unfortunately the precise measure of $^{14}CO_2$ remains challenging, and to date these observations can only be carried out through discrete samples (Sections 4.8 and 4.9, Annexes B.g. and B.h.), which generally does not allow sufficient observations. In addition to radiocarbon measurements, grab samples enable to measure GHGs mole fraction providing a quality control of the continuous time series. Beyond the additional compound measurements, it is also interesting to consider installing multiple sampling heights on the towers. The measurement of GHG vertical profiles provides information on the vertical stability of the atmosphere and the accumulation of those gases near the surface (Section 4.3. and Annex B.c.). Such an installation is not very expensive since the same instrument is used to successively measure air at different sampling heights.

B.a.4 References

Andrews A.E., Kofler J.D., Trudeau M.E. et al. (2014). CO_2, CO, and CH_4 measurements from tall towers in the NOAA Earth System Research Laboratory's Global Greenhouse Gas Reference Network: instrumentation, uncertainty analysis, and recommendations for future high accuracy greenhouse gas monitoring efforts. *Atmospheric Measurement Techniques* 7(2): 647–687.

Crotwell A.M., Lee H. and Steinbacher M. 20th WMO/IAEA Meeting on Carbon Dioxide, Other Greenhouse Gases and Related Measurement Techniques (GGMT-2019), *World Meteorological Organization GAW Report No. 255*, 2020.

Karion A., Lopez-Coto I., Gourdji S.M. et al. (2021). Background conditions for an urban greenhouse gas network in the Washington, D.C., and Baltimore metropolitan region. *Atmospheric Chemistry and Physics* 21(8): 6257–6273

Lopez-Coto I., Ghosh S., Prasad K. et al. (2017). Tower-based greenhouse gas measurement network design—The National Institute of Standards and Technology North East Corridor Testbed. *Advances in Atmospheric Sciences* 34(9): 1095–1105.

Mitchell L.E., Lin J.C., Bowling D.R. et al. (2018). Long-term urban carbon dioxide observations reveal spatial and temporal dynamics related to urban characteristics and growth. *Proceedings of the National Academy of Sciences* 115(12): 2912–2917.

Lian J., Bréon F.M., Broquet G. et al. (2019). Analysis of temporal and spatial variability of atmospheric CO_2 concentration within Paris from the GreenLITE™ laser imaging experiment. *Atmospheric Chemistry and Physics* 19(22): 13809–13825.

Miller J.B.,. Lehman S.J, Verhulst K.R. et al. (2020). Large and seasonally varying biospheric CO_2 fluxes in the Los Angeles megacity revealed by atmospheric radiocarbon. *Proceedings of the National Academy of Sciences* 117(43): 26681–26687.

Niu Z., Zhou W., Feng X. et al. (2018). Atmospheric fossil fuel CO_2 traced by $^{14}CO_2$ and air quality index pollutant observations in Beijing and Xiamen, China. *Environmental Science and Pollution Research* 25(17): 17109–17117.

Ramonet M., Ciais P., Apadula F. et al. (2020) The fingerprint of the summer 2018 drought in Europe on ground-based atmospheric CO_2 measurements. *Philosophical Transactions of the Royal Society B: Biological Sciences* 375(1810): 20190513.

Sargent M., Barrera Y., Nehrkorn T. et al. (2018) Anthropogenic and biogenic CO_2 fluxes in the Boston urban region. *Proceedings of the National Academy of Sciences* 115(29): 7491–7496.

Stanley K.M., Grant A., O'Doherty S. et al. (2018) Greenhouse gas measurements from a UK network of tall towers: technical description and first results. *Atmospheric Measurement Techniques* 11(3): 1437–1458.

Turnbull J.C., Sweeney C., Karion A. et al. (2015) Toward quantification and source sector identification of fossil fuel CO_2 emissions from an urban area: Results from the INFLUX experiment. *Journal of Geophysical Research Atmospheres* 120(1): 292–312.

Turner A.J., Shusterman A.A., McDonald B.C. et al. (2016) Network design for quantifying urban CO_2 emissions: assessing trade-offs between precision and network density. *Atmospheric Chemistry and Physics* 16(21): 13465–13475.

Verhuls K.R., Karion A., Kim J. et al. (2017) Carbon dioxide and methane measurements from the Los Angeles Megacity Carbon Project – Part 1: calibration, urban enhancements, and uncertainty estimates. *Atmospheric Chemistry and Physics* 17(13): 8313–8341.

Wang Y., Broquet G., Ciais P. et al. (2018) Potential of European $^{14}CO_2$ observation network to estimate the fossil fuel CO_2 emissions via atmospheric inversions. *Atmospheric Chemistry and Physics* 18(6): 4229–4250.

Wu L., Broquet G., Ciais P. et al. (2016) What would dense atmospheric observation networks bring to the quantification of city CO_2 emissions? *Atmospheric Chemistry and Physics* 16(12): 7743–7771.

Xueref-Remy I., Dieudonné E., Vuillemin C. et al. (2018) Diurnal, synoptic and seasonal variability of atmospheric CO_2 in the Paris megacity area. *Atmospheric Chemistry and Physics* 18(5): 3335–3362.

B.b. Tower and elevated point measurement data analysis

Jooil Kim[1], Anna Karion[2], Zoe Loh[3], Natasha Miles[4], Irene Xueref-Remy[5]

[1]Scripps Institution of Oceanography, University of California San Diego, La Jolla, CA, USA

[2]National Institute of Standards and Technology, Gaithersburg, Maryland, USA

[3]Commonwealth Scientific and Industrial Research Organization (CSIRO), Melbourne, Victoria, Australia

[4]Pennsylvania State University, University Park, Pennsylvania, USA

[5]Institut Méditerranéen de Biodiversité et d'Ecologie Marine et Continentale, Universitaires d'Aix-Marseille, France

B.b.1 Introduction

The interpretation of tower-based greenhouse gas (GHG) observations is strongly dependent on sound practices in general observational techniques and data quality control which are detailed in section B.a. Another important, and many times challenging, dependence is on background mole fractions defined for the network, including the consideration of biogenic signals (Section B.l). Readers are asked to consult the relevant chapters in this document for details on these topics. Here, we outline strategies that may be useful in analysing the data, once the prerequisite data needs have been fulfilled.

Generally, analysis can be done on the measured GHG mole fractions directly, or on "enhancements" (mole fractions after removal of a baseline). Calculation of enhancements isolates the local signal from the regional and larger scale contributions. When determination of the background also takes into consideration the biogenic signal, the enhancements more directly represent the signals from anthropogenic emissions. Of interest is identifying significant patterns in the observed variability, and one should expect a mix of factors to drive this variability in the complex urban environment. Some factors to consider include the following.

B.b.2 Sub-annual temporal factors

Short-term (sub-hourly) variability in mole fractions may point to significant sources near the measurement site or identify certain very local conditions that can produce very high mole fractions that are difficult to interpret. In some cases these data points need to be filtered out to avoid inferring spuriously high fluxes. Local meteorology, including wind speed and atmospheric boundary layer height, for example, can drive diurnal to monthly/seasonal variability patterns in mole fraction enhancements. Note that some anthropogenic signals exhibit significant weekday/weekend differences.

- Inlet height differences: If GHGs are measured at multiple inlet heights, analysis of differences between these inlet heights can lead to better understanding of the surface fluxes near the measurement site. Generally, lower inlet heights will capture more of the surface influence but be sensitive to a smaller regional footprint, as compared to higher inlets (Annex B.a.).
- Correlations with on-site meteorology: Some of the observed mole fractions can be strongly correlated with certain wind directions/speeds. Analysis of temperature, humidity and other meteorological data may help identify specific meteorological conditions that bring distinct source signatures to the observation site.
- Annual trends in variability: Analysis should consider whether significant patterns exist in the variability over annual timescales. Note that some changes may be

gradual (e.g. changes in traffic emissions due to long-term policy or increased adoption of electric vehicles) while others may be relatively abrupt (e.g. power plant closure, COVID-19 shutdown).

- Site-to-site variability: Note that sites within the network may exhibit significantly different variability characteristics and identifying these differences may help better understand the factors that dominate variability at each site and across the network.
- Local time considerations: Note that some of the diurnal variability in the urban environment may follow daylight savings (e.g. emissions from traffic, buildings, industry), and one should consider whether the analysis can potentially be affected by this. It is recommended to adopt time stamp conventions that allow for programmatic, flexible conversion to suitable local time zones as necessary.
- Tracer-tracer ratio analysis between co-measured compounds can effectively factor out meteorology and help identify a direct source emission signature. Consult Section B.h. for more details on this topic.
- One special application of tower observations is in combination with air mass back trajectory footprint patterns, which becomes an integral part of forward modelling and inversions (Annex C).

It is important to point out that generally speaking, tower observations can capture a more temporally complete and precise signal of the emissions compared to other forms of measurement (e.g. remote sensing, aircraft measurements, flask sampling). As such, attempts to fully explore this temporal variability are greatly encouraged.

B.b.3 Graphs and plot types that may be useful

- Variability at various temporal scales: Consider composite plots of mole fractions at hour-of-day, day-of-week, day-of-year, month-of-year, seasonal, multi-annual, etc. Caution is necessary in interpreting patterns in enhancements, as changes can be driven by meteorology as opposed to a change in emissions. Missing data can affect the results and should be carefully considered. (Briber et al., 2013; Karion et al., 2020; McKain et al., 2012; Miles et al. 2017; Mitchell et al., 2018; Sargent et al., 2018; Verhulst et al., 2017; Xueref-Remy et al., 2018).
- Temporal changes in vertical gradients: Vertical gradients are directly related to local fluxes, with a footprint similar in size to an eddy covariance flux tower. There can be some benefit to a lower level measurement close to the ground for capturing a larger signal of the surface flux over a smaller footprint area, e.g. 10 m above ground level. (Miles et al., 2017).
- Tracer-tracer ratios: Caution is necessary to ensure enough data points exist for robust estimate of the ratio. The York bivariate fit method is effective in taking into account variance in both axes and reducing the influence of outliers (Cantrell, 2008). See also Annex B.h.
- Accumulation plots: Cumulative summing of the enhancement mole fractions over a period of time (typically day-of-year) can be useful in identifying the timing of significant change in emission patterns, but caution is necessary with accounting for missing data (Miles et al., 2017; Yadav et al., 2021).
- Wind roses and polar plots: Enhancements can be plotted against wind speeds/directions on a polar coordinate to analyse correlations between wind and pollution patterns (Miles et al., 2017; Xueref-Remy et al., 2018). Recent studies have expanded polar analysis to make statistical inferences on the pollution patterns (Balashov et al., 2020; Grange et al., 2016; Uria-Tellaetxe et al., 2014).
- Atmospheric boundary layer height and correlation to GHG mole fractions: In theory, lower atmospheric boundary layer heights will lead to increased GHG mole

fractions for a given surface emissions flux within a simplified well mixed atmospheric box model. Therefore, the correlation of the atmospheric boundary layer height, either directly measured or proxied from other tracers (e.g. Radon), against observed GHG mole fractions can provide information on the surface emissions flux rate for these GHGs (Vogel et al., 2012).

- Hourly standard deviations in mole fractions: In general, higher variability within a given time period (e.g. within an hour) is an indicator of larger local sources.
- Significant filtering of the data (e.g. in terms of wind speed, wind direction, time of day, day-of-year) may be necessary to derive coherent plots, and the recommendation is that the software tools for plotting are flexible and allow for experimentation.

B.b.4 References

Balashov N., Davis K., Miles N. et al. (2020) Background heterogeneity and other uncertainties in estimating urban methane flux: results from the Indianapolis Flux Experiment (INFLUX*) Atmospheric Chemistry and Physics* 20(7), 4545–4559.

Briber B.M., Hutyra L.R., Dunn A.L. et al. (2013) Variations in atmospheric CO_2 mixing ratios across a Boston, MA urban to rural gradient. *Land* 2(3), 304–327.

Cantrell C. (2008) Technical Note: Review of methods for linear least-squares fitting of data and application to atmospheric chemistry problems *Atmospheric Chemistry and Physics* 8(17), 5477 – 5487.

Grange S., Lewis A., Carslaw D. (2016) Source apportionment advances using polar plots of bivariate correlation and regression statistics *Atmospheric Environment* 145(), 128–134

Karion A., Callahan W., Stock M. et al. (2020) Greenhouse gas observations from the Northeast Corridor tower network, *Earth System Science Data*, 12, 699–717

McKain K., Wofsy S.C., Nehrkorn T. et al. (2012) Assessment of ground-based atmospheric observations for verification of greenhouse gas emissions from an urban region. *Proceedings of the National Academy of Sciences* https://dx.doi.org/10.1073/pnas.1116645109.

Miles N., Richardson S., Lauvaux T. et al. (2017) Quantification of urban atmospheric boundary layer greenhouse gas dry mole fraction enhancements in the dormant season: Results from the Indianapolis Flux Experiment (INFLUX) *Elementa-Science of the Anthropocene* 5, 27.

Mitchell L., Lin J., Bowling D. et al. (2018). Long-term urban carbon dioxide observations reveal spatial and temporal dynamics related to urban characteristics and growth *Proceedings of the National Academy of Sciences* 115(12), 2912–2917.

Sargent M., Barrera Y., Nehrkorn T. et al. (2018) Anthropogenic and biogenic CO_2 fluxes in the Boston urban area *Proceedings of the National Academy of Sciences*, https://doi.org/10.1073/pnas.1803715115.

Uria-Tellaetxe I. and Carslaw D. (2014) Conditional bivariate probability function for source identification *Environmental Modelling & Software* 59, 1–9,

Verhulst K., Karion A., Kim J. et al. (2017) Carbon dioxide and methane measurements from the Los Angeles Megacity Carbon Project – Part 1: calibration, urban enhancements, and uncertainty estimates *Atmospheric Chemistry and Physics* 17(13), 8313 – 8341.

Vogel F.R., Ishizawa M., Chan E. et al. (2012) Regional non-CO_2 greenhouse gas fluxes inferred from atmospheric measurements in Ontario, Canada. *Journal of Integrative Environmental Sciences*, *9*(sup1), 41–55.

Xueref-Remy I., Dieudonné E., Vuillemin C. et al. (2018) Diurnal, synoptic and seasonal variability of atmospheric CO_2 in the Paris megacity area *Atmospheric Chemistry and Physics* 18(5), 3335–3362.

Yadav V., Ghosh S., Mueller K. et al. (2021) The Impact of COVID-19 on CO_2 Emissions in the Los Angeles and Washington D.C./ Baltimore Metropolitan Areas. *Geophysical Research Letters*, 48(11).

B.c. Greenhouse gas and other trace gas vertical profile measurements

Kenneth J. Davis[1]

[1]Pennsylvania State University, University Park, Pennsylvania, USA

B.c.1 Introduction

Measurements of greenhouse gases (GHGs) and other trace gases are typically collected at discrete altitudes with in situ sensors. This measurement process requires decisions about measurement altitudes, and raises the possibility of multiple measurement altitudes, providing vertical profile measurements. This section describes some basic understanding of trace gas profile measurements in the atmospheric boundary layer, their potential applications to urban GHG flux monitoring, and recommendations for their use in these applications.

B.c.2 Micrometeorological background

Vertical profiles of GHGs and other trace gases are linearly related to the surface fluxes of these gases, but the relationship between these two properties is a highly nonlinear function of the distance above ground, and is strongly dependent on the stability of the atmosphere (Monin and Obhukhov, 1954; Wyngaard and Brost, 1984; Wang et al, 2006). These relationships are rooted in the concept of eddy diffusivity (Stull, 1988; Garratt, 1992),

$$F_C = -K\frac{\partial C}{\partial z}, \qquad (1)$$

where F_C is the flux of the scalar, in this case a trace gas, K is the eddy diffusivity, z is altitude above ground, and dC/dz is the vertical gradient of the mean mole fraction of the trace gas. Note that C represents the mean (typically time-averaged) mole fraction, not an instantaneous measurement that includes turbulent fluctuations. K is strongly dependent on atmospheric stability and altitude above ground.

Surface layer and mixed layer similarity theories provide a rich body of literature on this topic, and these are summarized in many micrometeorological text (e.g. Wyngaard 2010) in addition to a growing body of research literature. Many empirical relationships exist that convert similarity theories into quantitative descriptions of the eddy diffusivity.

Robust similarity theory does not yet exist, however, for heterogeneous surfaces (which includes either heterogeneous fluxes or heterogeneous surface turbulence), or condition where the surface forcing evolves more rapidly than the timescales of turbulent mixing. Large eddy simulations and field experiments can in principle be used to investigate specific conditions, but this is only applicable, at this point, to case studies.

To facilitate this discussion, we define the time-averaged GHG mole fraction at a specific measurement location as,

$$C = \frac{1}{T}\int_0^T c\partial t, \qquad (2)$$

where T is the averaging time, often one hour, chosen to average over microscale turbulent eddies, but to resolve the daily cycle and c is the GHG mole fraction as measured over time at a point in space. We also define the boundary layer mean value of the time-averaged GHG mole fraction as,

$$\langle C\rangle = \frac{1}{h}\int_0^h C\partial z, \qquad (3)$$

where h is the atmospheric boundary layer (ABL) depth. Figure 5 shows a typical near-surface and whole ABL time-averaged GHG mole fraction profile, and the properties defined in equations (2) and (3).

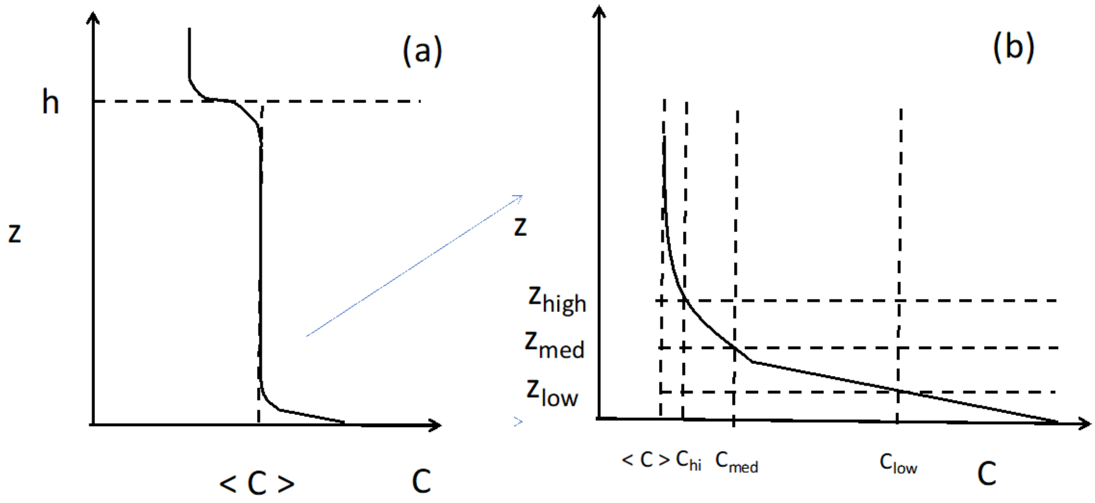

Figure 5: (a) Typical profile of the time-averaged GHG mole fraction vs. altitude above ground showing the ABL depth, h, and the ABL-averaged, time-averaged GHG mole fraction, <C>. (b) Expanded view of the atmospheric surface layer showing the relationship between <C> and the time-averaged mole fractions at three hypothetical measurement altitudes, C_{low}, C_{med} and C_{hi}. This profile would be typical for CH_4 or for CO_2 in the biologically dormant season, where surface fluxes would be positive (into the atmosphere), and the ABL mole fraction is greater than the free tropospheric mole fraction.

B.c.3 Applications

B.c.3.1 Daytime urban GHG enhancements

The fundamental measurement used for most urban GHG emissions estimates is the change in the ABL mean GHG mole fraction between upwind and downwind locations. This quantity ideally represents both a time-averaged, and ABL-averaged quantity,

$$\Delta\langle C\rangle = \langle C^{down}\rangle - \langle C^{up}\rangle, \tag{4}$$

where $<C^{down}>$ is the ABL mean, time-averaged mean mole fraction downwind of the city and $<C^{up}>$ is the ABL mean, time-averaged mean mole fraction upwind of the city. These upwind and downwind ABL mean mole fractions can either be matched in time or the upwind data can be collected prior to the downwind data with an appropriate time lag for advection (Section 4.13; Annex B.I). In practice, however, we rarely if ever measure the true ABL mean mole fraction. Instead we most often collect measurements at a point within the ABL and compute a mole fraction difference between these points,

$$\Delta C = C^{down} - C^{up}, \tag{5}$$

and commonly refer to this quantity, ΔC, as the mole fraction enhancement. We then use an atmospheric model to simulate the urban ABL and compare the modelled version of equation (3) to the measured quantity to infer the urban GHG emissions. Mesoscale atmospheric models often struggle to simulate near-surface vertical gradients accurately, so atmospheric transport uncertainty resulting from the inability to simulate these near-surface gradients is minimized if

$$\Delta C \approx \Delta\langle C\rangle. \tag{6}$$

As shown in Figure 5, mole fractions measured at different altitudes will be offset from the ABL mean by varying amounts. The larger this difference,

$$\Delta C_z = C - \langle C \rangle, \tag{7}$$

the greater the dependence on the atmospheric model to simulate the ABL vertical profile. Vertical profile measurements, for example the difference between a lower and upper altitude, can be used to approximate this offset, as suggested in Figure 5,

$$\Delta C_z \approx C_{med} - C_{high}. \tag{8}$$

In addition to quantifying the degree to which an urban GHG inversion depends on the ability of the atmospheric transport model to simulate the GHG mole fraction vertical profile, the vertical difference can be compared to the urban mole fraction enhancement (3). The sensitivity of the observational setup to the simulation of the vertical GHG profile is minimized if

$$|\Delta C_z| \approx |C_{med} - C_{high}| \ll |\Delta C|. \tag{9}$$

Equations (7) and (4) are proposed as guides for the construction of an urban observational network and can be assessed most easily if vertical profile measurements are collected.

Equation (1) notes that the vertical gradient in ABL GHG mole fractions is a function of the surface flux, the altitude above ground, and the atmospheric stability (or eddy diffusivity), so that site-to-site difference in any of these quantities will lead to site-to-site differences in vertical gradients. These site-to-site differences in the vertical gradient could be misinterpreted as differences in ΔC. Profile measurements should be deployed at representative sites around the study area. If local surface fluxes and stability conditions are known moderately well and vertical profile measurements are not available, flux-gradient relationships (Wang et al, 2007; Moeng and Wyngaard, 1989; Patton et al, 2001), can be used to estimate the GHG mole fraction profile.

The recommendation most commonly used in urban GHG flux studies (e.g. Lauvaux et al, 2016; Miles et al, 2017), is to limit the time period used for urban observations to midday, when turbulence is strong and ABL mean mole fractions are nearly constant with height (Bakwin et al, 1998; Moeng and Wyngaard, 1989). Note again, that we are describing measurements of the mean mole fraction, where time-averaging eliminates turbulent fluctuations. Fast-response, short-term measurements, such as aircraft profiles or time-resolved ground-based measurements, will show turbulent fluctuations. These fluctuations do not represent a failure of micrometeorological theory; they are simply instantaneous realizations of a turbulent atmosphere.

Miles et al, (2017) explored the vertical differences in GHG mole within the INFLUX network and found that, for tower sites with strong local surface fluxes, the mean mole fraction differences in the vertical for measurements within the surface layer can be as large as the mean mole fraction enhancement across the city of Indianapolis, but that this difference decreases rapidly as a function of altitude above ground, consistent with past measurements and models of flux-gradient relationships in the lower portion of the convective boundary layer (Wang et al, 2006; Patton et al, 2001). In the case where the upwind data are chosen to be lagged in time with respect to the downwind measurements, the upwind conditions for a midday to afternoon downwind measurement is likely to be early morning, stably stratified conditions (Karion et al, this report). In this case the vertical gradients are likely to be quite large, and the profile measurements can help to approximate the upwind ABL mean value.

B.c.3.2 Night-time urban GHG enhancements

At night mixing is often weak and the ABL column is typically poorly represented by a single measurement altitude in the stably stratified lower ABL (Bakwin et al, 1998). Measurements of the GHG profile, if obtained from a tall tower (Bakwin et al, 1998; Wang, 2006) can be used to

directly measuring column accumulation up to the ABL top in calm conditions. In calm conditions, the nocturnal boundary layer depth is often only a few hundred meters (Yi et al, 2001; Wang, 2006), and tall communications towers can often span most or all of the depth of this layer. As noted previously, GHG profile measurements can also add valuable information to an inversion system that ingests night-time or early morning data, whether for upwind (Karion et al, this report) or downwind measurements. The use of night-time data in urban inversions is, at this time, experimental, and will rely upon improved understanding of our ability to simulate the nocturnal ABL in urban atmospheric transport reanalyses (Lopez-Coto et al, this report, Lopez-Coto et al., 2020b).

B.c.3.3 Direct flux inference

Vertical GHG gradients are proportional to local fluxes. Profile measurements, therefore, can be used to infer local fluxes. This is the basis of the well known Bowen ratio method of quantifying the surface energy balance (Stull, 1988). Flux-gradient relationships have been adapted to the convective boundary layer and other trace gases (e.g. Davis et al, 1994). This approach for quantifying fluxes has a number of strengths and weaknesses.

The spatial extent of such a flux estimate is both a strength and a weakness. The flux footprint of a vertical gradient is similar to that of an eddy covariance flux measurement (Horst, 1999). The upwind fetch of the fluxes derived from a GHG vertical difference measured at altitudes of tens to a few hundred meters above ground will vary from a few hundred meters to a maximum of a few kilometres depending on stability conditions and altitude above ground of the measurement. Vertical profiles in the lower ABL, therefore, are sensitive to relatively local fluxes. This makes attribution relatively simple. Emissions can also be inferred on an hourly basis since gradients evolve from hour to hour in response to fluxes and turbulence. The clear disadvantage of this approach, similar to eddy covariance flux measurements, is that it would take an unrealistic number of measurement locations to directly quantify the emissions from an entire urban area. Local flux measurements, however, to understand urban flux processes which can then be extrapolated over space and time with flux models and inventories, is a promising route forward (e.g. Wu, 2018).

Unlike eddy covariance measurements, flux-gradient relationships are a more indirect approach to inferring emissions. Flux-gradient relationships also do not yet exist for heterogeneous surfaces. Profile measurements are more likely, therefore, to be valuable as a measure of the relative change in emissions, rather than as a direct flux measurement. Work is underway, for example, to demonstrate the value of tracer ratio methods tied to eddy covariance flux measurements (Wu, 2019).

B.c.4 Complementary nature of GHG profile and other boundary layer measurements

Eddy covariance flux measurements can greatly improve our ability to interpret GHG profile measurements. The vertical gradients measured in the lower ABL (equation 1, Figure 5) are caused by local fluxes. As noted previously, the flux footprint of a vertical gradient is similar to that of an eddy covariance flux measurement (Horst, 1999). The upwind fetch of an eddy covariance flux footprint observed at altitudes of tens to a few hundred meters above ground will vary from a few hundred meters to a maximum of a few kilometres (Kljun et al, 2015; Wang et al, 2008) depending on stability conditions and altitude above ground of the measurement. An eddy covariance system that observes both GHG fluxes and fluxes related to atmospheric stability (momentum flux, latent and sensible heat flux), and mean winds and turbulent kinetic energy (TKE) provides a complete set of micrometeorological data, fluxes and stability, needed to evaluate the GHG profiles and any numerical models used to evaluate these data (Baidar et al, this report; Papale et al, this report). Efforts are underway to integrate eddy covariance measurements into urban GHG emissions studies (Sarmiento et al, 2017; Wu, 2018).

Atmospheric boundary layer profile measurements, particularly continuous, remote profiling with lidar and sodar can also prove highly complementary to GHG profile and eddy covariance measurements (e.g. Helbig et al, 2021). Profiling systems can be used to quantify the depth and vigour of vertical mixing, providing critical context to the GHG profile measurements.

B.c.5. Recommendations

- Measure vertical GHG profiles at sites representative of the urban area. Urban enhancements (equation 3) are the primary observation used at present for urban emission estimates. These enhancements effectively capture emissions from an entire urban area. Ideally the measured enhancements are close approximations to the ABL-averaged enhancement (equation 4). It is generally advantageous, therefore, to collect GHG measurements high enough to avoid strong vertical differences driven by local fluxes that will mix with and complicate interpretation of the urban enhancement (equation 7). The sensitivity of the measurement network to local fluxes and vertical gradients can be assessed with profile measurements at sites representative of your urban area.
- Measure at common altitudes. Measurements collected at common altitudes across your network make comparison across profile measurements easier, since the vertical gradients in the lower ABL are strong functions of altitude above ground.
- Measure GHG profiles at upwind sites to improve background characterization. Vertical profile measurements, particularly on tall communications towers, can provide valuable upwind constraints particularly in stably stratified conditions.
- Measure GHG profiles at urban or downwind sites to explore experimental night-time enhancement measurements. It is likely that night-time measurements can be used to constrain urban emissions as our understanding of the nocturnal, urban boundary layer improves. Vertical profile measurements are likely to contribute to that improved understanding and improve the accuracy of night-time emissions estimates.
- Measure GHG profiles for local flux inference. GHG profiles can be used to infer local fluxes. While absolute quantification with flux-gradient relationships is challenging, relative changes over time can be tracked. Low altitude sampling points are beneficial to this objective.
- Consider coupling vertical GHG profile measurements with eddy covariance flux measurements. Micrometeorological measurements of atmospheric turbulence, energy fluxes, and GHG fluxes are complementary to profile measurements, and enable additional quantification of flux-gradient relationships and local fluxes. Atmospheric profiling using lidar, rawinsondes, sodar or radar are similarly complementary to GHG profile measurements.

B.c.6 References

Bakwin P.S., Tans P.P., Hurst D.F. et al. (1998) Measurements of carbon dioxide on very tall towers: results of the NOAA/CMDL program. *Tellus B: Chemical and Physical Meteorology* 50(5):401–15.

Davis K, Lenschow D.H, Zimmerman P.R. (1994) Biogenic non-methane hydrocarbon emissions estimated from tethered balloon observations. *Journal of Geophysical Research: Atmospheres* 99(D12):25587–98.

Horst TW. (1999) The footprint for estimation of atmosphere-surface exchange fluxes by profile techniques. *Boundary Layer Meteorology* 90(2):171–88.

Kljun N., Calanca P., Rotach M.W. et al. (2015) A simple two-dimensional parameterization for Flux Footprint Prediction (FFP), *Geoscience Model Development*, 8, 3695–3713.

Lauvaux T, Miles N.L, Deng A. et al. (2016) High-resolution atmospheric inversion of urban CO_2 emissions during the dormant season of the Indianapolis Flux Experiment (INFLUX). *Journal of Geophysical Research: Atmospheres* 121(10):5213–36.

Lopez-Coto I., Hicks M., Karion A. et al. (2020) Assessment of Planetary Boundary Layer Parameterizations and Urban Heat Island Comparison: Impacts and Implications for Tracer Transport. *Journal of Applied Meteorology and Climatology* 59(10):1637–53.

Patton E.G., Davis K.J., Barth M.C. et al. (2001) Decaying scalars emitted by a forest canopy: A numerical study. *Boundary Layer Meteorology* 100(1):91–129.

Miles N.L., Richardson S.J., Lauvaux T. et al. (2017) Quantification of urban atmospheric boundary layer greenhouse gas dry mole fraction enhancements in the dormant season: Results from the Indianapolis Flux Experiment (INFLUX). *Elementa: Science of the Anthropocene* 5.

Moeng C.H. and Wyngaard J.C. (1989) Evaluation of turbulent transport and dissipation closures in second-order modelling. *Journal of the Atmospheric Sciences* 46(14): 2311–30.

Monin A.S. and Obukhov A.M. (1954). 'Osnovnye zakonomernosti turbulentnogo peremeshivanija v prizemnom sloe atmosfery (Basic Laws of Turbulent Mixing in the Atmosphere Near the Ground)'. *Trudy Geofiz. Inst.* AN SSSR 24(151): 163–187.

Obukhov A.M. (1946). 'Turbulentnost' v temperaturnoj–neodnorodnoj atmosfere (Turbulence in an Atmosphere with a Non-uniform Temperature)'. *Trudy Inst. Theor. Geofiz.* AN SSSR 1:95–115.

Sarmiento D.P., Davis K.J., Deng A. et al. (2017) A comprehensive assessment of land surface-atmosphere interactions in a WRF/Urban modelling system for Indianapolis, IN. *Elementa: Science of the Anthropocene* 5.

Stull R.B. (1988) An introduction to boundary layer meteorology. *Springer Science & Business Media*.

Wang W., Davis K.J., Yi C. et al. (2007) A note on the top-down and bottom-up gradient functions over a forested site. *Boundary Layer Meteorology* 124(2):305–14.

Wang W. and Davis K.J. (2008) A numerical study of the influence of a clearcut on eddy covariance fluxes of CO_2 measured above a forest. *Agricultural and Forest Meteorology* 148(10):1488–500.

Wyngaard J.C. and Brost R.A. (1984) Top-down and bottom-up diffusion of a scalar in the convective boundary layer. *Journal of Atmospheric Sciences* 41(1):102–12.

Wu K., Lauvaux T., Davis K.J. et al. (2018) Joint inverse estimation of fossil fuel and biogenic CO_2 fluxes in an urban environment: An observing system simulation experiment to assess the impact of multiple uncertainties. *Elementa: Science of the Anthropocene* 6.

Wyngaard J.C. (2010) Turbulence in the Atmosphere. *Cambridge University Press*.

Yi C., Davis K.J., Berger B.W. et al. (2001) Long-term observations of the dynamics of the continental planetary boundary layer. *Journal of the Atmospheric Sciences* 58(10):1288–99.

B.d. Mobile (ground-based) surveys

Felix Vogel[1], Sebastien Ars[1], Thomas Röckmann[2], Irene Xueref-Remy[3]

[1]Environment and Climate Change Canada, Canada

[2]University of Utrecht, The Netherlands

[3]Institut Méditerranéen de Biodiversité et d'Ecologie Marine et Continentale, Universitaires d'Aix-Marseille, France

B.d.1 Introduction

Over recent years mobile ground-based surveys have been used in many studies to detect and quantify greenhouse gas sources and to identify unknown/untapped mitigation potentials. Especially the work on methane sources from facilities and infrastructure has progress significantly.

Many studies have used mobile surveys in combination with tracer release experiments or modelling to infer CH_4 emissions from facilities (landfills, wastewater treatment plants, etc.). Typically, emission rates can be estimated with an uncertainty of 20–50%.

Larger scale studies in urban areas have often focussed on mapping enhancements of atmospheric methane resulting from natural gas infrastructure (von Fischer et al 2017, Weller et al., 2020). These studies were initiated in US cities and used empirical calibrations to translate CH_4 enhancement maps to emission rate estimates (e.g. von Fischer et al. 2017, Weller et al. 2019). Besides individual research studies there are also multiple coordinated efforts underway to accelerate the application of this approach in different regions (e.g. CCAC/UNEP) and to work towards a better scientific understanding as well as training of early career researchers, e.g. in within the MEMO2 project (https://h2020-memo2.eu/).

Beyond these short-term studies targeting specific events of facilities, the use of third-party platforms has emerged as a viable option for city scale monitoring, for example, using a city tram line to collect frequent transect data on GHGs in Salt Lake City (Mitchell et al. 2018).

Campaigns as well as more routine surveys follow similar principles and the core issues to address in our recommendation are survey planning, technical requirements and auxiliary observations.

B.d.2 Survey planning

B.d.2.1 Facility monitoring

The key issues to consider when planning a survey are:

- Ensuring that the observed GHG variability is caused by the target facility. This can be achieved by performing a survey around (or at least upwind of) the site to identify other potential upwind sources that may contribute to the plume seen downwind of the site. Modelling tools or the use of tracer release techniques or tracer-tracer ratio methods could be reasonable alternatives, but in all cases, care must be taken to ensure upwind sources are clearly identified beforehand.

- Ensuring that the observed enhancements are representative to allow upscaling of results, either to monthly or annual emissions, from short-term surveys or to upscale emissions from a few facilities to a whole industrial (sub-)sector. To scale emissions collected during a short-term campaign to e.g. annual totals it is critical to understand if the emissions observed are constant, intermittent and/or predictable by external factors. For example, landfills emission rates can be affected by ambient temperature or atmospheric pressure changes, while many oil and gas related facilities might be affected by operational activities on-site. It is crucial to plan the surveys accordingly, either by revisiting the location or by gathering additional data on external factors and site operations. Another advantage of multiple measurements under different meteorological conditions (esp. wind direction) is that the source location on-site can be triangulated, which can reduce uncertainties if a Gaussian plume is used for emission rate estimation.

B.d.2.2 Urban surveys

When surveying atmospheric GHG in an urban area the issue of representativeness is of prime concern. The measurement plan should aim to reflect the whole domain. If not all roads or areas in a city can be accessed this is even more important as a sampling bias can limit the ability to upscale the results from the survey. Therefore, it is important to consider the right mobile platform beforehand. Public transit vehicles or other vehicles of opportunity do allow frequent revisits which reduces the uncertainty when quantifying temporal changes of emissions but might not allow to cover all areas. Smaller scale platforms like drones and bikes do allow access to more areas, but often have a limited range. Research trucks or cars typically allow larger areas to be covered but might not allow access to all areas in an urban environment.

Another important consideration for the campaign planning is related to the time of the campaign. Methane emissions from some sources (e.g. related to waste) can be influenced by seasonal and meteorological changes as well as differ during daytime and night-time. The campaign planning should reflect this fact.

B.d.3 Technical considerations

Given the wide range of technical considerations for urban GHG measurements this section does not aim for completeness, but rather highlight a few highly relevant aspects specific to vehicle-based measurements. General recommendations on measurements and traceability considerations can, for example, be found in the WMO/GAW GGMT recommendations.

B.d.3.1 Inlet system design

The setup in the vehicle of choice should ensure that the measurements are not contaminated by the vehicle (or passengers) itself as well as not too much influenced by the turbulence created by the vehicle. Typically, inlets installed on top of or on the front of vehicles have been shown to work well. The inlet height can also be a relevant choice. Inlets at the front bumper of vehicles have been shown to be more sensitive to roadside leaks, while higher inlets (e.g. on top of car or streetcars) tend to be preferable when sources are further away. Especially, for measurements around facilities a higher inlet seems suitable as emissions could be released from stacks.

As many instruments provide continuous observations a precise determination of the residence time of the gas in the inlet is critical. Any uncorrected delay in timing would eventually result in a spatial misplacement of an identified mixing ratio enhancement. To avoid too much diffusion in the tubing a residence time of under one minute in the inlet systems is advisable and generally also realizable with current instrumentation.

B.d.3.2 GHG analyser performance

For urban GHG surveys the most relevant quantity is the local GHG enhancement. To properly determine this quantity frequent measurements are required (multiple times per minute) as well as the use of stable instruments. Ideally, the short-term and long-term repeatability of the instrument used should allow a signal to noise ratio of better than 20.

The response time of the instrument should also reflect the platform used and the target spatial resolution, for example: a 1 Hz GHG measurement rate equals a spatial resolution of ca. 3 – 6 m when using a bike or 10 – 20 m when using a car.

Instruments should be calibrated on a regular basis. Frequent calibrations during the campaign are impractical and, in many cases, not required because the target quantity is the signal enhancement above background, but post and pre-campaign calibrations should be achievable in most circumstances.

The detection limit and detection range for urban GHG measurements is considerably higher than for continuous measurement stations and tower sites: CH_4 [1.8 – 20 ppm], CO_2 [300 – 5000 ppm], CO [50 -10000 ppb].

The choice of analyser might also be dependent on the gases investigated. Urban surveys of CH_4 have been conducted successfully in many cities and can also benefit from co-located measurements of $^{13}CH_4$, C_2H_6 or other hydrocarbons. To better interpret CO_2 enhancements (e.g. observed by tram) additional information can be gained from co-located CO, $^{13}CO_2$, NOx or other combustion related species.

B.d.3.3 Additional observations

To use the collected GHG data it is indispensable to provide aligned and accurate information about geolocation. High resolution and high-frequent (1–5Hz) GPS equipment is recommended and additional information from gyroscopes and accelerometers can be valuable. In the dense urban core of larger cities, surrounding buildings can affect the reception of GPS signal, so relying on this system alone can be limiting.

Many previous studies have also included the use of weather stations, but it is unclear if and how the collected data can be best used.

B.d.4 Further recommendations

- IG^3IS should consult with the MEMO-2 consortium and the UNEP/CCAC groups conducting urban methane surveys to continuously improve these recommendations.
- Further investigation of the (empirical) relationship proposed between emission rate of a GHG source and the observed GHG enhancements in different conditions is needed.
- The usefulness and application of mobile weather stations to urban survey studies requires further investigation.

B.d.5 References

Mitchell L.E., Crosman E.T., Jacques A.A. et al. (2018), Monitoring of greenhouse gases and pollutants across an urban area using a light-rail public transit platform, *Atmospheric Environment*, 187, 9–23.

Von Fischer J.C., Cooley D., Chamberlain S. et al. (2017), Rapid, Vehicle-Based Identification of Location and Magnitude of Urban Natural Gas Pipeline Leaks, *Environmental Science & Technology*, 51(7), 4091–4099.

Weller Z.D., Hamburg S.P. and von Fischer J.C. (2020), A National Estimate of Methane Leakage from Pipeline Mains in Natural Gas Local Distribution Systems, *Environmental Science & Technology*, 54(14), 8958–8967.

B.e. In situ airborne GHG mole fraction observations

Huilin Chen[1], Dominik Brunner[2], Joseph Pitt[3], Anke Roiger[4], Isaac Vimont[5]

[1]University of Groningen, The Netherlands

[2]Empa, Dübendorf, Switzerland

[3]Stony Brook University, School of Marine and Atmospheric Sciences, NY, USA

[4] German Aerospace Centre, Institute of Atmospheric Physics, Germany

[5]NOAA Global Monitoring Laboratory, Boulder CO, USA

B.e.1 Introduction

For urban monitoring of GHGs, airborne platforms provide a unique way of making in situ vertical profile measurements and surveying the entire urban area for quantification of surface fluxes, e.g. using a mass balance approach or inverse studies. The mobile platform includes large aircraft (O'Shea et al., 2014; Pitt et al., 2019), small aircraft (Karion et al., 2013; Mays et al., 2009; Klausner et al., 2020), unmanned aerial vehicles (UAVs) (Andersen et al., 2018; Tuzson et al., 2020), and promising helicopters, zeppelin, balloon, etc. Besides GHGs, airborne platforms also provide collocated meteorological measurements, other trace gases, and aerosols.

- Aircraft are suitable to make GHGs measurements to a few kilometres above ground level, sampling the atmosphere within and above the planetary boundary layer. There is usually a lower limit, e.g. ~150 m (500 ft) or ~300 m (1000 ft) over populated areas.
- Small UAVs are an emerging platform that is relatively cheap and suitable to make GHGs measurements from the surface up to a certain altitude, usually ~120 m (400 ft) above ground. UAVs can be flown at different locations, in contrast to fixed locations at which tower measurements are made. However, the horizontal range of UAVs is limited to a few hundred meters, mainly due to strict aviation regulations, not suitable for mass balance studies of the entire urban areas. Furthermore, the UAVs may be useful in quantification of GHGs from facilities, e.g. landfills, farms. In the urban area, UAVs may have stricter regulations compared to aircraft, e.g. a permission may be required to fly during night-time or above ~120 m.
- Other platforms such as helicopters, zeppelin, and balloons may be suitable for sampling the urban atmosphere from near the surface up to a few kilometres and can cover the urban area within a relatively short period (Wong et al., 2012).
- Priority of trace gas and isotope measurements should be given to continuous measurements of CO_2, CH_4, N_2O, discrete flask analyses for $^{14}CO_2$, ^{13}C and ^{2}H in CH_4. Other useful trace gas and isotope measurements include continuous tracers such as CO, C_2H_6, NO_2, H_2O (or RH, T, P) and discrete flask analyses for ^{13}C, ^{14}C, ^{18}O, ^{17}O in CO_2, ^{13}C, ^{2}H in CH_4, O_2/N_2, COS, hydrocarbons for source attribution (Section B.h.).

B.e.2 Data quality

The GHGs mole fraction measurements should be traceable to the WMO scales.

- For elevated regional scale measurements (> a few kilometres), we recommend network compatibility of 5% (or better) of the excess dry air mole fraction over the appropriate regional background
- For elevated local scale measurements (< a few kilometres), we recommend network compatibility of 10% (or better) of the excess dry air mole fraction over the appropriate regional background
- Besides the accuracy of GHGs mole fractions, attention should also be paid to the accuracy of altitude measurements, especially for small UAVs.

B.e.3 Recommendations for in situ airborne observations

- Make continuous measurements of CO_2, CH_4, N_2O and other useful tracers such as CO, C_2H_6, NO_2, H_2O (or RH, T, P), wind speed and wind direction measurements.
- Collect discrete flasks (section B.g) for offline analysis of tracers and isotopes e.g. O_2/N_2, COS, $^{14}CO_2$, ^{13}C and ^2H in CH_4.
- Careful background observations should be measured by UAVs and aircraft unless it has proven that no significant upwind sources are present.
- Make use of the synergy with commercial airliner programs, i.e. the Comprehensive Observation Network for Trace gases by Airliner (CONTRAIL; http://www.cger.nies.go.jp/contrail/index.html) and the In-Service Aircraft for a Global Observing System (IAGOS; https://www.iagos.org/).
- We encourage the development and validation of simultaneous wind speed and direction measurements on the UAVs.
- We encourage the development of quantification techniques using UAVs, e.g. by performing tracer release experiments or comparisons with other methods such as the tracer ratio method, the mobile van method, the integrated open path method.

B.e.4. References

Andersen T., Scheeren B., Peters W. et al. (2018) A UAV-based active AirCore system for measurements of greenhouse gases, *Atmospheric Measurement Techniques*, 11, 2683–2699.

Karion A., Sweeney C., Petron G. et al. (2013) Methane emissions estimate from airborne measurements over a western United States natural gas field. Geophysical Research Letters 40, 4393–4397.

Klausner T., Mertens M., Huntrieser H. et al. (2020) Urban greenhouse gas emissions from the Berlin area: A case study using airborne CO_2 and CH_4 in situ observations in summer *Elementa: Science of the Anthropocene*, 8.

Mays K.L., Shepson P.B., Stirm B.H. et al. (2009) Aircraft-based measurements of the carbon footprint of Indianapolis., *Environmental Science and Technology*, 43, 7816–7823.

O'Shea S.J., Allen G., Fleming Z.L. et al. (2012) Area fluxes of carbon dioxide, methane, and carbon monoxide derived from airborne measurements around Greater London: A case study during summer *Journal of Geophysical Research Atmospheres*, 119, 4940–4952.

Pitt J.R., Allen G., Bauguitte S.J.-B. et al. (2019) Assessing London CO_2, CH_4 and CO emissions using aircraft measurements and dispersion modelling, *Atmospheric Chemistry and Physics*, 19, 8931–8945.

Tuzson B., Graf M., Ravelid J. et al. (2020) A compact QCL spectrometer for mobile, high precision methane sensing aboard drones, *Atmospheric Measurement Techniques* 13, 4715–4726.

Wong C. and Wyles R. (2012) Mapping concentrations of airborne matter to quantify the fugitive emissions discharge rate from a landfill, *Greenhouse Gas Measurement and Managemen*t, 2:1, 50–60.

B.f. Mass balance

Joseph Pitt[1], Doyeon Ahn[2], Kenneth Davis[3], Beniamino Gioli[4], Kristian Hajny[1], Anna Karion[6], Paul Shepson[1]

[1]Stony Brook University, School of Marine and Atmospheric Sciences, NY, USA

[2]The George Washington University, Washington, D.C., USA

[3]Pennsylvania State University, University Park, Pennsylvania, USA

[4]Italian National Research Council, Institute for Biometeorology, Sesto Fiorentino (FI), Italy

[6]National Institute of Standards and Technology (NIST), Gaithersburg, Maryland, USA

B.f.1 Introduction

The principle of mass conservation has been employed to estimate trace gas emissions at spatial scales ranging from very local (e.g. individual emission sources) to global (e.g. box models). This section covers only aircraft mass balance techniques that have been used to quantify bulk urban emissions at the whole-city scale. The mass balance method is a conceptually simple approach that does not involve numerical transport modelling or sophisticated statistical methods. However, it relies on many implicit assumptions, the validity of which must always be considered when applying this approach. This section discusses these assumptions and their practical implications. Guidance on the appropriate use of the mass balance method in the context of other available tools is also given.

Greenhouse gas emission estimates have been made for many cities across the world using an aircraft mass balance approach, including Indianapolis (Mays et al., 2009; Cambaliza et al., 2015; Heimburger et al., 2017), Baltimore, MD-Washington, D.C. (Ren et al., 2018; Ahn et al., 2020), Sacramento (Turnbull et al., 2011; Ryoo et al., 2019), London (O'Shea et al., 2014; Pitt et al., 2019; Ashworth et al., 2020), Berlin (Klausner et al., 2020) and Rome (Gioli et al., 2014). All of these studies are fundamentally based on the conservation of mass principle, which for any trace gas within a given atmospheric volume is represented by the equation:

$$Q = \oiint \underline{F}.d\underline{S} + \iiint \frac{\partial C}{\partial t} dV \qquad (1)$$

Here Q represents the net source of the trace gas within the volume, $\underline{F}$ is the trace gas flux within the atmosphere, which is integrated over the closed surface of the atmospheric volume, and $\partial C/\partial t$ is the rate of change of trace gas concentration, which is integrated over the volume. If the lower surface of this atmospheric volume is taken to be the ground, and the trace gas species is assumed to be chemically inert on the timescale of advection through the volume, source Q represents the net surface emission of trace gas (i.e. emission minus uptake).

For sources with a spatial extent on the order of 10 km or less, it is possible to design an aircraft sampling strategy that enables all terms in Eq. 1 to be explicitly estimated (Gordon et al., 2015; Conley et al., 2017) in order to calculate the net surface emission rate Q. However, in most cases simplifying assumptions are made. A common approach is to assume the concentration within the volume does not change with time, such that the second term on the right-hand side of Eq. 1 can be neglected. By flying closed loops around a city, some studies then solve Eq. 1 directly by calculating the integrated flux through the closed surface bounded by the flight track (Gioli et al., 2014; Ryoo et al., 2019). To estimate the net flux through the upper surface bounding the volume, Ryoo et al. (2019) place this upper surface at the boundary between the convective boundary layer (CBL) and free troposphere, such that the advective flux through the surface can be assumed to be negligible. The turbulent entrainment flux through this upper surface is then calculated using high frequency measurements of trace gas mole fraction and vertical wind speed.

An alternative approach, employed by Gioli et al. (2014), is to place the upper surface of the volume within the free troposphere. This enables the assumption of zero turbulent flux through the surface. Gioli et al. (2014) then estimate the net advective flux through the upper surface using CO_2 concentration measurements from vertical profiles and a mean vertical wind speed calculated as a residual from the measured net mass flow of air through the lateral boundaries of the volume. This measured net mass flow is equal to the volume-integrated horizontal wind divergence. This approach assumes that there is no net change in the mass of air within the volume.

In principle, by explicitly estimating the closed surface flux integral in Eq. 1, these approaches avoid the need to infer a background mole fraction for the species of interest. However, for trace gas species with large background mole fractions, such as CO_2 and CH_4, uncertainty in the measurement of volume-integrated horizontal wind divergence can lead to large uncertainty in the flux estimated using Eq. 1 if this background is not subtracted (for details see Conley et al., 2017). Ryoo et al. (2019) demonstrate the impact of this effect when calculating the total net horizontal flux through a closed cylinder surrounding Sacramento. When raw wind measurements are used to evaluate Eq. 1, Ryoo et al. (2019) show that their flux estimate is highly sensitive to the choice of background value. However, when the average measured wind is used, they find that this sensitivity to the background mole fraction is greatly reduced. Using the average measured wind to evaluate Eq. 1 assumes that the actual flux due to horizontal wind divergence is negligible, in contrast to the approach of Gioli et al. (2014).

The approaches taken by Gioli et al. (2014) and Ryoo et al. (2019), solving Eq. 1 explicitly as a closed surface integral, enabled net urban emission rates to be estimated at spatial scales of 25–40 km. However, the time required for an aircraft to complete a closed loop bounding a larger urban area can render this approach impractical in such cases (unless multiple aircraft are used simultaneously). Most other studies (e.g. Mays et al., 2009; Cambaliza et al., 2015; Ren et al., 2018; Ahn et al., 2020; Turnbull et al., 2011; O'Shea et al., 2014; Klausner et al., 2020) that use a mass balance approach to estimate urban greenhouse gas emissions further simplify Eq. 1, based on the conceptual model shown in Figure 6. Typically, the following set of assumptions are made:

(1) Chemistry can be ignored, so the net source *Q* represents only the net surface emission (i.e. emission minus uptake) of trace gas.

(2) Winds are in steady-state and wind divergence can be neglected, such that the air transits from upwind of the city to downwind of the city at a constant speed.

(3) Net diffusion through the sides of the box shown in Figure 6 is zero.

(4) Either there must be zero net flux through the top of the box (i.e. no entrainment of air from above), or any flux must be accounted for by an appropriate choice of background.

(5) Any concentration changes within the volume (i.e. the second term on the right-hand side of Eq. 1) can be neglected. In general, concentration changes due to entrainment from above or variability in the composition of inflowing air can be handled in the background definition, but concentration changes due to violation of the steady-state wind assumption cannot (e.g. concentration build-up within the box due to storage). Therefore, the winds must be steady enough such that concentration changes can be assumed (or shown) to be zero.

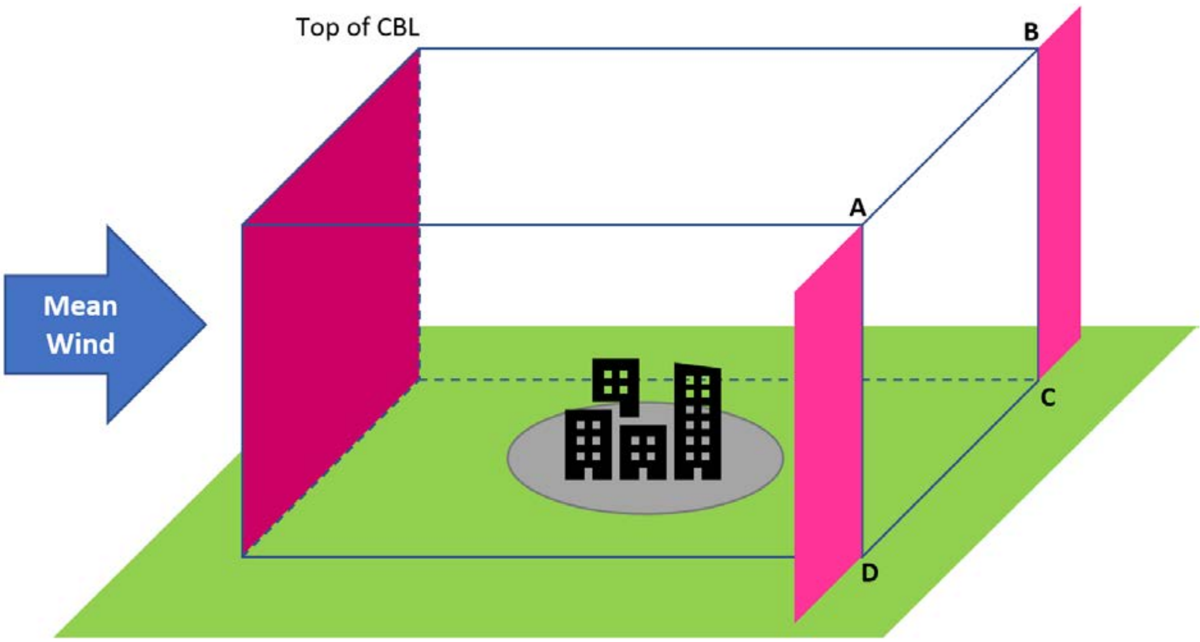

Figure 6: Conceptual model of the mass balance technique applied to measure emissions from an urban area. The two different shades of pink represent two possible choices of background.

On the basis of these assumptions, Eq. 1 can be simplified to:

$$Q_{surface} = \iint \left(X - X_{bgd}\right) n_{air}\, u_{\perp}\, dS_{downwind} \qquad (2)$$

Here $Q_{surface}$ represents the net surface emission rate of species X (in $mol_X\ s^{-1}$), X is the measured trace gas mole fraction, X_{bgd} is the background mole fraction (discussed in detail below), n_{air} is the molar air density (i.e. $mol_{air}\ m^{-3}$), $S_{downwind}$ is a hypothetical vertical surface downwind of the city on which the mole fraction measurements are being taken (bounded by points A, B, C and D in Fig. 6) and $u_{\perp}$ is the wind speed perpendicular to that surface.

Typically, n_{air} is calculated using the ideal gas law, yielding a molar air density that includes moles of water vapour. The trace gas mole fractions X and X_{bgd} should therefore be expressed as “wet” mole fractions, i.e. the moles of trace gas per mole of humid air. While using a dry trace gas mole fraction in Eq. 1 induces only a small bias for winter flights in temperate or polar regions, in high humidity conditions the use of wet mole fractions in Eq. 2 becomes more important.

Assumption (2) above requires that the winds throughout the domain are in steady-state. In such a hypothetical case, the perpendicular wind speed $u_{\perp}$ can be determined by aircraft measurements across the downwind surface $S_{downwind}$. However, in practice the steady-state wind assumption frequently does not hold on typical urban spatial scales. Some studies mitigate the impact of non-steady-state winds over large domains by calculating $u_{\perp}$ from modelled wind values, averaged over the history of the sampled air mass as it transited the domain (Karion et al., 2015; Ahn et al., 2020). Alternatively, if aircraft wind measurements covering the spatial and temporal scales of advection over the urban area can be made, the average measured wind can be used for this purpose (e.g. Ryoo et al., 2019). These approaches do not formally satisfy the assumptions required to reduce Eq. 1 to Eq. 2 but can reduce the error induced by non-steady-state winds in many cases.

In general, assumption 2) represents an important limitation on the use of Eq. 2 to derive mass balance emission rates, as it is often violated in practice. This is especially true at the larger urban spatial scales that, for logistical reasons, motivate the use of Eq. 2 over the explicit solution of the various terms in Eq. 1. It is important that all studies using Eq. 2 take steps to verify the legitimacy of this assumption and assess the potential impact of non-steady-state winds on their emission rate estimates.

B.f.2 Method

Solving Equation 2 requires mole fraction, temperature, pressure and wind measurements covering the spatial extent of the urban emission plume (in both the horizontal and vertical dimensions). Therefore, in situ measurements from research aircraft are well suited for use in conjunction with this method. Remote sensing instruments on board aircraft (Krautwurst et al., 2021) and satellites (Buchwitz et al., 2017; Pandey et al., 2021) have also been employed to estimate greenhouse gas emissions from area sources (or clusters of point sources) using a mass balance approach. Recent improvements in instrument precision may facilitate the increased use of such remote sensing mass balance approaches, including for estimating urban greenhouse gas emissions. However, as the majority of urban mass balance studies have derived emission estimates using in situ measurements in conjunction with Eq. 2, this section focusses on such an approach.

The first approach assumes that trace gas mole fractions are well mixed throughout the CBL, so the measured mole fraction in the downwind plane does not vary with height. Incomplete vertical mixing can be minimized by flying far enough downwind of the city to allow convective mixing to homogenize the CBL. The downwind distance required for complete mixing of the CBL is approximately 3 eddy turnover times (Weil and Horst, 1992), where the eddy turnover time, τ, is defined as:

$$\tau = {}^{z_i}/_{w_*} \qquad (2)$$

Here z_i is the altitude of the inversion above ground and w_* is the convective velocity scale. This can be converted to a distance using the mean boundary layer wind speed, M. Thus one can ensure sampling of a well mixed CBL by conducting measurements a distance of L or more downwind, where:

$$L \gtrapprox 3M\tau \qquad (3)$$

Given typical CBL conditions where z_i = 1000 m, w_* = 1 m s^{-1} and M = 5 m s^{-1}, this yields a recommended downwind distance of L > 15 km. Measurements at multiple heights throughout the boundary layer should be made to verify the vertical mixing, either by flying multiple horizontal transects through the urban emission plume at different heights, or by flying a single horizontal transect supported by vertical profiles within the plume. Eq. 2 is then reduced to a one-dimensional integral of mole fraction across the horizontal extent of the plume, multiplied by the integrated air density within the CBL and the average perpendicular wind (e.g. Turnbull et al., 2011).

Flying more than 15 km distance downwind of the source region can lead to complications. First, the mole fraction enhancement within the urban plume will become increasingly difficult to detect above background variability as the downwind distance increases. Second, the landscape in between the urban boundary and the downwind flight track is likely to include greenhouse gas emissions, and this complicates the task of isolating urban emissions. Thus it is sometimes preferable to fly very close to the urban boundary, in the region where the emission from the city will not yet be well mixed in the vertical.

In cases where emissions from the city are not vertically well mixed, the vertical structure of the plume must be resolved by flying multiple horizontal transects through the urban emission plume at a wide range of heights, covering as much of the CBL as possible. If the spatial distribution of aircraft sampling can be considered a representative sample of the entire downwind surface, the average flux (in mol_X m^{-2} s^{-1}) can simply be multiplied by the downwind surface area to calculate the area-integrated flux (Ahn et al., 2020). Otherwise mole fraction, pressure, temperature and wind measurements from these transects can be interpolated onto a two-dimensional grid covering the downwind surface in order to evaluate the integral in Eq. 2. Alternatively, the flux through the downwind surface can be calculated at each measurement point, then interpolated (for a comparison between these two approaches see Heimburger et al., 2017).

Previous studies have adopted a variety of interpolation methods, with many opting for an approach based on Kriging (Kitanidis, 1997). Tadić et al. (2015) discuss the importance of selecting an appropriate interpolation method for atmospheric data and evaluate multiple possible choices of technique. When working with mass balance data it is usually necessary to account for anisotropy, as discussed by Tadić et al. (2017), who develop a Kriging approach for use with anisotropic data on a cylindrical flight plan encircling an emission source. The most suitable interpolation method inherently varies from case to case, so it is not possible to prescribe a generally applicable approach. All studies should include a preliminary analysis of the data to identify an appropriate interpolation technique.

An important source of uncertainty when flying close to the urban boundary and evaluating Eq. 2 as a two-dimensional integral is the extrapolation of measured data from the lowest transect down to the ground (see discussion in Ryoo et al., 2019). To minimize this uncertainty, the lowest transect should be conducted as close to the ground as airspace and safety requirements allow. Where possible, flight plans should be designed to avoid the presence of strong emission sources just upwind of the transects. Future studies may consider the use of unmanned aerial vehicles (UAVs), aircraft missed approaches, airborne remote sensing, mobile ground measurements, or tall towers to provide mole fraction data below the lowest transect, although in all cases these measurements can be logistically challenging. Where airspace restrictions prevent transects from being conducted in the upper CBL, extrapolation between the highest transect and the CBL height also represents a source of uncertainty.

In all cases vertical profiles are required to estimate the CBL height. The CBL top is defined by the point where turbulence is capped when the atmosphere becomes dynamically stable (Stull, 1988). This is most rigorously defined by the gradient Richardson number, but in convective conditions the virtual potential temperature profile dominates dynamic stability. Gradients in virtual potential temperature, relatively easier to measure at high resolution than mean winds, are often used to define CBL depth (Dai et al., 2014). Direct measurements of atmospheric turbulence, when available, provide a method of determining turbulent mixing depth (Tucker et al., 2009).

Many practical methods of determining the CBL height from meteorological profiles have been tested (Dai et al., 2014). Airborne mass balance studies have employed many of these methods including the maximum virtual potential temperature gradient (Peischl et al., 2015), the height above which potential temperature exceeds a prescribed threshold (Mays et al., 2009), or simply by eye from the vertical structure in trace gas composition (Turnbull et al., 2011; Pitt et al., 2019). In principle trace gas gradients should not be used since they do not represent the stability of the atmosphere, and gradients may not exist even when a stability boundary exists in the atmosphere. In practice, however, the boundary is often also evident in trace gas profiles.

Boundary layer depth can also be measured continuously using remote sensing techniques such as LIDAR (e.g. Melfi et al., 1985; Davis et al., 2000). High-resolution LIDAR data (Kiemle et al., 1997; Grabon et al., 2010) and large eddy simulation studies (e.g. Sullivan et al., 1998) show the complexity of the convective boundary layer top. The instantaneous interface between the boundary layer and the free troposphere is typically thin (although variable in thickness), but the shape of the interface is turbulent and varies across space (Grabon et al., 2010). Definitions of the entrainment zone often confuse and blend these two issues. This confusion is compounded by the fact that a single aircraft profile cuts through this interface at one point, and at an angle. Thus, single in situ aircraft soundings should be viewed as single samples of a complex and turbulent surface, and not as horizontally averaged layers, as typically represented in texts describing the boundary layer (Stull, 1988). These lidar studies also reveal that single soundings of the boundary layer depth are single measurements of a turbulent property whose standard deviation is 5–10% of the CBL depth (Davis et al., 1997). Multiple soundings, or continuous measurement of CBL depth, will reduce sampling error in a property that is linearly related to the estimated urban emission rate.

B.f.3 Background

Implicit in the derivation of Eq. 2 from Eq. 1 is the definition of a background mole fraction, X_{bgd}, representing the mole fraction that would have been measured downwind of the city if there were no emissions from the city. In practice this is not a measurable quantity, so studies typically pick one of two background choices, then based on this choice they try to determine the surface area over which emissions can be considered to contribute to the calculated emission rate. The choice of background and its associated uncertainties is the focus of much of the active discussion regarding the implementation of the mass balance method; here we provide a summary of the two basic approaches commonly used. A broader discussion of background methods used in urban studies is presented in Annex B.l.

The first approach takes the background mole fraction from measurements downwind of the city either side of the plume (i.e. the light pink areas in Figure 6). Heimburger et al. (2017) found that a linear regression between these two edges yielded more consistent results from flight to flight than when a straight average was used; this approach has become typical in the literature. Taking background values downwind of a city minimizes the impact of temporal changes in the composition of the inflowing air. Another advantage is that taking a downwind background loosens assumption 4) above. Rather than requiring that there is no exchange through the top of the mass balance box, with this choice of background we only need to assume that any such exchange is the same both within and either side of the plume. Some studies have reported an urban heat island effect that results in enhanced CBL growth downwind of urban environments (Trainer et al., 1995; Cambaliza et al., 2014). In principle the impact of this effect could be accounted for, provided that the CBL height within and either side of the plume is known (e.g. from vertical profiles) and the free tropospheric mole fraction is well characterized.

Net surface emissions within the footprint of the two downwind edges present an issue with using a downwind background. Both emissions and uptake in these background footprint areas impact the background mole fraction measured either side of the urban plume. The calculated urban enhancement is then a function of the difference in net emission between the urban area and the background footprint, not the net urban emissions alone. This issue can be addressed by accounting for net emissions within the background footprint (for further details see Turnbull et al., 2019), although this approach assumes accurate knowledge of emissions and uptake within this region.

Defining the upwind boundary, within which net surface emissions can be assumed to contribute to the mass balance emission rate calculated using Eq. 2, presents a more complex issue. At a sufficiently large distance upwind, any surface emissions will contribute equally to enhanced mole fraction in the plume and the background, such that they should not be considered to contribute to the calculated mass balance emission rate. The determination of this upwind distance has not received careful study. It has typically been handled in an ad hoc basis within the literature and represents an unresolved issue associated with using a downwind background.

Taking the background mole fraction measurements upwind of a city (i.e. the dark pink region in Figure 6 mitigates the problems described above). In this case the net surface emission contributing to the calculated mass balance emission rate can be taken as the emissions within the area bounded by the upwind and downwind transects (e.g. Klausner et al., 2020).

Furthermore, spatial gradients in inflowing air can be explicitly resolved, and need not be assumed linear.

On the other hand, it is often challenging to design an experiment so that the upwind and downwind sampling are in the Lagrangian frame (i.e. sampling the same air). This renders an upwind background more sensitive to temporal changes in the composition of inflowing air. A practical consequence of the desire for Lagrangian frame sampling is that most studies conduct upwind transects in the late morning, prior to the afternoon downwind sampling. In many cases the CBL height during the upwind sampling is therefore lower than during the downwind sampling. Provided the composition of the air above the upwind CBL is well characterized, a simple dilution calculation could in principle be used to adjust the background mole fraction to account for CBL growth. In all cases, vertical profiles during the upwind sampling are vitally important to determine if CBL growth has occurred, and to account for the impact of any such growth.

As for the downwind sampling, multiple upwind transects may also be required to characterize the upwind background as a function of height if emissions within the footprint of the upwind sampling are not well mixed throughout the CBL. Where possible it is desirable that multiple horizontal transects and vertical profiles are incorporated into the upwind sampling even in well mixed cases, in order to ascertain that the well mixed assumption is justified.

Considering the different issues associated with the choice of either an upwind or a downwind background, where possible it is informative to employ both approaches, enabling a comparison to be made between them. Such an upwind-downwind background comparison was conducted by Ahn et al. (2020), using a numerical transport model to map upwind measurements onto the downwind surface.

The challenges discussed in this section, associated with the determination of the background mole fraction in Eq. 2, motivate the development of methods that are less heavily reliant on such a background choice. In particular, the approach of Ryoo et al. (2019) was shown to be relatively insensitive to background choice in cases where the average wind across the sampling domain was used (assuming zero wind divergence). While logistical constraints may limit the use of such methods for single aircraft studies of large urban areas, this constraint can be overcome when multiple aircraft are available.

B.f.4 Flight Planning

The methodological assumptions inherent in the mass balance method constrain the meteorological conditions under which sampling can take place. In particular, suitable days for an aircraft mass balance experiment require steady-state winds with minimal vertical shear. The ideal wind direction also minimizes nearby upwind sources, reducing spatial variability in the inflowing air.

The upper limit on desirable wind speed is often determined by the signal to noise ratio of the enhancement over background to the background variability. Larger cities with higher total emissions can be sampled under higher wind speeds than smaller cities. For some very large cities (e.g. New York City) aircraft safety constraints may ultimately determine the upper wind speed constraint. Also relevant to the signal to noise ratio is the choice of distance from the urban centre to the location of the downwind transects. As discussed above, flying further away from the urban centre improves mixing throughout the boundary layer but reduces the enhancement over background. As background uncertainty often dominates the uncertainty budget, downwind transects are frequently conducted as close to the urban centre as permitted by airspace restrictions.

The lower limit on wind speed is constrained in part by the accuracy of the aircraft wind measurements, although in practice at wind speeds below about 4 kt (2 m s^{-1}) variability in wind speed and direction often precludes sampling. Other operational requirements include the absence of low clouds, as flying at the requisite range of heights usually involves operating under visual flight rules. Cloudy conditions can also generate non-stationarity due to spatial variability in irradiance. Due to instrument limitations, some aircraft are unable to sample during precipitation events.

Even if adopting a downwind background (as described above), it is always advisable to perform at least one upwind transect to assess the potential impact of upwind emission sources and spatial variability in the inflowing air. As changes in boundary layer height and structure have a significant impact on the assumptions inherent in the mass balance method, vertical profiles are vital for assessing the corresponding uncertainty on the mass balance emission rate calculated using Eq. 2. Clearly there is a trade-off between the number of vertical profiles conducted, the amount of upwind data collected, and the time spent on the downwind transects. Where possible, however, it is beneficial to obtain vertical profile data before and after both the upwind and downwind sampling. The impact of this sampling trade-off can be alleviated through the use of multiple aircraft where available.

B.f.5 Recommendations

The mass balance method relies on many implicit assumptions, as discussed above. In cases where the legitimacy of these assumptions can be verified, the simplicity of the mass balance method renders it an appealing option for estimating net greenhouse gas emissions from urban areas. However, in many cases the assumption of steady-state winds across the space and time of the flights does not hold (Karion et al., 2015; Barkley et al., 2017). Urban aircraft flights cover distances of ~100 km and take hours to complete, often in complex landscapes. Wind fields in these conditions are rarely constant in space nor steady-state in time. At best, filtering for such idealized wind conditions can make it very difficult to obtain a good mass balance flight. At worst, large errors can be introduced by violations of the mass balance assumptions.

Another important source of error stems from the relationship between the chosen background definition and the boundaries of the area to which the mass balance emission rate estimate is assumed to pertain (Pitt et al., 2019; Turnbull et al., 2019). As noted above and in Section B.l., it is not usually possible to isolate the mole fraction enhancement resulting purely from emissions within a prescribed urban boundary. The net emission rate estimated using Eq. 2 is therefore representative of the difference between net emissions within the footprint of the plume measurements and net emissions within the footprint of the background measurements. Due to dispersion, the boundary between these two regions is not well-defined.

Both of these sources of error can be mitigated by interpreting aircraft data with a numerical weather prediction (NWP) model. NWP models run in reanalysis mode (Annex C.a.) are well-tested tools for simulating realistic temporally and spatially varying wind fields. These can be run over urban domains quite readily and can assimilate operational or city-specific regional weather data to improve the accuracy and precision of regional reanalyses (e.g. Deng et al., 2017), and avoid the data limiting, and often error-inducing, steady-wind assumption (Barkley et al., 2017). A simple use of NWP model data (discussed above) is to use the average modelled wind speed to calculate $u_\perp$ in Eq. 2 (Karion et al., 2015; Ahn et al., 2020), where the average is taken along the trajectory of the measured air mass as it crosses the urban domain.

If a reliable prior estimate of the spatial distribution of surface emissions within the domain is available, these data can be combined with a dispersion model, driven using NWP data, to produce a modelled time series of mole fraction enhancements corresponding to the aircraft observations. This approach explicitly represents the transport and dispersion of emissions, including the impact of variable wind speeds. In addition, explicitly modelling the transport of emissions from source to measurement location enables the mole fraction enhancement from emissions within the urban area to be isolated. Emission rate estimates can then be made via either a forward simulation model data matching calculation (Barkley et al., 2017; Karion et al., 2019; Pitt et al., 2019) or via a Bayesian inversion (Brioude et al., 2013; Lopez-Coto et al., 2020). Barkley et al. (2017) show that on meteorologically simple days a model data matching approach agreed fairly well with mass balance estimates, but it also allowed emissions to be calculated on days where the meteorology was not suitable for a mass balance calculation.

The best approach for calculating urban greenhouse gas emissions using aircraft data inevitably depends on the circumstances of each individual study. In cases where steady-state winds can reasonably be assumed (e.g. on small spatial and temporal timescales), urban emissions are spatially separated from other significant emission sources and reliable NWP model data is not available, the purely observation mass balance approach likely represents the best option. If NWP model data is available, but uncertainty regarding the spatial distribution of emissions and/or errors in dispersion modelling limit the ability to accurately model the observed mole fraction enhancements, NWP data can be used to assess the validity of the steady-state wind assumption used in the mass balance calculation (Ahn et al., 2020). If available, other ground-based wind measurements (e.g. ground-based lidar) can also be used to assess the steady-state wind assumption and evaluate NWP fields (Karion et al., 2015). Using the NWP model winds in the mass balance calculation can mitigate the impact of spatially or temporally varying winds in some cases. If a reasonable prior estimate of the spatial distribution of emissions can be obtained, and atmospheric dispersion can be represented with sufficient accuracy, then either a model data matching calculation or a Bayesian inversion may be most suitable, especially in cases where cities are surrounded by other significant emission sources.

The flight conditions and flight planning principles that are ideal for the mass balance calculation are equally ideal for a model-assisted estimate of net urban emissions. Different analysis approaches can be applied to the same sample data set, enabling a comparison between the different emission estimates. Such comparisons can help to identify biases in individual methods and provide a basis for inferring the best approach for any given case.

Averaging emission rate estimates from multiple flights within a short period of time can help to reduce the impact of random errors in all the approaches discussed above. In addition, multiple flights across different months and days of the week are required to capture seasonal and weekly emission patterns. The number of flights required to capture variability on these timescales is the subject of ongoing research. Diurnal emission patterns are difficult to capture using aircraft sampling as a consequence of the stably stratified night-time boundary layer.

B.f.6 References

Ahn D.Y., Hansford J.R., Howe S.T. et al. (2020) Fluxes of Atmospheric Greenhouse-Gases in Maryland (FLAGG-MD): Emissions of Carbon Dioxide in the Baltimore, MD-Washington, D.C. Area, *Journal of Geophysical Research Atmospheres*, 125, 1–23.

Ashworth K., Bucci S., Gallimore P.J. et al. (2020) Megacity and local contributions to regional air pollution: an aircraft case study over London, *Atmospheric Chemistry and Physics*, 20, 7193–7216.

Balashov N.V., Davis K.J., Miles N.L. et al. (2020) Background heterogeneity and other uncertainties in estimating urban methane flux: results from the Indianapolis Flux Experiment (INFLUX), *Atmospheric Chemistry and Physics*, 20, 4545–4559.

Barkley Z.R., Lauvaux T., Davis K.J. et al. (2017) Quantifying methane emissions from natural gas production in northeastern Pennsylvania, *Atmospheric Chemistry and Physics* 17, 13941–13966.

Brioude J., Angevine W.M., Ahmadov R. et al. (2013) Top-down estimate of surface flux in the Los Angeles Basin using a mesoscale inverse modelling technique: assessing anthropogenic emissions of CO, NOx and CO_2 and their impacts, *Atmospheric Chemistry and Physics* 13, 3661–3677.

Buchwitz M., Schneising O., Reuter M. et al. (2017) Satellite-derived methane hotspot emission estimates using a fast data-driven method, *Atmospheric Chemistry and Physics* 17, 5751–5774.

Cambaliza M.O.L., Shepson P.B., Caulton D.R. et al. (2014) Assessment of uncertainties of an aircraft-based mass balance approach for quantifying urban greenhouse gas emissions, *Atmospheric Chemistry and Physics* 14, 9029–9050.

Cambaliza M.O.L., Shepson P.B., Bogner J. et al. (2015) Quantification and source apportionment of the methane emission flux from the city of Indianapolis, *Elementa: Science of the Anthropocene*, 3.

Conley S., Faloona I., Mehrotra S. et al. (2017) Application of Gauss's theorem to quantify localized surface emissions from airborne measurements of wind and trace gases, *Atmospheric Measurement Techniques*, 10, 3345–3358.

Davis K.J., Gamage N., Hagelberg C.R. et al. (2000) An Objective Method for Deriving Atmospheric Structure from Airborne LIDAR Observations, *Journal of Atmospheric and Oceanic Technology*, 17, 1455–1468.

Deng A., Lauvaux T., Davis K.J. et al. (2017) Toward reduced transport errors in a high resolution urban CO_2 inversion system, *Elementa: Science of the Anthropocene*, 5, 20.

Gioli B., Carfora M.F., Magliulo V. et al. (2014) Aircraft mass budgeting to measure CO_2 emissions of Rome, Italy, *Environmental Monitoring and Assessment*, 186, 2053–2066.

Gordon M., Li S.-M., Staebler R. et al. (2015) Determining air pollutant emission rates based on mass balance using airborne measurement data over the Alberta oil sands operations, *Atmospheric Measurement Techniques* 8, 3745–3765.

Grabon J.S., Davis K.J., Kiemle C. et al. (2010) Airborne lidar observations of the transition zone between the convective boundary layer and free atmosphere during the International H2O Project (IHOP) in 2002, *Boundary Layer Meteorology*, 134, 61–83.

Heimburger A.M.F., Harvey R.M., Shepson P.B. et al. (2017) Assessing the optimized precision of the aircraft mass balance method for measurement of urban greenhouse gas emission rates through averaging, *Elementa: Science of the Anthropocene*, 5, 26.

Karion A., Sweeney C., Kort E.A. et al. (2015) Aircraft-Based Estimate of Total Methane Emissions from the Barnett Shale Region, *Environmental Science and Technology*, 49, 8124–8131.

Karion A., Lauvaux T., Lopez-Coto I. et al. (2019) Intercomparison of atmospheric trace gas dispersion models: Barnett Shale case study, *Atmospheric Chemistry and Physics*, 19, 2561–2576.

Kiemle C., Ehret G., Giez A. et al. (1997) Estimation of boundary layer humidity fluxes and statistics from airborne differential absorption lidar (DIAL), *Journal of Geophysical Research Atmospheres*, 102, 29189–29203.

Kitanidis P.K. (1997) Introduction to Geostatistics: Applications in Hydrogeology, *Cambridge University Press*, Cambridge, UK.

Klausner T., Mertens M., Huntrieser H. et al. (2020) Urban greenhouse gas emissions from the Berlin area: A case study using airborne CO_2 and CH_4 in situ observations in summer 2018, *Elementa: Science of the Anthropocene*, 8

Krautwurst S., Gerilowski K., Borchardt J. et al. (2021) Quantification of CH_4 coal mining emissions in Upper Silesia by passive airborne remote sensing observations with the Methane Airborne MAPper (MAMAP) instrument during the CO_2 and Methane (CoMet) campaign, *Atmospheric Chemistry and Physics*, 21, 17345–17371.

Lopez-Coto I., Ren X., Salmon O.E. et al. (2020) Wintertime CO_2, CH_4, and CO Emissions Estimation for the Washington, D.C.–Baltimore Metropolitan Area Using an Inverse Modelling Technique, *Environmental Science and Technology* 54, 2606–2614.

Mays K.L., Shepson P.B., Stirm B.H. et al. (2009) Aircraft-based measurements of the carbon footprint of Indianapolis., *Environmental Science and Technology* 43, 7816–7823.

Melfi S.H., Spinhirne J.D., Chou S.-H. et al. (1985) LIDAR Observations of Vertically Organized Convection in the Planetary Boundary Layer over the Ocean, *Journal of Climate and Applied Meteorology*, 24, 806–821.

O’Shea S.J., Allen G., Fleming Z.L. et al. (2014) Area fluxes of carbon dioxide, methane, and carbon monoxide derived from airborne measurements around Greater London: A case study during summer 2012, *Journal of Geophysical Research Atmospheres* 119, 4940–4952.

Pandey S., Houweling S., Lorente A. et al. (2021) Using satellite data to identify the methane emission controls of South Sudan’s wetlands, *Biogeosciences*, 18, 557–572.

Peischl J., Ryerson T.B., Aikin K.C. et al. (2015) Quantifying atmospheric methane emissions from the Haynesville, Fayetteville, and northeastern Marcellus shale gas production regions, *Journal of Geophysical Research Atmospheres* 120, 2119–2139.

Pitt J.R., Allen G., Bauguitte S.J.-B. et al. (2019) Assessing London CO_2, CH_4 and CO emissions using aircraft measurements and dispersion modelling, *Atmospheric Chemistry and Physics*, 19, 8931–8945.

Ren X., Salmon O.E., Hansford J.R. et al. (2018) Methane Emissions From the Baltimore-Washington Area Based on Airborne Observations: Comparison to Emissions Inventories, *Journal of Geophysical Research Atmospheres* 123, 8869–8882.

Ryoo J.-M., Iraci L.T., Tanaka T. et al. (2019) Quantification of CO_2 and CH_4 emissions over Sacramento, California, based on divergence theorem using aircraft measurements, *Atmospheric Measurement Techniques* 12, 2949–2966.

Stull R.B. (1988) An introduction to boundary layer meteorology, *Kluwer Academic*, Dordrecht, The Netherlands.

Sullivan P.P., Moeng C.-H., Stevens B. et al. (1998) Structure of the Entrainment Zone Capping the Convective Atmospheric Boundary Layer, *Journal of Atmospheric Science*, 55, 3042–3064.

Tadić J.M., Ilić V. and Biraud S. (2015) Examination of geostatistical and machine learning techniques as interpolators in anisotropic atmospheric environments, *Atmospheric Environment*, 111, 28–38.

Tadić J.M., Michalak A.M., Iraci L. et al. (2017) Elliptic Cylinder Airborne Sampling and Geostatistical Mass Balance Approach for Quantifying Local Greenhouse Gas Emissions, *Environmental Science and Technology* 51, 10012–10021.

Trainer M., Ridley B.A., Buhr M.P. et al. (1995) Regional ozone and urban plumes in the southeastern United States: Birmingham, A case study, *Journal of Geophysical Research Atmospheres* 100, 18823.

Tucker S.C., Senff C.J., Weickmann A.M. et al. (2009) Doppler LIDAR Estimation of Mixing Height Using Turbulence, Shear, and Aerosol Profiles, *Atmospheric Measurement Techniques* 26, 673–688.

Turnbull J.C., Karion A., Fischer M.L. et al. (2011) Assessment of fossil fuel carbon dioxide and other anthropogenic trace gas emissions from airborne measurements over Sacramento, California in spring 2009, *Atmospheric Chemistry and Physics*11, 705–721.

Turnbull J.C., Karion A., Davis K.J. et al. (2019) Synthesis of Urban CO_2 Emission Estimates from Multiple Methods from the Indianapolis Flux Project (INFLUX), *Environmental Science and Technology* 53, 287–295.

Weil J.C. and Horst T.W. (1992) Footprint estimates for atmospheric flux measurements in the convective boundary layer, in: *Precipitation Scavenging and Atmosphere-Surface Exchange, vol. 2*, edited by S.E. Schwartz and W.G.N. Slinn, 717–728, Hemisphere Publishing, Washington D.C.

B.g. Discrete flask sampling

Isaac Vimont[1], Jocelyn C Turnbull[2,3], Peter Sperlich[4]

[1]NOAA Global Monitoring Laboratory, Boulder CO, USA

[2]GNS Science, Te Pū Ao, Lower Hutt, New Zealand

[3]CIRES, University of Colorado at Boulder, CO, USA

[4]NIWA, Wellington, New Zealand

B.g.1 Introduction

The use of sampling containers for discrete measurements of greenhouse gases (GHG's) and ozone depleting substances (ODS's) within urban areas is recommended by this working group due to the high level of precision achievable in current laboratory instrumentation relative to in situ sampling, the ability to measure numerous species within the same atmospheric sample, and the ability to measure species that are currently impossible using any other method, namely radiocarbon in CO_2 ($^{14}CO_2$). Sampling containers, or flasks, are the most common method used to capture atmospheric grab samples. However, careful consideration of several factors must be done to ensure the flask sampling method or the materials of the flasks themselves do not corrupt the sample during collection, transport, storage, and analysis. In this section we describe recommended methods for robust sampling of urban atmospheric constituents of interest.

B.g.2. Discrete Sampling system configuration

There are several considerations to take into account for the sampling set up. Firstly, if possible, the discrete system should be installed alongside the paired in situ sampling system. Inlet lines at a common location for both systems are ideal, as this allows for discrete versus in situ comparisons to assist in data quality control, diagnose failures, and directly compare observations from the two systems. The in situ sampling system can also be used to provide quality control checks for pollution events by looking at the variability in the in situ signal throughout the duration of the flask fill.

Secondly, an integrating volume sampling system is highly recommended (Turnbull et al., 2012). This form of sampling system has two main advantages over short, "grab" style sampling techniques. In a "grab" sample, the flask is filled over a short period of a few minutes, which captures a very small window of time and is easily influenced by any small, short-term fluctuations in mole fraction of the species of interest, and which may be difficult to interpret. An integrating sampler collects sample over the course of a set time period (typically one hour), and thus averages over short-term atmospheric fluctuations, and provides a more representative measurement of the overall atmospheric composition. The integrating technique further avoids biasing the sample towards the beginning of sample collection by allowing for collection of equal volume per unit time during pressurization (Turnbull et al., 2012). The integration time puts the discrete sample observations onto the same time step as in situ observations which are commonly averaged to hourly values (Section 4.2, Annex B.b), and model simulations (Section 5, Annex 5) also typically use time steps of one hour.

For mobile surveys both on the ground (Section 4.4, Annex B.d) and in the air (Section 4.5, Annex B.e), grab sampling is usually more appropriate than integrated sampling, as the short-term and spatial variability are of prime interest in these situations. Comparison of grab flask samples with in situ analysers is extremely useful but requires a precise match of the timing of the two systems.

For most analyses, comparison with the same species measured at a background location will be required, with the background considerations being similar to those for other observational methods (Section 4.12, Annex B.l). The wide range of species measured from flasks mean that potential contamination from local sources near the background site need to be considered for every species of interest.

Discrete sampling is, by its nature, limited in frequency. Practical constraints usually determine the sampling frequency. Manual samplers requiring an operator will be limited by access and availability of personnel. Automated sampling systems (e.g. Sweeney et al., 2015; Turnbull et al., 2012; Levin et al., 2020) offer the opportunity for sampling at any time, typically with an option to connect remotely, control the sampling times and monitor performance. Even with automation, flask samples will still need to be exchanged and returned to the laboratory for analysis on a routine basis. Laboratory capacity for flask analysis, and the number of flasks available are also constraints on sampling frequency.

A typical frequency is one flask per week per site, typically collected in the midafternoon, to match the time when models are able to best simulate the atmosphere, and usually on a consistent weekday to reduce the variability in sampling parameters. In some studies, conditional sampling is used to collect samples only when wind conditions mean that the urban emissions will be observed (e.g. Turnbull et al., 2015), although this necessarily biases the results since only certain conditions are sampled. It is well recognized that more frequent flask sampling is beneficial when practicalities allow, and sampling at different times of day and days of week will give insights into diurnal and other variability in emissions.

Collection of paired samples is recommended where practical, such that replicate measurements can be made. This allows assessment of repeatability as well as diagnosing problematic samples for which the pair disagree. In urban settings where signals are large, this is less critical than for background stations. Where in situ measurements are made at the same location, comparison of flask and in situ can provide a similar diagnosis. For some species with limited measurement capacity, most notably $^{14}CO_2$, replicate measurements may be omitted in favour of additional samples.

B.g.3 Sample collection and containment construction

For the preservation of all species of interest, all steps in sample collection, containment, and storage must be carefully considered. Firstly, the materials used in the construction of the collection system and the flasks must be chosen to preserve the integrity of the sample. Some species of interest may require material choices that are not compatible with materials that are necessary for other species. Prioritization of species will become necessary and/or separate sampling systems will be needed. For N_2O, CO, CH_4, CO_2 and their isotope ratios, borosilicate glass flasks with glass valves designed for high-vacuum applications have proven useful. While most polymers can be problematic for some tracers, Viton, PTFE and PCTFE have successfully been applied for the tracers above. Viton o-rings require a thin coating of ultralow vapour pressure vacuum grease, which requires caution. Further, flask air must be dried below 1% H_2O for preservation of the CO_2 mole fraction and for analysis of stable isotopes. Especially for the analysis of $\delta^{18}O$-CO_2, flasks need to be evacuated under heated conditions, to prevent isotopic exchange after sampling. Some programmes pre-fill flasks with dry natural air, zero air or N_2 to prevent leakage of undried ambient air into the flask before sampling. It is worth noting that when flasks are substantially over pressurized with the collected sample air, sampling of wet air into flasks previously stored with dry air can also be problematic.

Typical sampling systems collect between one and five litres of whole air at standard temperature and pressure, and where possible, flask pressures should be at least slightly higher than atmospheric pressure. Many analysis instruments require overpressure for measurements, and the overpressure ensures that any leaks can readily be identified (by lower than expected pressure at analysis) and leakage will usually be out of the flask rather than in. Some systems use smaller flasks with higher pressure to obtain a similar amount of air, but reducing the physical space required (Sweeney et al., 2015). The amount of air required for each analysis, and any other considerations of input pressure, etc., should be taken into account when determining flask size. It may be useful to collect multiple flasks simultaneously to allow analyses of more gases or for replicate analyses to meet data quality objectives.

B.g.4 Species measured, and considerations for individual species

Urban monitoring of greenhouse gases can include a large number of species. We recommend some key species here, but this list is not meant to be exhaustive or restrictive. The essential species recommended for continual monitoring, are CO_2, CO, CH_4. Additionally, the continuous monitoring of these species by in situ analysers is sufficiently precise to allow for direct comparison between flask and in situ samples. These measurements in flasks, with all sites analysed on the same laboratory instrument, are one method for ensuring consistency across in situ analysers within a network.

Radiocarbon measurements of CO_2 ($^{14}CO_2$) are essential for accurate quantification of fossil fuel CO_2 emissions within urban regions (Levin et al., 2003; Turnbull et al., 2006). For urban centres with populations less than 2 million, this measurement must have a precision of better than 2 ‰ in $\Delta^{14}C$ (1σ) in order to quantify small urban enhancements of 1 ppm in CO_2ff (Turnbull et al., 2016). Larger measurement uncertainties may be sufficient in locations with higher enhancements.

Other useful tracers in urban flask samples are stable isotopic measurements of CO_2 and CH_4, which can be used for source apportionment. Less common stable isotopic measurements of CO and N_2O have also been employed, and while these are not done as often, they can be powerful tools to aid understanding of the budgets of these species. Additionally, these measurements traditionally take less air and cost less per sample than radiocarbon analyses, in both cases by a significant amount. Thus, stable isotopic measurements can potentially be made at higher temporal and spatial resolution than radiocarbon.

Other species that are desirable to measure where possible include carbon monoxide (CO), hydrogen (H_2), non-methane hydrocarbons, halocarbons, and carbonyl sulfide (COS). CO and hydrocarbons can provide further information about fossil fuel distribution and storage emissions, while halocarbons may provide constraints on industrial sector emissions. Additionally, Halon-1211 is present only in miniscule amounts in the atmosphere, and thus a Halon-1211 fire extinguisher can be placed near the sampling system to detect leaks of room air into the sampling system, which can assist with data quality control. COS can be used in conjunction with $^{14}CO_2$ to understand the biogenic CO_2 fluxes relative to the fossil fuel emitted fluxes. However, this method is still being developed and careful consideration of other COS sources (such as combustion) must be considered. COS contamination in the sampling containers and drift in reference mixtures used in analyses further complicates the analysis of this species.

SO_2, NOx, O_3, particulates and other air quality species are often useful but typically cannot be measured in the same type of flask sampling system.

B.g.5 References

Davis K.J., Deng A.J., Lauvaux T. et al. (2017). The Indianapolis Flux Experiment (INFLUX): A testbed for developing urban greenhouse gas emission measurements. Elementa-Science of the Anthropocene, 5, 20.

Lauvaux T., Miles N.L., Deng A.J. et al. (2016). High-resolution atmospheric inversion of urban CO_2 emissions during the dormant season of the Indianapolis Flux Experiment (INFLUX). Journal of Geophysical Research Atmospheres, 121(10), 5213–5236.

Levin I., Kromer B., Schmidt M. et al. (2003). A novel approach for independent budgeting of fossil fuel CO_2 over Europe by $^{14}CO_2$ observations. *Geophysical Research Letters*, 30(23).

Levin I., Karstens U., Eritt M. et al. (2020) A dedicated flask sampling strategy developed for Integrated Carbon Observation System (ICOS) stations based on CO_2 and CO measurements and Stochastic Time-Inverted Lagrangian Transport (STILT) footprint modelling, *Atmospheric Chemistry and Physics*, 20, 11161–11180.

Miller J.B., Lehman S.J., Montzka S.A. et al. (2012) Linking emissions of fossil fuel CO_2 and other anthropogenic trace gases using atmospheric (CO_2)-C-14. *Journal of Geophysical Research Atmospheres*, 117, 23.

Nathan B.J., Lauvaux T., Turnbull J.C. et al. (2018). Source Sector Attribution of CO_2 Emissions Using an Urban CO/CO_2 Bayesian Inversion System. *Journal of Geophysical Research Atmospheres*, 123(23), 13611–13621.

Sweeney C., Karion A., Wolter S. et al. (2015) Seasonal climatology of CO_2 across North America from aircraft measurements in the NOAA/ESRL Global Greenhouse Gas Reference Network, *Journal of Geophysical Research: Atmospheres*, 120, 5155–5190.

Turnbull J., Guenther D., Karion A. et al. (2012). An integrated flask sample collection system for greenhouse gas measurements. Atmospheric Measurement Techniques, 5(9), 2321–2327.

Turnbull J.C., Karion A., Davis K.J. et al. (2019). Synthesis of Urban CO_2 Emission Estimates from Multiple Methods from the Indianapolis Flux Project (INFLUX). *Environmental Science & Technology*, 53(1), 287–295.

Turnbull J.C., Miller J.B., Lehman S.J. et al. (2006). Comparison of $^{14}CO_2$, CO, and SF6 as tracers for recently added fossil fuel CO_2 in the atmosphere and implications for biological CO_2 exchange. *Geophysical Research Letters*, 33(1).

Turnbull J.C., Sweeney C., Karion A. et al. (2015). Toward quantification and source sector identification of fossil fuel CO_2 emissions from an urban area: Results from the INFLUX experiment. *Journal of Geophysical Research: Atmospheres*, 120, 10.1002/2014jd022555.

Whetstone J. R. (2018). Advances in urban greenhouse gas flux quantification: The Indianapolis Flux Experiment (INFLUX). *Elementa-Science of the Anthropocene*, 6, 4.

Wu K., Lauvaux T., Davis K.J. et al. (2018). Joint inverse estimation of fossil fuel and biogenic CO_2 fluxes in an urban environment: An observing system simulation experiment to assess the impact of multiple uncertainties. *Elementa-Science of the Anthropocene*, 6, 19.

B.h. Isotope, Correlate Tracer and Tracer Ratio Methods

Jocelyn Turnbull[1,2], Samuel Hammer[3,4], Peter Sperlich[5]

[1]GNS Science, Te Pū Ao, Lower Hutt, New Zealand

[2]CIRES, University of Colorado at Boulder, CO, USA

[3]Institute of Environmental Physics, Heidelberg University, Germany

[4]ICOS Central Radiocarbon Laboratory, Heidelberg University, Germany

[5]NIWA, Wellington, New Zealand

B.h.1 Introduction

Isotopes have long been used to partition and quantify trace gas sources and sinks, taking advantage of the different isotopic content of the various sources. Correlate tracers are tracers that are co-emitted with the greenhouse gas of interest, or emissions are co-located, thus allowing these gases to be used as proxies for the greenhouse gas source sector of interest. Quantitative estimates of GHG source and sink contributions can be drawn from observed changes in atmospheric isotopic composition or the surplus of the correlate tracers using appropriate modelling approaches. In this section, we present the methodology for isotope and tracer methods that are widely used in urban greenhouse gas research.

B.h.2 Recently added fossil fuel CO_2 (CO_2ff)

Radiocarbon (^{14}C) measurements can be used to determine the recently added fossil fuel CO_2 component (CO_2ff) of the atmospheric CO_2 mole fraction. Fossil fuels are entirely devoid of ^{14}C and therefore CO_2ff emissions dilute the relative ^{14}C content of atmospheric CO_2, usually presented as $\Delta^{14}CO_2$, the deviation in per mil (‰) of the $^{14}C/C$ ratio of a sample from an internationally accepted standard activity, corrected for fractionation and decay. Please note that the atmospheric radiocarbon community uses the symbol $\Delta^{14}CO_2$ but applies the definition for the Δ symbol in Stuiver and Polach (1977).

In the ^{14}C method, CO_2ff is determined as the decrease in $\Delta^{14}CO_2$ relative to a background $\Delta^{14}CO_2$ observation (Levin et al., 2003; Turnbull et al., 2016), and therefore the choice of background is critical (Section 4.12, Annex B.l). To calculate the fossil fuel CO_2 component, we can formulate two balance equations, one for the CO_2 mixing ratio and one for its isotopic composition $\Delta^{14}CO_2$:

$$CO_{2obs} = CO_{2bg} + CO_{2ff} + CO_{2npp} + CO_{2h\_res} \qquad (1)$$

$$\Delta_{obs}CO_{2obs} = \Delta_{bg}\, CO_{2bg} + \Delta_{ff}\, CO_{2ff} + \Delta_{npp}\, CO_{2npp} + \Delta_{h\_res}\, CO_{2h\_res} + \Delta_{nuc}\, CO_{2obs} \qquad (2)$$

In equations (1) and (2), CO_2 is the CO_2 mole fraction and Δ is the $\Delta^{14}C$ value of the observation (obs), background (bg), fossil fuel (ff), net primary productivity (npp), heterotopic respiration (h_res) and nuclear contamination (nuc).

In urban CO_2ff observations, the concentrations and their isotopic signature are observable at the background and the measurement sites containing the central part of the information about the urban CO_{2ff} admixture. The remaining terms in equations (1) and (2) account for second-order effects that imply bias corrections. For reasonably chosen background and measurement sites, these biases are modest and can be accounted for (Turnbull et al., 2006; Miller et al., 2012). In the following, we discuss the bias terms in detail:

CO_{2npp}: The CO_2 mole fraction change caused by the Net Primary Production represents the rapid carbon exchange between the atmosphere and the biosphere. The Δ_{npp} signature can thus be set to the Δ signature of the air, as both the photosynthetic uptake and the autotrophic respiration can be approximated by the atmospheric Δ signature. The atmospheric Δ signature can be expressed either by the background Δ_{bg} or by that of the urban measurement Δ_{obs}. It is recommended to choose Δ_{obs} for urban observations since this corresponds to the ^{14}C signature that the urban biosphere assimilates and respires. The formulation of $\Delta^{14}CO_2$ assures that isotope fractionation effects are mathematically removed, so photosynthetic uptake does not alter the atmospheric $\Delta^{14}CO_2$ (Stuiver and Polach, 1977).

$CO_{2h\ res}$: In urban areas, heterotrophic respiration is usually the main bias, as the heterotrophically respired CO_2 reflects the (higher) ^{14}C content of CO_2 fixed in earlier years. A quantitative consideration of this term requires assumptions on the age distribution of the heterotrophically respired carbon and the source strength of the heterotrophic respiration.

$CO_{2\ nuc}$: $^{14}CO_2$ released by nearby nuclear facilities or waste incineration plants burning radioactive waste can be a significant source of bias (Graven and Gruber, 2011, Kuderer et al., 2018). A judicious choice of background can reduce the effect of the nuclear bias for nuclear $^{14}CO_2$ emissions in the far-field. Any nuclear $^{14}CO_2$ emissions between the background and observational site should be avoided. The influence of nuclear $^{14}CO_2$ emissions can be considered a correction term in equation (2) by simulating their impact on the observation sites. Referencing the simulated nuclear $^{14}CO_2$ molecules to the observed CO_2 mole fractions allows the description of the nuclear influence in $\Delta^{14}CO_2$ units (Kuderer et al. 2018).

Depending on how Δ_{npp} signature of the NPP term is approximated, the following two equations result:

$$CO_{2ff} = \frac{CO_{2obs}(\Delta_{obs}-\Delta_{nuc}-\Delta_{bg})}{\Delta_{ff}-\Delta_{bg}} - \frac{CO_{2h\_res}(\Delta_{res}-\Delta_{bg})}{\Delta_{ff}-\Delta_{bg}} \tag{3}$$

$$CO_{2ff} = \frac{CO_{2bg}(\Delta_{obs}-\Delta_{nuc}-\Delta_{bg})}{\Delta_{ff}-\Delta_{bg}} - \frac{CO_{2h\_res}(\Delta_{res}-\Delta_{obs})}{\Delta_{ff}-\Delta_{bg}} \tag{4}$$

The two equations are equivalent, and in most urban cases, where both CO_2 mole fraction and $\Delta^{14}CO_2$ are measured in the same flasks, equation 3 is most appropriate. In cases where CO_2obs is not available, such as when plant material is used to determine $\Delta^{14}CO_2$, equation 4 must be used. In either case, the second term is a bias term to account for the effect of heterotrophic respiration CO_2 sources on $\Delta^{14}CO_2$. This bias is typically modest and can usually be reasonably accounted for (Turnbull et al., 2006; Levin et al., 2011; Miller et al., 2012). In urban areas heterotrophic respiration is usually the main bias, as the respired CO_2 reflects the (higher) ^{14}C content of CO_2 that was fixed a few years earlier. In some locations, ^{14}C produced by nearby nuclear power plants can be a large source of bias (Graven and Gruber, 2011). Judicious choice of background can reduce the effect of these biases, and typically also ensures that ocean sources do not bias the CO_2ff calculation. The formulation of $\Delta^{14}CO_2$ means that fractionation effects are mathematically removed, so photosynthetic uptake does not alter $\Delta^{14}CO_2$ (Stuiver and Polach, 1977).

^{14}C-based CO_2ff measurements can, in principle, be used to evaluate CO_2ff emissions in a similar manner to CO_2 observations in direct analysis (Section 4.2, 4.5, Annex B.b, B.f) and data assimilation systems (Section 5, Annex C), but because they cannot be made in situ, such analysis is likely to be limited by the small number of measurements. Instead, ^{14}C measurements are typically applied in other ways as described, along with other isotope and tracer methods, in the following sections.

B.h.3 Partitioning of CO_2 fluxes into fossil and biogenic components

A common approach is to use ^{14}C observations to partition the observed CO_2 enhancement or "excess" (CO_2xs) into CO_2ff and biogenic CO_2 (CO_2bio) components (e.g. Djuricin et al, 2010). During the dormant season, and with sufficient ^{14}C measurements, it can be possible to generalize this partitioning for a given city or site (e.g. Turnbull et al., 2015) and apply it in combination with in situ CO_2 and CO observations (Annex B.h.6) to obtain a high-resolution time series of CO_2ff and net biogenic CO_2 (CO_2bio) fluxes. It is important to note that to determine CO_2bio, the CO_2 enhancement over the background (CO_2xs) must be determined from observations along with CO_2ff, and for this analysis any bias in CO_2xs (such as from choice of background) will translate directly to bias in CO_2bio.

Furthermore, it is possible to separate fossil and biogenic contributions using the stable isotope $\delta^{13}CO_2$. The challenge is the small differences in the $\delta^{13}C$ source signature of biogenic (C3 plants) and solid and liquid fossil fuels. The study of Vardag et al. (2015) compares the theoretical discriminatory power between biogenic and fossil CO_2 contributions for the different tracers: CO_2, CO, $\delta^{13}CO_2$ and $\Delta^{14}CO_2$ as well as combinations of these in a model study, which they extend with the additional aspect of realistic measurement accuracy. $\Delta^{14}CO_2$ measurements have the largest discriminatory power, whereas CO and $\delta^{13}CO_2$ show comparable performance as CO_2ff surrogate tracers.

Partitioning CO_2 fluxes into fossil and biogenic components can also be achieved by using Atmospheric Potential Oxygen (APO) as a tracer for fossil fuel emissions. Carbon combustion consumes O_2 from the atmosphere, and the resulting O_2/CO_2 change allows different fuels to be distinguished by their oxidative ratios (Pickers, 2016). The oxidative ratios of fossil fuels can range between 1.2 and 1.9, with the global average fossil fuel mix resulting in 1.4 (e.g. Keeling and Manning, 2014), while biospheric APO signals, as well as biofuels, have an average exchange ratio of 1.1. APO is not a direct measurement but is constructed from O_2 (O_2/N_2) and CO_2 measurements, with the advantage that it can be measured continuously. The application of APO as a novel tracer for CO_2ff is a matter of current active research.

B.h.4 Partitioning of CO_2ff fluxes into fossil sectors

Further partitioning of CO_2ff into petroleum, coal and natural gas sources is possible using the stable isotope ^{13}C in CO_2 (e.g. Djuricin et al., 2010, Pugliese et al., 2017). Coal and petroleum have similar $\delta^{13}C$ signatures, and these are also quite similar to the $\delta^{13}C$ signature of C3 plant exchange, whereas natural gas has a strongly different signature. Thus when ^{14}C is used to partition CO_2xs into CO_2ff and CO_2bio, the natural gas component can also be partitioned by assuming the $\delta^{13}C$ values of each source sector. Some considerations:

- The $\delta^{13}C$ values of each fossil fuel source sector vary and may not be well constrained.
- This method requires that the CO_2bio and CO_2ff components are determined separately (typically from ^{14}C measurements).
- The diurnal and seasonal profiles of each source sector (both fossil and biogenic) are different, meaning that careful consideration of the sources of variability and the sampling regime to diagnose it are needed (Vardag et al., 2016).
- The CO_2bio $\delta^{13}C$ value of C3 (most woody plants, grasses in cooler regions) and C4 (some grasses, corn and sugar cane) plants are quite different, and improved characterization of these signatures may be needed. Because the relative abundance of C3 and C4 plants depends on geography, so will the potential of this application. When both plant types are present, the CO_2bio $\delta^{13}C$ may not be easily determined, and in locations with substantial C4 plant sources, this method may not be viable.

B.h.5 Partitioning of CO_2bio fluxes

- Carbonyl sulfide (COS) may be used to diagnose the photosynthetic uptake component of CO_2bio (e.g. Whelan et al., 2018). As yet most COS studies have been at regional scales, and the use in urban areas is under development. COS also has a source from fossil fuel combustion that may be confounding in urban areas.
- $\delta^{18}O$ has been occasionally used to partition respiration fluxes.

B.h.6 Correlate tracer methods

Correlate tracer methods rely on trace gases which have emissions co-located or co-emitted with the greenhouse gas of interest. If the emission ratio of the tracer to the greenhouse gas is known, then the correlate tracer can be used to infer emissions of the greenhouse gas.

To date, the most widely used correlate tracer to study CO_2ff is carbon monoxide (CO). During fossil fuel combustion, CO is co-emitted with CO_2ff as a by-product of incomplete combustion. The CO:CO_2ff ratio (R_{CO}) varies depending on combustion efficiency and any CO removal (e.g. catalytic converters). R_{CO} can also be influenced by other factors including combustion of biogenic materials (wildfires, wood burning in industrial and home settings, bioethanol usage, etc.), CO produced by oxidation of volatile organic compounds (VOCs), and oxidation of CO in the atmosphere.

In principle, these factors could be determined from bottom-up data products, but in practice R_{CO} for a particular location and time period is more easily determined by empirical evaluation from flask measurements of $^{14}CO_2$ and CO (Levin and Karstens, 2007; Vogel et al., 2010, Turnbull et al., 2006, Lopez et al, 2013, Ammoura et al, 2016). Once R_{CO} is established from paired CO and $^{14}CO_2$ measurements, it may be applied to in situ CO measurements to evaluate CO_2ff at high resolution, which can then be applied to further analyses.

- Sufficient observations of ^{14}C-derived CO_2ff and of CO are needed to robustly evaluate R_{CO}, considering the possibilities of spatial, diurnal, seasonal and interannual variability in R_{CO}. Information from other sources may supplement the observations (e.g. Vogel et al., 2010).
- R_{CO} varies by source sector, so that the method is more sensitive to some sectors than others. There can also be substantial variability in R_{CO} within a single sector. For example, traffic is often the largest source of CO in urban areas, but most vehicles produce very little CO and the majority of the traffic CO emissions come from the small number of vehicles with absent or failed catalytic converters (e.g. Bishop and Stedman, 2008).

There is potential for other tracers to be used in a similar manner to R_{CO}, and this area of research is currently in development.

- NO_x is another correlated tracer that is applied in an analogous manner as CO (Lopez et al., 2010) but has been used much less widely. The additional challenge of using NO_x as a CO_2ff correlate tracer is the shorter and variable atmospheric lifetime of NO_x compared to CO. As with CO, the NO_x/CO_2ff emission ratio is dependent on the fossil source type. Nevertheless, the use of NO_x as a correlated tracer is the subject of current research, especially since NO_x can be measured with high resolution and good accuracy from satellites.
- Other tracers may be co-located rather than co-emitted with CO_2ff, and emission ratios may be quite variable. For example, sulfur hexafluoride (SF_6) leaks from electrical facilities are often co-located with electrical CO_2ff emissions and correlate well at the regional scale. However, at the local scale, SF_6 and CO_2ff are often not sufficiently co-located (e.g. Turnbull et al., 2006).

- Some tracers may be correlated with a particular fossil emission sector or sectors. This may be exploited to examine a particular fossil emission sector (Nathan et al., 2018; Coakley et al., 2016). For example, in urban areas, acetylene and benzene primarily produced by vehicles, although care must be taken because they are also emitted by evaporation of spilled fuel (Nathan et al., 2018, LaFranchi et al., 2013). Some refrigerants are used only in particular sectors: HFC-134a is associated with vehicle air conditioning, others with commercial refrigeration, and others with stationary air conditioners (Hu et al., 2015, Miller et al., 2012). Consideration of changes in usage over time, and other possible sources is needed.

B.h.7 Emission flux estimates from tracer ratios.

When emissions of two trace gas species are co-located and their emission strength is linked to one another, the emission ratio of the two species will be preserved under many conditions. Thus if the atmospheric ratio of the two species is measured, then if the emission rate of one species is known, the emission rate of the second species can be inferred.

- CO_2ff:^{222}Rn has been used to determine CO_2ff emission rates in regions where the natural ^{222}Rn flux from the surface is well understood (e.g. van der Laan et al., 2010).
- CH_4:^{222}Rn has been used to determine regional CH_4 emissions (Levin et al., 2021), showing that the limited knowledge of the ^{222}Rn exhalation rate and its spatial and temporal variability is a fundamental limitation for the quantitative use of this approach.
- CH_4:CO_2 ratios have been used to evaluate the CH_4 flux in urban areas. In this case, it is assumed that the urban CO_2 emission rate is much more certain than the urban CH_4 emission rate, and therefore the CH_4 flux can be evaluated from the ratio of the two gases (Plant et al., 2019).
- CO:CO_2ff ratios have been used to evaluate CO emissions from urban areas, in addition to evaluating R_{CO} (Turnbull et al., 2011; Turnbull et al., 2018).

There are a number of considerations:

- Both species must be stable in the atmosphere at the scale of interest.
- The emissions must be co-located at the scale of interest, resulting in a strong correlation between the species in the atmosphere.
- Any incoming background mole fraction in either species must be accounted for.

B.h.8 Partitioning of CH_4 fluxes

- Stable isotopes of CH_4 can be used in a similar manner as for CO_2 isotopes. The predominant urban CH_4 fluxes – natural gas and waste (wastewater, landfills, etc.) – have quite different $^{13}CH_4$ signatures, allowing partitioning of CH_4 by source sector.
- ^2H in CH_4 may also be useful but is less commonly measured.
- Ethane is an excellent correlate tracer for CH_4, as ethane is associated with natural gas emissions but not with waste emissions.

B.h.9 References

Ammoura L., Xueref-Remy I., Vogel F. et al. (2016) Exploiting stagnant conditions to derive robust emission ratio estimates for CO_2, CO and volatile organic compounds in Paris, *Atmospheric Chemistry and Physics*, 16, 15653–15664.

Bishop G.A. and Stedman D.H. (2008) A Decade of Onroad Emissions Measurements, *Environmental Science & Technology*, 42, 1651–1656.

Coakley K.J., Miller J.B., Montzka S.A. et al. (2016) Surrogate gas prediction model as a proxy for $\Delta^{14}C$-based measurements of fossil fuel CO_2, *Journal of Geophysical Research: Atmospheres*, 121, 7489–7505.

Djuricin S., Pataki D.E. and Xu X. (2010) A comparison of tracer methods for quantifying CO_2 sources in an urban region, *Journal of Geophysical Research Atmospheres*, 115, 10.1029/2009jd012236.

Graven H.D. and Gruber N. (2011) Continental-scale enrichment of atmospheric $^{14}CO_2$ from the nuclear power industry: potential impact on the estimation of fossil fuel-derived CO_2, *Atmospheric Chemistry and Physics*, 11, 12339–12349.

Hu L., Montzka S.A., Miller J.B. et al. (2015) US emissions of HFC-134a derived for 2008–2012 from an extensive flask air sampling network, *Journal of Geophysical Research: Atmospheres*, 120, 801–825, 10.1002/2014jd022617.

Keeling R.F. and Manning A.C. (2014). Studies of recent changes in atmospheric O2 content. In *Treatise on Geochemistry: Second Edition* (pp. 385–404).

Kuderer M., Hammer S. and Levin I. (2018). The influence of $^{14}CO_2$ releases from regional nuclear facilities at the Heidelberg $^{14}CO_2$ sampling site (1986–2014). *Atmospheric Chemistry and Physics*, 18(11), 7951–7959.

LaFranchi B.W., Petron G., Miller J.B. et al. (2013) Constraints on emissions of carbon monoxide, methane, and a suite of hydrocarbons in the Colorado Front Range using observations of $^{14}CO_2$, *Atmospheric Chemistry and Physics*, 13, 11101–11120.

Levin I. and Karstens U.T.E. (2007) Inferring high resolution fossil fuel CO_2 records at continental sites from combined $^{14}CO_2$ and CO observations, *Tellus B*, 59, 245–250.

Levin I., Hammer S., Eichelmann E. et al. (2011) Verification of greenhouse gas emission reductions: the prospect of atmospheric monitoring in polluted areas. *Philosophical Transactions of the Royal Society A: Mathematical, Physical and Engineering Sciences*, 369(1943), 1906–1924.

Levin I., Karstens U., Hammer S. et al. (2021) Limitations of the radon tracer method (RTM) to estimate regional greenhouse gas (GHG) emissions–a case study for methane in Heidelberg. *Atmospheric Chemistry and Physics*, 21(23), 17907–17926.

Levin I., Kromer B., Schmidt M. et al. (2003) A novel approach for independent budgeting of fossil fuel CO_2 over Europe by $^{14}CO_2$ observations, *Geophysical Research Letters*, 30, 2194.

Lopez M., Schmidt M., Delmotte M. et al. (2013) CO, NOx and $^{14}CO_2$ as tracers for fossil fuel CO_2: results from a pilot study in Paris during winter 2010, *Atmospheric Chemistry and Physics*, 13, 7343–7358.

Miller J.B., Lehman S.J., Montzka S.A. et al. (2012) Linking emissions of fossil fuel CO_2 and other anthropogenic trace gases using atmospheric $^{14}CO_2$, *Journal of Geophysical Research Atmospheres*, 117, D08302, 10.1029/2011JD017048.

Nathan B., Lauvaux T., Turnbull J.C. et al. (2018) Investigations into the use of multi-species measurements for source apportionment of the Indianapolis fossil fuel CO_2 signal, *Elementa: Science of the Anthropocene*, 6, 10.1525/journal.elementa.131.

Pickers P. (2016). New applications of continuous atmospheric O_2 measurements: meridional transects across the Atlantic Ocean, and improved quantification of fossil fuel-derived CO_2 *Doctoral dissertation, University of East Anglia*.

Plant G., Kort E.A., Floerchinger C. et al. (2019) Large Fugitive Methane Emissions From Urban Centres Along the US East Coast, *Geophysical Research Letters*, 46, 8500–8507, 10.1029/2019GL082635.

Pugliese S.C., Murphy J.G., Vogel F. et al. (2017) Characterization of the $\delta^{13}C$ signatures of anthropogenic CO_2 emissions in the Greater Toronto Area, Canada. *Applied Geochemistry*, 83, 171–180.

Stuiver M. and Polach H.A. (1977) Discussion: Reporting of ^{14}C data, *Radiocarbon*, 19, 355–363.

Turnbull J.C., Karion A., Davis K.J. et al. (2019) Synthesis of urban CO_2 emission estimates from multiple methods from the Indianapolis Flux Project (INFLUX), *Environmental Science and Technology*, 10.1021/acs.est.8b05552.

Turnbull J.C., Graven H.D. and Krakauer N.Y. (2016) Radiocarbon in the atmosphere, in: *Radiocarbon and Climate Change*, edited by: Schuur, E. A. G., Druffel, E. R. M., and Trumbore, S. E., Springer International Publishing, 83–137.

Turnbull J.C., Karion A., Fischer M.L. et al. (2011) Assessment of fossil fuel carbon dioxide and other anthropogenic trace gas emissions from airborne measurements over Sacramento, California in spring 2009, *Atmospheric Chemistry and Physics*, 11, 705–721, 10.5194/acp-11–705–2011.

Turnbull J.C., Miller J.B., Lehman S.J. et al. (2006) Comparison of $^{14}CO_2$, CO and SF_6 as tracers for determination of recently added fossil fuel CO_2 in the atmosphere and implications for biological CO_2 exchange, *Geophysical Research Letters*, 33, L01817, 10.1029/2005GL024213.

Turnbull J.C., Sweeney C., Karion A. et al. (2015) Toward quantification and source sector identification of fossil fuel CO_2 emissions from an urban area: Results from the INFLUX experiment, *Journal of Geophysical Research: Atmospheres*, 120, 10.1002/2014jd022555.

Van der Laan S., Karstens U., Neubert R.E.M. et al. (2010) Observation based estimates of fossil fuel-derived CO_2 emissions in the Netherlands using $\Delta^{14}C$, CO and ^{222}Radon, *Tellus B*, 62, 389–402, 10.1111/j.1600–0889.2010.00493.x.

Vardag S.N., Gerbig C., Janssens-Maenhout G. et al. (2015). Estimation of continuous anthropogenic CO_2: model-based evaluation of CO_2, CO, $\delta^{13}C$ (CO_2) and $\Delta^{14}C(CO_2)$ tracer methods. *Atmospheric Chemistry and Physics*, 15(22), 12705–12729.

Vardag S.N., Hammer S. and Levin I. (2016). Evaluation of 4 years of continuous $\delta^{13}C(CO_2)$ data using a moving Keeling plot method. *Biogeosciences*, 13(14), 4237–4251.

Vogel F.R., Hammer S., Steinhof A. et al. (2010) Implication of weekly and diurnal ^{14}C calibration on hourly estimates of CO-based fossil fuel CO_2 at a moderately polluted site in southwestern Germany, *Tellus B*, 62, 512–520, 10.1111/j.1600–0889.2010.00477.x.

Whelan M.E., Lennartz S.T., Gimeno T.E. et al. (2018) Reviews and syntheses: Carbonyl sulfide as a multi-scale tracer for carbon and water cycles, *Biogeosciences*, 15, 3625–3657.

B.i. Eddy covariance flux observations

Dario Papale[1], Andreas Christen[2], Kenneth Davis[3], Christian Feigenwinter[4], Beniamino Gioli[5], Leena Järvi[6], Bradley Matthews[7], Erik Velasco[8], Roland Vogt[4]

[1] Università degli Studi della Tuscia, Viterbo, Italy

[2]Albert-Ludwigs-Universität Freiburg, Freiburg, Germany

[3]Pennsylvania State University, University Park, Pennsylvania, USA

[4]University of Basel, Department of Environmental Sciences, Basel, Switzerland

[5]Italian National Research Council, Institute for Bioeconomy, Sesto Fiorentino (FI), Italy

[6]University of Helsinki, Institute for Atmospheric and Earth System Research, Finland

[7]University of Natural Resources and Life Sciences, Vienna, Austria

[8]Molina Centre for Energy and the Environment, USA

B.i.1 General introduction to the method

The Eddy Covariance (EC) technique measures the net exchange of one or more scalars between a surface (the footprint) and the atmosphere at high temporal resolution (typically half-hourly). The method is unique in terms of urban greenhouse gas (GHG) monitoring in that it is the only method whereby local net surface-atmosphere fluxes are inferred directly from measurements at single locations. The working assumption is that, under certain conditions the measured turbulent fluxes, properly corrected for other flux components not directly detected (storage, advection, see below) are in equilibrium with net surface-atmosphere exchange integrated over a footprint extending upwind. The footprint of the measurements is variable in time and a function of the measurement height, turbulence and wind direction. It typically extends hundreds of meters around the measurement point. Eddy Covariance can be applied to measure greenhouse gas (GHG) fluxes that can be analysed in relation to emission control strategies applied in the cities (e.g. vehicular traffic limitations, house heating strategies etc.), to infer integral emission factors and integral emission signatures for an entire urban area, to assess the role of urban vegetation in the GHG balance of cities or to assess the accuracy of gridded emissions inventories (e.g. Velasco et al., 2014). Eddy covariance is also used to measure latent and sensible heat fluxes, and the momentum flux, all of which are important drivers of turbulent mixing in the atmospheric boundary layer.

The method provides unique information in terms of temporal resolution and integration of emission sources (e.g. traffic, building emissions, human metabolism etc.) and sinks (e.g. vegetation uptake). It is the only method that measures directly net GHG fluxes over a relatively large area, typically at neighbourhood scale in cities, integrating all the sources and sinks in the footprint. The method is also quasi-instantaneous, as the time from the sources/sinks to the measurement point is in the order of minutes, hence fluxes, particularly under well mixed conditions and when properly processed, represent an instantaneous flux at the surface below. However, it is challenging (but not impossible) to retrieve long-term GHG budget estimates from Eddy Covariance data in urban areas due to changing footprints and the more heterogeneous surface and source/sink patchiness in comparison to more uniform natural ecosystems. The measurements integrate over a relatively small area (up to few square kilometres) and cannot be used to measure the GHG budget of an entire city. Nonetheless, the area of the city sampled flux towers can be expanded by increasing measurement heights and/or by operating multiple stations within the city. Surface exchanges measured using the Eddy Covariance technique have shown good correspondence with high resolution inventory techniques in urban areas (Christen et al. 2011, Gioli et al. 2015, Goret et al. 2019, Ward et al. 2015, Järvi et al., 2019). They have also been used to evaluate the land surface models used in urban meteorological simulations (e.g. Sarmiento et al, 2017). The direct flux measurements at the high temporal resolution offered by the technique are a unique resource also in studying rapid changes in behaviour such as the case of the COVID lockdown analysis done in ICOS very rapidly (Papale et al. 2020) and then in other following studies (Nicolini et al. 2022, Sugawara et al. 2021, Lamprecht et al. 2021) where looking to relative changes in time allowed for a quantification of local emission reductions. Relative changes in time are robust in their estimation and the use of wind sectors can also highlight local differences in the composition of emission sources and sinks. Integrated with other data such vehicular traffic counts can be used to disentangle the different contributions. There are several studies where the Eddy Covariance technique has been applied to measure GHG fluxes and to understand the source / sink dynamics of GHGs in urban areas (e.g. Ao et al. 2014, Christen 2014, Crawford et al. 2011, Crawford et al. 2015, Gioli et al. 2012, Grimmond et al. 2002, Helfter et al 2016, Karl et al. 2017, Järvi et al. 2018, Lietzke et al. 2015, Stagakis et al. 2019, Velasco et al. 2014, Vogt et al. 2005).

B.i.2 Principles of the observational technique

The method is based on high frequency measurements of vertical wind speed and mole fraction of a GHG and through the analysis of the covariance between the two over a pre-fixed integration period. From the covariance, it is possible to calculate the turbulent exchange between the surface and the atmosphere. The measurement system requires an ultrasonic 3D anemometer and a fast gas analyser that must be synchronized. Data are in general collected at a frequency of 10 to 20 Hz in order to capture the smaller eddies that contribute to the turbulent mixing of the GHG. The Eddy Covariance system should ideally be placed high enough above the surface to measure in the well mixed surface layer and avoid the influence of the local elements. The optimal measurement height is above the roughness sublayer which is typically 2–5 times the mean surrounding building height in an urban area (for details see Oke et al. 2017). A second recommendation is that, although GHG emission sources and sinks in the measurement region can be dispersed spatially in a heterogeneous manner, sources and sinks of GHGs in the measurement region should ideally be homogenously distributed; however, this criterion is less critical that the requirement that the urban roughness creating the turbulence should be uniform. This means that an urban Eddy Covariance system should ideally be placed in areas with roughly uniform building heights and densities with regard to approaching flow directions. More details about setting up an EC system in urban environments can be found in Feigenwinter et al. (2012) or Velasco et al. (2010).

Data collected are then processed to apply quality controls and final calculation of the fluxes over an integration period of 30 to 60 minutes typically (i.e. each flux estimates represent the average flux in the integration period).

The flux measured at the measurement point represents the average flux from the variable footprint and is expressed in µmol m^{-2} s^{-1} or nmol m^{-2} s^{-1} depending on the gas species. Improvements in instrumentation have made it relatively easy to measure methane (CH_4) fluxes (Gioli et al. 2012, Helfter et al. 2016, Pawlak and Fortuniak 2016). Other GHG fluxes can also be measured (such as N_2O; Famulari et al. 2010, Järvi et al. 2014 or O_3, Karl et al. 2020) given analysers fast enough (about 10Hz) to detect the high frequency turbulent variations.

The methods and tools for the fluxes quality control and calculation are already well established thanks to the experience in the natural ecosystem applications and for this reason mostly ready to be applied also in the context of urban environments (e.g. Aubinet et al. 2012). Nevertheless the is a strong need to evaluate their direct applicability in the urban environment and the possible adaptation to the urban context or the development of new tests.

B.i.2.1 Flux partitioning

Eddy Covariance measurements of GHGs track the net sources and sinks of the footprint, irrespective of whether they are of fossil fuel or biogenic origin. For CO_2, the net flux is the sum of all fossil fuel emissions, biomass and, in some contexts, garbage burning, and human, plant and soil respiration minus photosynthesis by urban vegetation. Several studies have shown that human respiration can make up a significant fraction (>10%) of total net emissions in densely populated areas (Björkegren & Grimmond, 2018, Järvi et al. 2019, Velasco et al., 2013, Moriwaki & Kanda, 2004). Eddy covariance measurements of CH_4 and N_2O also integrate fossil fuel emissions (leakage, incomplete combustion) and biogenic processes in cities (Christen, 2014, Annex A.b.). Hence a challenge with EC measurements in cities is separating the net emissions into different contributors. This is not straightforward, and for urban applications, no standard method currently exists. Different approaches have shown the potential using modelling for selected processes to remove them (e.g. Järvi et al. 2019), statistical modelling (e.g. Crawford et al. 2014), artificial neural networks (e.g. Menzer et al. 2015) or stable isotope fluxes.

B.i.2.2 Storage and advection fluxes

The Eddy Covariance setup described above measures the exchanges between the urban surface and the atmosphere happening through the turbulent transport. There are however conditions where the turbulence is not sufficient and in these cases the city emissions are either accumulated below the EC system (referred to in the EC literature as the storage flux) and/or transported out through lateral non-turbulent transport (horizontal advection). Situations with low turbulence, however, are less common in cities than over rural or natural surfaces, as the surface layer over a city is much more commonly neutral and unstable due to the significant roughness and the substantial releases of sensible heat, especially at night (Christen and Vogt 2004).

Storage can be calculated using measurements of the mole fraction of the scalar below the EC system (typically along a vertical profile, see for example Bjorkeren et al. 2015; Yi et al, 2000) while for the advection, although there have been tests to measure it (e.g. Yi et al, 2000), the most common approach is to detect periods where advection is likely and remove them from the data set (see for example Aubinet et al. 2012). The complexity of the urban environment may necessitate a different level of complexity in the measurements and methods. The storage component (CO_2 or other gas accumulated below the EC system) can be quite spatially heterogeneous due to the distribution of emission sources and the structure of the city including the near-surface air flow (size of the roads, height of the buildings, presence of trees, etc.) as demonstrated in Crawford et al. (2014). For this reason, the number of mole fraction measurement points needed to estimate the rate of change of storage under the system with high accuracy is larger than the number required for a more homogeneous environment. For the horizontal advection the complexity is in the selection of the threshold level of turbulence (quantified by a threshold in the square root of the momentum flux, also knowns as the friction velocity, u_*) that is site dependent. The methods to estimate this site specific threshold value are based on assumptions that cannot be made in an urban environment and for this reason the only solution available is to use a predefined threshold value that however adds uncertainty in particular to calculate budgets.

B.i.2.3 Footprint estimation

There are different modelling approaches to estimate the footprint of the flux measurements that are in general function of the measurement height, buildings mean height, variability in the surface (e.g. if all the buildings have the same height or if there is large heterogeneity) and wind characteristics (wind speed, wind direction and their variability).

Most of the methods have been developed for aerodynamically homogeneous surfaces and for this reason are not easily applicable to most urban environments. Some of these models are also relatively fast and straightforward to apply (e.g. Kljun et al., 2015) and are typically used as first guess and rough estimate on the extent of the footprint.

There are also more complex models and approaches available that can be used in strongly complex situations like in cities, but they are often difficult to use and resources demanding. The most common approach is based on large eddy simulation modelling that has been also applied for urban footprint estimation (e.g. Glazunov et al. 2016, Auvinen et al. 2017).

Depending on the position of the EC system and the characteristic of the footprint, important and useful information can be also retrieved without a proper estimation of the footprint area but analysing the fluxes for specific wind sectors, for example characterized by a specific source (traffic, heating, vegetation, etc.). This is particularly useful when measurements from the same sector are compared to detect anomalies, peaks and trends (see for example Crawford et al. 2014).

B.i.3 Instrument maintenance

An EC system can be operated unsupervised, yet all sensors require regular standard maintenance, cleaning and factory calibrations. The gas analyser also needs a periodic field calibration to check and correct the readings at zero (an air mixture without the target gas) reading and a known mole fraction (e.g. around 400 ppm for CO_2), with the first more important than the second because it directly affects the mole fraction variation measurements used as basis to calculate the fluxes (see Fratini et al. 2014). Unlike the mole fraction measurements used for urban inversions, which must be calibrated with very high absolute accuracy, EC measurements rely on the fast-response, relative precisions of the sensors, so lower quality gas calibration standards are acceptable (e.g. for CO_2 1 ppm is sufficient).

B.i.4 Companion measurements

Eddy Covariance measurements, while unable to encompass an entire city's GHG emissions, are excellent for studying local processes and testing the process-based models used to estimate fluxes. In the urban environment these models include ecosystem flux models, models or inventories of anthropogenic GHG emissions, and land surface energy balance and momentum flux models. The EC flux measurements are most easily interpreted if local measurements that would be used as inputs to these models are collected simultaneously.

Ecosystem and surface energy balance analyses benefit from on-site measurements of common meteorological variables such as air temperature, relative humidity (in some cases also vertical profiles), air pressure, precipitation and radiation (shortwave up/down and longwave up/down). Additional measurements could also include soil temperature, soil water content, water table depth, soil physical properties and soil heat fluxes in case of vegetated areas present in the footprint. In these cases, other ecosystem properties commonly measured at rural EC sites (including but not limited to leaf area index, above and below ground carbon stocks, species distributions, and leaf chemistry) are also valuable. Urban flux measurements benefit from the long history of ecosystem studies using this technique. Recommended measurements from well known long-term EC measurement programs (NEON, AmeriFlux, ICOS) serve as excellent references.

Information about anthropogenic activities is needed if the objective is to evaluate the mechanisms driving anthropogenic emissions. The variables needed to develop urban emissions inventories provide a sound guide for potential process-level measurements in these settings. The most obvious and useful example is accurate and time-resolved information on vehicular traffic within the footprint, ideally with sensors distributed along the most important and representative roads (e.g. see Buckley et al. 2016). Cameras can be used to count the number of cars or monitor their amount in parking lots in commercial areas. In case of footprints characterized by residential or commercial areas, information about the heating systems is also important and could be collected using consumption and inventory approaches. Finally, although generally not easily accessible, mobility data generally collected by smartphones have been demonstrated to be of extreme interest in identifying emissions coming from humans and vehicles (e.g. Nicolini et al. 2022, Velasco 2021).

B.i.5 Data quality considerations

The assumptions underlying the EC technique are based on a number of conditions that can be difficult to satisfy in an urban environment. One condition is that observations should be made above the roughness sublayer where turbulence is uniform and GHG fluxes from individual sources/sinks are blended. In urban areas, the height of the buildings can be quite heterogeneous, making this condition very difficult to satisfy, and complicating the interpretation of measurements. In addition, in areas where emissions are heterogeneous, the storage component is difficult to estimate accurately (see above) and so only data when turbulence is sufficient can be considered in case storage correction is not feasible. The spatial heterogeneity of emissions and a possible uneven distribution of the wind direction distribution should be also considered if the aim is to calculate a flux value representative of the measurement area. In these cases, Schmutz et al. (2016) propose to use methods based on a directional horizontal averaging, where all the wind sectors and emissions areas are weighted in order to reduce the risk of biases. This approach however can work only when long-term time series are available because a sufficient number of observations are needed also from the less represented sectors.

Data quality check and filtering procedures including stationary test and despiking can be adapted from natural ecosystem studies where significant development has been accomplished (e.g. Vitale et al., 2020). Gap filling can be made using statistical tools already largely applied in natural ecosystems ranging from moving look-up tables to multiple imputation methods and machine learning tools (e.g. see Järvi et al. 2012, Menzer et al. 2015, Schmutz et al. 2016) or simple models of emissions. In all cases however a careful evaluation of the direct applicability of the already existing methods and their adaptation to the specific urban environment conditions is needed.

B.i.6 Sampling location considerations

The choice of sampling location depends on the research objective. For the study of GHG emissions from urban systems we envision three possible objectives: 1) direct measurement of anthropogenic GHG emissions; 2) direct measurement of the GHG fluxes from vegetation within the urban environment and 3) measurements of the surface energy and momentum fluxes that drive atmospheric turbulence. In all cases the limitations noted about the height of the roughness sublayer, heterogeneous turbulence conditions and heterogeneous GHG fluxes should be considered. Sites with relatively homogeneous flux footprints, and with towers that extend above the roughness sublayer are ideal. Siting of an EC flux tower-based on these considerations is a simple matter for low-stature, urban vegetation such as turfgrass, but is more challenging if the objective is to measure anthropogenic GHG emissions which are often mixed with urban vegetation and are often heterogeneous relative to the dimensions of an EC flux footprint, also considering that EC towers cannot be used to measure large point sources (such as chimneys of power plants). In terms of platforms, it is necessary to find a compromise among the technical EC requirements, the legal aspects and the feasibility in terms of maintenance of the instruments. In general, thin and tall telecommunication towers are a good option because they are ready to host sensors and in general accessible. Locating the EC system on a building top is not advisable, as the turbulence near the rooftop could be severely altered by the building, unless a tower can be extended from the top of the building to install the EC system (Feigenwinter et al., 2012). In general, isolated and bulky high-rise buildings should be avoided not only as measurement platforms but also in the footprint as they can cause severe anomalies in the turbulence field making the data difficult to interpret.

B.i.7 Sampling strategy

Short-term (weeks to months) and long-term (years) measurements are both valuable. The high temporal resolution of the EC method enables a site's fluxes to be characterized relatively quickly and the time needed to sample all wind directions sufficiently in the case of a heterogeneous flux footprint. Short-term measurement can be deployed and redeployed across an urban area to capture variability in urban emissions across space. The ability to maintain these systems for years in the same location also enables the establishment of long-term monitoring important to detect trends and patterns. Currently there are between 10 and 20 long-term urban EC stations active in Europe and an estimation of about 40 globally. A coordination of the existing stations is under construction in the context of the ICOS European Research Infrastructure where, also thanks to the Pilot Application in Urban Landscapes (PAUL) Horizon2020 European project, new methods for data processing will be developed and the use of tall towers with large footprint for multiple GHGs monitoring will be tested (https://cordis.europa.eu/project/id/101037319). Shorter-term deployments intended to quantify urban turbulence conditions or for specific local studies have been deployed in different examples in Europe and USA, like the study still ongoing around the city of Indianapolis in the US (Sarmiento et al, 2017).

Today it is also possible to have near-real-time products with the fluxes processed and made available in a few hours, providing useful information for real time ingestion in models or to provide indications in the context of the emissions management by public administrations. Co-location with other instruments to monitor different emission compartments in the footprint would clearly help the attribution and could contribute to an integrated monitoring system. For example, the co-location with isotopes mixing ratios can help the partitioning and attribution of the fluxes to different sources (e.g. Venturi et al., 2020).

B.i.8 References

Ao X., Grimmond C.S.B., Chang Y. et al. (2016), Heat, water and carbon exchanges in the tall megacity of Shanghai: challenges and results, *International Journal of Climatology*, 36(14), 4608–4624, doi:10.1002/joc.4657.

Aubinet M., Vesala T. and Papale D. (Eds.) (2012), *Eddy Covariance*, doi:10.1007/9784–007–2351–1.

Auvinen M., Järvi L., Hellsten A. et al. (2017), Numerical framework for the computation of urban flux footprints employing large eddy simulation and Lagrangian stochastic modelling, *Geoscientific Model Development*, 10(11), 4187–4205, doi:10.5194/gmd-10–4187–2017.

Björkegren A.B., Grimmond C.S.B., Kotthaus S. et al. (2015), CO_2 emission estimation in the urban environment: Measurement of the CO_2 storage term, *Atmospheric Environment*, 122, 775–790, doi:10.1016/j.atmosenv.2015.10.012.

Buckley S.M., Mitchell M.J., McHale P.J. et al. (2016), Variations in carbon dioxide fluxes within a city landscape: Identifying a vehicular influence, Urban *Ecosystems*, 19(4), 1479–1498, doi:10.1007/s11252–013–0341–0.

Christen A. and Vogt R. (2004), Energy and radiation balance of a central European city, *International Journal of Climatology*, 24(11), 1395–1421, doi:10.1002/joc.1074.

Christen A., Coops N.C., Crawford B.R. et al. (2011), Validation of modelled carbon dioxide emissions from an urban neighbourhood with direct eddy covariance measurements, *Atmospheric Environment*, 45(33), 6057–6069, doi:10.1016/j.atmosenv.2011.07.040.

Christen A. (2014), Atmospheric Measurement Techniques to quantify greenhouse gas emissions from cities, *Urban Climate*, 10, 241–260, doi:10.1016/j.uclim.2014.04.006.

Crawford B., Grimmond C.S.B. and Christen A. (2011), Five years of carbon dioxide fluxes measurements in a highly vegetated suburban area, *Atmospheric Environment*, 45(4), 896–905, doi:10.1016/j.atmosenv.2010.11.017.

Crawford B. and Christen A. (2014), Spatial source attribution of measured urban eddy covariance CO_2 fluxes, *Theoretical and Applied Climatology*, 119(3–4), 733–755, doi:10.1007/s00704–014–1124–0.

Famulari D., Nemitz E., Di Marco C. et al. (2010), Eddy covariance measurements of nitrous oxide fluxes above a city, *Agricultural and Forest Meteorology*, 150(6), 786–793, doi:10.1016/j.agrformet.2009.08.003.

Feigenwinter C., Vogt R. and Christen A. (2011), Eddy Covariance Measurements Over Urban Areas, *Eddy Covariance*, 377–397, doi:10.1007/9784–007–2351–1_16.

Fratini G., McDermitt D.K. and Papale D. (2014), Eddy covariance flux errors due to biases in gas concentration measurements: origins, quantification and correction, *Biogeosciences*, 11(4), 1037–1051, doi:10.5194/bg-11–1037–2014.

Gioli B., Toscano P., Lugato E. et al. (2012), Methane and carbon dioxide fluxes and source partitioning in urban areas: The case study of Florence, Italy, *Environmental Pollution*, 164, 125–131, doi:10.1016/j.envpol.2012.01.019.

Gioli B., Gualtieri G., Busillo C. et al. (2015), Improving high resolution emission inventories with local proxies and urban eddy covariance flux measurements, *Atmospheric Environment*, 115, 246–256, doi:10.1016/j.atmosenv.2015.05.068.

Glazunov A., Rannik Ü., Stepanenko V. et al. (2016), large eddy simulation and stochastic modelling of Lagrangian particles for footprint determination in the stable boundary layer, *Geoscientific Model Development*, 9(9), 2925–2949, doi:10.5194/gmd-9–2925–2016.

Goret M., Masson V., Schoetter R. et al. (2019), Inclusion of CO_2 flux modelling in an urban canopy layer model and an evaluation over an old European city centre, *Atmospheric Environment* 3, 100042, doi:10.1016/j.aeaoa.2019.100042.

Grimmond C.S., King T., Cropley F. et al. (2002), Local scale fluxes of carbon dioxide in urban environments: methodological challenges and results from Chicago, *Environmental Pollution* 116, 243–254, doi:10.1016/s0269–7491(01)00256–1.

Helfter C., Tremper A.H., Halios C.H. et al. (2016), Spatial and temporal variability of urban fluxes of methane, carbon monoxide and carbon dioxide above London, UK, *Atmospheric Chemistry and Physics*, 16(16), 10543–10557, doi:10.5194/acp-16–10543–2016.

Järvi L., Nordbo A., Junninen H. et al. (2012), Seasonal and annual variation of carbon dioxide surface fluxes in Helsinki, Finland, in 2006–2010, *Atmospheric Chemistry and Physics*, 12(18), 8475–8489, doi:10.5194/acp-12–8475–2012.

Järvi Leena; Nordbo A., Rannik Ü. et al. (2014), Urban nitrous oxide fluxes measured using the eddy covariance technique in Helsinki, Finland, *Boreal Environment Research* 19(supplement B, 2014): 108–121.

Järvi L., Rannik Ü., Kokkonen T.V. et al. (2018), Uncertainty of eddy covariance flux measurements over an urban area based on two towers, *Atmospheric Measurement Techniques*, 11(10), 5421–5438, doi:10.5194/amt-11–5421–2018.

Järvi L., Havu M., Ward H.C. et al. (2019), Spatial Modelling of Local-Scale Biogenic and Anthropogenic Carbon Dioxide Emissions in Helsinki, *Journal of Geophysical Research: Atmospheres*, 124(15), 8363–8384, doi:10.1029/2018jd029576.

Karl T. et al. (2017), Urban eddy covariance measurements reveal significant missing NOx emissions in Central Europe, *Scientific Reports*, 7(1), doi:10.1038/s41598–017–02699–9.

Karl T. et al. (2020), Studying Urban Climate and Air Quality in the Alps: The Innsbruck Atmospheric Observatory, *Bulletin of the American Meteorological Society*, 101(4), E488–E507, doi:10.1175/bams-d-19–0270.1.

Kljun N., Calanca P., Rotach M.W. et al. (2015), A simple two-dimensional parameterization for Flux Footprint Prediction (FFP), *Geoscientific Model Development*, 8(11), 3695–3713, doi:10.5194/gmd-8–3695–2015.

Lamprecht C., Graus M., Striednig M. et al. (2021), Decoupling of urban CO_2 and air pollutant emission reductions during the European SARS-CoV-2 lockdown. *Atmospheric Chemistry and Physics*, 21(4), 3091–3102, https://doi.org/10.5194/acp-21–3091–2021.

Lietzke B., Vogt R., Feigenwinter C. et al. (2015), On the controlling factors for the variability of carbon dioxide flux in a heterogeneous urban environment, *International Journal of Climatology*, 35(13), 3921–3941, doi:10.1002/joc.4255.

Menzer O., Meiring W., Kyriakidis P.C. et al. (2015), Annual sums of carbon dioxide exchange over a heterogeneous urban landscape through machine learning based gap filling *Atmospheric Environment* 101, 312–327, 10.1016/j.atmosenv.2014.11.006.

Moriwaki R. and M. Kanda (2004), Seasonal and Diurnal Fluxes of Radiation, Heat, Water Vapour, and Carbon Dioxide over a Suburban Area, *Journal of Applied Meteorology*, 43(11), 1700–1710, doi:10.1175/jam2153.1.

Nicolini G., Antoniella G., Carotenuto F. et al. (2022), Direct observations of CO_2 emission reductions due to COVID-19 lockdown across European urban districts. *Science of the Total Environment*, 154662, https://doi.org/10.1016/j.scitotenv.2022.154662.

Oke T.R., Mills G., Christen A. et al. (2017), *Urban Climates*, doi:10.1017/9781139016476.

Papale D., Antoniella G., Nicolini G. et al. (2020) Clear evidence of reduction in urban CO_2 emissions as a result of COVID-19 lockdown across Europe. Integrated Carbon Observation System (ICOS). https://data.icos-cp.eu/objects/w6pTmRGYKqAm3c-siQrg5kgd, accessed 27 October 2021.

Pawlak W. and Fortuniak K. (2016), Eddy covariance measurements of the net turbulent methane flux in the city centre – results of 2-year campaign in Łódź, Poland, *Atmospheric Chemistry and Physics*, 16(13), 8281–8294, doi:10.5194/acp-16–8281–2016.

Sarmiento D.P., Davis K.J., Deng A. et al. (2017), A comprehensive assessment of land surface-atmosphere interactions in a WRF/Urban modelling system for Indianapolis, IN, edited by D. Helmig and P. Palmer, *Elementa: Science of the Anthropocene*, 5, doi:10.1525/elementa.132.

Schmutz M., Vogt R., Feigenwinter C. et al. (2016), Ten years of eddy covariance measurements in Basel, Switzerland: Seasonal and interannual variabilities of urban CO_2 mole fraction and flux, *Journal of Geophysical Research: Atmospheres*, 121(14), 8649–8667, doi:10.1002/2016jd025063.

Stagakis S., Chrysoulakis N., Spyridakis N. et al. (2019), Eddy Covariance measurements and source partitioning of CO_2 emissions in an urban environment: Application for Heraklion, Greece, *Atmospheric Environment*, 201, 278–292, doi:10.1016/j.atmosenv.2019.01.009.

Sugawara H., Ishidoya S., Terao Y. et al. (2021), Anthropogenic CO_2 emissions changes in an urban area of Tokyo, Japan, due to the COVID-19 pandemic: A case study during the state of emergency in April–May 2020, *Geophysical Research Letters*, 48, doi.org/10.1029/2021GL092600.

Velasco E. and Roth M. (2010), cities as net sources of CO_2: Review of atmospheric CO_2 exchange in urban environments measured by eddy covariance technique, *Geography Compass*, 4(9), 1238–1259, https://doi.org/10.1111/j.1749–8198.2010.00384.x.

Velasco E., Perrusquia R., Jiménez E. et al. (2014), Sources and sinks of carbon dioxide in a neighbourhood of Mexico City, *Atmospheric Environment*, 97, 226–238, 10.1016/j.atmosenv.2014.08.018.

Velasco E. (2021) Impact of Singapore's COVID-19 confinement on atmospheric CO_2 fluxes at neighbourhood scale. *Urban Climate* 37, 100822, 10.1016/j.uclim.2021.100822

Venturi S. et al. (2020), Seasonal and diurnal variations of greenhouse gases in Florence (Italy): Inferring sources and sinks from carbon isotopic ratios, *Science of the Total Environment*, 698, 134245, doi:10.1016/j.scitotenv.2019.134245.

Vitale D., Fratini G., Bilancia M. et al. (2020), A robust data cleaning procedure for eddy covariance flux measurements, *Biogeosciences*, 17(6), 1367–1391, doi:10.5194/bg-17–1367–2020.

Vogt R., Christen A., Rotach M.W. et al. (2005), Temporal dynamics of CO_2 fluxes and profiles over a central European city, *Theoretical and Applied Climatology*, 84(1–3), 117–126, doi:10.1007/s00704–005–0149–9.

Yi C., Davis K.J., Bakwin P.S. et al. (2000), Influence of advection on measurements of the net ecosystem-atmosphere exchange of CO_2 from a very tall tower, *Journal of Geophysical Research: Atmospheres*, 105(D8), 9991–9999, doi:10.1029/2000jd900080.

B.j. Ground-based Remote Sensing for Urban Monitoring

Jia Chen[1], Florian Dietrich[1] and Frank Hase[2]

[1]Technical University of Munich, München, Germany

[2]Karlsruhe Institute of Technology, Karlsruhe, Germany

B.j.1 Introduction

In order to quantify the GHG emissions of large area sources such as cities, ground-based remote sensing approaches that determine column average dry air mole fractions are of growing interest. In comparison to the state of the art in situ measurements, they are less influenced by the variation of the planetary boundary layer height and nearby point sources. Furthermore, they are more compatible with the scale of atmospheric models, as they are not only measuring the mole fractions at a certain point next to the surface but in the total column between the instrument and the Sun (Chen et al., 2016b).

As a standard for ground-based remote sensing, the Total Carbon Column Observing Network (TCCON; Wunch et al., 2011) was accepted in the WMO/GAW guideline in 2009 (WMO, 2016). The measurements are subject to strict controls on instrumentations and data analysis. TCCON stations are mainly built to measure the global background mole fractions of GHGs. It is generally difficult to use the delicate stationary high-resolution laboratory FTIR spectrometers for measuring urban GHG mole fraction gradients. However, a subset of TCCON sites located in or near metropolitan areas is useful for quantifying GHG emissions, for example the Pasadena site (Hedelius et al., 2017) or the Tsukuba site near Tokyo (Babenhauserheide et al., 2020).

Therefore, compact and portable solar-tracking Fourier transform infrared (FTIR) spectrometers with relatively low-resolution (0.5 cm-1), such as the EM27/SUN from Bruker (Gisi et al., 2012; Hase et al., 2016) are preferred for urban monitoring. By placing these instruments upwind and downwind of an urban emission source, the mole fraction gradients between at least two instruments are an indication for the urban emissions (Figure 7, Chen et al., 2016b; Dietrich et al., 2020; Hase et al., 2015). Recently, several international campaigns showed that this approach is well suited to quantify the emissions of cities and local sources (Chen et al., 2016b; Dietrich et al., 2020; Hase et al., 2015; Jones et al., 2018; Luther et al., 2019; Makarova et al., 2020; Toja-Silva et al., 2017; Viatte et al., 2017; Vogel et al., 2019; Zhao et al., 2019). However, all these studies were conducted as campaigns and, therefore, were limited in time. In order to better understand the urban carbon cycle, a long-term observation of the urban emissions is necessary.

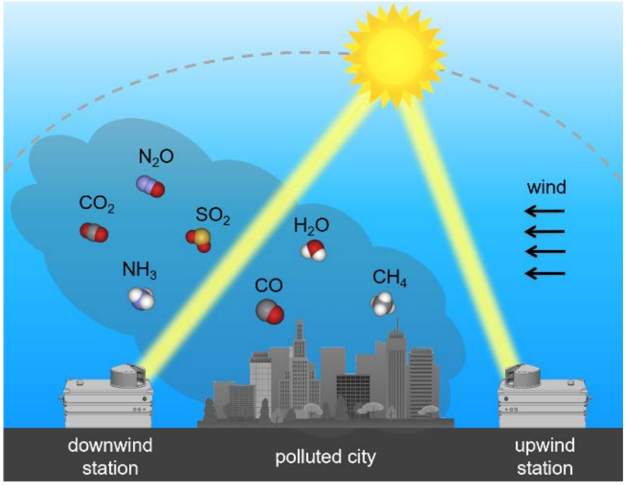

Figure 7: Principle of the differential column methodology (Chen et al., 2016b; Dietrich et al., 2020)

The EM27/SUN spectrometer requires a shelter and additional software solutions achieving autonomous and permanent operation. An automated enclosure system is necessary to protect the instruments (Dietrich et al., 2020; Heinle and Chen, 2018). With the help of such enclosure systems, it is possible to set up ground-based remote sensing networks for long-term operations to observe not only the trend in urban GHG emissions but also to validate urban mole fraction gradients measured by GHG satellites such as OCO-2/3, TROPOMI, MethaneSat, etc.

As TCCON is already defined as a standard for ground-based remote sensing, the compact FTIR spectrometers for urban emission monitoring should follow similar guidelines with regard to instrument calibration and data quality control (Wunch et al., 2011). The following recommendations go beyond these already defined standards.

B.j.2 Instrumentation

The current recommended instrument choice for measuring the urban city gradient is a low-resolution (resolution in the range of ~ 0.2 to 1 cm^{-1}), compact robust FTIR spectrometer, performing solar absorption measurements in the near infrared spectral region (the same spectral region used by TCCON). The choice of the near infrared spectral range allows the co-observation of molecular oxygen column and rationing of the target gas column over the oxygen column delivers the dry air molar fraction. This rationing significantly reduces the propagation of various error sources into the derived GHG abundances (Washenfelder et al., 2006). As source noise is an important degrading impact factor for FTIR observations, the FTIR spectrometer should record DC-coupled interferograms for allowing the compensation of variable atmospheric transmission during recording (Keppel-Aleks et al., 2007). The spectrometer needs to be equipped with an actively controlled solar tracker for ensuring proper line-of-sight control (Gisi et al., 2011). As it has been known for decades that double-sided interferogram recording is highly advantageous over single-sided recording whenever high photometric accuracy is required (e.g. Learner et al., 1995), only spectrometers recording double-sided interferograms should be accepted. Other possible factors compromising photometric accuracy are periodic sampling errors during interferogram recording (Messerschmidt et al., 2010) and detector nonlinearity. For the detection of the presence of these and other detrimental effects, the optical bandpass of the spectrometer needs to be well-defined using suitable optical filters. For the purpose of source attribution, it is desirable that the device also records XCO.

Different low-resolution FTIR spectrometers have been tested for their suitability of measuring GHGs (Chen et al., 2016a; Petri et al., 2012; Sha et al., 2019). Among the spectrometers investigated far, the EM27/SUN spectrometer developed by KIT in collaboration with Bruker and commercially available since 2014 has proven the best characteristics concerning noise level and instrumental stability over periods of several years. This spectrometer therefore should serve as performance benchmark for other devices. An additional spectral channel has been added to the EM27/SUN for measuring XCO (Hase et al, 2016).

B.j.3 Design of a city network

Ground-based remote sensing network design has some commonalities with tower and elevated point network design (see section B.a.), but also differs in some respects. It is necessary to place at least one instrument upwind and one downwind of the city. However, five instruments (one in the centre, one in each compass direction or distributed along the periphery of the region of interest) is the preferred setup when local topography allows, as it always results in instruments being upwind and downwind, regardless of the wind direction (Dietrich et al., 2020; Hase et al., 2015; Vogel et al., 2019).

It is preferable to set up these instruments on rooftops to be not shaded by any obstacles throughout the day and seasons and also allows for a safe long-term operation.

In order to perform the source attribution (see section “tracer-tracer methods”), it is beneficial to measure at least the species CO_2, CH_4 and CO. In addition, it might be helpful to include an extra grating spectrometer in the UV-VIS range to also measure NO_2 and O_3 using the same solar tracker setup (Butz et al., 2017).

B.j.4 Measurements

The optimum integration time is derived as 10 min using Allan variance analysis (Chen et al., 2016b). For resolving high frequency atmospheric signal 5 min integration time is recommended.

In order to ensure and maintain a high precision and accuracy of the column gradient measurement, the instruments of a city need to be calibrated using side by side measurements twice a year. In addition, the calibration of at least one of these instruments with a TCCON instrument is suggested once per year.

For ensuring consistent instrumental performance, the operation of a central testing and calibration facility for the devices is advisable. Each instrument should be tested and calibrated at the central facility. The calibration is commonly performed by performing side by side observations with another instrument. In addition, checks of optical alignment and open path measurements are performed in the framework of the procedure (Frey et al., 2019).

B.j.5 Retrievals

Retrieval algorithms such as GFIT (Wunch et al., 2011) or PROFFAST (Sha et al., 2019) can be used to translate observations to mole fraction values that are intercomparable within different groups and study regions. The recommendation is to store the mole fractions and relevant auxiliary data in a common data format such as NetCDF to combine all important parameters in one file.

The resulting mole fractions should be filtered according to common regulations. This includes cloud-filtering, air mass filtering and averaging.

B.j.6 Results

There are primarily two goals that can be reached using ground-based remote sensing in an urban environment: quantification of urban emissions and validation of the urban-rural gradients measured by GHG satellites. For the first, the mole fraction measurements should be combined with inverse modelling approaches (Annex C) using atmospheric models such as STILT to generate column footprints (Annex C.c.) driven by global meteorological models like ERA5 or GDAS (Annex C.a.). As mentioned in Annex B.l., obtaining accurate background information is essential for a reliable emission determination in the urban area. Background mole fractions can be obtained in different ways. Typically, the background information is taken from one of the upwind stations in the network, depending on the wind direction (Chen et al., 2016b; Dietrich et al., 2020). However, the air mass passing the upwind station does not travel along the downwind station at the same time. Therefore, the optimization of the background mole fraction within an inversion framework is recommended, where the influence of the mole fraction at the city boundary (background) to the city measurements is determined using a Lagrangian particle dispersion model and the travelling time of the air mass is taken into account.

The satellite validation can be done as a by-product of the urban emission network. It can be used to validate not only the absolute mole fractions measured by the satellites but also the mole fraction gradients such as urban-rural gradients.

B.j.7 References

Babenhauserheide A., Hase F. and Morino I. (2020). Net CO_2 fossil fuel emissions of Tokyo estimated directly from measurements of the Tsukuba TCCON site and radiosondes. *Atmospheric Measurement Techniques* 13, 2697–2710. https://doi.org/10.5194/amt-13–2697–2020

Butz A., Dinger A.S., Bobrowski N. et al. (2017). Remote sensing of volcanic CO_2, HF, HCl, SO2, and BrO in the downwind plume of Mt. Etna. *Atmospheric Measurement Techniques* 10, 1–14. https://doi.org/10.5194/amt-10–1–2017

Chen J., Samra J., Wofsy S. et al. (2016a). Diffuser-based solar-tracking with camera for atmospheric measurements. WO2016187502A1.

Chen J., Viatte C., Hedelius J.K. et al. (2016b). Differential column measurements using compact solar-tracking spectrometers. *Atmospheric Chemistry and Physics* 16, 8479–8498. https://doi.org/10.5194/acp-16–8479–2016

Dietrich F., Chen J., Voggenreiter B. et al. (2020) Munich permanent urban greenhouse gas column observing network. *Atmospheric Measurement Techniques*, in review.

Frey M., Sha M.K., Hase F. et al. (2019) Building the COllaborative Carbon Column Observing Network (COCCON): long-term stability and ensemble performance of the EM27/SUN Fourier transform spectrometer. *Atmospheric Measurement Techniques* 12, 1513–1530. https://doi.org/10.5194/amt-12–1513–2019

Gisi M., Hase F., Dohe S. et al. (2011) Camtracker: a new camera controlled high precision solar tracker system for FTIR spectrometers. *Atmospheric Measurement Techniques* 4, 47–54. https://doi.org/10.5194/amt-47–2011

Gisi M., Hase F., Dohe S. et al. (2012) XCO_2 measurements with a tabletop Fourier transform spectrometry (FTS) using solar absorption spectroscopy. *Atmospheric Measurement Techniques* 5, 2969–2980.

Hase F., Frey M., Blumenstock T. et al. (2015) Application of portable FTIR spectrometers for detecting greenhouse gas emissions of the major city Berlin. *Atmospheric Measurement Techniques* 8, 3059–3068.

Hase F., Frey M., Kiel M. et al. (2016) Addition of a channel for XCO observations to a portable FTIR spectrometer for greenhouse gas measurements. *Atmospheric Measurement Techniques* 9, 2303–2313. https://doi.org/10.5194/amt-9–2303–2016

Hedelius J.K., Feng S., Roehl C.M. et al. (2017) Emissions and topographic effects on column CO_2 (X CO_2) variations, with a focus on the Southern California Megacity. *Journal of Geophysical Research: Atmospheres* 122, 7200–7215. https://doi.org/10.1002/2017JD026455

Heinle L. and Chen J. (2018) Automated enclosure and protection system for compact solar-tracking spectrometers. *Atmospheric Measurement Techniques* 11, 2173–2185. https://doi.org/10.5194/amt-11–2173–2018

Jones T., Franklin J., Chen J. et al. (2018) Estimating methane emissions from cities using Portable Ground-based Total Column Spectrometers. *AGU Fall Meeting Abstracts* 52.

Keppel-Aleks G., Toon G.C., Wennberg P.O. et al. (2007) Reducing the impact of source brightness fluctuations on spectra obtained by Fourier transform spectrometry. *Appl. Opt.*, AO 46, 4774–4779. https://doi.org/10.1364/AO.46.004774

Learner R.C.M., Thorne A.P., Wynne-Jones I. et al. (1995) Phase correction of emission line Fourier transform spectra. *Journal of the Optical Society of America A* 12, 2165–2171. https://doi.org/10.1364/JOSAA.12.002165

Luther A., Kleinschek R., Scheidweiler L. et al. (2019) Quantifying CH_4 emissions from hard coal mines using mobile Sun-viewing Fourier transform spectrometry. *Atmospheric Measurement Techniques* 12, 5217–5230. https://doi.org/10.5194/amt-12–5217–2019

Makarova M.V., Alberti C., Ionov D.V. et al. (2020) Emission Monitoring Mobile Experiment (EMME): an overview and first results of the St. Petersburg megacity campaign-2019. *Atmospheric Measurement Techniques Discussions* 1–45. https://doi.org/10.5194/amt-2020–87

Messerschmidt J., Macatangay R., Notholt J. et al. (2010) Side by side measurements of CO_2 by ground-based FTS. *Tellus B: Chemical and Physical Meteorology* 62, 749–758. https://doi.org/10.1111/j.1600–0889.2010.00491.x

Petri C., Warneke T., Jones N. et al. (2012) Remote sensing of CO_2 and CH_4 using solar absorption spectrometry with a low-resolution spectrometer. *Atmospheric Measurement Techniques* 5, 1627–1635. https://doi.org/10.5194/amt-5–1627–2012

Sha M.K., Mazière M.D., Notholt J. et al. (2019) Intercomparison of low and high resolution infrared spectrometers for ground-based solar remote sensing measurements of total column concentrations of CO_2, CH_4 and CO. *Atmospheric Measurement Techniques Discussions* 1–67. https://doi.org/10.5194/amt-2019–371

Toja-Silva F., Chen J., Hachinger S. et al. (2017) CFD simulation of CO_2 dispersion from urban thermal power plant: Analysis of turbulent Schmidt number and comparison with Gaussian plume model and measurements. *Journal of Wind Engineering and Industrial Aerodynamics* 169, 177–193. https://doi.org/10.1016/j.jweia.2017.07.015

Viatte C., Lauvaux T., Hedelius J.K. et al. (2017) Methane emissions from dairies in the Los Angeles Basin. *Atmospheric Chemistry and Physics* 17, 7509–7528. https://doi.org/10.5194/acp-17–7509–2017

Vogel F.R., Frey M., Staufer J. et al. (2019) XCO_2 in an emission hotspot region: the COCCON Paris campaign 2015. *Atmospheric Chemistry and Physics* 19, 3271–3285. https://doi.org/10.5194/acp-19–3271–2019

World Meteorological Organization, Global Atmosphere Watch (2016) WMO/GAW aerosol measurement procedures: guidelines and recommendations.

Wunch D., Toon G.C., Blavier J.F. et al. (2011) The Total Carbon Column Observing Network. *Philosophical Transactions A Mathematics Physics Engineering Sciences* 369, 2087–112.

Zhao X., Marshall J., Hachinger S. et al. (2019) Analysis of Total Column CO_2 and CH_4 Measurements in Berlin with WRF-GHG. *Atmospheric Chemistry and Physics Discussions* 1–26. https://doi.org/10.5194/acp-2018–1116

B.k. Dense networks

Ron Cohen[1], Felix Vogel[2] and Dominik Brunner[3]

[1]University of California, Berkeley, California, USA

[2]Environment and Climate Change Canada, Canada

[3]Empa, Dübendorf, Switzerland

B.k.1 Introduction

Dense networks are an approach to urban GHG emissions assessment that relies on large numbers of sensors, each with a small, locally dominated, footprint of two-five kilometres diameter that overlaps with the footprint of adjacent observing stations. In principle, such networks could use any instruments, however, in practice low-cost sensors make the idea attractive. The conceptual advantages of the approach include 1) much lower capital investments than some of the alternatives, 2) the small footprint of each sensor allows for more direct attribution to individual source types, 3) addition of low-cost air quality observations can enhance attribution to sectors for an incremental additional cost that is a small percentage of overall capital cost and 4) there is a square root N advantage in signal to noise of some analyses. Within the mix of approaches described in this document, dense networks are a newer idea, one that is not as extensively vetted as the others.

There is growing interest in mapping experiments that rely on instrumented vehicles including cars and trucks whose path can be user defined or public transit that repeatedly samples the same route through a city. These have some parallel benefits to dense networks in that they can map the city emissions with many small footprints at an affordable price point.

B.k.2 Instrumentation, Calibration and Performance

Instruments for measuring CO_2 using IR spectroscopy at prices from ~$ \100-$ \1000 are commercially available. Many of these instruments have a folded pathlength comparable to that used in state-of-the-art instruments. As a result, the short-term precision of these measurements is little different from those instruments and frequent calibration with gas standards might well result in equivalent accuracy (~0.1ppm). However, the dense network deployment of dozens to hundreds of sensors makes direct on-site calibration cost prohibitive. Instead alternative approaches that rely on slow drift and correlation across the network have been proposed. For example, the slope response of the sensors can be calibrated before deployment and drift in the instrument zero is tracked by assuming the bottom x% (x = 5 – 10) of the observations are identical across the network (Shusterman et al., 2016). Adjustments to the instrument zero are tracked and treated as a linear drift. Observed drifts are of order 1ppm/month.

One hypothesis about dense networks is that the large numbers of instruments reduce the constraints on choice of site. If sensors randomly sample a wide range of realistic environments, then they will effectively observe the emissions from a city. It is important that the sensors not be unduly influenced by direct emissions from the building they are mounted on—or that such times as they are influenced are easily recognized and removed from the data set.

Performance of a hypothetical dense network was evaluated by Turner et al (2016) who compared the efficacy of equivalent capital investment in three state of the art instruments and as many as 30 low-cost instruments configured in a dense network. The analysis showed that if model and observation error are held below 1ppm the low-cost network can deliver a more precise estimate of emissions when used as a constraint on an identical inverse model. 1 ppm accuracy was also found as a useful target in the analysis of Wu et al (2018).

In addition, Lopez-Coto et al., 2017 also found that very high-density networks of low-cost sensors can provide useful information if the uncertainties remain moderated and that careful consideration should be put into characterizing possible long-term sensors drifts.

A recent analysis of the decrease in emissions immediately following the COVID-19 shelter-in-place order in the San Francisco Bay Area (Turner et al., 2020), showed that overall emissions decreased by 25%. The analysis showed that vehicle emissions decreased by 45% and by a larger percentage at night—estimates that are consistent with measures of highway traffic.B.k.3.   Ongoing Research

The BEACO_2N network (Shusterman et al., 2016) aims for one sensor per 2 square kilometres, but it is not yet established if this is an optimal density. In any case, the optimal density will depend on the goals of the network, the type of data analysis and/or modelling, and the particular city geography and meteorology.

B.k.4. References

Lopez-Coto I., Ghosh S., Prasad K. et al. (2017) Tower-based greenhouse gas measurement network design—The National Institute of Standards and Technology North East Corridor Testbed. *Advances in Atmospheric Science* 34, 1095–1105, doi.org/10.1007/s00376–017–6094–6.

Shusterman A.A., Teige V.E., Turner A.J. et al. (2016) The Berkeley atmospheric CO_2 observation network: Initial evaluation. *Atmospheric Chemistry and Physics* 16(21):13449–13463.

Turner A.J., Shusterman A.A., McDonald B.C. et al. (2016) Network design for quantifying urban CO_2 emissions: Assessing trade-offs between precision and network density. *Atmospheric Chemistry and Physics* 16(21):13465–13475.

Turner A.J., Kim J., Fitzmaurice H. et al. (2020) Observed impacts of COVID-19 on urban CO_2 emissions. *Geophysical Research Letters*.

Wu K., Lauvaux T., Davis K.J. et al. (2018) Joint inverse estimation of fossil fuel and biogenic CO_2 fluxes in an urban environment: An observing system simulation experiment to assess the impact of multiple uncertainties. *Elementa: Science of the Anthropocene* 6:17.

B.I. Choice of background

Anna Karion[1], Jia Chen[2], Kenneth J Davis[3], Irene Xueref-Remy[4]

[1]National Institute of Standards and Technology (NIST), Gaithersburg, Maryland, USA

[2]Technical University of Munich, München, Germany

[3]Pennsylvania State University, University Park, Pennsylvania, USA

[4]Institut Méditerranéen de Biodiversité et d'Ecologie Marine et Continentale, Universitaires d'Aix-Marseille, France

B.I.1 Background method overview

Analysis of urban area greenhouse gas (GHG) concentration (or mole fraction) data for the purpose of estimating emissions requires isolating the portion of the observed mole fraction that is attributed to emissions from the domain of interest. Here we refer to the portion not attributable to emissions within the domain as “background”. For urban analyses, the domain of interest is often small compared with the domains of regional or continental analyses, complicating the choice of background. Air masses entering an urban area are influenced by emissions (and depletions) upwind that occurred in the recent past, and upwind terrestrial and anthropogenic fluxes of both carbon dioxide (CO_2) and methane (CH_4) can be quite large and heterogeneous. Thus, unlike background conditions for global or continental analyses, the incoming air mole fraction can have significant variability both in space and time (Mueller et al., 2018; Balashov et al., 2020; Xueref-Remy et al, 2018; Pal et al, 2020). Each urban research project must determine the level of variability to be expected, and if a background analysis method is chosen, should take steps to evaluate that background as much as possible. Evaluation of background mole fraction and variability not only aids in the selection of the best possible background for the application at hand, but it also helps quantify uncertainties that should be propagated to the analysis. Below we outline methods that have been used in the literature for background determination.

When urban analyses use stationary in situ observations (e.g. sensors placed on building rooftops or cell towers, including high accuracy systems, whole air flask sampling, or high-density networks), background mole fractions are often established using observations from stations that are located close to or just outside the urban region, upwind and/or in an area far from local emissions. The background station might be selected when it is upwind of the urban area (Miles et al, 2017; Sargent et al., 2018; Xueref-Remy et al, 2018; Bréon et al, 2015; Staufer et al, 2016; Lian et al, 2019; Balashov et al, 2020) or at all times for a station that generally samples air unaffected by the urban area, such as off-shore or at high elevation (Lauvaux et al., 2013; Verhulst et al., 2017; Mitchell et al., 2018). Data from this station may be sampled at the same time as the observations inside the urban area (Lauvaux et al., 2016, Miles et al., 2017; Xueref-Remy et al., 2018, Bréon et al., 2015, Staufer et al., 2016; Balashov et al., 2020), or may be incorporated in a more sophisticated backward trajectory method (Sargent et al., 2018). In the case of a “clean air” monitoring station, the observations are often filtered and smoothed in order to achieve the background conditions, to remove synoptic pollution events near the background station (Verhulst et al., 2017; Mitchell et al., 2018). Some studies use a lowest percentile of data to define the background (e.g. the lowest 5% of measurements during a 24 or 48-hour period, or the network-wide daily minimum value (Ammoura et al., 2016; Shusterman et al., 2018)), but this method can yield incorrect values depending on the goal of the study, so care should be taken to validate them.

Caution must be exercised when using upwind or rural stations to define a background, no matter which of the above methods are employed. For CO_2 in the summer, for example, strong local biospheric fluxes near the rural station may bias the background time series. Thus, additional understanding of the biosphere in the rural area surrounding the upwind or background measurement sites may be required. In some studies, local biospheric fluxes have been accounted for by subtracting model-based estimates of local fluxes (Lauvaux et al., 2016). In addition, it may be necessary to select or filter data according to wind speed and wind direction relative to the upwind site in analysis (Miles et al., 2017; Bréon et al., 2015; Staufer et al., 2016). Complex meteorology (e.g. recirculation, land-sea breeze) also complicates the choice of background, so additional considerations for data filtering and upwind station choice are required (Xueref-Remy et al., 2017; Milne et al., in prep). The choice of instrumentation for the background site should ensure a precision within 5% of the urban signal that is studied, as recommended by the GAW/WMO for regions of dense emissions (WMO, 2017). The background station measurements should be monitored for temporal drift and precision relative to the urban network, i.e. measurements must be compatible with the calibration scales for the urban stations, to ensure that calculated enhancements are accurate.

Background stations should be located so that they are well exposed to regional atmospheric flow, and not contaminated by local anthropogenic emissions, as much as possible. Although both anthropogenic CO_2 and CH_4 emissions can be highly heterogeneous in space, making upwind boundary conditions highly complex (Heimburger et al., 2017; Balashov et al., 2020), large CH_4 emissions may exist in rural areas (e.g. livestock, oil and gas operations, coal mines) and must be considered when siting background measurements. The spatial distribution of large emitters, however, may be relatively well known (Massakkers et al, 2016), enabling the boundary conditions to be simulated with good confidence (Barkley et al., 2017). Unlike CO_2, CH_4 boundary conditions may not be highly seasonal if natural biogenic sources (wetlands) are not a significant source in the region. Alternatives to using upwind measurements for in situ enhancement analyses include solving for the boundary condition within an inversion (Nickless et al., 2018), or nesting the urban domain inside a large global model in order to propagate the background into the domain (Ammoura et al., 2016).

Some urban analyses rely on in situ measurements of GHGs from airborne platforms, either using a mass balance method (e.g. Heimburger et al., 2017), a tracer ratio method (e.g. Plant et al., 2019), a forward model data comparison (Barkley et al., 2017), an inverse model (e.g. Cui et al., 2017; Lopez-Coto et al., 2020), or some combination of the above. Background for modelling-based airborne studies may be constructed similarly to the methods for a mass balance technique (Karion et al., 2019), but not always. A lowest percentile method could be used for each flight (Cui et al., 2017), or a model could be used to remove background influences (Barkley et al., 2017) or to optimize the background along with fluxes (Lopez-Coto et al., 2020). Lagrangian model back-trajectories from flight observations have also been used to inform the background conditions used for each flight (Pitt et al., 2019). Additional details on the choice of background for aircraft analyses can be found in the Mass Balance Annex B.f.

Satellite-based and other column remote sensing observations require information about background mole fractions for determining urban enhancements as well. Methods are similar to those for in situ stationary sensors. One possibility is to use observations outside the urban area, for example from a satellite observation outside the region that is not influenced by the urban emissions (Kort et al., 2012; Shekhar et al. 2020). Alternatively the background is taken from a ground-based spectrometer that is upwind on a given day (Chen et al., 2016; Vogel et al, 2019; Makarova et al., 2020) or from the measurements of various upwind stations depending on the wind direction during the course of the day (Dietrich et al. 2020, in review). As with in situ stationary or aircraft measurements, the background mole fraction for column measurements can be also optimized within a flux inversion (Jones et al., in prep), using a Lagrangian particle backward trajectory model to determine the influence of the background to the measurements. The daily network minimum has also been used as a background (Viatte et al. 2017), but as with the in situ networks, care must be taken with this method especially if measuring CO_2 during summer months, as biospheric influence will bias the background. More details on backgrounds used for ground-based column measurements are found in the section on Ground-based Remote Sensing (Annex B.j.).

The choice of background can be the largest contributor to uncertainty in urban studies, especially in metropolitan areas with smaller enhancements. Most troublesome is the possibility of a bias in the background (e.g. instrumental drift, local biogenic impacts, contamination by local anthropogenic emissions), which is difficult to account for in modelling studies that rely on unbiased error distributions. Thus, any analysis of urban GHG enhancements should assess and evaluate the options for determining background conditions, including careful placement of observation sites for use as background stations. One option for evaluating the quality of the background choice is to compare the background mole fraction with the mole fraction at measurement sites during periods of low urban influence, for example during high-wind events (Xueref-Remy et al, 2018), or if using a modelling framework, for hours with small surface influence (low footprint magnitudes). Another method is to use a synthetic data experiment to directly evaluate the representativity of whatever background choice (e.g. the measurement from an upwind tower) compared to the “true” background; such a study could also be performed as part of network design (e.g. Mueller et al., 2018; Wu et al., 2016). A direct and highly recommended approach is to deploy multiple background measurements (Miles et al., 2017). This allows for direct evaluation of the total uncertainty in the background (Balashov et al., 2017), as well as for the selection of the appropriate upwind observation based on wind direction. As noted previously, if upwind sources are relatively well known, an atmospheric model can also be used to correct for upwind contamination (Barkley et al., 2017). This approach is not recommended, however, when the upwind contamination is so large that the urban emission of interest is small compared to the background correction. Such evaluation and error analysis may give guidance as to which observations should be either de-weighted or removed due to large background errors in an analysis.

B.I.2 References

Ammoura L., Xueref-Remy I., Vogel F. et al. (2016) Exploiting stagnant conditions to derive robust emission ratio estimates for CO_2, CO and volatile organic compounds in Paris, *Atmospheric Chemistry and Physics*, 16, 15653–15664, https://doi.org/10.5194/acp-16–15653–2016.

Barkley Z.R. et al. (2017), Quantifying methane emissions from natural gas production in northeastern Pennsylvania, *Atmospheric Chemistry and Physics* 17(22), 13941–13966, doi:10.5194/acp-17–13941–2017.

Bréon F.M., Broquet G., Puygrenier V. et al. An attempt at estimating Paris area CO_2 emissions from atmospheric concentration measurements, *Atmospheric Chemistry and Physics* 15, 1707–1724, https://doi.org/10.5194/acp-15–1707–2015, 2015, https://www.atmos-chem-phys.net/15/1707/2015/acp-15–1707–2015.html.

Chen J., Viatte C., Hedelius J.K. et al. Differential column measurements using compact solar-tracking spectrometers, *Atmospheric Chemistry and Physics* 16, 8479–8498, https://doi.org/10.5194/acp-16–8479–2016, 2016.

Cui Y.Y. et al. (2017), Top-down estimate of methane emissions in California using a mesoscale inverse modelling technique: The San Joaquin Valley, *Journal of Geophysical Research Atmospheres*, 122, 3686–3699, doi:10.1002/2016JD026398.

Dietrich F., Chen J., Voggenreiter B. et al. (2022) Munich permanent urban greenhouse gas column observing network, *Atmospheric Measurement Techniques*, in review.

Heimburger A.M.F. et al. (2017), Assessing the optimized precision of the aircraft mass balance method for measurement of urban greenhouse gas emission rates through averaging, *Elementa: Science of the Anthropocene*, 5, 15, doi:10.1525/elementa.134.

Karion A. et al. (2019), Intercomparison of atmospheric trace gas dispersion models: Barnett Shale case study, *Atmospheric Chemistry and Physics* 19(4), 2561–2576, doi:10.5194/acp-19–2561–2019.

Kort E.A., Frankenberg C., Miller C.E. et al. (2012), Space-based observations of megacity carbon dioxide, *Geophysical Research Letters*, 39, L17806, doi:10.1029/2012GL052738.

Lauvaux T., Miles N.L., Richardson S.J. et al. (2013) Urban emissions of CO_2 from Davos, Switzerland: the first real time monitoring system using an atmospheric inversion technique, *Journal of Applied Meteorology and Climatology*, 52, 2654–2668, http://dx.doi.org/10.1175/JAMC-D-13–038.1.

Lauvaux T., Miles N.L., Deng A. et al. (2016) High resolution atmospheric inversion of urban CO_2 emissions during the dormant season of the Indianapolis Flux Experiment (INFLUX), *Journal of Geophysical Research Atmospheres* 121, doi:10.1002/2015JD024473.

Lian J., Breon F.M., Broquet G. et al. (2019), Analysis of temporal and spatial variability of atmospheric CO_2 concentration within Paris from the GreenLITE laser imaging experiment, *Atmospheric Chemistry and Physics* 19 (22), 13809–13825, https://doi.org/10.5194/acp-19–13809–2019.

Lopez-Coto I., Ren X., Salmon O.E. et al. (2020), Wintertime CO_2, CH_4, and CO Emissions Estimation for the Washington, D.C.–Baltimore Metropolitan Area Using an Inverse Modelling Technique, *Environmental Science & Technology*, 54(5), 2606–2614, doi:10.1021/acs.est.9b06619.

Makarova M.V., Alberti C., Ionov D.V. et al. (2020) EMME: an overview and first results of the St. Petersburg megacity campaign-2019, *Atmospheric Measurement Techniques Discussions,* https://doi.org/10.5194/amt-2020–87, in review, 2020.

Miles N.L., Richardson S.J., Lauvaux T. et al. (2017) Quantification of urban atmospheric boundary layer greenhouse gas dry mole fraction enhancements: Results from the Indianapolis Flux Experiment (INFLUX), *Elementa: Science of the Anthropocene* 5:27, http://doi.org/10.1525/elementa.127.

Milne M., Xueref-Remy I., Zoghbi N. et al. (2019), Analysing the atmospheric CO_2 variability in the Mediterranean region of the Aix-Marseille metropolis and its coastal region area at different timescales, Atmospheric Environment, in prep.

Mitchell L.E. et al. (2018), Long-term urban carbon dioxide observations reveal spatial and temporal dynamics related to urban characteristics and growth, *Proceedings of the National Academy of Sciences*, 115(12), 2912–2917, doi:10.1073/pnas.1702393115.

Mueller K., Yadav V., Lopez-Coto I. et al. (2018), Siting Background Towers to Characterize Incoming Air for Urban Greenhouse Gas Estimation: A Case Study in the Washington, D.C./Baltimore Area, *Journal of Geophysical Research: Atmospheres*, 123(5), 2910–2926, doi:doi:10.1002/2017JD027364.

Nickless A., Rayner P.J., Engelbrecht F. et al. (2018), Estimates of CO_2 fluxes over the city of Cape Town, South Africa, through Bayesian inverse modelling, *Atmospheric Chemistry and Physics*, 18(7), 4765–4801, doi:10.5194/acp-18–4765–2018.

Pal S., Davis K.J., Lauvaux T. et al. (2020) Observations of greenhouse gas changes across summer frontal boundaries in the eastern United States. *Journal of Geophysical Research: Atmospheres*, 125, e2019JD030526. https://doi.org/10.1029/2019JD030526.

Pitt J.R., Allen G., Bauguitte S.J.B. et al. (2019), Assessing London CO_2, CH_4 and CO emissions using aircraft measurements and dispersion modelling, *Atmospheric Chemistry and Physics*, 19(13), 8931–8945, doi:10.5194/acp-19–8931–2019.

Plant G., Kort E.A., Floerchinger C. et al. (2019), Large Fugitive Methane Emissions From Urban Centres Along the US East Coast, *Geophysical Research Letters*, 46(14), 8500–8507, doi:10.1029/2019gl082635.

Sargent M. et al. (2018), Anthropogenic and biogenic CO2 fluxes in the Boston urban region, *Proceedings of the National Academy of Sciences*, 115(29), 7491–7496, doi:10.1073/pnas.1803715115.

Shekhar A., Chen J., Dietrich F. et al. (2020) Anthropogenic CO_2 emissions assessment of Nile Delta using XCO_2 and SIF data from OCO-2 Satellite *Environmental Research Letters*, doi: 10.1088/1748–9326/ab9cfe.

Shusterman A.A., Teige V.E., Turner A.J. et al. (2016), The Berkeley Atmospheric CO_2 Observation Network: initial evaluation, *Atmospheric Chemistry and Physics*, 16(21), 13449–13463, doi:10.5194/acp-16–13449–2016.

Staufer J., Broquet G., Bréon F.-M. et al. (2016), A first year-long estimate of the Paris region fossil fuel CO_2 emissions based on atmospheric inversion, *Atmospheric Chemistry and Physics* 16, 14703–14726.

Verhulst K.R. et al. (2017), Carbon dioxide and methane measurements from the Los Angeles Megacity Carbon Project – Part 1: calibration, urban enhancements, and uncertainty estimates, *Atmospheric Chemistry and Physics* 17(13), 8313–8341, doi:10.5194/acp-17–8313–2017.

Viatte C., Lauvaux T., Hedelius J.K. et al. (2017) Methane emissions from dairies in the Los Angeles Basin, *Atmospheric Chemistry and Physics* 17, 7509–7528, https://doi.org/10.5194/acp-17–7509–2017, 2017.

Vogel F.R., Frey M., Staufer J. et al. (2019), XCO_2 in an emission hotspot region: the COCCON Paris campaign 2015, *Atmospheric Chemistry and Physics* 19, 3271–3285, https://doi.org/10.5194/acp-19–3271–2019.

WMO (2018), 19th WMO/IAEA Meeting on Carbon Dioxide, Other Greenhouse Gases and Related Measurement Techniques (GGMT-2017) Rep. Report No. 242, WMO / GAW.

Wu L., Broquet G., Ciais P., Bellassen V., et al. (2016), What would dense atmospheric observation networks bring to the quantification of city CO_2 emissions?, *Atmospheric Chemistry and Physics* 16, 7743–7771, https://doi.org/10.5194/acp-16–7743–2016

Xueref-Remy I., Dieudonné E., Vuillemin C. et al. (2018), Diurnal, synoptic and seasonal variability of atmospheric CO_2 in the Paris megacity area, *Atmospheric Chemistry and Physics* 18, 3335–3362, https://doi.org/10.5194/acp-18–3335–2018

Xueref-Remy I., Zoghbi N., Yohia C. et al. (2017), T., Assessing the atmospheric forcing of CO_2 emissions issued by the Aix-Marseille metropolis region from a top-down approach : towards verifying bottom-up regional inventories and estimating the anthropogenic impacts on regional ecosystems, 10th International Carbon Dioxide Conference, Interlaken, Switzerland, 20–27 August 2017, p. 380, https://www.icdc10.unibe.ch/unibe/portal/fak_naturwis/micro_icdc10/content/e342182/e588294/e591299/ICDC10_Abstracts_14082017.pdf

B.m. Meteorological Observations for Urban Greenhouse Gas Analysis

Sunil Baidar[1,2], Kenneth Davis[3], and Alan Brewer[1]

[1]NOAA Chemical Sciences Laboratory, Boulder, CO, USA

[2]CIRES, University of Colorado at Boulder, USA

[3]Pennsylvania State University, University Park, Pennsylvania, USA

B.m.1 Introduction

Meteorological measurements are essential for improving the accuracy and precision of Greenhouse gases (GHG) emissions inferred from atmospheric GHG observations. Meteorological parameters like wind speed and direction are often concurrently measured with greenhouse gases for the purpose of filtering and interpreting GHG data for different atmospheric conditions. Regional backgrounds needed to quantify local excess GHG mole fractions may strongly depend on the meteorological conditions (wind speed, direction, mixing height) (Turnbull et al., 2015). Methods such as mass balance used to estimate GHG fluxes from source regions require knowledge of wind speed, direction and mixing height (e.g. Cambaliza et al., 2015). Atmospheric models used for inverse modelling of GHG emissions either assimilate meteorological observations to improve model performance (e.g. Deng et al., 2017) or use the meteorological observations for evaluating model performance (e.g. Lac et al., 2013, Sarmiento et al., 2017).

The WMO Guide to Meteorological Instruments and Methods of Observations (WMO 2018) provide information about different instruments for measuring various meteorological parameters and should be followed.

B.m.2 Key meteorological measurements

Urban atmospheric boundary layer (ABL) wind speed and direction, and mixing height are the main measurements that can constraint atmospheric transport errors in inverse modelling of GHG fluxes.

B.m.2.1 Urban ABL wind speed and direction

ABL wind speed and direction are directly relevant to the estimation of urban GHG emissions. These can be used to evaluate and improve the atmospheric models used for urban inversions (e.g. Lac et al., 2013, Sarmiento et al, 2017). These data can also be used to filter atmospheric GHG data that are used in inversion (e.g. Bréon et al., 2015). Wind profiles are also readily assimilated into numerical weather prediction models and have been shown to improve model performance and inverse flux estimation (e.g. Deng et al., 2017). Periodic or continuous urban ABL wind speed and direction measurements, therefore, are highly beneficial for urban GHG emissions estimation.

ABL wind speed and direction profiles can be measured using radiosondes, tethered balloons, masts, aircrafts, radar wind profilers and Doppler lidars. In practice, it might not be feasible to make vertical profile measurements close to the surface, where most of the atmospheric GHG measurements are made, using aircrafts in urban areas. ABL winds and temperature profiles are also available at airports from instrumented commercial aircrafts via NOAA's Meteorological Assimilation Data Ingest System (MADIS, 2020). Measurements from radiosondes and tethered balloons will be limited to launch times. Remote sensors such as Doppler lidars (Henderson et al., 2005), and radar wind profilers (Ecklund et al., 1990) provide continuous measurements of wind profiles, and these would be very useful for evaluating the diurnal cycle in the models.

B.m.2.2 Urban Mixing height

The mixing height (MH) is the height of the layer adjacent to the ground over which pollutants or any constituents emitted within this layer or entrained into it become vertically dispersed by convection or mechanical turbulence within a timescale of about an hour (Seibert et al., 2000). Thus, the measured urban GHG mole fractions are directly related to the mixing height and their interpretation would require knowledge of the mixing height (e.g. de Arellano et al., 2004). Like the ABL winds, mixing height can also be used to evaluate numerical prediction models (e.g. Lac et al., 2013, Sarmiento et al., 2017, Lopez-Coto et al., 2020). Therefore, periodic or continuous measurements of urban mixing height greatly improves urban GHG emissions estimation.

Mixing height can be estimated using temperature, pressure, and wind profiles measured by radiosondes using parcel method (Seibert et al., 2000). This instantaneous mixing height from radiosondes might not be representative of the mean mixing height, especially if the radiosonde ascends through a significant updraft or downdraft. Remote sensors such as elastic backscatter lidar (Lewis et al., 2013, Caiecdo et al., 2017), Doppler lidar (Tucker et al., 2009, Bonin et al., 2018) and radar wind profilers (Angevine et al., 1994, Bianco and Wilczak, 2002) provide continuous or semi-continuous measurements of the mean mixing height over a certain time interval.

Low pulse energy elastic backscatter lidars (e.g. Ceilometers, Micropulse LIDAR (MPL)) and Doppler lidars are increasingly being used for continuous measurements of mixing height. These lidars are eye safe and capable of continuous unattended operation. They have high vertical resolution (5–30 m) and low minimum range (100 m or less). The returned signal originates directly from aerosols. Elastic backscatter lidars use aerosol gradient to determine mixing height (Davis et al., 2000, Brooks, 2003). As a consequence, these elastic backscatter lidars have difficulty detecting the mixing height, at night-time and during morning and evening transitions, in the presence of residual layers. Networks of these lidars with standardized products for clouds and mixing height are starting to be formed (Welton et al., 2001, UMBC 2020) and data from these networks could be beneficial for evaluating atmospheric models.

Doppler lidars have additional advantage of directly measuring atmospheric turbulence. They can also provide horizontal wind speed and direction measurements if they employ one of a variety of scanning modes. Vertical velocity w statistics from the Doppler lidar can even be used to evaluate turbulence in atmospheric models or turbulent kinetic energy (TKE) can be directly measured from Doppler lidar using sophisticated scanning techniques (Bonin et al, 2017). Minimum range of Doppler lidars can be lowered by making off-axis and scanning measurements (Bonin et al., 2018). Mixing height is retrieved using information from turbulence, wind and aerosol backscatter profiles (Tucker et al., 2009, Bonin et al., 2018). Doppler lidars can provide continuous measurements of the two key ABL variables, ABL winds and mixing height, needed to ensure high quality GHG flux, and hence, a Doppler lidar measurement at one urban site would greatly benefit urban GHG estimates (e.g. Davis et al., 2017).

The low pulsed energy lidars may not be sensitive enough to detect the mixing height accurately when the aerosol loading is low and the mixing height is deep. This would result in low biased mixing height, and hence, such periods should be identified.

B.m.2.3 Measurement location

We recommend urban ABL measurements on the downwind end of the city, to capture the ABL characteristics of the air exiting the city. This will enable the observed urban GHG enhancement to be matched to its ABL environment.

B.m.2.4 Measurement frequency

We recommend continuous measurements of urban ABL measurements to ensure diurnal variation are captured and well simulated in atmospheric models. This will help reduce uncertainty in attribution of the distribution of greenhouse gas fluxes (Sarmiento et al., 2017). However, periodic daily ABL measurements provided by radiosondes and commercial aircraft would still be extremely helpful in evaluating the atmospheric models.

B.m.3 Other measurements

These variables will help improve atmospheric model simulations of urban ABL and should be considered if possible.

B.m.3.1 ABL clouds

The presence of clouds has a large influence on the ABL structure (e.g. Lareau et al., 2018). Transport within the ABL can be significantly influenced by ABL clouds and ABL pollutant mole fractions (e.g. Cotton et al., 1995, Greenhut, 1986). Measurements of cloud-base and fractional coverage, readily available with lidar remote sensing, are likely to benefit evaluation of model simulations of the urban ABL. These measurements will also aid in filtering atmospheric GHG data for improved flux inversion estimates.

B.m.3.2 ABL heterogeneity

Some urban environments are complex (e.g. coastal cities; cities with heterogeneous surface conditions). In these situations, multiple urban ABL sounding sites may be needed to fully characterize the urban environment. Resources, however, may be limited. If so, even a single measurement point in a characteristic portion of the city will enable evaluation of the numerical weather model used to quantify atmospheric transport over the city. A mobile ABL profiling system will also enable capturing effects of spatial heterogeneity (e.g. Pal et al., 2012).

B.m.3.3 Urban Heat Island

Urban heat island plays an important role in defining the urban-rural contrasts on the mixing height (Pal et al., 2012) and the GHG diurnal cycle (Lac et al., 2013). Choice of urban parameterization is crucial for reproducing the urban-rural contrast on BLH and GHG diurnal cycle in atmospheric models (Lac et al., 2013). Measurements of temperature, humidity, and winds across rural, suburban and urban locations will help urban parametrization selection.

B.m.3.4 Diagnostic meteorological measurements

The ABL properties needed to ensure high quality GHG flux estimates are the variables described above, urban mixing height, and urban ABL wind speed and direction. Measurement of these properties enables a strong check of the quality of GHG emissions estimates from a city. These measurements are not sufficient, however, to diagnose the causes of any observed biases in the simulated ABL properties. Biases are common, and diagnostic measurements, if feasible are recommended.

B.m.3.5 Upwind ABL boundary conditions.

The ABL conditions upwind of the city play an important role in the properties of the urban ABL (e.g. Sarmiento et al, 2017). Measurements of the ABL depth, wind speed and wind direction in the upwind environment, paired with the same urban measurements, enable this to be examined as a source of bias in the urban meteorological simulation.

B.m.3.6 Surface fluxes

The ABL, by definition, is strongly linked to surface fluxes of heat, moisture and momentum, and these are driven by the net radiation at the Earth’s surface (Santanello et al., 2018). Simulating these fluxes has proven to be a significant challenge for the numerical weather modelling community (e.g. Yang et al., 2006). Observations of these fluxes including incoming solar radiation, both upwind of the city and over representative urban surfaces, can provide great insight into biases that may exist in the numerical simulation of ABL properties.

B.m.4 References

Angevine W.M., White A.B. and Avery S.K. (1994) Boundary layer depth and entrainment zone characterization with a boundary layer profiler. *Boundary Layer Meteorology,* 68, 375–385.

Bianco L., and Wilczak J.M. (2002) Convective boundary layer depth: Improved measurement by Doppler radar wind profiler using fuzzy logic methods, *Journal of Atmospheric and Oceanic Technology,* 19, 1745–1758, https://doi.org/10.1175/1520–0426(2002)019,1745:CBLDIM.2.0.CO;2.

Bonin T.A., Choukulkar A., Brewer W.A. et al. (2017) Evaluation of Turbulence Measurement Techniques from a Single Doppler LIDAR, *Atmospheric Measurement Techniques,* doi:10.5194/amt-10–3021–2017.

Bonin T.A., Carrol B., Hardesty R.M. et al. (2018) Doppler lidar observations of the mixing height in Indianapolis using an automated composite fuzzy logic approach, *Journal of Atmospheric and Oceanic Technology* https://doi.org/10.1175/JTECH-D-17–0159.1

Bréon F.M., Broquet G., Puygrenier V. et al. (2015) An attempt at estimating Paris area CO_2 emissions from atmospheric concentration measurements, *Atmospheric Chemistry and Physics* 15, 1707–1724, doi:10.5194/acp-15–1707–2015.

Brooks I.M. (2003) Finding Boundary Layer Top: Application of a Wavelet Covariance Transform to LIDAR Backscatter Profiles, *Journal of Atmospheric and Oceanic Technology* 20, 1092–1105, https://doi.org/10.1175/1520–0426(2003)020<1092:FBLTAO>2.0.CO;2.

Caicedo V., Rappenglück B., Lefer B. et al. (2017) Comparison of aerosol lidar retrieval methods for boundary layer height detection using ceilometer aerosol backscatter data, *Atmospheric Measurement Techniques* 10, 1609–1622, https://doi.org/10.5194/amt-10–1609–2017.

Cambaliza M.O.L., Shepson P.B., Bogner J. et al. (2015) Quantification and source apportionment of the methane emission flux from the city of Indianapolis, *Elementa: Science of the Anthropocene* 3, 37, http://doi.org/10.12952/journal.elementa.000037.

Cotton W.R., Alexander G.D., Hertenstein R. et al. (1995) Cloud venting – A review and some new global annual estimates, *Earth Science Reviews*, 39, 169–206.

Davis K.J., Gamage N., Hagelberg C.R. et al. (2000) An Objective Method for Deriving Atmospheric Structure from Airborne LIDAR Observations. *Journal of Atmospheric and Oceanic Technology* 17, 1455–1468.

Davis K.J. et al. (2017) The Indianapolis Flux Experiment (INFLUX): A testbed for developing urban greenhouse gas emission measurements. *Elementa: Science of the Anthropocene* 5, 21, https://doi.org/10.1525/elementa.188.

De Arellano J.V.-G., Gioli B., Miglietta F. et al. (2004) Entrainment process of carbon dioxide in the atmospheric boundary layer, *Journal of Geophysical Research Atmospheres,* 109, D18110, doi:10.1029/2004JD004725.

DengA., Lauvaux T., Davis K.J. et al. (2017) Toward reduced transport errors in a high resolution urban CO_2 inversion system, *Elementa: Science of the Anthropocene* 5, 20, http://doi.org/10.1525/elementa.133

Ecklund W.L., Carter D.A., Balsley B.B. et al. (1990) Field tests of a lower tropospheric wind profiler, *Radio Science*, 25, 899–906.

Greenhut G.K. (1986) Transport of Ozone Between Boundary Layer and Cloud Layer by Cumulus Clouds, *Journal of Geophysical Research Atmospheres* 91, 8613–8622.

Henderson S.W. et al. (2005) Wind LIDA in *Laser Remote Sensing,* T. Fuji and T. Fukuchi, eds. (CRC Press, 2005), pp. 266–290.

Lac C., Donnelly R.P., Masson V. et al. (2013) CO_2 dispersion modelling over Paris region within the CO_2-MEGAPARIS project, *Atmospheric Chemistry and Physics* 13, 4941–4961, doi:10.5194/acp-13–4941–2013.

Lareau N.P., Zhang Y. and Klein S.A. (2018) Observed Boundary Layer Controls on Shallow Cumulus at the ARM Southern Great Plains Site. *Journal of Atmospheric Science* 75, 2235–2255, https://doi.org/10.1175/JAS-D-17–0244.1.

Lewis J.R., Welton E.J., Molod A.M. et al. (2013) Improved boundary layer depth retrievals from MPLNET, *Journal of Geophysical Research Atmospheres* 118, 9870–9879, doi:10.1002/jgrd.50570.

MADIS (2020) Meteorological Assimilation Data Ingest System, https://madis.ncep.noaa.gov/, accessed August 2020.

Lopez-Coto I., Hicks M., Karion A. et al. (2020) Assessment of Planetary Boundary Layer Parameterizations and Urban Heat Island Comparison: Impacts and Implications for Tracer Transport. *Journal of Applied. Meteorology and Climatology*, **59**, 1637–1653, https://doi.org/10.1175/JAMC-D-19–0168.1.

Pal S., Xueref-Remy I., Ammoura L. et al. (2012) Spatio-temporal variability of the atmospheric boundary layer depth over Paris agglomeration: an assessment of the impact of urban heat island intensity, *Atmospheric Environment* 63, 261–275, doi:10.1016/j.atmosenv.2012.09.046.

Santanello J.A. et al. (2018) Land–Atmosphere Interactions. The LoCo Perspective, *BAMS,* 99(6), 1253–1272, doi:10.1175/BAMS-D-17–0001.1

Sarmiento D.P., Davis K.J., Deng A. et al. (2017) A comprehensive assessment of land surface-atmosphere interactions in a WRF/Urban modelling system for Indianapolis, IN *Elementa: Science of the Anthropocene* 5: 23. http://doi.org/10.1525/elementa.132.

Seibert P., Beyrich F., Gryning S.-E. et al. (2000) Review and intercomparison of operational methods for the determination of the mixing height, *Atmospheric Environment* 34, 1001–1027, https://doi.org/10.1016/S1352–2310(99)00349–0.

Tucker S.C., Senff C.J., Weickmann A.M. et al. (2009) Doppler lidar estimation of mixing height using turbulence, shear, and aerosol profiles, *Journal of Atmospheric and Oceanic Technology* 26, 4, 673–688.

Turnbull J.C. et al. (2015) Toward quantification and source sector identification of fossil fuel CO_2 emissions from an urban area: Results from the INFLUX experiment, *Journal of Geophysical Research Atmospheres* 120, 292–312, doi:10.1002/2014JD022555.

UMBC (2020) Enhanced-PAMS Profiler and Ceilometer Network, https://alg.umbc.edu/ceilometer-testbed/, accessed August 2020.

Welton E.J., Campbell J.R., Spinhirne J.D. et al. (2001) Global monitoring of clouds and aerosols using a network of micropulse lidar systems, *Proc. SPIE,* 4153, 151–158.

WMO (2018) WMO guide to meteorological instruments and methods of observations, https://www.wmo.int/pages/prog/www/IMOP/CIMO-Guide.html

Yang F., Pan H., Krueger S.K. et al. (2006) Evaluation of the NCEP Global Forecast System at the ARM SGP Site. *Monthly Weather Reviews* 134, 3668–3690, https://doi.org/10.1175/MWR3264.1.

B.n. Satellite Remote Sensing of XCO_2

Sujong Jeong[1], Hayoung Park[1], David Crisp[2], Janne Hakkarainen[3]

[1]Seoul National University, Seoul, Korea

[2]Jet Propulsion Laboratory/California Institute of Technology, CA, USA

[3]Finnish Meteorological Institute, Helsinki, Finland

B.n.1 Introduction

To overcome the current spatial limitations of ground-based measurements, surface measurements can be augmented with high precision, spatially resolved estimates of the column-averaged dry air mole fractions of CO_2, i.e. XCO_2, retrieved from space-based remote sensing observations. While the space-based estimates are usually less precise and accurate than ground-based results, they complement ground-based measurements with their much greater spatial resolution and coverage.

Spatially resolved satellite remote sensing of XCO_2 has opened up opportunities to quantify the urban carbon cycle. With the advantage of satellite remote sensing, many studies have utilized XCO_2 to monitor urban carbon emissions and uptake from a single megacity, such as the Los Angeles Basin (Kort et al., 2012), to many cities across the globe (Hakkarainen et al., 2019; Labzovskii et al., 2019; Park et al., 2021). In this chapter, we introduce various ways to utilize satellite remote sensing of XCO_2 for analysis of the urban carbon cycle.

B.n.2 Available data sets

In this section, we cover only the satellites that are currently in orbit and measuring atmospheric mole fractions of CO_2 from space.

Table 1. Ongoing satellite missions for CO_2 observations

Satellite instrument	Observations	IFOV at nadir	Revisit time
OCO-2	CO_2, SIF	~3km^2	16 days
OCO-3	CO_2, SIF	~4km^2	Varies
GOSAT	CO_2, CH_4, SIF	10.5 km	3 days
GOSAT-2	CO_2, CH_4, CO, SIF	8~10.5km	6 days
TanSat	CO_2, SIF	2 km x 2 km	16 days

The Orbiting Carbon Observatory-2 (OCO-2) is the first NASA satellite that measures column-averaged CO_2 dry air mole fraction (XCO_2) from space with high accuracy, spatial resolution, and coverage over the globe. The OCO-2 carries a single instrument that has three co-boresighted, long-slit imaging grating spectrometers, which collect high resolution spectra by measuring the absorption by CO_2 and O_2 in reflected sunlight in three independent wavelength bands: the O_2 *A* band at around 0.765 μm, the weak CO_2 band at around 1.61 μm, and the strong CO_2 band at around 2.06 μm (Crisp et al. 2017). OCO-2 was launched in July 2014 and flies at an altitude of 705 km at the front of the Afternoon Constellation (A-Train), in an ascending-node, Sun-synchronous orbit that crosses the equator at 1336h local time. OCO-2 has a repeat cycle of 16 days. It collects data across a narrow (< 10 km) swath either along its ground track or in the direction of the apparent glint spot, where sunlight is specularly reflected from the surface. The swath is resolved into eight soundings, each with a footprint of an along-track dimension of ~2.25 km and a cross-track dimension that varies from 0.1 to 1.3 km, having a total area of < 3 km^2 at nadir (Crisp et al., 2017; Eldering et al., 2017). The instrument returns almost 1 million soundings each day over the sunlit hemisphere. On monthly timescales, 7~12% of these soundings pass the cloud and other data quality screenings to provide column-averaged estimates of XCO_2, yielding ~3 million XCO_2 estimates each month. In addition to its routine nadir and glint observations, OCO-2 collects thousands of observations in "target mode" over dedicated surface locations such as TCCON stations, which are used for validation, or large urban areas.

In May 2019, the OCO-2 flight spare instrument was installed on the International Space Station (ISS) as the Orbiting Carbon Observatory-3 (OCO-3) mission. Like OCO-2, the OCO-3 mission has been designed to collect high precision and highly spatially resolved global measurements of XCO_2 to improve our understanding of surface sources and sinks of CO_2 and the processes that control their seasonal variability. Since OCO-3 uses the OCO-2 flight spare instrument, it records spectra in the same three spectral channels, centred on the oxygen *A* band at 0.765 µm and the two CO_2 bands at 1.61 µm and 2.06 µm. Unlike OCO-2, which flies at 705 km and has a Sun-synchronous polar orbit, the ISS has a ~418 km altitude precessing orbit, which allows OCO-3 to collect observations at all hours between dawn and dusk. The OCO-3 footprints are < 4 km^2 and changes in aspect ratio with the viewing geometry. The instrument field of view is approximately 13 km, divided into eight footprints of 1.6 km width. Also, unlike OCO-2, which manoeuvres the entire spacecraft to point its instrument, OCO-3 is in a fixed position on the ISS and uses an agile pointing mirror assembly (PMA), which facilitates rapid transitions between nadir, glint, and target observations. In addition to these pointing modes, the PMA provides the ability to make observations in the Snapshot Area Map (SAM) mode, which scans the instrument field of view over a large contiguous area (80 km by 80 km) such as a city or forest, in a single overpass (Eldering et al., 2018; Taylor et al., 2020).

The Greenhouse Gases Observing Satellite "IBUKI" (GOSAT) was launched in 2009 and was the world's first spacecraft specifically dedicated to measure the mole fractions of two main greenhouse gases, CO_2 and CH_4, from space. The original objectives of the GOSAT mission are to monitor the global distribution of CO_2 and CH_4, estimate the sources and sinks of CO_2 on a subcontinental scale, and to verify the reduction of GHG emissions required by the Kyoto Protocol. GOSAT flies in a Sun-synchronous orbit at an altitude of 666 km. It has an equatorial overpass at a local solar time of 1300h with a revisit interval of three days. GOSAT is equipped with two sensors: Thermal and Near infrared Sensor for Carbon Observation – Fourier Transform Spectrometer (TANSO-FTS) and the Cloud and Aerosol Imager (TANSO-CAI). TANSO-FTS detects near infrared (NIR) and shortwave-infrared (SWIR) light reflected from the Earth's surface, along with the thermal infrared (TIR) radiation emitted from the ground and atmosphere. It has three narrow bands in the NIR and SWIR region (0.76, 1.6, and 2.0 µm) and a wide TIR band (5.5–14.3 µm). The NIR band has a resolution of ~0.36 cm^{-1} while the SWIR and TIR bands have a spectral resolution of about 0.25 cm^{-1} (Kuze et al., 2009). The TANSO-FTS instantaneous field of view (IFOV) is 15.8 mrad, corresponding to a nadir footprint diameter of 10.5 km (Shiomi et al., 2008). TANSO-CAI has four narrow bands in the near-ultraviolet to near infrared region at 0.38, 0.674, 0.87 and 1.6 µm with a higher spatial resolution than TANSO-FTS. TANSO-CAI can detect optically thick clouds inside the TANSO-FTS IFOV, which are used to correct the effect of aerosols in the TANSO-FTS spectrum data.

The GOSAT-2 mission was launched in 2018 and is aimed at continuing and advancing the GOSAT mission and providing useful information that contributes to environmental decision-making for global warming. GOSAT-2 monitors CO_2, CH_4, and CO globally from a Sun-synchronous, 613 km orbit that crosses the equator at a local time of 1300h and has a revisit time of six days. GOSAT-2 carries TANSO-FTS-2, which can measure the oxygen *A* band (0.76 µm), weak and strong CO_2 bands (1.6 µm and 2.0 µm), weak and strong CH_4 bands (1.6 µm and 2.3 µm), the weak CO band (2.3 µm), as well as a midwave TIR band (5.5–8.4 µm) and a longwave TIR band (8.4–14.3 µm) with 0.2 cm^{-1} spectral resolution. TANSO-CAI-2 on GOSAT-2 is an imaging radiometer for the ultraviolet (UV), visible, and SWIR regions providing cloud and aerosol information. Moreover, TANSO-FTS-2 carries a camera that has an intelligent pointing functionality which can identify cloudy areas in the TANSO-FTS-2 field of view before observation and relocate the observation point to a cloud-free area (Suto et al., 2020).

TanSat, China's first satellite for monitoring atmospheric CO_2, was launched in December 2016. TanSat is a Sun-synchronous polar-orbiting satellite with a local equator crossing time of ~1330h and a revisit period of 16 days; it has an orbit altitude of approximately 700 km (Du et al., 2018). TanSat provides CO_2 measurements with nine footprints along a swath of ~20 km, each with a spatial resolution of 2 km x 2 km in nadir mode. Like the OCO-2, TanSat measures CO_2 in three observations modes of nadir, glint and target. TanSat carries two key sensors: The Atmospheric Carbon dioxide Grating Spectroradiometer (ACGS) and the Cloud and Aerosol Polarization Imager (CAPI). The ACGS measures solar radiation reflected in the O_2 *A* band (0.76- 0.78 μm), the weak CO_2 absorption band (1.59–1.62 μm) and the strong CO_2 absorption band (2.04–2.08 μm). CAPI provides the cloud and aerosol optical properties and also allows the removal of cloudy soundings of the ACGS. The ground track of TanSat typically passes between two OCO-2 tracks, allowing potential future opportunities of increased spatial coverage with the combined usage of the two satellites (Yang et al., 2020; Wang et al., 2020).

B.n.3 XCO_2 urban enhancement

It is challenging to detect urban emission plumes in the atmospheric signal of CO_2 (i.e. CO_2 urban enhancement or CO_2 anomaly) given the fundamental linkage of atmospheric CO_2 with biospheric sources and influences from other processes such as atmospheric transport. Moreover, CO_2 has a long atmospheric lifetime and a comparably large background mole fraction that adds up to almost 410 ppm and insignificantly varies from pole-to-pole (Hakkarainen et al., 2019). For urban-scale studies, it is important to extract the local effect of fossil fuel combustion and anthropogenic emissions have on the atmospheric CO_2 mole fraction. The biospheric contribution to the urban signal represents an immensely strong source of interference as the biosphere regulates a significant portion of atmospheric variability of CO_2 at large scales, and this variability depends on the urban extent, vegetation type, biome, and season (Hutyra et al., 2014). Therefore, it is necessary to remove the non-anthropogenic (i.e. natural) portion of the atmospheric signal from the urban, fossil fuel based CO_2 enhancement. This procedure normally requires the elimination of vegetation-driven seasonal variability from the final urban CO_2 enhancement.

Many studies have utilized different methods to disaggregate the anthropogenic fluxes of CO_2. Kort et al. (2012) calculated the CO_2 enhancement of two megacities by differentiating the XCO_2 enhancement over the Los Angeles Basin megacity with nearby 'clean' observations that are less influenced by emissions and represent the background air. This method has been shown to work for other megacities such as Mumbai. With an addition of wind speed analysis in the process of calculating urban XCO_2 enhancement, it is also applicable in Seoul as demonstrated by Park et al. (2020). Another method to extract XCO_2 anomalies from pollution regions was used by Hakkarainen et al. (2016), where each individual satellite XCO_2 sounding was subtracted from the daily median value of the selected study regions to detrend and deseasonalize the CO_2 data. The mean of all the XCO_2 anomalies was then calculated from the defined regional grid box. In a different study, Hakkarainen et al. (2019) expanded on the anomaly calculation method to extract global XCO_2 anomalies, which are defined as the difference between the individual XCO_2 value and the daily background. The daily background value to calculate global XCO_2 anomalies is defined as the daily median for each 10-degree latitude band, which has been linearly interpolated to the location of each measured XCO_2 value. The anomalies are then aggregated, for example, in a $1^\circ \times 1^\circ$ spatial grid and averaged over a defined period of time.

Labzovskii et al. (2019) combined the urban to rural gradient method and statistical filtering approach to retrieve XCO_2 anomalies for each type of urban area. The XCO_2 anomaly is defined as the urban XCO_2 soundings subtracted by the background value. The urban soundings are constrained to satellite XCO_2 observations falling within the boundaries of any city or urban areas defined by the MODIS urban extent map (Schneider et al., 2009). A "background box" with an area of ~500,000 km^2 was set centred on the central point of each city. All the soundings that do not fall on urban pixels were considered rural observations, and the monthly median of the rural soundings were defined as the background value which are then subtracted from the urban soundings. Park et al. (2021) further developed the anomaly calculation method by creating a 10 km buffer zone around each urban area to filter out any contaminated rural observations that surround the urban area. Finally, instead of using monthly medians, daily medians analogous to the satellite track of rural soundings falling within the background box for each urban area were used as the background value.

B.n.4 Synergy of multi-satellites

A multitude of satellites are currently in orbit making atmospheric observations which range from mole fractions of greenhouse gases to air pollutants, aerosols, clouds, etc. Using a synergy of multiple satellites has proven to be effective in delineating fossil fuel CO_2 emissions and capturing emission characteristics. Comparing CO_2 together with air pollutants such as CO and ozone has multiple benefits in assessing the characteristics of urban air quality as it aids in disentangling urban enhancements of CO_2 from biogenic influences and attributing its anthropogenic sources (see also Section 4.8 and Annex B.h). Also, as atmospheric CO_2 shares common combustion sources with air pollutants such as CO and NO_2, the emission ratios of CO/CO_2 and NO_2/CO_2 vary with combustion efficiency, thus enabling us to better characterize their emission sources and their link to air quality. Therefore, improved quantification of greenhouse gas and pollutant co-emission patterns and characteristics can support mitigation strategies to reduce CO_2 and air pollutant emissions in urban areas.

Many studies have exploited satellite observations to analyse urban enhancements of anthropogenic CO_2 mole fractions together with other atmospheric constituents such as CO and NO_2. Hakkarainen et al. (2019, 2021) and Reuter et al. (2019) used satellite-based observations of NO_2 to estimate the emissions and spatio-temporal variability of CO_2 from point sources, while Berezin et al. (2013) used satellite measurements of NO_2 to verify CO_2 emissions from fossil fuel combustion. Since air pollutants like CO and NO_2 are feasible tracers of anthropogenic CO_2, the combination of CO_2, CO, and NO_2 can also compensate for the uncertainties associated with the inaccurate knowledge of technology and combustion conditions affecting CO and NO_2 separately (Konovalov et al., 2016). Silva et al. (2013) took retrievals of CO from the Measurement of Pollution in the Troposphere (MOPITT) and CO_2 from the Greenhouse Gases Observing Satellite (GOSAT) to analyse the CO_2/CO enhancement ratios ($\Delta CO_2/\Delta CO$) over megacities. The observed $\Delta CO_2/\Delta CO$ showed a distinct pattern of correlation with combustion activity as well as the “developed” and “developing” status of megacities. In a following study, Silva et al. (2017) used satellite observations of CO_2, CO, and NO_2 across 14 regions obtained from GOSAT, MOPITT, and the Ozone Monitoring Instrument (OMI), respectively, and demonstrated that spaceborne observations of enhancement patterns can distinguish combustion source characteristics such as combustion activity and efficiency on a regional scale.

Several studies have used TROPOMI NO_2 and OCO-2 XCO_2 observations together to analyse anthropogenic plumes and emissions (e.g. Reuter et al., 2019; Hakkarainen et al., 2019, 2021). Figure 7 illustrates an example of joint CO_2 and NO_2 analysis for the Highveld region in South Africa including several strong emissions sources. Individual plumes from Matimba power station, as well as the emission area south of Pretoria, are clearly visible from both OCO-2 XCO_2 and TROPOMI NO_2 observations. Park et al. (2021) used co-located urban enhancements of CO_2 and air pollutants CO and NO_2 to analyse emission characteristics of cities across the Northern Hemisphere. The ratios of $\Delta CO/\Delta CO_2$ and $NO_2/\Delta CO_2$ show distinct emission patterns located in different regions of the world. The ratios also showed a positive relationship to city population and GDP. In addition, when cities were divided into “developed” and “developing” cities, developing cities showed higher degradation of air quality with the increase of CO_2 and GDP.

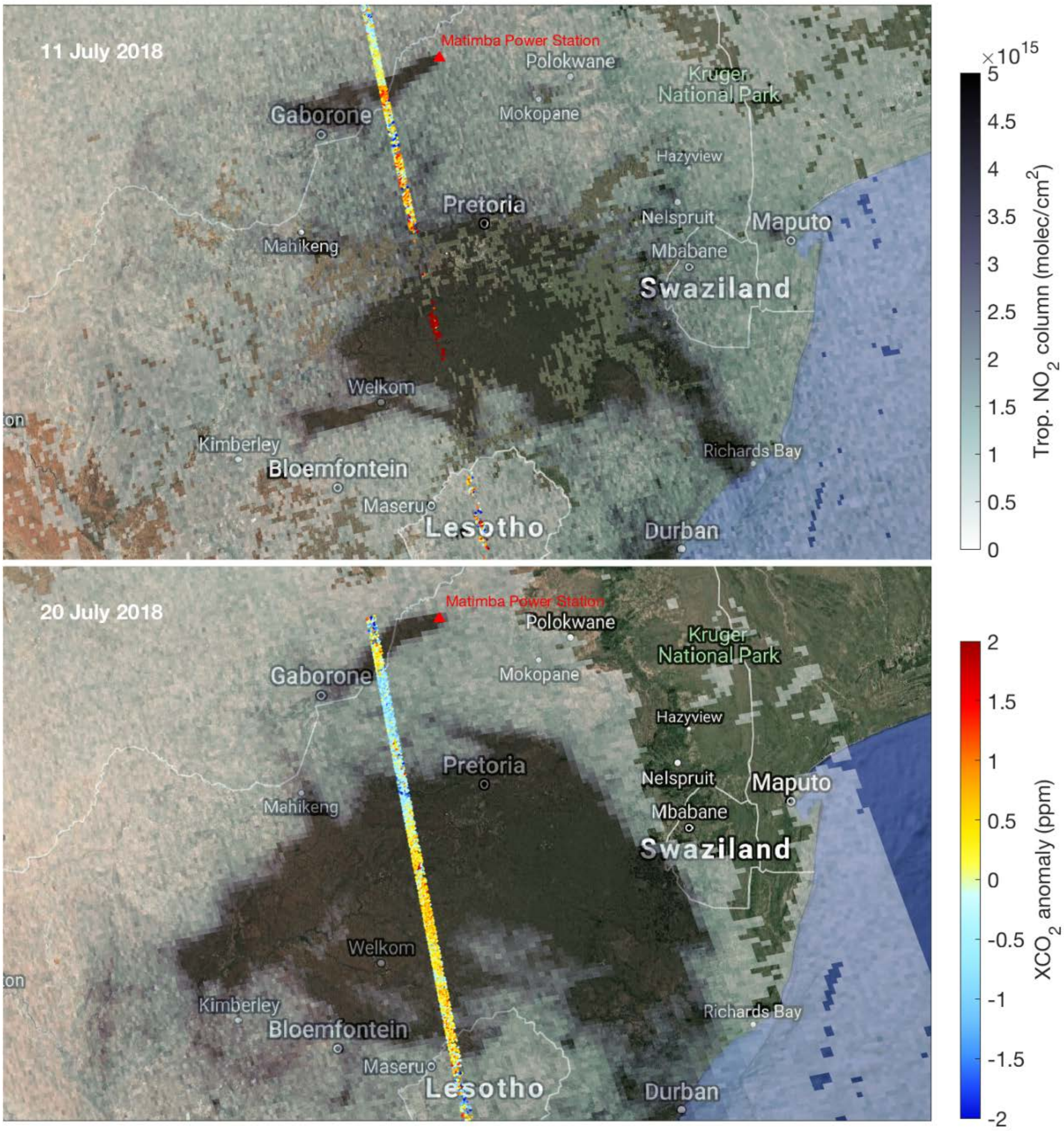

Figure 7. OCO-2 XCO_2 anomalies overlaid under TROPOMI NO_2 measurements (grey) show that positive XCO_2 anomalies (yellow-red colours) are visible over the plumes with the largest NO_2 enhancements (Hakkarainen et al., 2019).

B.n.5 Quantifying CO_2 fluxes from space-based observations

Satellite measurements of CO_2 have been used to quantify CO_2 fluxes on scales ranging from continents and large urban areas down to individual power plants. Estimates of CO_2 fluxes can be made from space-based column-averaged measurements using mass balance methods, plume dispersion models, or with more sophisticated atmospheric inversion systems. These methods can be used to predict or optimize the surface CO_2 fluxes that are required to reproduce observed XCO_2 distributions with considerations of atmospheric transport and wind fields varying with time. The mass balance method is a simple way of tracking CO_2 that move into and out of the domain of interest with the point source. With the assumption that the ambient wind profile is known and nearly constant in the mass balance method, flux estimations of CO_2 can be quantified over the set domain and interval. Plume dispersion models using satellite observations first distinguish the XCO_2 enhancements of the plume from background values. Then, by fitting the observed enhancements to a plume from a dispersion model and prior emissions, with consideration of meteorological conditions, a scaling factor is determined. The calculated scaling factor can be used to estimate the CO_2 emissions from the observed point source. Finally, atmospheric inversion models assimilate CO_2 data and adjust the surface fluxes to decrease the uncertainties when matching the model simulations to observations. In the inversion process, atmospheric transport models are used to improve prior estimates of surface fluxes and to relate them to spatially and temporally resolved CO_2 measurements. The atmospheric transport models, such as the Lagrangian particle dispersion model (LDPM), can use XCO_2 results gathered over a wider atmospheric footprint than those from a ground measurement at a specific site. As shown in Figure 8, the pixels represent the spatial extent and degree of influence (footprints) on the measurement site. The higher the modelled footprint value, the bigger the influence on the CO_2 mole fractions at the measurement site (See also Annex C.b).

Multiple studies have been made on quantifying CO_2 emissions from space-based observations. Nassar et al. (2017) first used OCO-2 observations to quantify CO_2 emissions from individual power plants. Their method modelled the plume profile as a Gaussian distribution that expands as it continues to be transported downwind. The best fit for the observed and model plume defined as XCO_2 enhancements is determined and used as a scale factor to estimate emissions of the point source. In this study, results of the emission estimates of US power plants were within 1–17% of EPA daily values. Ye et al. (2020) utilized XCO_2 observations from the OCO-2 to optimize whole-city fossil fuel CO_2 ($ffCO_2$) emissions using a Bayesian inversion system and high-resolution atmospheric transport model to reproduce fine-scale structures of $ffXCO_2$ plumes and to also link the surface CO_2 emissions with the XCO_2 observations. Their model also evaluates the contributions from transport model and measurement errors as well as the local variability of biospheric fluxes. Reuter et al. (2019) used OCO-2 with TROPOMI NO_2 observations to estimate CO_2 emissions with cross-sectional flux method. Wu et al. (2018) developed a forward simulation approach called 'X-STILT', which extends the Stochastic Time-Inverted Lagrangian Transport (STILT) model with column features and includes several comprehensive characteristics such as column transport error analysis, background XCO_2 approximation and enhancement calculation, and identification of upwind emitters using backward time runs from column receptors based on satellite overpasses. Top-down assessments using satellite models that include an accurate knowledge of atmospheric transport are important, as they enable the isolation of urban enhancements from background influences. In addition, quantifications of CO_2 fluxes using satellite models can help improve fossil fuel emission estimates and reduce uncertainties in CO_2 emission monitoring networks and emissions reporting.

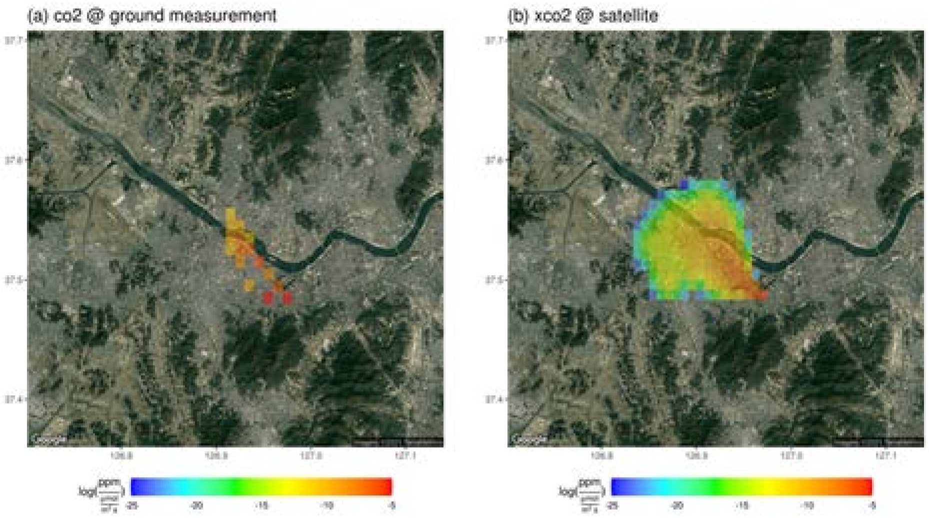

Figure 8. Atmospheric footprint of (a) one location of a ground measurement site and (b) a satellite pixel from the OCO-2 at the same location of the ground measurement modelled from the Weather and Research Forecasting–Stochastic Time-Inverted Lagrangian Transport (WRF–STILT) model simulation on a specific date (e.g. 20186–01).

The pixels represent the spatial extent and degree of influence (footprints) on the measurement site. The higher the modelled footprint value, the bigger the impact on CO_2 mole fractions at the measurement site.

B.n.6 Challenges in satellite data

Despite the benefits of satellite measurements having high precision and a global coverage, space-based observations still face multiple limitations. In exchange for the high resolution, high precision, and good accuracy of the measurements, satellites have irregular or infrequent observations over cities and are also prone to cloud and aerosol contamination during the retrieval, which results in lack of data availability. Moreover, the swath width of satellites such as OCO-2 limits the detection of individual CO_2 sources or plumes. As illustrated in Figure 1, only a cross-section of the plume can be seen with by the OCO-2 track. To overcome this limitation, the new OCO-3 SAM mode has allowed for a dense sampling of observation sites. Future missions of satellites, such as the Copernicus CO_2 Monitoring system (CO_2M) and the GOSAT-GW, in addition to constellation satellites, geostationary satellites, and cubesats observing CO_2 and other greenhouse gases, will allow for better coverage and larger sampling of atmospheric CO_2 mole fractions over urban areas.

B.n.6 References

Berezin E.V., Konovalov I.B., Ciais P. et al. (2013). Multiannual changes of CO_2 emissions in China: Indirect estimates derived from satellite measurements of tropospheric NO_2 columns. *Atmospheric Chemistry and Physics*, *13*(18), 9415–9438.

Crisp D., Pollock H.R., Rosenberg R. et al. (2017). The on orbit performance of the Orbiting Carbon Observatory-2 (OCO-2) instrument and its radiometrically calibrated products. *Atmospheric Measurement Techniques*, *10*(1), 59–81.

Du S., Liu L., Liu X. et al. (2018). Retrieval of global terrestrial solar induced chlorophyll fluorescence from TanSat satellite. *Science Bulletin*, *63*(22), 1502–1512.

Eldering A., Wennberg P.O., Crisp D. et al. (2017). The Orbiting Carbon Observatory-2 early science investigations of regional carbon dioxide fluxes. *Science*, *358*(6360).

Eldering A., Taylor T.E., O'Dell C.W. et al. (2018). The OCO-3 mission: Measurement objectives and expected performance based on 1 year of simulated data. *Atmospheric Measurement Techniques*, *12*(4), 2341–2370.

Hakkarainen J., Ialongo I. and Tamminen J. (2016). Direct space-based observations of anthropogenic CO_2 emission areas from OCO-2. *Geophysical Research Letters*, *43*(21), 11–400.

Hakkarainen J., Ialongo I., Maksyutov S. et al. (2019). Analysis of four years of global XCO_2 anomalies as seen by Orbiting Carbon Observatory-2. *Remote Sensing*, *11*(7), 850.

Hakkarainen J., Szeląg M.E., Ialongo I. et al. (2021). Analysing nitrogen oxides to carbon dioxide emission ratios from space: A case study of Matimba Power Station in South Africa, *Atmospheric Environment:* X, 10.

Hutyra L.R., Duren R., Gurney K.R. et al. (2014). Urbanization and the carbon cycle: Current capabilities and research outlook from the natural sciences perspective. *Earth's Future*, *2*(10), 473–495.

Konovalov I.B., Berezin E.V., Ciais P. et al. (2016). Estimation of fossil fuel CO 2 emissions using satellite measurements of “proxy” species. *Atmospheric Chemistry and Physics*, *16*(21), 13509–13540.

Kort E.A., Frankenberg C., Miller C.E. et al. (2012). Space-based observations of megacity carbon dioxide. *Geophysical Research Letters*, *39*(17).

Kuze A., Suto H., Nakajima M. et al. (2009). Thermal and near infrared sensor for carbon observation Fourier transform spectrometer on the Greenhouse Gases Observing Satellite for greenhouse gases monitoring. *Applied Optics*, *48*(35), 6716–6733.

Labzovskii L.D., Jeong S.J., and Parazoo N. C. (2019). Working towards confident spaceborne monitoring of carbon emissions from cities using Orbiting Carbon Observatory-2. *Remote Sensing of Environment*, *233*, 111359.

Nassar R., Hill T.G., McLinden C.A. et al. (2017). Quantifying CO_2 emissions from individual power plants from space. *Geophysical Research Letters,* 44.

Park C., Jeong S., Park H. et al. (2021). Evaluation of the potential use of satellite-derived XCO_2 in detecting CO_2 enhancement in megacities with limited ground observations: a case study in Seoul using Orbiting Carbon Observatory-2. *Asia-Pacific Journal of Atmospheric Sciences*, *57*(2), 289–299.

Park H., Jeong S., Park H. et al. (2021). An assessment of emission characteristics of Northern Hemisphere cities using spaceborne observations of CO_2, CO, and NO_2. *Remote Sensing of Environment*, *254*, 112246.

Reuter M., Buchwitz M., Schneising O. et al. (2019). Towards monitoring localized CO_2 emissions from space: co-located regional CO_2 and NO_2 enhancements observed by the OCO-2 and S5P satellites. *Atmospheric Chemistry and Physics* 19, 9371–9383.

Schneider A., Friedl M. A. and Potere D. (2009). A new map of global urban extent from MODIS satellite data. *Environmental Research Letters*, *4*(4), 044003.

Shiomi K., Kawakami S., Kina T. et al. (2008). GOSAT Level 1 processing and in orbit calibration plan, *Sensors, Systems, and Next-Generation Satellites XII*, 7106.

Silva S.J. and Arellano A.F. (2017). Characterizing regional scale combustion using satellite retrievals of CO, NO_2 and CO_2, *Remote Sensing*, *9*(7), 744.

Silva S.J., Arellano A.F. and Worden H.M. (2013). Toward anthropogenic combustion emission constraints from space-based analysis of urban CO_2/CO sensitivity, *Geophysical Research Letters*, *40*, 4971–4976.

Suto H., Kataoka F., Kikuchi N. et al. (2020). Thermal and near infrared sensor for carbon observation Fourier transform spectrometer-2 (TANSO-FTS-2) on the Greenhouse Gases Observing Satellite-2 (GOSAT-2) during its first year on orbit. *Atmospheric Measurement Techniques Discussions*, 1–51.

Taylor T.E., Eldering A., Merrelli A. et al. (2020). OCO-3 early mission operations and initial (vEarly) XCO_2 and SIF retrievals. *Remote Sensing of Environment*, *251*, 112032.

Wang S., Van Der A. R.J., Stammes P. et al. (2020). Carbon dioxide retrieval from TanSat observations and validation with TCCON Measurements. *Remote Sensing*, *12*(14), 2204.

Wu D., Lin J.C., Fasoli B. et al. (2018). A Lagrangian approach towards extracting signals of urban CO_2 emissions from satellite observations of atmospheric column CO 2 (XCO 2): X-Stochastic Time-Inverted Lagrangian Transport model (“X-STILT v1”). *Geoscientific Model Development*, *11*(12), 4843–4871.

Yang D., Boesch H., Liu Y. et al. (2020). Toward High Precision XCO_2 Retrievals from TanSat Observations: Retrieval Improvement and Validation against TCCON Measurements. *Journal of Geophysical Research: Atmospheres*, *125*(22), e2020JD032794.

Ye X., Lauvaux T., Kort E.A. et al. (2020). Constraining fossil fuel CO_2 emissions from urban area using OCO-2 observations of total column CO_2. *Journal of Geophysical Research: Atmospheres*, *125*(8), e2019JD030528.

Annex C. Data Assimilation Systems

C.a. Meteorological Inputs Needed for Urban Monitoring Systems

Israel Lopez-Coto[1], Kim Mueller[1], John Lin[2], Thomas Nehrkorn[3], Anna Agusti-Panareda[4], Richard Engelen[4], Irene Xueref-Remy[5], Ken Davis[6], James R. Whetstone[1]

[1]National Institute of Standards and Technology (NIST), Gaithersburg, Maryland, USA

[2]The University of Utah, Department of Atmospheric Sciences, Salt Lake City, UT, USA

[3]Atmospheric and Environmental Research, Lexington, MA, USA

[4]European Centre for Medium-Range Weather Forecasts, Reading, United Kingdom

[5]Institut Méditerranéen de Biodiversité et d'Ecologie Marine et Continentale, Universitaires d'Aix-Marseille, France

[6]Pennsylvania State University, University Park, Pennsylvania, USA

C.a.1. Background

All urban greenhouse gas (GHG) monitoring systems rely on meteorological inputs. In this section, we refer to “meteorological inputs” as the drivers of an atmospheric transport model(s), either offline or online, and mainly focus on how these models relate to an atmospheric inversion (AIM) rather than to other types of urban monitoring systems. Herein, we briefly describe atmospheric transport models, their function in an AIM, and provide guidelines and considerations for applying these models for the purpose of estimating urban emissions. Note that atmospheric dispersion is mainly discussed in the “Footprint Section” and only briefly discussed below.

C.a.2 Link to atmospheric inversion systems

The quantification of emissions is, by definition, an inverse problem because we use observable mole fractions of GHG in the atmosphere to infer the underlying/unknown emission distribution in both space and time. Inversions are used when the underlying emission distribution cannot be directly observed. A “transfer function” is needed to translate one state (e.g. concentration or mole fraction) to another (e.g. flux).

In general terms, this relationship can be written as follows:

$$G(m) = d \qquad \text{(Eq. 1)}$$

where the transfer function (G) relates the atmospheric observations of mole fraction (d) to the unknown “true” emissions fluxes (m) to estimate emissions. This relationship forms the backbone of any AIM. For a more detailed discussion of atmospheric inversion systems (AIM) including other components and equations, refer to Section 5.4, Annex 5.d.

The transfer function (G) in Eq. 1 is constructed using an atmospheric transport and dispersion model. The model characterizes the transport of GHG from an emission location, in both time and space, to where it is measured in the atmosphere using our understanding of atmospheric dynamics, physics, and chemistry. These atmospheric transport models can be as simple as a box or plume model or as complex as a model that attempts to solve the governing equations of atmospheric dynamics. The ability of the transport model to correctly or adequately simulate actual transport will directly impact the quality of the estimated emissions. That is why much care should be used in selecting, developing, and applying the atmospheric transport model in an AIM – the more accurately the model simulates actual conditions, the better the inferred emissions. Figure 8 provides a pictorial representation of an atmospheric transport model in an AIM.

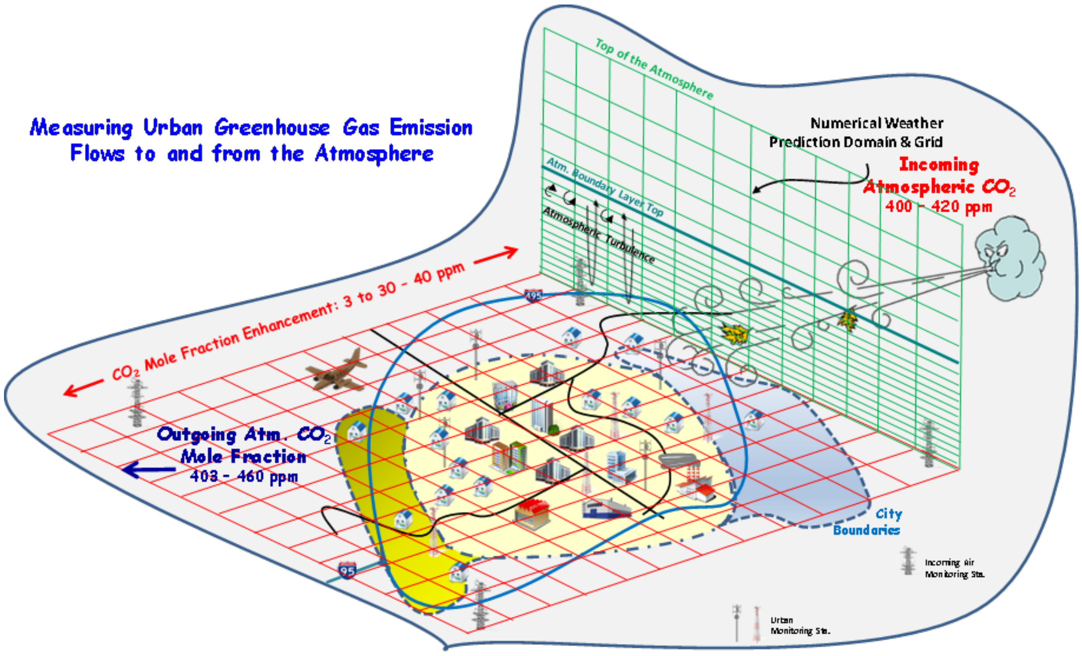

Figure 8: Measuring GHGs in an urban area is influenced by the region's characteristics.

Urban areas often contain several local governmental jurisdictions (shaded areas), various typology mixes of businesses, manufacturing and power generation plants, commercial and residential buildings, and various transportation systems. The incoming atmosphere carries CO_2 and other GHG's into the urban domain. The city emits GHG's dispersed in the atmosphere by turbulent motions of the atmospheric boundary layer. These emissions mix with the incoming air to enhance the amount and mole fraction of outgoing atmospheric GHG's. Measuring GHG fluxes within the domain can be accomplished with atmospheric GHG mole fraction measurements coupled with atmospheric transport and dispersion model and statistical optimization methods. Atmospheric GHG mole fraction measurements are observed from a surface network located in and around the region. Mass balance experiments are often accomplished with airborne measurements that give whole-city GHG fluxes.

C.a.3 Different Approaches to Modelling Atmospheric Transport

Two conceptually different approaches are used to model the atmospheric transport: Eulerian and Lagrangian models, as well as hybrid approaches, e.g. semi-Lagrangian. Eulerian models simulate transport using grid boxes that remain stationary, while Lagrangian models follow air parcels that move with the wind (Annex C.b). Both approaches are driven offline or online by NWP models with global or regional coverage with different resolution in time and space depending on the scope of the problem. For urban areas, high resolution meso-scale models are most common given their relatively finer temporal, horizontal and vertical resolutions. For street-level studies, a building-scale large eddy simulation (LES) model may be needed to properly represent the complexity of atmospheric flows. However, unresolved LES as well as other simpler approaches ranging from parameterized/diagnostic treatments to RANS-based CFD models might be helpful as well. A RANs model is a mathematic model based on average values of variable for both steady-state and dynamic flows. However, unresolved LES as well as other simpler approaches ranging from parameterized/diagnostic treatments to RANS-based CFD models might be helpful as well." "A RANs model is a mathematic model-based on average values of variable for both steady-state and dynamic flows.

C.a.4 Evaluating Atmospheric Models for AIM Applications

Since atmospheric transport modelling is a primary component of an inversion, understanding the model and any associated uncertainties and systematic errors (biases) is fundamental for improving the estimation of emissions. In general, advection (by wind fields resolved by the model) drives the transport while the turbulence (by generally unresolved/parameterized turbulent velocities, represented as needed for each model type) drives the mixing. Thus, an effort must be made to ensure that winds, mixing depth, turbulent kinetic energy and velocity variances are as accurately reproduced throughout the boundary layer as possible.

This is important for both the urban environment and rural areas surrounding it. The residence time of air over any urban environment is limited, and biases in the air inflow to the urban area may persist throughout the entire urban domain. Evaluation of the atmospheric transport in the study area and regions upwind is therefore, of great importance.

The accuracy and uncertainty of the meteorological fields are assessed using a variety of techniques. Any model performance assessment should be in line with the specific application to quantify urban emissions, and the required performance may vary with the objectives (e.g. long-term bias vs short-term precision).

C.a.5 Custom Meteorological Data Assimilation

The assimilation of meteorological data has been shown is some studies to reduce errors. However, it is unclear whether data assimilation would significantly improve the atmospheric transport model if the meteorological observations are sparse or difficult to represent by the underlying NWP model because they are influenced by hyper-local conditions. This is especially true if the meteorological observations suffer from systematic errors or for those meteorological variables that cannot be observationally constrained (e.g. TKE, etc.). Additionally, physical conservation laws within atmospheric transport model may be violated so these techniques must be used carefully and evaluated thoroughly.

C.a.6 Ensembles

As uncertainty associated with transport affects the interpretation of observed mole fractions in AIM, it is a required AIM input in the form of error covariance matrices (Annex C.d). To include those, covariances of atmospheric transport error can be computed using an ensemble of simulations where the different sources of uncertainty are perturbed within their uncertainty range (e.g. initial meteorological input, transport model parameters/tendencies). Numerical Weather Prediction Centres can provide information on uncertainties associated with meteorological analysis (https://www.ecmwf.int/sites/default/files/elibrary/2010/10125-ensemble-data-assimilations-ecmwf.pdf).

Atmospheric transport model ensembles are an effective means of characterizing uncertainty in atmospheric transport simulations. A long history of ensemble modelling exists in the atmospheric sciences research literature. As an ensemble, to properly represent uncertainty in the atmospheric modelling system, the mean of the ensemble should be unbiased, and the spread of the ensemble members should represent the random error in the modelling system. Ensembles can be based on initial conditions perturbations, in different physical parametrizations or a combination of them. For GHG studies, the key goal is to generate enough plausible variability. Recent research has explored the development of small transport ensembles and “calibration” methodologies based on techniques like the Rank histogram (“Talagram plots”). The ensemble methods represent an effective approach to empirically quantifying the complex uncertainty in atmospheric transport simulations.

C.a.7 Model Improvement Avenues

The planetary boundary layer (PBL) turbulent mixing parametrization drives the vertical mixing of mass, heat and momentum in the PBL and therefore directly impacts the prediction of temperature, winds, mixing depth and ultimately the tracer mole fractions in different parts of the atmosphere as well as its evolution. The physical processes involved are complex and two main theory branches for PBL parametrizations exist: local vs non-local mixing. However, there is a trend in the research community to unify both types of concepts by using hybrid parametrizations where local and non-local concepts are included. In addition, as the model resolution becomes smaller, “grey zone” issues start to appear where the turbulence is partially resolved but the PBL scheme is still parameterized. Models that are “scale-aware” are starting to emerge to mitigate this problem. Lastly, stable conditions remain a challenge as well as typical turbulence scales are largely reduced. These complex issues would benefit from further research.

The surface layer parametrization is responsible for the calculation of the heat and latent fluxes, which act as the surface boundary condition for the PBL scheme and strongly influence the near-surface variables and PBL mean properties. As a result, accurate simulations of the energy and momentum fluxes at the Earth’s surface are perhaps the most important input to accurate and precise simulation of atmospheric boundary layer mixing. Robust simulation of land surface fluxes remains a challenge because of the complexity of the soil-vegetation-atmosphere system. This challenge is amplified by the heterogeneity of the urban land surface. The evaluation of modelled surface fluxes, both upwind of and within the urban environment, can help diagnose the causes of biases in urban atmospheric boundary layer simulations to aid the refinement of the model.

In Lagrangian models, the mixing is often parametrized using different schemes than those employed in the meteorological models used to drive them. These can lead to inconsistencies between the Eulerian and Lagrangian models and additional research and development is needed to unify the coupling of these two approaches.

C.a.8 Definitions

Below we provide specific definitions and recommendations for selecting and using meteorological inputs (an atmospheric meteorological model) in urban monitoring systems. In the following, we use the American Meteorological Society (AMS) definition for the following four terms (http://glossary.ametsoc.org/wiki/Background_field):

- Analysis: An analysis may be looked upon as a space–time interpolation system. It is a procedure to project the state of the atmosphere (or any system) as known from a finite set of imperfect and irregularly distributed observations onto a regular grid or to represent it by the amplitude of standard mathematical functions.
- Reanalysis: Like an analysis but interpolates retrospectively and the background field[1] is made by a NWP model that does not change over the entire period of the reanalysis. A reanalysis yields complete, gridded data that is as temporally homogeneous as possible. Reanalysis data include many derived fields for which direct meteorological observations are nearly absent.
- Forecast: An assessment of the future state of the atmosphere. Such assessments are usually made by national/international organizations or private meteorologists, often using numerical simulations. Such simulations are the result of representing the atmosphere mathematically as a fluid in motion.

[1] http://glossary.ametsoc.org/wiki/Background_field

- Forecast Verification: Any process for determining the accuracy of a weather forecast by comparing the predicted weather with the observed weather of the forecast period.

C.a.9 Recommendations for use in an AIM model

Define a horizontal resolution relevant to the target problem size and terrain complexity. Depending on the application and feasibility, finer resolution models are preferred up to the limit that the physical approximations intrinsic to the parameterizations adopted in the model hold. If the option is available, nested domains or adaptive grid solutions may be considered.

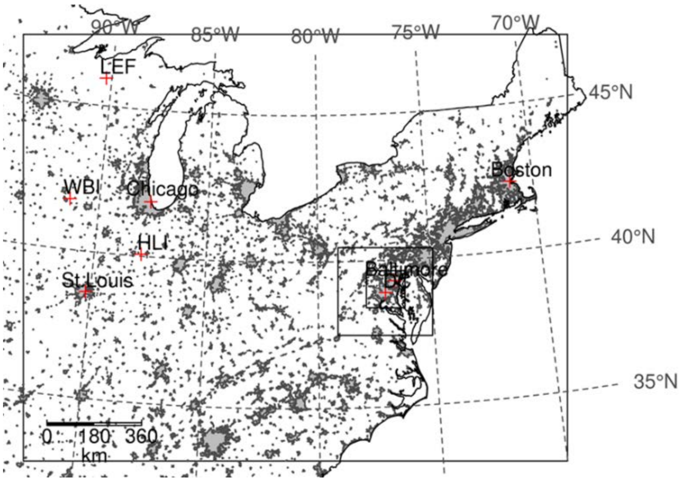

Figure 9: Example Nested Domain Configuration for the USA Northeastern Corridor

C.a.9.1 Vertical resolution

The vertical resolution should be fine enough to resolve the vertical development of the PBL over time and to resolve vertical gradients in GHGs corresponding with the atmospheric GHG measurements used within the AIM.

C.a.9.2 Domain size.

The size of the domain should also be in accordance with the target problem domain. In general, the area for which emissions are to be estimated should be far enough from the domain's edges to avoid boundary effects and allow for some spatial spin up of the simulation so that numerical anomalies are minimized.

C.a.9.3 Meteorological products

If "off-the-shelf" meteorological products are used, preference should be given to well known products generated by national or international agencies or other certifiable sources, like the NOAA-NWS, ECMWF[2], or similar. In general, these products include state of the art data assimilation and are verified on a regular basis. They also use consistent versions of the system for long periods of time, update previous data to some extent and have robust documentation. For increased vertical resolution, "model levels" data should be preferred against "pressure levels" for the offline model to better reproduce atmospheric transport in the native meteorological model and reduce interpolation errors. Reanalysis, analysis and forecast

---

[2] NOAA-NWS: US National Oceanic and Atmospheric Administration, National Weather Service and ECMWF: European Centre for Medium-Range Weather Forecasts

products should be considered in that order. In general, forecasts should only be used if no other alternative is available because it will diverge from the "true state" as the forecast horizon increases due to the chaotic nature of the atmosphere because it is a complex dynamical system. Short-range forecasts could be used if timeliness is of essence, or the temporal and spatial resolutions are much better than that of available reanalysis products.

C.a.9.4 LES Models

For city scale modelling, finer horizontal, vertical and temporal resolutions might be needed. Specifically, if GHG measurements are within urban canyons and/or within building wakes, much higher fidelity modelling including LES may be needed. Mesoscale models should not be used on grid spacings less than ~1 km without careful consideration of "grey zone" issues.

C.a.9.5 Regional simulations

In the case of custom regional simulations, well established and tested meteorological models like the Weather Research and Forecasting Model (WRF) or similar (open source community models for transparency) should be considered for use in an AIM. The physical parametrizations should be selected relative to previous studies for the period and area of interest or to perform sensitivity tests specifically conducted to test the ability of the model to simulate actual conditions.

The hierarchy of meteorological drivers to be used for initial and boundary conditions for customized systems should follow the same order as Item #3, i.e. reanalysis, analysis and forecast products. As before, forecast should only be used if no other alternative is available.

Custom meteorological data assimilation may be used to improve model performance, but physical conservation laws within atmospheric transport model may be violated with some techniques like "nudging". In any case, the performance improvements should not be taken as a given as undesirable side-effects can appear by ingesting "bad" observations or by using poorly configured systems and thus data assimilation techniques must be used carefully and evaluated thoroughly.

C.a.9.6 Evaluation

In all cases, evaluation against independent observations (those not used in custom meteorological data assimilation) of the most important variables affecting tracer transport (e.g. wind direction, wind speed, mixing depth and turbulence) should be used – if available. This step provides useful information about the reliability of the simulations for specific locations and times. Both surface and upper air performance should be investigated. Refer to the "Meteorological and Boundary Layer Observation Section" for more information. Examples of observations useful for evaluation are:

- Mixing depth (micropulse LIDAR, inferred from aircraft and ACARS, ceilometers, radiosondes, etc.).
- Turbulence statistics (3D sonic, Doppler LIDAR, aircraft measurements, etc.).
- Wind speed/direction (Doppler lidar, ground stations, ACARS, radiosondes, wind profilers, etc.).

Despite any meticulous attempt to set up a meteorological model, in general, significant biases in mixing depth, wind speed, wind direction and turbulence characteristics for specific locations and times may occur due to errors in boundary conditions or model physics/numerics approximations. Therefore, it is desirable to use at least two meteorological models with similar overall performance metrics that are sufficiently independent to evaluate the impact of the choice of atmospheric transport on inferred emissions. If possible given resources, an ensemble of transport models should be used to help quantify transport model uncertainties. Consideration of the AIM application should be taken into consideration.

Transparency is of paramount importance and, thus, model configurations, observations used, and performances should be fully assessed, documented, justified and referenced.

Refer to the WMO/GAW Urban Research Meteorology and Environment (GURME) project for any additional guidance.

C.a.10 References

American Meteorological Society (2020) "Analysis, Reanalysis, Forecast". Glossary of Meteorology, http://glossary.ametsoc.org/wiki/

Agustí-Panareda A., Diamantakis M., Massart S. et al. (2019) Modelling CO_2 weather – why horizontal resolution matters, 19, *Atmospheric Chemistry and Physics* 7347–7376, https://doi.org/10.5194/acp-19–7347–2019.

Angevine et al. (2013) Pollutant transport among California regions, *Journal of Geophysical Research: Atmospheres* 118, 1–14, doi:10.1002/jgrd.50490

Angevine et al. (2012) Meteorological model evaluation for CalNex 2010, *Monthly Weather Reviews* 140, 3885–3906, DOI: 10.1175/MWR-D-12–00042.1

Angevine et al. (2020) Transition Periods in the Diurnally-Varying Atmospheric Boundary Layer Over Land, *Boundary Layer Meteorology.*

Deng A., Lauvaux T., Davis K.J. et al. (2017) Toward reduced transport errors in a high resolution urban CO_2 inversion system. *Elementa: Science of the Anthropocene* 5:20. DOI: http://doi.org/10.1525/elementa.133

Díaz-Isaac L.I., Lauvaux T., Bocquet M. et al. (2019) Calibration of a multi-physics ensemble for estimating the uncertainty of a greenhouse gas atmospheric transport model, *Atmospheric Chemistry and Physics* 19, 5695–5718, https://doi.org/10.5194/acp-19–5695–2019, 2019.

Feng S., Lauvaux T., Davis K. et al. (2019). Seasonal characteristics of model uncertainties from biogenic fluxes, transport, and large-scale boundary inflow in atmospheric CO_2 simulations over North America. *Journal of Geophysical Research: Atmospheres*,124, 14,325–14,346. https://doi.org/10.1029/2019JD031165

Gaudet B.J., Lauvaux T., Deng A. et al. (2017) Exploration of the impact of nearby sources on urban atmospheric inversions using large eddy simulation. *Elementa: Science of the Anthropocene* 5:60. DOI: http://doi.org/10.1525/elementa.247

Han B.-S., Park S.-B., Baik J.-J. et al. (2017), Large-eddy simulation of vortex streets and pollutant dispersion behind high-rise buildings. *Q.J.R. Meteorol. Soc,* 143: 2714–2726. doi:10.1002/qj.3120

Hanna S.R. et al. (2006) Detailed simulations of atmospheric flow and dispersion in downtown Manhattan: An application of five computational fluid dynamics models. *Bulletin of the American Meteorological Society* 87 (12), 1713–1726.

Hanna S.R. et al. (2011) Comparisons of JU2003 observations with four diagnostic urban wind flow and Lagrangian particle dispersion models. *Atmospheric Environment* 45 (24), 4073 – 4081, doi:10.1016/j.atmosenv.2011.03.058.

Karion A., Lauvaux T., Lopez-Coto I. et al. (2019) Intercomparison of atmospheric trace gas dispersion models: Barnett Shale case study, *Atmospheric Chemistry and Physics* 19, 2561–2576

Lac C. et al. (2013) CO_2 dispersion modelling over Paris region within the CO_2 MEGAPARIS project, *Atmospheric Chemistry and Physics* 4941–4961

Lateb M., Meroney R., Yataghene M. et al. (2016) On the use of numerical modelling for near-field pollutant dispersion in urban environments A review. *Environmental Pollution*, 208, 271 – 283, doi:10.1016/j.envpol.2015.07.039.

Lopez-Coto I., Ren X., Salmon O.E. et al. (2020) Wintertime CO_2, CH_4, and CO Emissions Estimation for the Washington, D.C.–Baltimore Metropolitan Area Using an Inverse Modelling Technique *Environmental Science & Technology* 54 (5), 2606–2614. DOI: 10.1021/acs.est.9b06619

Lopez-Coto I., Hicks M., Karion A. et al. (2020) Assessment of Planetary Boundary Layer Parameterizations and Urban Heat Island Comparison: Impacts and Implications for Tracer Transport. *Journal of Applied Meteorology and Climatology* 59, 1637–1653, https://doi.org/10.1175/JAMC-D-19–0168.1.

Sargent M., Barrera Y., Nehrkorn T. et al. (2018) Anthropogenic and biogenic CO_2 fluxes in the Boston urban region. *Proceedings of the National Academy of Sciences* 115(29):7491?7496, 2018. doi:10.1073/pnas.1803715115.

McNorton J.R., Bousserez N., Agustí-Panareda A. et al. (2020) Representing model uncertainty for global atmospheric CO_2 flux inversions using ECMWF-IFS-46R1, *Geoscientific Model Development 13*, 2297–2313, https://doi.org/10.5194/gmd-13–2297–2020, 2020.

Nehrkorn T., Henderson J., Leidner M. et al. (2013) WRF simulations of the urban circulation in the Salt Lake City area for CO_2 modelling. *Journal of Applied Meteorology and Climatology* 52 (2), 323?340, doi: 10.1175/JAMC-D-12–061.1.

Pal S., Xueref-Remy I., Ammoura L. et al. (2012) Spatio-temporal variability of the atmospheric boundary layer depth over the Paris agglomeration: An assessment of the impact of the urban heat island intensity. *Atmospheric Environment*, Elsevier, 2012, 63, pp.261–275. ⟨10.1016/j.atmosenv.2012.09.046⟩. ⟨hal-00748695⟩

Sarmiento D.P., Davis K.J., Deng A. et al. (2017) A comprehensive assessment of land surface-atmosphere interactions in a WRF/Urban modelling system for Indianapolis, IN, *Elementa: Science of the Anthropocene* 5:23. DOI: http://doi.org/10.1525/elementa.132

Solazzo et al. (2017) Evaluation and error apportionment of an ensemble of atmospheric chemistry transport modelling systems: multivariable temporal and spatial breakdown, *Atmospheric Chemistry and Physics* 3001–3054

Stauffer D.R. and Seaman N.L. (1990) Use of Four-Dimensional Data Assimilation in a Limited-Area Mesoscale Model. Part I: Experiments with Synoptic-Scale Data. *Monthly Weather Reviews* 118, 1250–1277.

Wennberg P.O., Wunch D., Roehl C. et al. (2014) TCCON data from California Institute of Technology, Pasadena, California, USA, ReleaseGGG2014R1, TCCON data archive, hosted by Caltech-DATA, California Institute of Technology, Pasadena, CA, USA, https://doi.org/10.14291/tccon.ggg2014.pasadena01.R1/1182415,2014.

Xueref-Remy I. et al. (2018) Diurnal, synoptic and seasonal variability of atmospheric CO_2 in the Paris megacity area, *Atmospheric Chemistry and Physics* 3335–3362

Y. Barrera, Nehrkorn T., Hegarty J. et al. (2019) Using LIDAR technology to assess urban air pollution and improve estimates of greenhouse gas emissions in Boston. *Environmental Science & Technology* 53(15):8957–8966, 2019. doi:10.1021/acs.est.9b00650.

C.b. Forward modelling

Thomas Lauvaux[1], Kim Mueller[2], Lee Murray[3], Anna Agusti-Panareda[4]

[1]Laboratoire des Sciences du Climat et de l'Environnement, Gif sur Yvette, France

[2]National Institute of Standards and Technology (NIST), Gaithersburg, Maryland, USA

[3]Earth and Environmental Sciences, University of Rochester, NY, USA

[4]European Centre for Medium-Range Weather Forecasts, Reading, United Kingdom

Atmospheric modelling of GHGs in forward mode remains common practice at global scale. Different approaches associated with forward modelling of tracer transport exist depending on whether the meteorological parameters are computed online by the model or pre-processed offline from a numerical weather prediction model. Observational footprints may be generated using Green's response functions from forward runs transporting multiple tracers separately, each of them representing a specific area of the model surface. At regional and urban scales, backward in time simulations (e.g. using Lagrangian Particle Dispersion Modelling) become more computationally efficient as particles representing air masses leave the simulation domain more rapidly. Hence, forward simulations of passive tracers are often discarded. Despite the computational advantage, forward modelling often remains the unique approach able to evaluate the performances of backward Lagrangian simulations. Therefore, they are a valuable tool when interpreting complex observations at regional scale. For known source locations such as point sources or whole-city emissions, forward simulations produce the link between the mole fractions and the sources. Equally important, they are a means to evaluate transport model errors.

Across all scales, forward modelling provides information beyond observations (unobserved areas) and offers more flexibility in observing systems by simulating the whole spatio-temporal dimensions of the mole fraction space. Atmospheric forward modelling is also able to explicitly represent mixing heights and not boundary layer height, as well as path-integrated measurements (e.g. columns from space borne instruments). However, representing accurately the atmospheric transport of passive tracers requires careful consideration of the model configuration and its numerical schemes.

Considerations

- Conservation of mass remains the main and foremost issue to be considered at each step of the modelling system, from advection to convection. Relatively small imbalanced terms can generate large losses/gains in mass. Specific physical schemes tend to create/remove mass more often than others. While advection represents a linear motion at fine timescales, convection involves pressure perturbations and water exchanges prone to disequilibrium. Meteorological data assimilation also perturbs the mass balance by adjusting pressure and humidity making mass adjustment at each model time step necessary.
- All Eulerian models are subject to numerical diffusion, which may exceed the real-world diffusion that results from turbulence and other mixing processes. It is impossible for a model to resolve concentrated plumes that exist at finer horizontal and vertical resolutions than those of the model unless one transports higher-order moments of the subgrid tracer distribution. In practice, this is rarely done due to computational cost (e.g. the Quadratic Upstream Method requires transporting 9x the tracers). Certain numerical advection methods are more diffuse than others. Similarly, numerical diffusion happens regardless of whether the model runs forward or backwards in time. That is, it is numerically impossible to represent the

gathering (i.e. reverse diffusion) of dispersed particles into a concentrated plume when running Eulerian models backwards in time. Other numerical artifacts of advection schemes introduce errors that can include a lack of positive definiteness, monotonicity, locality, transportivity or correlativity.

- Continuous injection of mass fluxes into the atmosphere guarantees the fair representation of plume structures. The injection height for point sources above the surface should be considered. Short-term wind and turbulence variability are responsible for fine-scale structures that only frequent mass injection can represent.
- Conservation of GHG mass/concentration at the boundaries (e.g. global to regional scale) when running a bounded simulation domain involves different horizontal resolutions, hence different surface pressures that makes it nearly impossible to reconcile mass and concentration over the column. Depending on the observing systems, one strategy should be used: conserving the total mass coming from outside the domain (path-integrated) or modifying the mass but conserving the concentration (in situ).
- Spin up time ensures that the modelling system is theoretically at equilibrium. At global scale, the point is defined in time when a specific tracer has diffused so broadly that spatial gradients in concentrations have vanished entirely. At the regional scale, it is better represented by the absence of initial conditions, meaning that the air present at the start of the simulation has been entirely replaced by air from the domain boundaries.
- Drying air mole fraction remains challenging in specific instances. Convection schemes, which involve multiple phases being constantly adjusted within clouds, can pose major challenges to accurately dry air masses when calculating mixing ratios. Alternatively, drying can take place when mixing ratios are extracted from the simulation.
- For online forward models, regional models tend to deviate from the meteorological analysis. This is because the highly non-linear equations of motion effectively lose all memory of their initial conditions within 10 days. It is highly recommended to re-start simulations on a regular basis (i.e. every week at least). Looping simulation periods generates discontinuities in atmospheric transport, while GHG mixing ratios are simply looped continuously. This important detail can generate unrealistic structures by abruptly changing the air flow and must be adjusted (e.g. taking place at night) or smoothed (by overlapping simulation windows).
- An important consideration for offline models is inconsistencies between the meteorological parameters (e.g. from analysis) and the regional transport model, particularly regarding horizontal, vertical, and temporal resolution as well as the vertical coordinate.
- Near-surface mole fractions remain challenging as the surface is often poorly represented and the vertical resolution is too coarse compared to existing structures on the ground. This problem is particularly impactful when buildings cover most of a model grid cell, in urban areas for example. Some urban schemes do not allow high vertical resolutions so that ground structures can be parameterized within the first model layer. The vertical resolution must be defined to allow proper land surface modelling while being sufficiently high to represent mixing ratios near the surface. Furthermore, the accuracy of boundary layer heights and their diurnal variations in forward models remains poorly constrained, which directly translates to uncertainties in calculating surface mole fractions from recent emissions; for these reasons, many studies limit their analyses to local midafternoon.

Ongoing Research

- Global simulations with adaptive mesh models able to simulate parts of the globe at higher resolutions
- Online adjoint modelling at regional scales able to invert for surface and boundary fluxes within the forward simulation
- Convection and advection schemes including accurate representation of vertical transport, aerosol interactions, and mass balance conservation.

C.c. Calculation of atmospheric footprints needed for urban monitoring

John C. Lin[1], Ignacio Pisso[2], Israel Lopez-Coto[3]

[1]The University of Utah, Department of Atmospheric Sciences, Salt Lake City, UT, USA

[2]Norwegian Institute for Aire Research (NILU), Atmosphere and climate department, Kjeller, Norway

[3]National Institute of Standards and Technology (NIST), Gaithersburg, Maryland, USA

C.c.1 Introduction

With the availability of atmospheric GHG observations, a natural question arises in order to apply atmospheric GHG data to understand emissions: what is the source region that influences the air observed by the "receptor"—i.e. the GHG sensor? Clearly, to answer this question, knowledge of atmospheric transport—e.g. wind direction, wind speed, and atmospheric mixing—is necessary to elucidate the exact source regions upwind of the receptor that are influencing the measurements at the sensor location.

One of the most straightforward approaches to glean the impact of atmospheric transport is to examine the observed wind directions during the GHG measurements. However, this simple approach, often referred to as a "wind rose", only yields qualitative information and cannot provide the quantitative linkage between the source region and the receptor. For instance, knowledge that the wind was westerly during a spike in GHG merely suggests that the source is somewhere to the west of the receptor, without informing the researcher the amount of change in GHG mole fraction for a given unit emission from a particular location. Instead, the use of GHG measurements to provide quantitative information about GHG emissions requires knowledge about the sensitivity of the receptor observation to a particular source area. Known as the "footprint" (Lin et al. 2003) or the "source-receptor relation (SRR)" (Seibert and Frank 2004), the sensitivity is often quantified in units of mixing ratio per surface flux—e.g. [(ppm)/(µmole m^{-2} s^{-1})] —meaning the amount of change in GHG mole fraction at the receptor, given an unit emission of 1 µmole m^{-2} s^{-1} at a source area. The transported quantity in the models is often a conserved one, such as mixing ratio (sinks and sources are explicitly represented). Different factors and additional hypotheses about, for example, mixing can be applied at the source or the receptor for changing units. The footprint is the quantitative information used to construct the Jacobian matrix in inverse analysis (Rodgers 2000). The relevant GHG observations to understand GHG emissions take place in the lower atmosphere, within the PBL, where the surface emissions translate into large mole fraction changes (Gerbig et al. 2003a). Even changes in atmospheric column-averaged GHG mole fractions mainly reflect changes within the PBL, with the caveat that the mole fraction changes are smaller due to dilution of the signal throughout the atmospheric column (Rayner and O'Brien 2001).

C.c.2 Accounting for turbulent dispersion

Atmospheric transport within the PBL is strongly dominated by turbulence and turbulent dispersion (Stull 1988). The stochastic nature of turbulence means that the path between the source and the receptor can never be defined by a single air parcel trajectory (Stohl and Wotawa 1993). Instead, the transport is more closely approximated by an ensemble of air parcels, each of which traces a stochastic trajectory incorporating the random nature of turbulent eddies, drawing upon classical work by G.I. Taylor (Taylor 1920). Models which adopt the stochastic, ensemble trajectory (Figure 10) approach are referred to as Lagrangian particle dispersion models (LPDM). Even until the 1990s, the usage of LPDMs to reveal atmospheric footprints has been limited, mainly due to the computational cost and the difficulty of obtaining meteorological fields to drive the LPDM. However, in recent decades LPDMs have been widely adopted by atmospheric researchers in general to simulate atmospheric footprints with the widespread availability of computational resources and meteorological fields (Lin et al. 2012).

C.c.3 Constructing the footprint

The air parcels within LPDMs can be simulated either forward or backward in time. Whether forward-time or backward time simulation is more computationally efficient depends on the number of sources versus receptors (Lin et al. 2012). If receptors outnumber sources, then simulating air parcels forward in time from the sources would be more efficient. An example could be trying to assess the impact of large point sources such as a few power plants or methane emission hotspots on downwind regions. Conversely, if there are fewer receptors than sources, then tracing air parcels backward in time receptors to upwind sources would be more efficient (Figure 10). This is generally the case in urban applications, where the number of GHG measurement locations (i.e. receptors) is typically dwarfed by the large number of sources (see Emission Inventory section).

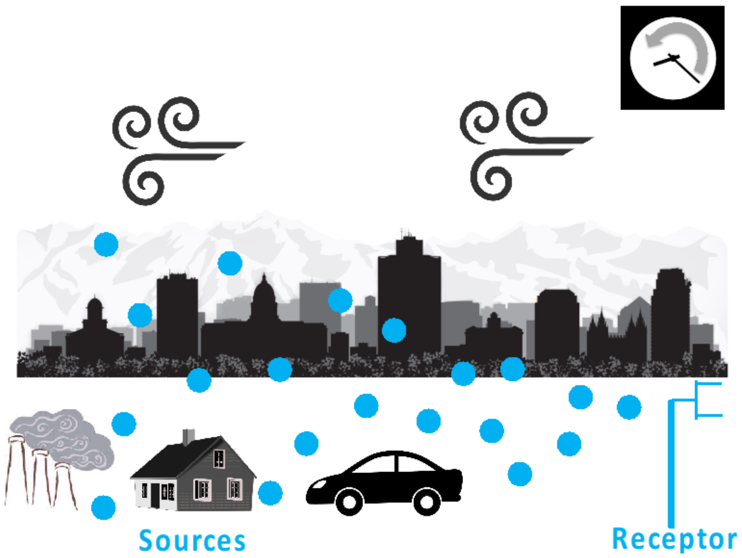

Figure 10: Application of Lagrangian particle dispersion model (LPDM) to link the receptor (where GHG measurements take place) to upwind sources by simulating the transport of an ensemble of air parcels backward in time. Turbulent dispersion is modelled through the stochastic motions of the parcels. The atmospheric "footprint", or source-receptor relationship, is calculated by the amount of time the air parcels spend near the sources, typically at the ground surface.

The LPDM setup must reflect the nature of the GHG sensor. For in situ sensors, the receptor is a point location, and the air parcel ensemble is released at a single point matching the sensor inlet height (Figure 10). Alternatively, remote sensing instruments can also measure GHG mole fractions averaged over the atmospheric column—either from the ground surface (Wunch et al. 2011)(Chen et al. 2016) or from space (Yokota et al. 2009)(Crisp et al. 2004). In this case, the air parcel ensemble is released over the column, and the contributions from various vertical levels need to be properly weighted by the sensor's averaging kernel and by the air pressure in order for an "apples-to-apples" comparison between the simulations and the GHG sensor (Wu et al. 2018).

C.c.4 Importance of Driving Meteorology

The movement of air parcels within LPDMs is driven by interpolating gridded winds down to each parcel's location and also parameterizing the stochastic eddies based on meteorological variables. Therefore, the veracity of the meteorological fields used to drive LPDMs is of utmost importance for the quality of the resulting air parcel trajectories and the simulated footprints (Bowman et al. 2013). The proverbial "garbage-in, garbage-out" expression is apt: no matter how well-constructed the LPDM is, the model cannot generate footprints that reflect true atmospheric transport if the driving meteorology is erroneous.

In particular, special attention should be paid to the representation of the height of the boundary layer, as the turbulent mixing in the free troposphere is much weaker. The failure of the input wind or the parameterization in the LPDM to represent the height of the PBL and of its daily variations could have a significant impact on the representation transport and hence on the sensitivity of the receptor points to the emission areas that are responsible for the measurement values.

As such, the errors within the driving meteorological fields should be quantified (see meteorological inputs section) by comparisons against meteorological measurements (Lin and Gerbig 2005)(Gerbig et al. 2008). In the absence of these comparisons, at least the sensitivity to meteorological input should be assessed by carrying out multiple simulations driven with more than one meteorological field (Pisso et al. 2019).

C.c.5 How to test LPDM models?

A comparison of time-forward and time-backward simulations using LPDM models should yield similar source-receptor information: i.e. the number of air parcels released from a source that arrive at the receptor should be similar to the number released from the receptor that arrive at the source, subject to statistical fluctuations. Discrepancies between time-forward versus time-backward simulations have been used to reveal internal inconsistencies and violations of physical principles within the model(Lin et al. 2003)(Nehrkorn et al. 2010)(Hegarty et al. 2013), such as mass conservation and the well mixed criterion, a manifestation of the Second Law of Thermodynamics (Thomson 1987).

In addition to testing for internal consistency and adherence to fundamental physical principles, the LPDM models should also be evaluated against real-world atmospheric dispersion. In a number of instances, known quantities of tracers have been released to the atmosphere from identified locations and whose mole fractions were measured downwind. Such "tracer release" experiments are important for testing the real-world behaviour of the LPDM models. Thus, data from multiple tracer release experiments have been compiled into a single data set and made readily available to the community (Draxler et al. 2001). In addition, tracer releases at the city scale (Allwine et al. 2002) are of particular value to urban applications.

While tracer release measurements are critical, they are typically carried out over a short period of time (a few days) as part of field campaigns. To test the LPDM models over a longer period of time, an alternative data set is to rely on information from relatively well characterized emissions, such as from power plants.

C.c.6 Technical Details Regarding Footprint Simulation

Footprints are generally a truncated representation of the transport, in space (domain) and time (backward time). Thus, the size of the domain and the backward time needed are mainly determined by the area of interest and the upwind sources to be studied in the simulation. For example, large, nearby sources should be included so that the superposition of the sources of interest plus the upwind sources in the measurements can be accounted for (Lopez-Coto et al. 2020). What is a large, nearby source? The qualitative answer would be a source that it is close enough or large enough to have a measurable impact in the observations. In practice, because of the exponential decay of the footprints with time as air is exchanged between the PBL and the free troposphere, one or two days backward in time from the receptor is often adequate for city problems although situations with recirculation may need more time.

The spatio-temporal domain chosen is directly related to the representation of the background, which reflects the influences from sources before the maximum time-backward. Although the background composition in isolated areas can be represented with a single number, this is rarely adequate in urbanized areas. If known, the 3D composition of the atmosphere (from another model, or observed) at the temporal edge of the footprint can be used to represent the background.

Due to the finite number of air parcels that can be simulated in a LPDM to approximate the effectively infinite number of molecules (order $>10^{23}$) in an atmospheric volume, a common consideration in footprint generation is the size of the air parcel ensemble—i.e. how many air parcels to simulate in order to simulate the atmospheric footprint. The number is problem-dependent and hinges on the interaction between heterogeneity in the GHG emissions within the model domain and complexity of the footprint geometry. Thus, in setting up the LPDM it is advisable to carry out a sensitivity analysis to see how results vary as the number of air parcels increases. Typically, the simulated footprint and resulting GHG values stabilize with the size of the air parcel ensemble. Therefore, an ensemble size where the simulation stabilizes, beyond which the simulation results change minimally can be selected (Mallia et al. 2015)(Wu et al. 2018).

It is worth noting that the size of the air parcel ensemble where the stabilization occurs depends upon the smoothing algorithm applied to the footprint yielded by the limited number of air parcels. Smoothing algorithms can include, for instance, simple averaging over multiple grid boxes (Gerbig et al. 2003b). More recently, it has been shown that a more sophisticated kernel density estimation method could reconstruct most of the footprint details from a large ensemble (10^5 parcels) within an urban context by using a small number (order 10^2) of air parcels (Fasoli et al. 2018). However, special attention is needed to address calculations of footprints in the “hyper near-field”, less than an hour’s worth of transport before arrival at the receptor (Gaudet et al. 2017)(Fasoli et al. 2018)(Sargent et al. 2018).

C.c.7 Footprint Generation Approaches as part of GHG Simulation Systems

Obtaining atmospheric transport information as encapsulated in footprints can be undertaken at different levels of effort, increasing in complexity and sophistication from simplest to most complex:

- Tier 1. No footprint generation, per se. Atmospheric transport information is instead gleaned from simple wind rose analyses or single backward trajectories originating from the receptor that only accounts of mean winds (no turbulence).
- Tier 2. Footprint generated using LPDMs.
- Tier 3. Footprint generated using LPDMs, as well as an assessment of transport errors in both the meteorological fields using meteorological observations and the atmospheric dispersion using tracer release data.
- Tier 4. Footprint generated using LPDMs, combined with an assessment of transport errors within an inverse analysis system.

C.c.8 References

Allwine K.J., Shinn J.H., Streit G.E. et al. (2002) Overview of URBAN 2000. *Bulletin of the American Meteorological Society* 83, 521–536.

Bowman K.P., Lin J.C., Stohl A. et al. (2013) Input Data Requirements for Lagrangian Trajectory Models. *Bulletin of the American Meteorological Society* 94, 1051–1058, doi:10.1175/BAMS-D-12–00076.1.

Chen J. et al. (2016) Differential column measurements using compact solar-tracking spectrometers. *Atmospheric Chemistry and Physics* 16, 8479–8498, doi:10.5194/acp-16–8479–2016. http://www.atmos-chem-phys.net/16/8479/2016/.

Crisp D. et al. (2004) The Orbiting Carbon Observatory (OCO) mission. *Advances in Space Research,* 34, 700–709.

Draxler R.R., Heffter J.L. and Rolph G.D. (2001) DATEM Data Archive of Tracer Experiments and Meteorology. NOAA Air Resources Laboratory, Silver Spring, Maryland, 27 pp. http://www.arl.noaa.gov/datem.

Fasoli B., Lin J.C., Bowling D.R. et al. (2018) Simulating atmospheric tracer concentrations for spatially distributed receptors: updates to the Stochastic Time-Inverted Lagrangian Transport model's R interface (STILT-R version 2). *Geoscientific Model Development* 11, 2813–2824, doi:10.5194/gmd-11–2813–2018.

Gaudet B.J., Lauvaux T., Deng A. et al. (2017) Exploration of the impact of nearby sources on urban atmospheric inversions using large eddy simulation. *Elementa: Science of the Anthropocene* 5, doi:10.1525/elementa.247.

Gerbig C., Lin J.C., Wofsy S.C. et al. (2003a) Toward constraining regional scale fluxes of CO_2 with atmospheric observations over a continent: 1. Observed spatial variability from airborne platforms. *Journal of Geophysical Research Atmospheres* 108, doi:10.1029/2002JD003018.

Gerbig C., Lin J.C., Wofsy S.C. et al. (2003b) Toward constraining regional scale fluxes of CO2 with atmospheric observations over a continent: 2. Analysis of COBRA data using a receptor-oriented framework. *Journal of Geophysical Research Atmospheres* 108, doi:10.1029/2003JD003770.

Gerbig C., Korner S., and Lin J.C. (2008) Vertical mixing in atmospheric tracer transport models: error characterization and propagation. *Atmospheric Chemistry and Physics* 8, 591–602.

Hegarty J. et al. (2013) Evaluation of Lagrangian Particle Dispersion Models with Measurements from Controlled Tracer Releases. *Journal of Applied Meteorology and Climatology* 52, 2623–2637.

Lin J.C. and Gerbig C. (2005) Accounting for the effect of transport errors on tracer inversions. *Geophysical Research Letters* 32, doi:10.1029/2004GL021127.

Lin J.C., Gerbig C., Wofsy S.C. et al. (2003) A near-field tool for simulating the upstream influence of atmospheric observations: The Stochastic Time-Inverted Lagrangian Transport (STILT) model. *Journal of Geophysical Research Atmospheres* 108, doi:10.1029/2002JD003161.

Lin J.C., Brunner D., Gerbig C. et al. (2012) Lagrangian Modelling of the Atmosphere. *Geophysical Monographs* 200, 349.

Lopez-Coto I. et al. (2020) Wintertime CO_2, CH_4, and CO Emissions Estimation for the Washington, D.C.–Baltimore Metropolitan Area Using an Inverse Modelling Technique. *Environmental Science and Technology* 54, 2606–2614, doi:10.1021/acs.est.9b06619.

Mallia D.V, Lin J.C., Urbanski S. et al. (2015) Impacts of upstream wildfire emissions on CO, CO_2, and PM2.5 concentrations in Salt Lake City, Utah. *Journal of Geophysical Research Atmospheres* 120, doi:10.1002/2014JD022472.

Nehrkorn T., Eluszkiewicz J., Wofsy S.C. et al. (2010) Coupled Weather Research and Forecasting–Stochastic Time-Inverted Lagrangian Transport (WRF–STILT) model. *Meteorol. Atmos. Phys.,* 107, 51–64.

Pisso I., Patra P., Takigawa M. et al. (2019) Assessing Lagrangian inverse modelling of urban anthropogenic CO_2 fluxes using in situ aircraft and ground-based measurements in the Tokyo area. *Carbon Balance Management* 14, 6, doi:10.1186/s13021–019–0118–8.

Rayner P.J. and O'Brien D.M. (2001) The utility of remotely sensed CO_2 concentration data in surface source inversions. *Geophysical Research Letters* 28, 175–178.

Rodgers C.D. (2000) Inverse methods for atmospheric sounding: theory and practice. World Scientific, Singapore.

Sargent M. et al. (2018) Anthropogenic and biogenic CO_2 fluxes in the Boston urban region. *Proceedings of the National Academy of Sciences* 201803715, doi:10.1073/PNAS.1803715115.

Seibert P. and Frank A. (2004) Source-receptor matrix calculation with a Lagrangian particle dispersion model in backward mode. *Atmospheric Chemistry and Physics* 4, 51–63.

StohlA. and Wotawa G. (1993) A method for computing single trajectories representing boundary layer transport. *Atmospheric Environment* 29, 3235–3238.

Stull R.B. (1988) An introduction to boundary layer meteorology. Kluwer, Dordrecht, The Netherlands.

Taylor G.I. (1920) Diffusion by continuous movements. *Proceedings of the London Mathematical Society* Ser.2, 20, 196–212.

Thomson D.J. (1987) Criteria for the selection of stochastic models of particle trajectories in turbulent flows. *J. Fluid Mech.,* 180, 529–556.

Wu D., Lin J.C., Oda T. et al. (2018) A Lagrangian Approach Towards Extracting Signals of Urban CO_2 Emissions from Satellite Observations of Atmospheric Column CO_2 (XCO_2): X-Stochastic Time-Inverted Lagrangian Transport model ("X-STILT v1"). *Geoscientific Model Development* 11, 4843–4871, doi:10.5194/gmd-2018–123.

Wunch D. et al. (2011) The Total Carbon Column Observing Network. *Philos. Trans. R. Soc. London A Math. Phys. Eng. Sci.,* 369, 2087–2112.

Yokota T., Yoshida Y., Eguchi N. et al. (2009) Global Concentrations of CO_2 and CH_4 Retrieved from GOSAT: First Preliminary Results. *SOLA,* 5, 160–163, doi:10.2151/sola.2009–041.

C.d. Use of inverse modelling methods for urban monitoring

Frédéric Chevallier[1]

[1]Laboratoire des Sciences du Climat et de l'Environnement, Gif sur Yvette, France

C.d.1 Introduction

The title of this chapter implies the inversion of a model: we go up the causal chain that is represented by this model, in order to infer some target variables from some observed variables that they have influenced. Target variables include emissions fluxes but also other variables that have influenced the observations and that are not known with sufficient accuracy (e.g. the initial state of CO_2 in the atmosphere, wind speed, etc.). Observations for us have been made in the atmosphere (atmospheric mole fractions and, possibly, meteorological observations) or from space but still about the atmosphere.

We focus the inversion concept on atmospheric models in the following. Atmospheric models are mainly chemistry transport models here. They can even be reduced to transport models for some species (CO_2) or for some short-enough timescales or regional domains, but they can also include prognostic equations for meteorological variables (online transport model rather than offline transport model). Together with the core atmospheric model, we need its numerical interfaces with the target variables on one side and with the observations on the other one.

Atmospheric dispersion is irreversible. Even if it was reversible, atmospheric observations are limited in spatial coverage (all of them) and quality (ground-based or satellite retrievals). Atmospheric models therefore cannot be inverted in a deterministic way but rather in a statistical way with the help of prior information to guide the inversion within a plausible subspace of the solutions. Prior refers to knowledge about the target variables (estimates with associated uncertainties, accounting for known characteristics of the target variables, e.g. positivity for some emission variables) made before the moment when the model is inverted with these observations.

What is the probability of the target variables given the model, the available observations and the prior information? This question can be rigorously posed in a Bayesian framework. Geostatistics, with less reliance on prior information, can also be used. Inversion aims to achieve the best statistical (aka optimal) compromise between the various information pieces. Inversion should be the ultimate combination of “bottom-up” (prior) and “top-down” (observations + model) information.

The inversion output is made of a multivariate probability density function, usually made of values of the control variables with maximum likelihood and of the uncertainty of those maximum likelihood values.

Some extensive literature already exists on the inversion methodology (e.g. Rayner et al. 2019 and Michalak et al. 2017) for a recent general overview of the topic.

C.d.2 Recommendations

The first requirement for inverse modelling is expertise in the corresponding applied statistics. Second requirement is expertise or access to expertise in all the ingredients that go into in the inversion.

All elements of Inverse modelling should be made explicit within the appropriate mathematical framework. For instance, an error covariance matrix is primarily an error covariance matrix before being a weight in a cost function. The Bayesian framework allows this clarity, unlike, e.g. artificial intelligence, and should therefore be favoured.

C.d.2.1 Explicit definition of configuration

Inverse modelling involves the following questions that should drive the inversion configuration:

- What are the observations that are to be assimilated? Raw or processed data, individually or as averages, ratios or differences (subtract background site). Data selection (wind direction, local time daily periods, outlier detection for observations or for models, ...).
- What are the variables that are controlled? Emission totals at some scale or gridded, sectoral emission variables, representation of atmospheric initial state and lateral boundary conditions, "nuisance" variables as well (e.g. vegetation fluxes for radiocarbon observations), hyper-parameters of the statistical distributions? Make the atmospheric model a weak rather than strong constraint (incl. winds, boundary layer heights, atmospheric mass fluxes, etc.)?
- What is the atmospheric model (incl. resolution in space and time, incl. other input variables, incl. pre-processor of the control variables and post-processor to compare with the observations)?
- How non-linear is the model? This question bears implication on the validity of linearized form or of linear form (impact on monotonicity of the advection scheme). The answer depends on the control variables (e.g. emission fluxes vs. meteorological variables).
- What is the source of prior information?
- How do the errors of the prior control vector look like? What are the statistical moments that can fairly be estimated (Gaussian modelling possible with the first 2)? Correlations between errors? This is resolution dependent.
- Same question about the errors of the observations.
- Same question about the error of the (full) atmospheric model. Important when assimilating profile measurements, or when coupling the atmospheric model with emission process models (see P Rayner's chapter) or when assimilating co-emitted species (emission ratio). Note that the interfaces can potentially dominate the model error budget, e.g. when disaggregating annual national totals into hourly grid cell values.
- Are the errors of the prior control vector correlated in some way with the observation errors or with the errors of the model (i.e. is an inversion crime being committed)?
- Is any bias suspected in the inversion system? Biases in the prior may not be a problem but will still distort the posterior statistics. "Large" model or observation biases may dominate the inversion.
- How is the inversion problem solved? Are there any additional statistical assumptions implied by the inversion method?
- Are there any independent data for evaluation? We mean independent, knowing that the model may make the comparison dependent.

C.d.2.2 Diagnostics

The inversion data provider should also communicate about the following diagnostics:

- The underlying cost function has to be reduced (because the optimal state is come closer to the provided information than the prior state).
- The gradient of the cost function has to be much reduced (because the optimal state is a minimum).
- Realism of ALL optimized variables (e.g. winds or temperature if they are optimized as well, or connected variables like surface pressure, respect of physical laws like continuity equation or mass conservation), or good reasons not to get it.
- Uncertainty statistics of the inversion result at any space-timescale (is it realistic, even when ratio-ed to the prior uncertainty?) or good reasons not to get it.
- Statistical consistency between the various internal elements (observation-minus-background O-B, observation minus analysis O-A, background-minus-analysis B-A consistent with H, B and R for Gaussian frameworks, reduced $\chi 2$ close to 1) or good reasons not to get it.
- Statistical consistency when comparing with external information, after accounting for the uncertainty of that information (can go as far as reliability diagrams to visualize the agreement between the predicted probabilities and the verifying observations, ...).
- Diagnostics can be qualitative as well (e.g. evaluation of the sign or the amplitude of the result) and sensitivity to some of the key choices should be shown.

C.d.2.3 Transparency

Transparency implies the possibility for others to reproduce inversion results. It is challenging because, strictly speaking, it implies the availability of the full model, the inversion system and the observations for these “others”. For the code, availability depends on portability and long-term maintenance and continuously evolving computer environments. Transparency should therefore be seen as a long-term goal, with achievements ranked in successive tiers, to be defined.

C.d.3. References

Michalak A.M., Randazzo N.A. and Chevallier F. (2018) Diagnostic methods for atmospheric inversions of long-lived greenhouse gases, *Atmospheric Chemistry and Physics* 17, 7405–7421.

Rayner P.J., Michalak A.M. and Chevallier F. (2019) Fundamentals of data assimilation applied to biogeochemistry, *Atmospheric Chemistry and Physics* 19, 13911–13932.

Annex D. Recommendations for Data Management, Archiving and Distribution

Logan Mitchell[1] and Alex Vermuelen[2]

[1]The University of Utah, Department of Atmospheric Sciences, Salt Lake City, UT, USA

[2]Integrated Carbon Observation System (ICOS), Helsinki, Finland

Successful data management, archiving and distribution are critical factors to cultivate urban carbon cycle science. The following recommendations are based on best practices for data management drawn from several fields to ensure consistency.

D.a. FAIR data principles

Urban greenhouse gas and ancillary data should follow 'FAIR' data principles, meaning they should be Findable, Accessible, Interoperable, and Reusable/Reproducible. A key component of creating data sets that follow FAIR principles is utilizing the Climate and Forecast (CF) conventions for data and metadata (http://cfconventions.org/).

D.a.1 Findable data sets

Findable datasets will have the following characteristics:

- A globally unique and persistent identifier such as a Handle PID or Digital Object Identifier (https://www.doi.org/).
- Data should be archived at a long-term trusted (community) repository that warrants the data integrity and preserves the data and metadata for the far future beyond the lifetime of projects or careers. Ideally these repositories commit to principles like CoreTrustSeal. Examples are Pangaea, Zenodo, ICOS CP and ORNL DAAC.
- Data that are described with rich metadata following CF and ISO19139 (e.g. WIGOS profile) conventions that is easy to interpret for both humans and computers and can facilitate automatic discovery.

D.a.1.1 Accessible data

Once data has been found, it needs to be accessed. Accessible data should have the following characteristics:

- Data and metadata should be accessed using a standardized communications protocol such as HTTPS, or a RESTful API. In cases where authentication or authorization are necessary, the protocol to access the data should be explicit, open, free, and universally implementable.
- Data and metadata should be accessible in open data formats such as NetCDF (https://www.unidata.ucar.edu/software/netcdf/), HDF5 (https://www.hdfgroup.org/) or plain text.

D.a.1.2 Interoperable data

Data is usually integrated with other data or model output and therefore it needs to be interoperable with applications or workflows for data analysis, storage, and processing. Interoperable data should have the following characteristics:

- Data and metadata should follow CF naming conventions for the description of the measured variables. The conventions define metadata that provide a definitive description of what the data in each variable represents, and the spatial and temporal properties of the data. This enables users of data from different sources to decide which quantities are comparable, and facilitates building applications with powerful extraction, regridding, and display capabilities. If an appropriate standard name does not exist in the CF conventions, the CF community has the ability to add it.
- Data and metadata should include references to primary literature, protocols or other qualified references as appropriate.

D.a.1.3 Reusable/reproducible data

Data becomes more useful if it is reused by others across several applications or settings. Reusable/Reproducible data should have the following characteristics:

- Data and metadata should be richly described as discussed above.
- Data and metadata are released with a clear and accessible 'Fair Use' policy or data usage license.
- Data and metadata are associated with a detailed provenance.
- Methods to produce data should be well documented so that results or products can be reproduced by others.

D.a.2 Date and time formats

Best practices for formatting date and timestamps are to follow the recommendations from the Air Sensor Workgroup (https://www.edf.org/health/data-standards-date-and-timestamp-guidelines). The recommended guidelines are derived from the ISO 8601 standard, IETF RFC 3339 and the W3C profile. It is recommended that data use a combination of Epoch time and a human readable timestamp.

- Epoch time (aka Unix time or POSIX time) is time in seconds since Unix Epoch (19701–01T00:00:00Z) as a 64-bit unsigned integer.
- A human readable timestamp should follow the ISO 8601 format that includes the time zone field. All data should be reported relative to UTC using the following format: YYYY-MM-DDThh:mm:ss.nnn±hh:mm (Example: 20161–25T15:23:22.635+00:00). UTC times have format YYYY-MM-DDThh:mm:ss.nnnZ. The part in fraction of seconds (.nnn) can be omitted in most applications.

D.a.3 Programming tools

Applications to develop and access data sets should be archived on open access code repositories such as GitHub (https://github.com/) and be developed on open source collaborative platforms like Jupyter Notebooks (https://jupyter.org/). Utilizing these collaborative platforms will expand the reach of the tools developed.

D.a.4 Examples

Several example data products that follow the aforementioned recommendations are:

- The ICOS Carbon Portal (https://www.icos-cp.eu/data-services)
- The CO_2-Urban Synthesis and Analysis data product (https://doi.org/10.3334/ORNLDAAC/1743)
- The NOAA ESRL ObsPack data product (https://www.esrl.noaa.gov/gmd/ccgg/obspack/)

____

For more information, please contact:

World Meteorological Organization

Science and Innovation Department

7 bis, avenue de la Paix – P.O. Box 2300 – CH 1211 Geneva 2 – Switzerland

Tel.: +41 (0) 22 730 81 11 – Fax: +41 (0) 22 730 81 81

Email: GAW@wmo.int

Website: https://public.wmo.int/en/programmes/global-atmosphere-watch-programme

JN 22329